Diplomarbeit

# Downstream processing in the ethanol production from lignocellulosic biomass

A process simulation with ASPEN PLUS including an energy analysis

ausgeführt zum Zwecke der Erlangung des akademischen Grades
eines Diplom-Ingenieurs
unter der Leitung von

Ao.Univ.Prof. Dipl.-Ing. Dr.techn. Anton Friedl,
Dipl.-Ing. Philipp Kravanja

E 166 - Institut für Verfahrenstechnik, Umwelttechnik
und Techn. Biowissenschaften

**Fakultät für Maschinenwesen und Betriebswissenschaften**

von

Tino Lassmann
0325476

Wien am 30.01.2012

_____

(Tino Lassmann)

## Acknowledgement

This thesis would not have been possible without Prof. Anton Friedl, who always gave me the support I needed and who had a lot of patience with me during that time.

I would also like to show my gratitude to my supervisor, Philipp Kravanja, for letting me work independently and never shying away from questioning my ideas or statements.

It is a pleasure to thank Ala Modarresi and Walter Wukovits, not only for their support in terms of simulation and analysis, but also for providing a wonderful working atmosphere.

I owe my deepest gratitude to all members of my family for their never ending support - especially to mention my mother, Veronika Lassmann, who can finally spend her money "with warm hands" on her own needs.

Thank you to my girlfriend, for being so patient with me.

Thank you to all my friends, for enriching my life.

Tack till alla mina kompisar från Sverige – ni berikar mitt liv!

And special thanks to those, who went with me for a coffee when I needed it.

Last but not least, I would like to thank my dad, Dr. Georg Lassmann, who gave me life, endowed me with a certain technical understanding and who would have surely been very proud of me right now.

"The journey is the reward!" – I have to admit, it was a pretty long journey.

# Abstract

The utilization of bioethanol as fuel in the transport industry is one of the most promising alternatives to gasoline. Besides the well established manufacturing method for conventional bioethanol based on raw materials containing sugar and starch, the production of bioethanol from lignocellulosic biomass is a another step in advancing renewable fuels. But its energy intensive downstream process still limits the ability to compete with conventional bioethanol or petroleum. It is therefore essential to find a process setup that provides possibilities for heat integration and consequently results in a more efficient overall process. The comparison of the different heat integrated configurations, based on the data obtained from simulation, provides information about the well-designed concept.

In this thesis, two different distillation concepts, with an annual production of 100,000 tons of ethanol from straw, are simulated with the modeling tool ASPEN Plus®. In addition to the 2-column and 3-column distillation configuration, simulations of an evaporation system and an anaerobic digester to produce biogas provide results for these two possibilities of subsequent stillage treatment. For the multi-stage evaporation system, an evaluation of different configurations gives information about possible energy savings in this process section.

By applying Pinch Analysis, the concepts are compared from an energy point of view, to find the optimal distillation concept in context with the background process for the respective subsequent stillage treatment. The results from Pinch Analysis show that in combination with a 5-stage co-current evaporation process, the 3-column distillation setup is preferable. For the whole process its minimum energy consumption per kg of ethanol accounts for 17.2 $MJ/kg_{EtOH}$ with a respective process overall heating and cooling demand of 60.3 MW and 59.1 MW. When anaerobic digestion is used to treat the distillation stillage, 10 $MJ/kg_{EtOH}$ have to be provided for the whole process. The overall process's heating and cooling demand accounts for 35.2 MW and 33.7 MW respectively, which again favors the 3-column distillation configuration. In both stillage treatment concepts, the overall process heating demand could easily be covered by the utilization of the dried solid residues from solid-liquid separation. Depending on the chosen concept, either the biogas produced could be upgraded and sold as a product or the evaporation concentrate could be used for further energy production.

# Kurzfassung

Eine der vielversprechendsten Alternativen zu Benzin als Kraftstoff im Transportsektor ist die Nutzung von Bioethanol. Neben den etablierten Herstellungsverfahren für Bioethanol basierend auf Rohstoffen die Zucker und Stärke enthalten, ist die Produktion von Bioethanol aus lignozellulosehaltiger Biomasse ein weiterer Schritt die Entwicklung erneuerbarer Energieträger voranzutreiben. Der energieintensive „down stream"-Prozess begrenzt jedoch dessen Konkurrenzfähigkeit gegenüber herkömmlichem Bioethanol und Benzin. Es ist daher unerläßlich ein Prozeß Setup zu finden, das die Möglichkeiten für eine Wärme-Integration bietet und somit in einen effizienteren Gesamtprozeß resultiert. Ein Vergleich der unterschiedlichen wärmeintegrierten Prozeß-Konfigurationen, basierend auf den Daten die aus der Simulation gewonnen wurden, gibt Auskunft über das bestgeeignete Konzept.

In dieser Arbeit wurden zwei verschiedene Destillationsvarianten, zur jährlichen Produktion von 100,000 Tonnen Ethanol aus Stroh, mit dem Modellierungswerkzeug ASPEN Plus® simuliert. Zusätzlich zu diesen 2-Kolonnen- und 3-Kolonnen-Destillationskonzepten wurden eine Mehrstufen-Eindampfanlage und ein anaerober Fermenter zur Erzeugung von Biogas simuliert, welche Ergebnisse für diese beiden Möglichkeiten der anschließenden Schlempenaufbereitung liefern. Eine Evaluierung der unterschiedlichen Betriebsweisen der Mehrstufen-Eindampfanlage liefert wiederum Informationen über mögliche Energieeinsparungen in diesem Prozeßabschnitt.

Mittels Pinch-Analyse werden die im Gesamtprozeß implementierten Konzepte aus energetischer Sicht verglichen, um das optimale Destillationkonzept für die jeweilige Form der Schlempenaufbereitung zu finden. Die Ergebnisse aus der Pinch-Analyse zeigen, dass für die Kombination mit der 5-stufigen Gleichstrom-Verdampferanlage das 3-Kolonnen-Destillationsmodell die effizientere Variante darstellt. Der entsprechende minimale Energieverbrauch pro kg Ethanol beträgt 17.2 MJ/$kg_{EtOH}$ mit einem Heiz- und Kühlbedarf für den Gesamtprozess von 60.3 MW und 59.1 MW. Wenn anaerobe Vergärung verwendet wird um die Destillations-Schlempe aufzubereiten, müssen bei der Variante mit einer 3-Kolonnen-Destillation 10 MJ/$kg_{EtOH}$ für den Gesamtprozess bereitgestellt werden. Für diese Anordnung betragen der Heiz- und Kühlbedarf des Gesamtprozesses 35.2 MW und 33.7 MW, welches somit die günstigste Konfiguration darstellt. In beiden Schlempen-Aufbereitungskonzepten könnte der Wärmebedarf des Gesamtprozesses durch die Nutzung der getrockneten festen Rückstände aus der Fest-Flüssig-Trennung abgedeckt werden. Je nach gewähltem Konzept, könnte entweder das produzierte Biogas aufgereinigt und als Produkt

verkauft werden oder das Konzentrat der Eindampfung zu weiterer Energieerzeugung herangezogen werden.

## Sammanfattning

Bioetanol är ett lovande, mer miljövänligt, alternativ till bensin som drivmedel inom transportsektorn. Förutom de etablerade metoderna för produktion av bioetanol baserat på råvaror innehållande socker och stärkelse, kan produktion av bioetanol baseras på lignocellulosa. Detta är en ytterligare möjlighet för utvecklingen av förnyelsebara energikällor, även om den energiintensiva nedströms-processen begränsar konkurrenskraften gentemot bensin och konventionellt producerad etanol. Det är därför viktigt att utveckla en process som har förutsättning för värmeintegration och därmed resulterar i en, totalt sett, mer effektiv process. Genom att jämföra simulerad data av olika värmeintegrerade processer, kan slutsats dras om vilken process-design som är bäst lämpad.

I detta arbete har två olika varianter av destillation, med kapacitet för årlig produktion på 100.000 ton etanol från halm, simulerats med modelleringsverktyget ASPEN Plus®. Ytterligare till 2-kolonns och 3-kolonns destillationssystemer, har data simulerats en flerstegs-indunstare och en anaerob fermentor för biogasproduktionen, för att få kunskap om de båda metodernas möjligheter av efterföljande drank behandlingen.

En evaluering vid olika driftsbetingelser av flerstegs-indunstaren gav ytterligare information om möjliga energibesparingar i detta processteg.

Pinch-analys användes för att jämföra de olika process koncepter ur energisynpunkt för att hitta den optimala destillationstypen i kombination med efterföljande drank behandling.

Jämförelsen resulterade i att vid användning av 5-stegs-indunstare av motströmstyp är 3-kolonnsdestillationen den mest energieffektiva metoden. För denna uppställning är den minimala energiförbrukningen per kilogram etanol 17.2 MJ, med ett värme- och kylbehov för den övergripande processen på 60.3 MW respektive 59.1 MW. Även då anaerob fermentering används för att behandla dranken, så är 3-kolonnsdestillationen mest effektiv då det åtgår 10 $MJ/kg_{EtOH}$. Vid denna uppställning är värme- och kylbehovet för den totala processen 35.2 MW respektive 33.7 MW, och utgör därmed den mest fördelaktiga framställningen. I båda fallen kan hela processens värmebehov täckas, genom att antingen använda den producerade biogasen eller de torkade fasta biprodukterna efter en fast-flytande separation.

# Index

# List of figures

# List of tables

# List of symbols

## Latin Latters

| | | |
|---|---|---|
| $BR$ | Boil up rate | - |
| $c_1$ | Concentration of organic substances at evaporator stage 1 | % |
| $c_2$ | Concentration of organic substances at evaporator stage 2 | % |
| $c_3$ | Concentration of organic substances at evaporator stage 3 | % |
| $c_4$ | Concentration of organic substances at evaporator stage 4 | % |
| $c_5$ | Concentration of organic substances at evaporator stage 5 | % |
| $c_S$ | Concentration of organic substances | % |
| $COP_{HP}$ | Coefficient of performance for a heat pump | - |
| $CP_{eff}$ | Effective heat capacity | kJ/(kg*K) |
| $f_i^0$ | Fugacity at standard conditions | bar |
| $f_i^l$ | Fugacity of component *i* in the liquid phase | bar |
| $f_i^v$ | Fugacity of component *i* in the vaporous phase | bar |
| $E_{MV}$ | Murphree efficiency | % |
| $\dot{F}$ | Load of volatile solids | kg/d |
| $g$ | Standard gravity | $m/s^2$ |
| $g^E$ | Gibb's excess energy | kJ |
| $h_B$ | Specific enthalpy of bottom product | kJ/kg |
| $h_F$ | Specific enthalpy of the feed | kJ/kg |
| $h_F$ | Specific enthalpy of the feed | kJ/kg |
| $h_H$ | Specific enthalpy of the head product | kJ/kg |
| $h_L$ | Specific enthalpy of the concentrate | kJ/kg |
| $h_{es}$ | Specific enthalpy of the evaporated solvent | kJ/kg |
| $h_{in}$ | Specific enthalpy of the incoming stream | kJ/kg |

| | | |
|---|---|---|
| $h_{out}$ | Specific enthalpy of the outgoing stream | kJ/kg |
| $H$ | Geodetic height | m |
| $HRT$ | Hydraulic retention time | d |
| $\dot{m}_B$ | Mass flow of bottom product | kg/s |
| $\dot{m}_{BU}$ | Mass flow of boil up | kg/s |
| $\dot{m}_F$ | Mass flow of feed | kg/s |
| $\dot{m}_F$ | Mass flow of the feed | kg/s |
| $\dot{m}_H$ | Mass flow of head product | kg/s |
| $\dot{m}_L$ | Mass flow of the concentrate | kg/s |
| $\dot{m}_R$ | Mass flow of reflux | kg/s |
| $\dot{m}_S$ | Amount of substrate fed to the digester | kg/d |
| $\dot{m}_{es}$ | Mass flow of the evaporated solvent | kg/s |
| $\dot{m}_{in}$ | Mass flow of incoming stream | kg/s |
| $\dot{m}_{out}$ | Mass flow of outgoing stream | kg/s |
| $\dot{m}_{sol}$ | Mass flow of the solution | kg/s |
| $OLR$ | Organic loading rate | kg/(l*d) |
| $p$ | Pressure from ASPEN simulation | bar |
| $p_2$ | Pressure at evaporator stage 2 | bar |
| $p_3$ | Pressure at evaporator stage 3 | bar |
| $p_4$ | Pressure at evaporator stage 4 | bar |
| $p_5$ | Pressure at evaporator stage 5 | bar |
| $p_i{}^0$ | Saturated vapor pressure | bar |
| $p_S$ | Saturated vapor pressure | bar |
| $p^l$ | Pressure of the liquid phase | bar |
| $p^v$ | Pressure of the vaporous phase | bar |
| $p_{stage\ x}$ | Pressure at evaporator stage x | bar |

| | | |
|---|---|---|
| $p_{stage\ x-1}$ | Pressure at evaporator stage x-1 | bar |
| $P_{el}$ | Electric power | W |
| $\dot{Q}$ | Transferred heat | kW |
| $\dot{Q}_c$ | Condenser duty | kW |
| $Q_{C\ min}$ | Minimum cold utility | kW |
| $Q_{H\ min}$ | Minimum hot utility | kW |
| $\dot{Q}_{Loss}$ | Heat loss | kW |
| $\dot{Q}_R$ | Reboiler duty | kW |
| $Q_{Rec}$ | Amount of heat recovered | kW |
| $R$ | Ideal gas constant | kJ/(kmol*K) |
| $RR$ | Reflux ratio | - |
| $T^l$ | Temperature of the liquid phase | °C |
| $T^v$ | Temperature of the vaporous phase | °C |
| $T_1$ | Temperature at evaporator stage 1 | °C |
| $T_2$ | Temperature at evaporator stage 2 | °C |
| $T_3$ | Temperature at evaporator stage 3 | °C |
| $T_4$ | Temperature at evaporator stage 4 | °C |
| $T_5$ | Stage temperature | °C |
| $T_5$ | Temperature at evaporator stage 5 | °C |
| $T_{boiling,stage\ 1}$ | Boiling temperature at stage 1 in the evaporation system | °C |
| $T_{boiling,stage\ 5}$ | Boiling temperature at stage 5 in the evaporation system | °C |
| $T_{boiling,stage\ x}$ | Boiling temperature at stage x | °C |
| $T_{es}$ | Temperature of the evaporated solvent | °C |
| $T_F$ | Temperature of the feed entering the evaporator | °C |
| $T_{feed,stage\ x}$ | Feed temperature at stage x | °C |
| $T_{stage\ x}$ | Temperature at evaporator stage x | °C |

| | | |
|---|---|---|
| $V_R$ | Reactor volume | l |
| $\dot{V}_S$ | Amount of substrate fed to the digester | l/d |
| $x_B$ | Mole fraction of low-boiling component in the bottom product | kmol/kmol |
| $x_F$ | Mole fraction of low-boiling component in the feed | kmol/kmol |
| $x_H$ | Mole fraction of low-boiling component in the head product | kmol/kmol |
| $x_i$ | Composition of component *i* in liquid phase | kmol/kmol |
| $y_i$ | Composition of component *i* in vaporous phase | kmol/kmol |
| $y_n$ | Mole fraction of component in gas phase at stage n | kmol/kmol |
| $y_{n-1}$ | Mole fraction of component in gas phase at stage n-1 | kmol/kmol |
| $y_n^*$ | Achievable equilibrium concentration for the composition of liquid leaving tray n | kmol/kmol |

**Greek Letters**

| | | |
|---|---|---|
| $\eta$ | Efficiency of the pump | - |
| $\rho_{Sol}$ | Density of the solution | $kg/m^3$ |
| $\varphi_i^v$ | Fugacity coefficient | - |
| $\gamma_i$ | Activity coefficient of component i | - |
| $\Delta G$ | Free Gibb's energy | kJ |
| $\Delta G^E$ | Extensive Gibb's energy | kJ |
| $\Delta G^{ideal}$ | Ideal Gibb's energy | kJ |
| $\Delta H_{evap,H}$ | Specific enthalpy of evaporation of the head product | kJ/kg |
| $\Delta H_{evap,w}$ | Latent heat of water | kJ/kg |
| $\Delta H_{v,i}$ | Latent heat of component i | kJ/kg |
| $\Delta p$ | Pressure difference between two stages | Pa |
| $\Delta T_{min}$ | Minimum temperature difference | °C |
| $\Delta T_{total}$ | Total temperature difference | °C |

**Short form**

| | |
|---|---|
| BE | Bioethanol |
| BOD | Biological oxygen demand |
| CCC | Cold composite curve |
| CE | Column efficiency |
| CHP | Combined heat and power |
| COD | Chemical oxygen demand |
| $COP_{HP}$ | Coefficient of performance in a heat pump |
| DDG | Distillers dried grain |
| DDGS | Dried distillers grains with solubles |
| DM | Dry matter |
| DMEA | Di-methyl ethanol amine |
| E-100 | Fuel consisting of pure ethanol |
| E-25 | Fuel with a 25% admixture of ethanol to petroleum |
| EO | Equation oriented |
| EtOH | Ethanol |
| EU-25 | First 25 European Union member states (until end of 2006) |
| FFV | Flexi fuel vehicles |
| FGBE | First generation ethanol |
| GCC | Grand composite curve |
| GHG | Greenhouse gases |
| GRFA | Global renewable fuels alliance |
| GWP | Global warming potential per unit mass |
| HCC | Hot composite curve |
| HRT | Hydraulic retention time |
| IEA | International energy agency |
| LLE | Liquid-liquid equilibrium |
| ME | Murphree efficiency |
| MEA | Mono ethanol amine |

| | |
|---|---|
| MP | Middle pressure |
| NMOC | Non-methane organic compounds |
| NREL | National Renewable Energy Laboratory |
| NRTL | Non-random two-liquid |
| OLR | Organic loading rate |
| PSA | Pressure swing adsorption |
| SE | Steam pretreatment |
| SGBE | Second generation ethanol |
| SHF | Separate hydrolysis and fermentation |
| SSF | Simultaneous saccharification and fermentation |
| VLE | Vapor-liquid equilibrium |
| VLLE | Vapor-liquid-liquid equilibrium |
| VS | Volatile solids |
| WIS | Water insoluble solids |
| WSS | Water soluble solids |

**Molecular formula**

| | | |
|---|---|---|
| $C_2H_4O_2$ | $CH_3COOH$ | Acetic acid |
| $C_2H_6O$ | $C_2H_5OH$ | Ethanol |
| $C_3H_6O$ | $CH_3CH_2COOH$ | Propionic acid |
| $C_3H_8O_3$ | | Glycerol |
| $C_5H_4O_2$ | | Furfural |
| $C_5H_8O_4$ | $C_5(H_2O)_4$ | Xylan |
| $C_5H_9NO_4$ | | L-Glutamic acid (Protein) |
| $C_5H_{10}O_5$ | | Xylose ($C_5$-sugar) |
| $C_6H_{10}O_5$ | $(C_6H_{10}O_5)_n$ | Cellulose |
| $C_6H_{12}O_6$ | | Glucose ($C_6$-sugar) |
| $C_{7.3}H_{13.5}O_{1.3}$ | | Lignin |
| $C_{14}H_{28}O_2$ | $CH_3(CH_2)_{12}COOH$ | Myristic acid |
| $C_{15}H_{30}O_2$ | $CH_3(CH_2)_{13}COOH$ | Pentadecanoic acid |
| $C_{16}H_{32}O_2$ | $CH_3(CH_2)_{14}COOH$ | Palmitic acid |
| $C_{18}H_{32}O_2$ | | Linoleic acid (extractives) |
| $C_{18}H_{34}O_2$ | | Oleic acid |
| $CH_{1.64}N_{0.23}O_{0.39}S_{0.0035}$ | | Yeast |
| $CH_{1.8}O_{0.5}N_{0.2}$ | | Enzymes |
| $CH_4$ | | Methane |
| $CH_4N_2O$ | $(NH_2)_2CO_2$ | Urea |
| $CO_2$ | | Carbon dioxide |
| $H_2$ | | Hydrogen |
| $H_2CO_3$ | $OC(OH)_2$ | Carbonic acid |
| $H_2O$ | | Water |
| $H_2SO_3$ | | Sulphurous acid |
| $H_2SO_4$ | | Sulphuric acid |
| $H_3PO4$ | | Phosphoric acid |
| HCl | | Hydrochloric acid |

| | |
|---|---|
| $HCO_2H$ | Formid acid |
| HF | Hydroflouric acid |
| HNO3 | Nitric acid |
| N | Nitrogen |
| $N_2O$ | Nitrous oxide |
| NaOH | Natrium hydroxid |
| $NH_3$ | Ammonia |
| $O_2$ | Oxygen |
| P | Phosphor |
| S | Sulfur |
| $SiO_2$ | Silicon dioxide |

# 1 Introduction

## 1.1 Motivation

Not only since the Deepwater Horizon oil spill in the Gulf of Mexico in 2010, critical voices against the dependency on oil and associated consequential environmental damages are raised. The facts, that fossil fuels availability expires and that they cause emissions, are undeniable drawbacks of its utilization as energy source. These adverse effects are intensified by the increasing demand in oil, whether as raw material for commodities or as energy source. According to IEA's Oil Market Report [IEA, 2011] the world oil production in 2010 accounted for 13.9 billion liters per day with 16.5% (2.3 billion liters per day) of it consumed by the OECD countries to produce motor gasoline. To reduce world's oil consumption, a reduction of motor gasoline demand is therefore inevitable.

An alternative to gasoline in the transport industry is the use of bioethanol as fuel. First generation bioethanol, or conventional bioethanol, is derived from raw materials containing sugar or starch. The production of bioethanol from these sugar- or starch-rich residues is a mature process, well established in the biofuels market and increased tremendously over the last 10 years, with Brazil and the United States contributing to a large part in this development. These two countries are, not only in terms of production but also in consumption, world market leaders. With rising production of first generation bioethanol, the demand in raw materials such as wheat, corn, potatoes sugar cane and sugar beet also increases. This results in a negative effect on the food industry, which is probably the biggest conflict in the fuel-ethanol-theme. Crops intended for food use are utilized as raw material for the ethanol production – this is better known as the "dinner plate or fuel tank" discussion.

To avoid a conflict between dinner plates and fuel tanks, the utilization of lignocellulosic biomass as raw material for the production of bioethanol seems promising. The advantage of this so called second generation bioethanol is that plant residues, emerged during harvesting, are utilized and the crops can serve its proper purpose. The lignocellulose-to-ethanol process

is, however, still not available in a commercial scale, and it requires an improvement in the process's efficiency, a wise use of its by-products and residues to make it economically competitive. When taking a look at the overall process of the bioethanol production from lignocellulosic raw materials, the downstream process, containing distillation and subsequent stillage treatment, turns out to be extremely energy intensive. Especially the multi-stage evaporation of the distillation stillage, which is a common treatment process, contributes a large share in the total energy demand. An optimization of the evaporation section provides one option to reduce the energy consumption of the process. Another option is the production of biogas due to fermentation of the distillation residue, which turns out to be an attractive alternative for the stillage treatment. Not only savings in energy demand, also the generation of another by-product, which can be used as source for heat and electricity or as commodity, are reasons to believe that the biogas production can have a positive effect on the overall efficiency.

Hence, the modeling and optimization of the downstream part in 2$^{nd}$ generation bioethanol production is an interesting and important task for the development of a commercial plant.

## 1.2 Goal of this work

In this work, the energy intensive downstream process of the bioethanol production from straw is investigated. To find the most efficient concept from an energetic point of view, process simulation along with Pinch Analysis is used. Therefore, the conceptual design and simulation of two different distillation concepts has to be done, maintaining a targeted ethanol production of 100,000 t/a. The results should serve as basis for the two different subsequent stillage treatment concepts, the multi-stage evaporation and the anaerobic digestion for biogas production.

By designing and optimizing two different multi-stage evaporation systems, a co-current and a counter-current, the energetic best fitting evaporation concept has to be identified. With the design and simulation of an anaerobic fermentation process, information about the possible yield in biogas production should be determined.

The process data obtained from all simulations will provide information about the energy demand of the respective parts in the process. To evaluate the ideal combination of distillation and evaporation or distillation and biogas production, the 2-column and the 3-column

distillation concepts in connection with the respective stillage treatment method are compared with each other.

For all simulations in this work, the process modeling tool ASPEN PLUS is implemented.

## 1.3 Scheme of this thesis

For a better understanding of this works purpose, it is important to get an overview about the state of the art in bioethanol production. Therefore, information about the different bioethanol production concepts, the common feedstock and current data about the ethanol market is listed in section 2.1. In this section a summary of the different ethanol production procedures, their advantages and disadvantages, is also given. The common by-products of first and second generation bioethanol processes can be found in section 2.2. Another important topic, always mentioned in bioethanol's favor, is the environmental impact or the respective $CO_2$ emissions, which is described in section 2.3. This is followed by the utilization of bioethanol as main product in section 2.4.

In chapter 3, the process setup for the distillation and the subsequent treatment of the distillation residue from lignocellulosic broths is addressed. The underlying theoretical background of the respective process sections is stated, as well as fundamentals of Pinch Analysis. In chapter 3.7, general information about the process modeling tool ASPEN PLUS and the chosen thermodynamic model for all simulations are provided. After that, the conceptual design and the ASPEN PLUS models of the different process parts as distillation, evaporation and biogas production are described. Chapter 3 concludes with the possibilities for heat integration, including information about the units and requirements of the background process.

All important findings from the flow sheet simulations are presented in chapter 4. This includes the two different distillation variations, the evaporation system and the biogas results, as well as the Pinch Analysis of the 5-stage evaporation system. Subsequently, the findings obtained are discussed, with an attention focused on determining the most effective combination of distillation and subsequent stillage treatments.

In chapter 5, the energetic evaluation of the different process configurations in context with the background process is described. The findings from that are described and discussed in chapter 6. A summary of the main results and an outlook is given to finalize this work in chapter 7.

# 2 State of the art

## 2.1 Bioethanol production

The term "bioethanol" identifies an undenatured ethanol with an alcohol content higher than 99 vol%, generated from biogenic feedstock [Winter et al., 2011]. As shown in Figure 2-1, today sixty percent of the global fuel bioethanol is produced in North and Central America and about one third finds its origin in South America. The bioethanol production in South America is mainly from sugar cane, while the United States ethanol production uses corn as raw material. In a press release, the GRFA (Global Renewable Fuels Alliance) stated that the global fuel ethanol production in 2010 was more than 23 billion gallons (approx. 85 $x10^9$ liter) [Global Renewable Fuels Alliance, 2011].

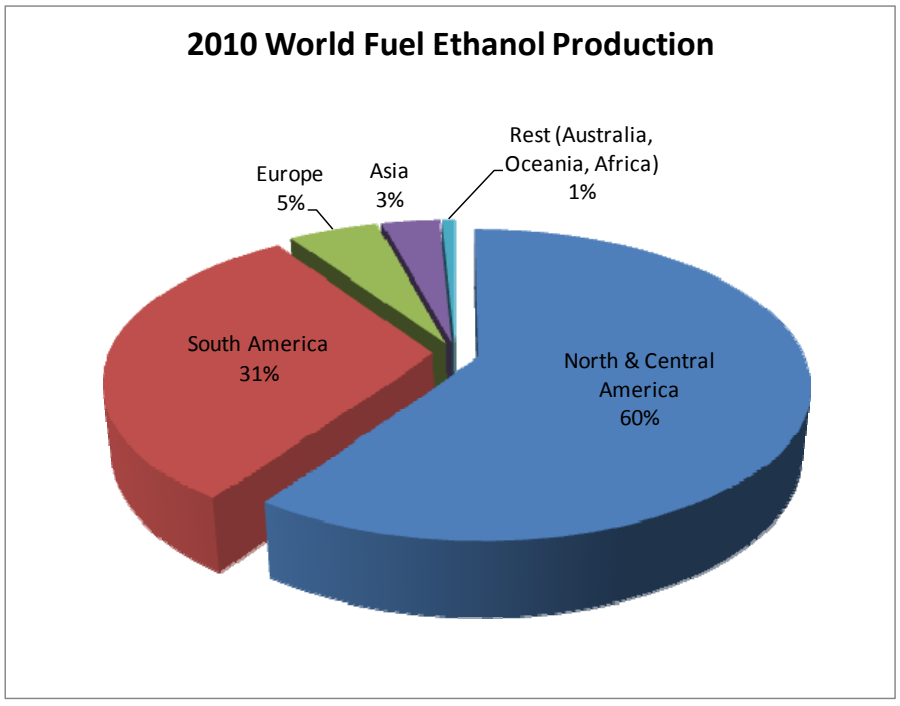


**Figure 2-1: World fuel ethanol production in 2010, with a total of 85 $x10^9$ liters; source: [Renewable Fuels Association, 2011]**

Europe's portion is only 5% and accounts for 1.2 billion gallons (approx. 4.6 $x10^9$ liters). Even though the European market is still small, it is steadily growing, which is proven by an increase of 280% since 2006. For the year 2011 the GRFA predicts a production of 5.467 billion liters fuel ethanol in Europe and a global production of 88.7 billion liters. France is the biggest producer in Europe with about 3.7 billion liters in 2009, followed by Germany and Spain.

As mentioned above, the feedstock varies depending on the regional availability, which in turn restricts the capabilities of various technologies. Common feedstocks for ethanol production in Europe are beets, corn, barley and wheat. In 2007, the proportion of wheat as feedstock was 48%, whilst sugar beet accounted for 29% of the total European ethanol production [Balat and Balat, 2009]. Based on the raw material, two different manufacturing methods of bio-ethanol are identified:

1.) First generation bioethanol (FGBE)

2.) Second generation bioethanol (SGBE)

Though the product bioethanol remains the same, a change in feedstock entails changes in the overall process. Therefore, the respective characteristics and setup are described subsequently.

### 2.1.1 First generation bioethanol

Today, most of the commercially available bioethanol is a first generation product. This manufacturing method is well established and utilizes raw materials containing starch and sugar, such as potatoes, wheat, corn, sugar beet and sugar cane to produce bioethanol. For illustration and easier understanding, the bioethanol production is described in Figure 2-2 by an industrial example – in this case, the Lurgi Bioethanol process based on wheat.

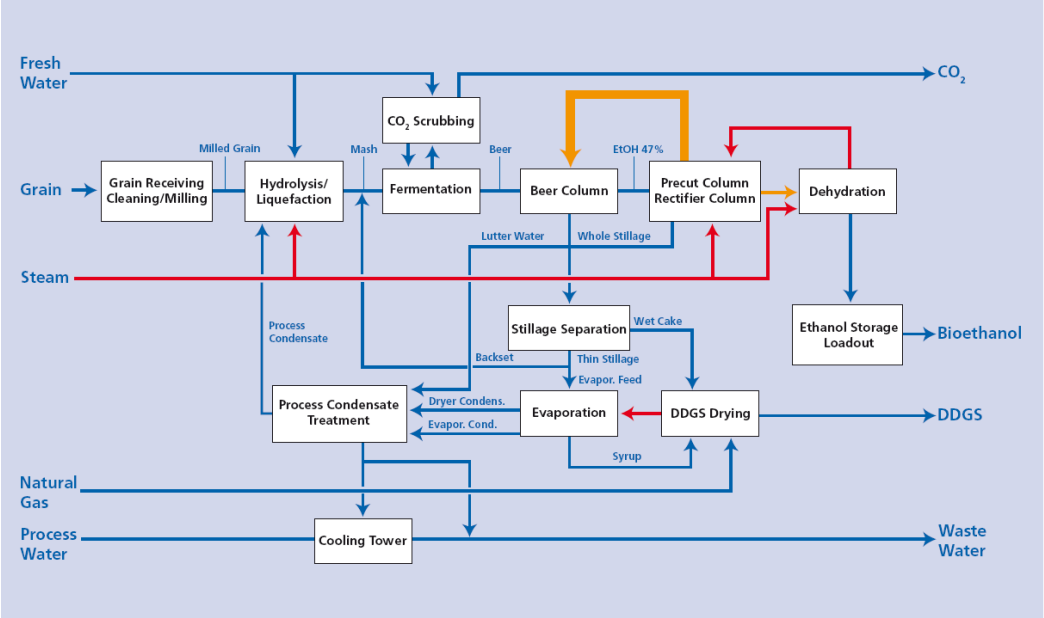


**Figure 2-2:** **Simplified process flow sheet of the Lurgi bioethanol process; source: [Lurgi GmbH, 2011]**

The main parts of the FGBE production are the pretreatment steps, hydrolysis, fermentation, distillation and treatment of the residues. The incoming grain is cleaned and reduced in size by wet or dry milling. After these pretreatment procedures, the raw material undergoes a hydrolysis/liquefaction step, where starch is degraded to fermentable sugars by enzymes or bacteria [Roehr, 2001]. Equation *EQ 1* describes a simplified sum-reaction for the degradation of starch to sugar. Depending on the conversion rate, a certain amount of the sugars present in the mash is fermented to ethanol, which is then concentrated in the distillation step. The chemical reaction during the fermentation of mash to ethanol is given by equation *EQ 2*.

$$(C_6H_{10}O_5)_n + n\,H_2O \xrightarrow{amylases} n\,C_6H_{12}O_6 \qquad \textit{EQ 1}$$

$$C_6H_{12}O_6 \rightarrow 2C_2H_5OH + 2CO_2 \qquad \textit{EQ 2}$$

The stillage coming from distillation is separated into a solid part, named wet cake, and a liquid part, termed thin stillage. The latter is treated by evaporation and the accruing syrup is fed to the dried distillers grains with soluble (DDGS) drying step, together with the wet cake from the solid-liquid-separation. The distillations top product is subjected to a dehydration

step using pressure swing adsorption (PSA). The PSA-residue is fed back to the rectifier, which results in an ethanol product with a purity of 99.6 wt%.

In order to get an idea of the Lurgi bioethanol plant's scale, the amount of produced ethanol, its byproducts and the consumed raw materials are presented in Table 2-1.

**Table 2-1: Key figures of the 100,000 t/a Lurgi bioethanol plant (large scale)**

| | | |
|---|---|---|
| **Production** | | |
| Ethanol 99.6 wt% | 12.5 t/h | 100,000 t/a |
| DDGS | 13.7 t/h | 110,000 t/a |
| **Consumption** | | |
| Wheat | 40.5 – 45 t/h | max. 360,000 t/a |
| Steam | 35 – 42 t/h | 280,000 t/a |
| Electricity | 3.6 MW | 28,800 MWh/a |
| Light Heating Oil | 1.7 t/h | 13,600 t/a |
| Fresh Water | 15 $m^3$/h | 129,000 $m^3$/a |
| **Effluents** | | |
| Waste Water | 15 $m^3$/h | 120,000 $m^3$/a |
| $CO_2$ | | max. 105,000 t/a |

Source: [**Lurgi GmbH, 2011]**

As explained in Table 2-1, for a large-scale bioethanol plant (100,000 t EtOH/a) a maximum of 360,000 tons of wheat needs to be fed into the process and 28,800 MWh of electricity are annually consumed. Even though with every kilogram of ethanol produced, about one kilogram of $CO_2$ will be released into the atmosphere, it is not a disadvantage of the process. The $CO_2$ formed in fermentation is biogenic and quite pure, which makes it capable for the utilization in other industries, like the beverage industry for example.

### 2.1.2 Second generation bioethanol

In Figure 2-3, one of the possible processes variations for the production of bioethanol based on lignocellulosic raw material is shown. In this particular case, the downstream process steps for SGBE, from distillation to the end product, are similar to the ones in the FGBE production. After fermentation the ethanol concentration is about 4 wt%. In the subsequent

distillation step it is enriched up to more than 94 wt% and afterwards dehydrated to 99.6 wt% ethanol content. Due to the low ethanol concentration after fermentation, the distillation in the SGBE production is more energy intensive than in the FGBE production. For comparison, after fermentation ethanol concentrations up to 17 wt% can be reached in the FGBE production [Jacques, Lyons and Kelsall, 2003]. The distillation stillage, whose main constituents are water and organic compounds, is fed to a solid-liquid separation step, where the liquid fraction can either be evaporated or used for biogas production.

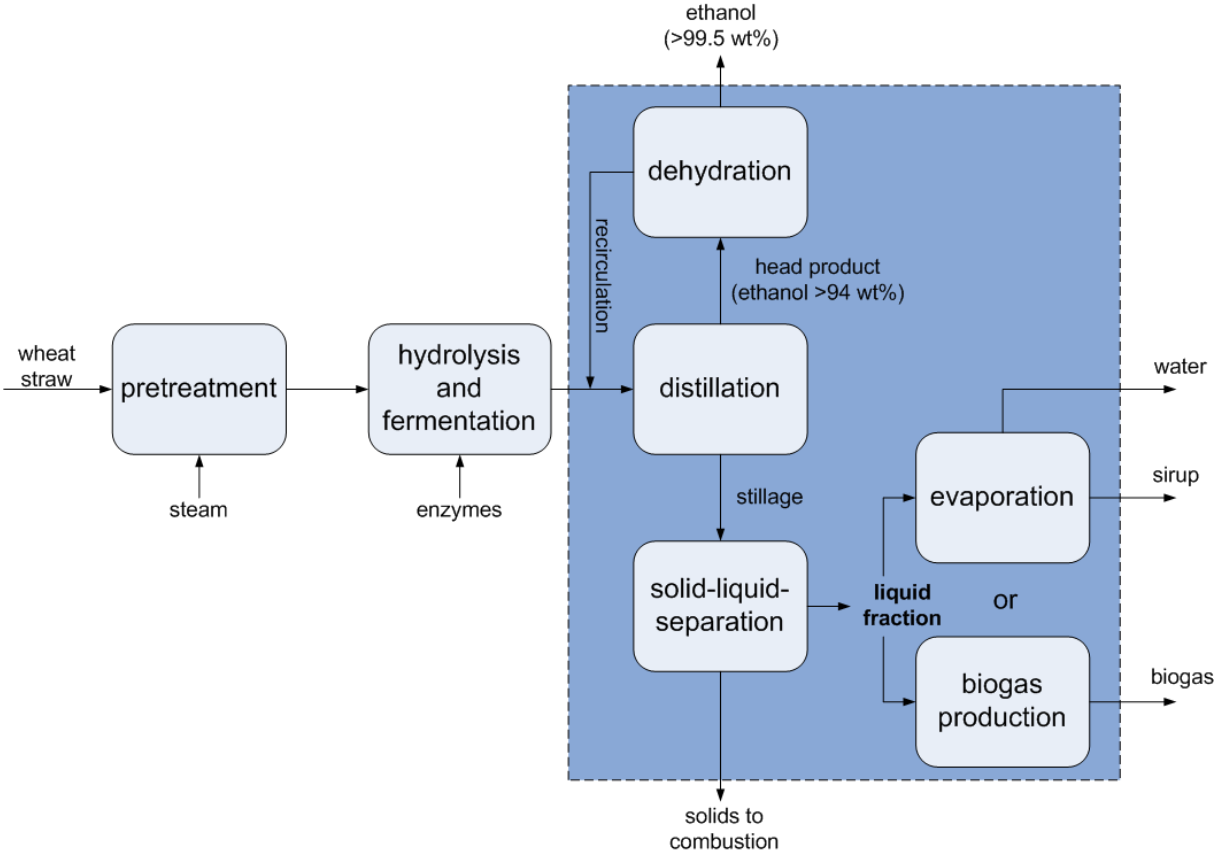


**Figure 2-3: Simplified flow sheet of the SGE process; blue framed: in this work simulated process steps**

Besides the higher energy demand of the downstream process, the main techno-economic challenges are in the pretreatment, hydrolysis and fermentation process steps. Since lignocellulosic material consists of celluloses, hemicelluloses and lignin, a better accessibility for hydrolysis has to be provided. Therefore the surface area should be increased, which can be done by milling for example. This is important for the efficiency of the de-polymerization of cellulose and hemicellulose to soluble sugars, which is done in hydrolysis [Hahn-Hägerdal,

et al., 2006]. There, the $C_5$- and $C_6$-polysaccharides are broken down to monosaccharides which can be fermented to ethanol, as equations *EQ 3* and *EQ 4* describe.

$$(C_6H_{10}O_5)_n + n\,H_2O \rightarrow n\,C_6H_{12}O_6 \qquad \textit{EQ 3}$$

$$(C_5H_8O_4)_n + n\,H_2O \rightarrow n\,C_5H_{10}O_5 \qquad \textit{EQ 4}$$

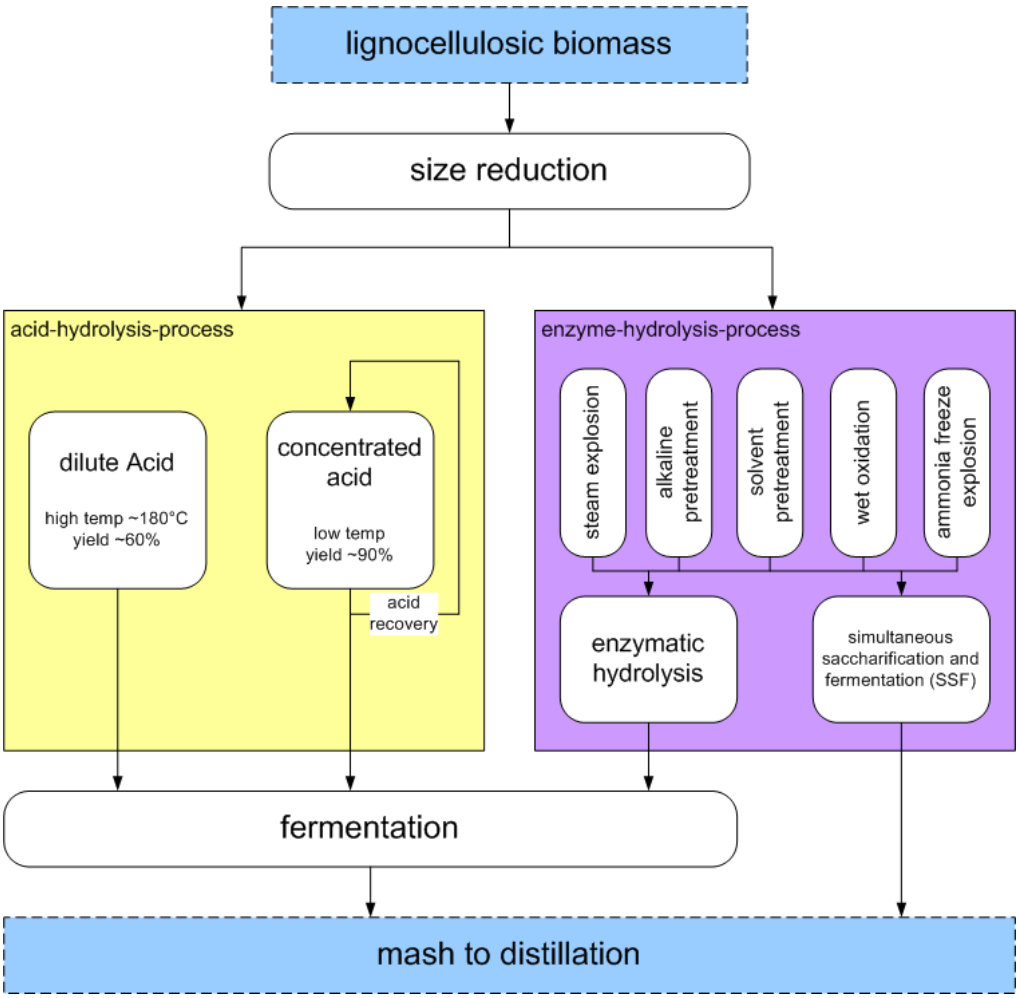


**Figure 2-4: Hydrolysis methods for lignocellulosic materials,**

**source: [Kaltschmitt, Hartmann and Hofbauer, 2009, p.809, figure 15.5]**

The main two different hydrolysis methods in the lignocellulosic ethanol process are shown in Figure 2-4 where, either enzymes or acids are used. Depending on the procedure chosen, the acids in the acid-hydrolysis-process can be diluted or concentrated. Typical acids are $H_2SO_3$,

$H_2SO_4$, HCl, HF, $H_3PO_4$, $HNO_3$ and $HCO_2H$ [Galbe and Zacchi, 2002]. In addition to the difference in acid concentration, also the operational conditions differ. The concentrated acid hydrolysis is performed at low temperature where high yields can be achieved. One of this process's drawbacks is that the high amount of acid can cause problems. In contrast, the acid consumption in the dilute acid hydrolysis is much lower, but it requires high temperatures and the yield is just 50-60% [Kaltschmitt, Hartmann and Hofbauer, 2009].

In enzymatic hydrolysis cellulose is converted to glucose by the use of enzymes and occurs at moderate temperatures. Due to the composite-like lignocellulosic structure, an additional pretreatment step is necessary to make the material accessible for enzymatic attack. Steam explosion, alkaline pretreatment, or wet oxidation are common methods for that purpose [Hahn-Hägerdal, et al., 2006]. Subsequently, enzymes are added and the polysaccharides are hydrolyzed to monomeric sugar. According to Kaltschmitt, Hartmann and Hofbauer [2009, p.811], 80-95% of the cellulose can be converted to glucose in 5-7 days at 50°C. This value refers to the separate hydrolysis and fermentation process (SHF), where hydrolysis and fermentation are performed subsequently in separate reactors. A second option is the simultaneous saccharification and fermentation process (SSF), where both process steps are executed in the same reactor. Whether in SHF or SSF, the optimum temperature for yeast is 32-37°C and the optimum activity for cellulase is at 50°C [Kaltschmitt, Hartmann and Hofbauer, 2009]. This difference in operating conditions seems to be a bit of a drawback when running the SSF. In attempt to achieve the highest values for both, saccharification and fermentation a tradeoff for enzymes and yeast is needed. Olofsson et.al. [2008] found an optimum temperature at 34°C for steam pretreated wheat straw and a specific yeast strain. The main advantages of SSF are the reduction of end-product inhibition by sugars formed in the hydrolysis, metabolization of the inhibitors from pretreatment by the microorganisms and the reduction in investment costs [Olofsson, et al., 2008]. Furthermore, it is pointed out that a yield, based on total pentoses and hexoses, higher than 70% can be reached with an ethanol concentration close to 40 g $L^{-1}$.

For fermentation, the most common organism used in first generation bioethanol production is baker's yeast (*S. cerevisiae*). Its main advantages are the stability, a high productivity and ethanol tolerance, as well as a high yield that can be reached. With baker's yeast, fructose, galactose, glucose, maltose and sucrose can be fermented [Roehr, 2001]. Unfortunately it cannot be utilized for the fermentation of $C_5$-sugars, which means that pentoses like xylose and arabinose remain unfermented in the slurry. For the production of second generation bioethanol, a $C_6$- and $C_5$-fermenting organism would be desirable, to increase the fermentation

efficiency. Actually, there are two efforts in making pentoses accessible – one, where baker's yeast is genetically modified for xylose fermentation and the other one, where naturally occurring, pentose fermentable microorganisms are modified to effectively produce ethanol [Kim, 2004, p.30; Sassner, 2007, p.23]. Standard conditions for fermentation are pH values of 3.5 to 6.0 and temperatures between 28 and 35°C. From net reaction, one can calculate that each gram of glucose can theoretically result in 0.51 g of alcohol [Roehr, 2001, p.92].

The downstream process steps, such as distillation, solid-liquid separation and evaporation will be described in detail in sections 3.1 and following.

## 2.2 By-products

Depending on the process type and the feedstock used, the amount and kind of by-products varies. Subsequently, the most common by-products in both, the first and the second generation bioethanol production, are listed:

A.) **DDG and DDGS (in case of FGBE from starch):** Dried distillers grain (DDG) consists of concentrated proteins, minerals, fat and vitamins. Dried distillers grain with solubles (DDGS) is a mixture of DDG and the bottom product in the distillation. The latter is labeled as feedstuff additive with a high quality.

B.) **Bagasse (in case of FGBE from cane):** Is gained during the pretreatment steps of the sugar cane based first generation bioethanol process. The bagasse describes the cellulose, hemicelluloses and lignin containing residue from sugar cane juice extraction. As one of the primary co-products from the sugar cane to ethanol process, it is used for combustion to supply the process with heat and electricity. It can also be utilized as feedstock for the production of enzymes, amino acids, pharmaceuticals, organic acids and animal feed on one hand [Cardona and Sanchez, 2007]. On the other hand, it is also used in the production of activated carbon.

C.) **$CO_2$:** Carbone dioxide is mainly formed during fermentation which is described by equation *EQ 2* in chapter 2.1.1. Depending on the energy supply of the process, $CO_2$ can also be formed in the combined heat and power (CHP) plant. As long as no fossil fuels are utilized for heat and electricity supply, the resulting $CO_2$ is bionic. If its purity corresponds to a certain quality, which could be reached by upgrading, the $CO_2$ can be sold to industries like the beverage industry. Otherwise, it will be released to the atmosphere.

**D.) Biogas:** Whether in first generation bioethanol production or in case of the lignocellulosic ethanol process, biogas as by-product figures big. On one hand, the proportion of organic material in the distillation stillage provides a high potential for biogas production and on the other hand, there is an already existing technology and market for it. The biogas formed during anaerobic fermentation can be directly used as a source for heat and electricity. Another option is upgrading to certain quality- respectively purity-standards, which makes it possible to feed the biogas into the gas grid.

**E.) Lignin (for material use):** Is the main component of the solid fraction after the solid-liquid-separation in the second generation bioethanol process. It can be used as raw material for several products as listed in Table 2-2.

**Table 2-2: Examples for lignin products and uses**

| Category of use | Explanation/example of application |
|---|---|
| Food & perfumes | Flavorings or scent for perfume, e.g. Vanilla (Borregaard) |
| Binder/glue | Fertilizer, plywood, dust suppressants, ceramics |
| Dispersant | Reduces binding with other substances, e.g. oil drilling muds, paints, dyes, pigments |
| Emulsifier | Mixes 2 immiscible liquids together, usually for a limited length of time, e.g. the mixing of oil and water |
| Sequestrant | Lignosulfonates can be used for cleaning compounds and for water treatments for boilers, cooling systems, micro-nutrient systems |

source: [**European Biomas Industry Association, 2008]**

**F.) Pellets:** Are the dried and pelletized solid residues after solid-liquid separation. They consist of mainly lignin and other insoluble, not fermentable organic compounds and can either be sold or used as solid fuel in the process. Depending on the bioethanol process, the fuel characteristics differ and additional treatment steps can be necessary to match the specifications on the residential pellet market [Sassner, 2007].

**G.) Electricity and Heat:** Are not direct by-products of the process, but can be generated from before mentioned by-products as pellets, biogas or the concentrate from evaporation. Simulations show, that the overall bio-ethanol process's electricity demand can easily be covered by the amount of electricity produced in the CHP plant and the excess electricity can be sold to the grid [Kravanja and Friedl, 2011]. Heat in the form of high- and low-pressure steam is generated to be utilized in the process. Latent heat from the flue gases and heat from the turbine condenser enable an advisable use in a district heating system [Sassner, 2007].

## 2.3 GHG emissions and environmental impacts

Whether in first or second generation processes, the $CO_2$ reduction potential and the accompanied mitigation of climate change promote the use of bioethanol as fuel in the transport industry. Several studies about greenhouse gas (GHG) emissions of bioethanol are published, unfortunately with widely varying results. For the most part, the results are not comparable, because the system boundaries differ. Reviews of life-cycle studies of conventional biofuels and second generation biofuels are done by Larson [2006], as well as by Eisentraut [2010].

In order to determine GHG emissions of a process and the resulting environmental impacts, the right choice of the system boundaries and key parameters is of great importance. Therefore, the emissions released by bioethanol production itself, as well as the emissions resulting from the product utilization and the supply-chain, have to be taken into account, which is shown in Figure 2-5. This assessment is also known as well-to-wheel or cradle-to-grave analysis.

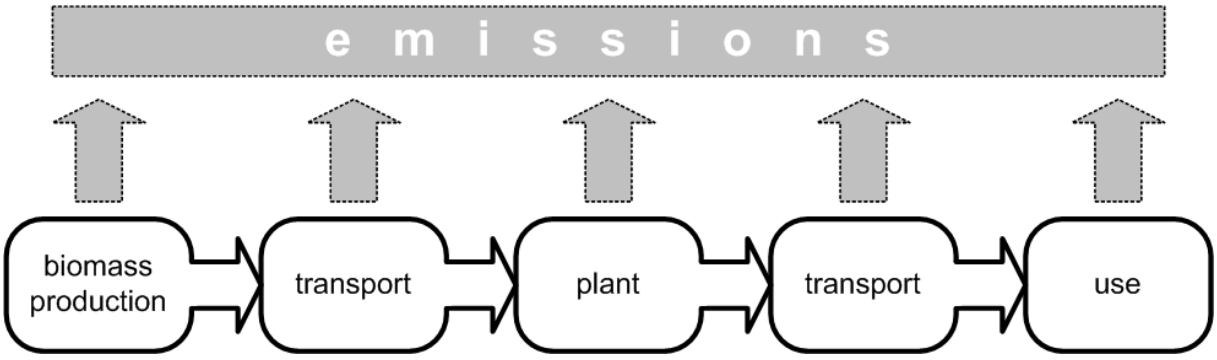


**Figure 2-5: Supply chain emissions**

Additionally to the determination of system boundaries, an evaluation of the emitted climate relevant gases $CO_2$, $CH_4$ and $N_2O$ is necessary. This is done by the introduction of the global warming potential (GWP), which is a measure of the relative radiative effect of a greenhouse gas compared to $CO_2$, integrated over a chosen time interval [Houghton, et al., 2001]. Over a period of 100 years, $CO_2$, $CH_4$, and $N_2O$ account for 1, 23 and 296 $CO_2$-equivalents, respectively [Houghton, et al., 2001]. For comparison purposes, the $CO_2$-equivalents are usually relative to per-km-driven, but sometimes they are also based on per-GJ of fuel produced or on per-ha/a.

Some aspects, that can increase the supply chain emissions dramatically, are land-use change and fertilizer replacement. The former can either be direct, which describes a change from previously uncultivated land to an area under cultivation for biomass feedstock. Or it can also be indirect, which refers to the impact that arises with increasing demand in biofuels, accompanied with increasing commodity prices or displacement of other crops [Slade, et al., 2009]. The contribution of $N_2O$ to total GHG emissions can play a major role due to its high GWP. Concerning the supply-chain, $N_2O$ emissions arise from fertilizer application and the decomposition of biomass waste spread onto the fields [Larson, 2006].

For first and second generation bioethanol, the $CO_2$ emitted during combustion of byproducts, such as lignin, does not contribute to new emissions of carbon dioxide, because the emissions are already part of the fixed carbon cycle [Fulton, et al., 2004]. But it is important to mention, that in a well-to-wheel analysis, certain differences in emissions and environmental effects between conventional bioethanol and ethanol from lignocellulosic feedstock occur.

Depending on the feedstock used, the reduction of GHG emissions in the first generation ethanol process compared to conventional gasoline varies from 13% for corn ethanol [Farrell,

et al., 2006], up to 58% for bioethanol gained from sugar beets [Fulton, et al., 2004]. Additionally to the raw material, also the form of process energy supply can limit the GHG emission reduction potential of the first generation bioethanol process. If the high energy demand for ethanol production is covered by fossil fuels, emissions are ascribed to the bioethanol. This can lead to the extent, that even more $CO_2$-equivalents will be released compared to the use of conventional petroleum [Slade, et al., 2009].

The utilization of second generation bioethanol as fuel seems to have a promising impact on the environment, because large reductions can be achieved [Farrell, et al., 2006]. Net GHG emission reductions from 70% up to 90% compared to conventional gasoline are estimated [Fulton, et al., 2004]. This is corroborated by the directive 2009/28/EC of the European parliament and of the council, where a standard value of 85% for GHG reduction in case of wheat straw is stated [Directive 2009/28/EC of the European Parliament and of the Council, 2009]. As listed in Table 2-3, Edwards, et al. [2007] compared the $CO_2$-equvalents per kilometer of petroleum with those of ethanol from straw, resulting in a ten times reduction. For this analysis, all climate-relevant gases that are associated with the supply and use are taken into account.

**Table 2-3: Comparison of petroleum and ethanol in GHG emissions (according to "Well-to-Wheel"-Analysis); source: [Edwards, 2007]**

| Fuel | Emissions (g $CO_2$-equivalents / km) | | | |
|---|---|---|---|---|
| | *$CO_2$* | *$CH_4$* | *$N_2O$* | *Sum* |
| Petroleum | 139 | 0 | 1 | 140 |
| Ethanol from straw | 14 | 1 | 1 | 16 |

In case of the bioethanol production from lignocellulosic feedstock, the lignin containing residues can be utilized to cover the process energy demand, which can boost the GHG reduction [Fulton, et al., 2004]. If the electricity is provided by a power plant, as mentioned for the first generation process, the enzymatic process is identified as the one with greater GHG emissions compared with the dilute acid process, due to the higher amount of electricity consumed during enzyme manufacturing [Slade, et al., 2009].

## 2.4 Bioethanol utilization

Originally, ethanol was produced mainly for the use in the food industry, but with approximately 13%, this industry turned into the smallest consumer over the recent years [Schmitz, 2003]. Today, the transportation sector is by far the largest customer followed by the chemical industry.

**Transportation sector:**

Compared to gasoline, a higher octane number (108), broader flammability limits, higher flame speeds and higher heats of vaporization favor the use of bioethanol as fuel [Balat and Balat, 2009]. Already in 2003 more than 60% of the bioethanol produced was utilized in the transport-industry [Schmitz, 2003]. Whether as direct blend with gasoline, as it is present in the EU-25, or as pure ethanol, the utilization possibilities in the transport industry are wide ranged.

The Brazilian market is a good example where the launch of first generation bioethanol as fuel worked well. Today there are fuels available containing 25% ethanol (E-25) and pure ethanol (E-100) which, however, requires the use of adapted engines, in so called flexi fuel vehicles (FFV). These engines can be run with both, ethanol and conventional fuel. Ethanol-free fuel is not available in the Brazilian market [Schmitz, 2006].

From a European perspective, the market for the utilization of pure bioethanol as fuel is still in its infancy. However, there is a considerable market potential for blends, because it is possible to blend up to 5 percent of ethanol with petroleum in conventional gasoline engines according to present day fuel norms [Schmitz, 2006]. Not only to promote renewable energy sources or to meet climate change commitments, the European Parliament and the Council of the European Union issued the Directive 2003/30/EC on the promotion of the use of biofuels or other renewable fuels for transport. This directive aims to annually replace 5.75% of all petrol and diesel by biofuels or other renewable fuels from 2010-12-31 on [Winter, et al, 2011]. To meet this target in Austria, at least 3.4% of the fossil petrol has to be substituted by biofuels annually. As a consequence 106,201 tons of bioethanol were sold during the year 2010 [Winter et al, 2011].

**Chemical industry:**

Besides the use as fuel, about one fifth of worlds ethanol demand is in the chemical industry, where it is used as a solvent, purifying agent, anti-freezing agent or medium for odorous substances [Schmitz, 2003]. With one-third of the overall ethanol sales in the chemical industry, its main field of application is the utilization as raw material for chemical synthesis [Schmitz, 2003].

**Food sector:**

In the food industry, bioethanol is utilized to produce spirits or acids, but the demand declines slightly and a change in this trend is not expected [Schmitz, 2003].

Besides these three main fields of application, bioethanol can also be utilized as fuel in a cogeneration unit to produce heat and electricity, but according to Schmitz [2006] this is still a small market and he assumes that the market growth is unlikely to rise.

# 3 Material & methods

## 3.1 Downstream processing in the ethanol production from lignocellulosic biomass

The scope of this work is a simulation of downstream processes for the ethanol production from lignocellulosic residue, such as wheat straw. The overall production process was modeled on the Institute of Chemical Engineering at the Technical University of Vienna using IPSEpro [Kravanja and Friedl, 2011]. The upstream process from IPSEpro-simulation provided the basis for the simulation in this work, done with ASPEN PLUS.

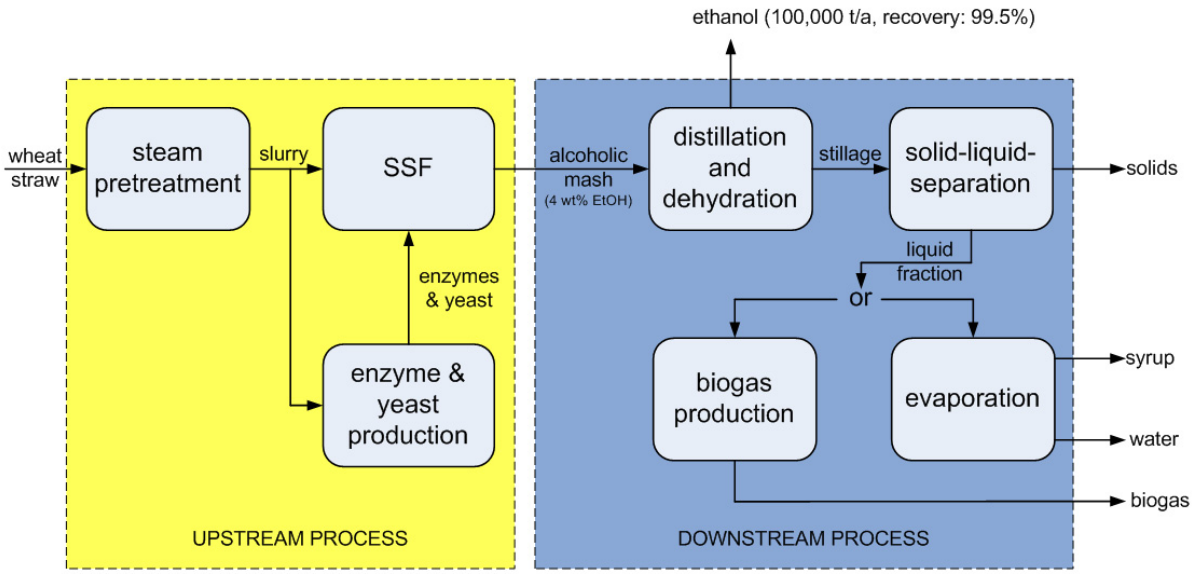


**Figure 3-1:** **Simplified flow sheet of the upstream and down stream process parts of the wheat straw to ethanol process**

As a starting situation, the process stream entering the distillation is specified, which is described in Table 3-1. Its composition and conditions emerge from the upstream process steps, where steam explosion is chosen as pretreatment method and the conversion to ethanol is performed by SSF at atmospheric pressure and a temperature of 37°C. Furthermore, it is assumed that the enzyme production is done on-site and only the $C_6$-sugars are converted to ethanol. Detailed information about the up-stream process can be obtained from Kravanja and Friedl [2011] and a simplified flow sheet of the respective process parts in upstream and downstream processing is presented in Figure 3-1. The alcoholic mash has an ethanol mass fraction of around 4 wt% and the main component of the stream is water with more than 80 wt%, as listed in Table 3-1.

**Table 3-1: Condition and composition of the process stream fed to the distillation column**

| Condition | | |
|---|---|---|
| **Pressure p [bar]** | **1.013** | |
| **Temperature T [°C]** | **37** | |
| **Composition** | | |
| **Component** | **mass flow** [kg/s] | **mass fraction** [wt%] |
| Water | 69.8 | 80.35% |
| Ethanol | 3.5 | 4.007% |
| Acetic acid | 0.6 | 0.63% |
| Furfural | 0.26 | 0.30% |
| Glycerol | 0.07 | 0.085% |
| $CO_2$ | 0.07 | 0.078% |
| Cellulose | 0.5 | 0.575% |
| Xylan | 0.24 | 0.27% |
| Lignin | 3.6 | 4.15% |
| $C_5$-monosaccharides | 4.04 | 4.66% |
| $C_6$-monosaccharides | 0.0 | 0.00% |
| Yeast | 0.5 | 0.56% |
| Enzymes | 0.16 | 0.18% |
| Ash | 1.2 | 1.385% |
| Extractives | 1.6 | 1.85% |
| Plant protein | 0.8 | 0.92% |
| SUM | 86.8 | 100% |

The water insoluble solids (WIS) fraction in the process stream has a share of more than 6% and consists of cellulose, xylan, lignin and ash.

For the subsequent downstream processes, it is specified that a production of 100,000 tons of anhydrous bioethanol per year and a bioethanol recovery of at least 99.8 % have to be maintained.

In the upcoming chapters, fundamentals and the applied lignocellulosic specific downstream processes are described. The feed is first treated in a distillation step to produce a head-product with 92.5 wt% ethanol. The residual 7.5 wt% in the head-product is mainly water, which is removed in a dehydration step by PSA. The distillation bottom residue, called stillage, contains all solids, most of the water and all other volatile compounds and is fed to a solid-liquid-separation step. Two possible applications for the liquid fraction treatment are considered in this work. First, the evaporation, which is a common process step to concentrate the liquid until a desired dry matter (DM) content on the one hand and to recycle the condensate on the other hand [Aden, et al., 2002; Wingren, et al., 2008; Sassner, 2007]. The second option is the biogas production, where the liquid stillage undergoes an anaerobic fermentation to produce a gas containing mainly $CH_4$ and $CO_2$.

## 3.2 Distillation and dehydration of lignocellulosic broths

For ethanol recovery, water and all organic compounds have to be separated from the head-product in the distillation step. In the subsequent chapters, the distillation principles and the specific designs for lignocellulosic broths are described.

### 3.2.1 Fundamentals of distillation

The distillation is a thermal separation technique to separate liquid mixtures. It utilizes the effect of different concentrations between the vaporous phase and the liquid phase of a boiling mixture if there is a difference in boiling point (or vapor pressure) of the two substances. The vaporous phase is enriched with the lower-boiling substance, whilst the higher-boiling substance remains in the liquid phase.

To strengthen this effect, a rectification column is used where the vaporous phase and the liquid phase get in contact in a counter-current mode. This causes a maximization of the driving force for mass transfer. The rising vapor enriches with the lower-boiling component

and the draining liquid is enriched with the higher boiling component. As a result, the latter is concentrated in the bottom of the column and the former is concentrated at the top of the column.

**Thermodynamic fundamentals:**

The Vapor-liquid equilibrium (VLE)

For an equilibrium state the following equations have to be the same in all phases:

$$T^l = T^v \qquad \textit{EQ 5}$$

$$p^l = p^v \qquad \textit{EQ 6}$$

$$\mu^l = \mu^v \qquad \textit{EQ 7}$$

The thermodynamic equilibrium can also be described by the fugacity of the components in the two phases:

$$f_i^{\,l} = f_i^{\,v} \quad (i = 1, \dots n) \qquad \textit{EQ 8}$$

The variables $f_i^l$ and $f_i^v$ describe the fugacity in the vapor phase and the liquid phase. The latter can be determined by using Dalton's law for real solutions:

$$f_i^{\,v} = y_i \times \varphi^v \times p \qquad \textit{EQ 9}$$

The factor $\varphi^v$ describes the difference to the ideal case.

To determine the fugacity of component *i* in the liquid phase, Raoult's law is used:

$$f_i^{\,l} = \gamma_i * x_i + f_i^{\,0} \qquad \textit{EQ 10}$$

The factor $f_i^0$ describes the fugacity at standard conditions of component *i* and $\gamma_i$ is named activity coefficient of component *i*.

For simplification, the fugacity at standard conditions $f_i^0$ can be substituted by the saturated vapor pressure $p_i^0$.

The saturated vapor pressure of component *i* can be calculated by using either the Antoine equation or the Othmer equation:

Antoine: $$log\ p_i = A_i - \frac{B_i}{C_i + T}$$ ***EQ 11***

Othmer: $$log\ p_i = m \times log\ p_{water} + C$$ ***EQ 12***

$$m = \frac{\Delta H_{v,i}}{\Delta H_{evap,w}}$$ ***EQ 13***

C = constant

The dependency of the activity coefficient on concentration, temperature and pressure is described by the excess Gibb's energy, which is the difference between the free Gibb's energy and the ideal Gibb's energy:

$$\Delta G^E = \Delta G - \Delta G^{ideal}$$ ***EQ 14***

The ideal and non-ideal parts are defined as following:

$$\Delta G^{ideal} = R \times T \times \sum(x_i \times ln\, x_i)$$ ***EQ 15***

$$\Delta G^E = R \times T \times \sum(x_i * ln\, \gamma_i)$$ ***EQ 16***

The derivate results in the Gibb's excess energy:

$$g^E = \left[\frac{\partial G^E}{\partial n_i}\right]_{T,p.n_j} = R \times T \times \ln \gamma_i$$ ***EQ 17***

For the calculation of the Gibb's excess energy, several models are available, such as Margules, Van Laar, Wilson, NRTL, UNIQUAC and UNIFAC.

**Distillation specific parameters:**

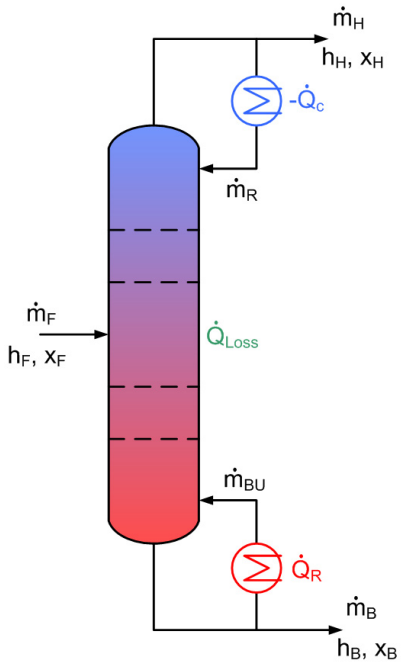


**Figure 3-2: Principle of a rectification column**

Reflux ratio:

$$RR = \frac{\dot{m}_R}{\dot{m}_H} \qquad \textit{EQ 18}$$

Is the ratio of distillate fed back to the column ($\dot{m}_R$) and the amount of head product ($\dot{m}_H$). The higher the RR, the more liquid is recirculated.

Boilup rate:

$$BR = \frac{\dot{m}_{BU}}{\dot{m}_B} \qquad \textit{EQ 19}$$

Condenser duty:

$$\dot{Q}_C = (\dot{m}_H + \dot{m}_R) \times \Delta H_{evap,H} = \dot{m}_H \times (RR + 1) \times \Delta H_{evap,H} \qquad \textit{EQ 20}$$

Reboiler duty:

$$\dot{Q}_R = \dot{Q}_C + \dot{m}_H \times h_H + \dot{m}_B \times h_B - \dot{m}_F \times h_F + \dot{Q}_{Loss} \quad \textit{EQ 21}$$

$\dot{m}_H, \dot{m}_B, \dot{m}_R, \dot{m}_{BU}, \dot{m}_F$ … mass flow of head product, bottom product, reflux, boil up and feed in kg/s

$h_F, h_H, h_B$ … specific enthalpy of the feed, the head product and the bottom product in kJ/kg

$x_F, x_H, x_B$ … mole fraction of low-boiling component in the feed, head and bottom

$\dot{Q}_c, \dot{Q}_R, \dot{Q}_{Loss}$ … condenser duty, reboiler duty and heat loss in kW

$\Delta H_{evap,H}$ … specific enthalpy of evaporation of the head product in kJ/kg

Column efficiency (CE):

The column efficiency is described by the ratio of actual trays to theoretical plates, which defines the number of stages in the distillation column block in the simulation. It depends on composition and purity of the different components.

Murphree efficiency (ME):

This efficiency can be defined for the various phases and components, and represents the ratio of achieved concentration change for the possible change in concentration at equilibrium. For the vapor phase, the Murphree efficiency of an arbitrary component is defined as follows:

$$E_{MV} = \frac{y_n - y_{n-1}}{y_n^* - y_{n-1}} \times 100 \quad \textit{EQ 22}$$

$E_{MV}$ … Murphree efficiency in %

$y_n^*$ … represents the achievable equilibrium concentration for the composition of liquid leaving tray n

$y_n$ … mole fraction of component in gas phase at stage n

$y_{n-1}$ … mole fraction of component in gas phase at stage n-1

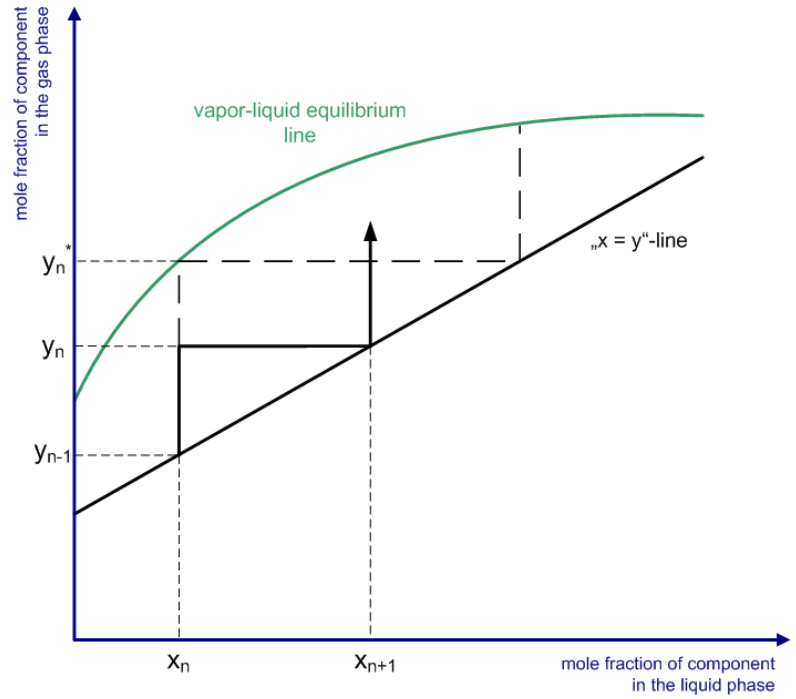


**Figure 3-3: Illustration of the Murphree efficiency in a distillation column; source: [Gmehling and Brehm, 1996]**

## 3.2.2 Distillation in lignocellulosic ethanol production

Detailed models for the distillation of lignocellulosic fermentation broth were performed by the National Renewable Energy Laboratory (NREL) and the Technical University of Lund. They differ in design and operational mode, the former is a 2-column and the latter a 3-column setup. The following chapters provide information about the two different distillation configurations.

### 3.2.2.1 The 2-column distillation

NREL modeled the complete process for the conversion of lignocellulosic feedstock to ethanol in detail [Aden, et al., 2002]. All subsequent information about the distillation of the NREL process relates to section II.5 in Aden, et al. [2002].

Figure 3-4 shows the simplified flow sheet of this distillation variant, which consists of two columns, the beer column and the rectification column. Both are operated at an overhead pressure smaller than 2 bar, whereas the number of stages, the related column efficiency and the reflux ratio differ. The beer column consists of 32 actual trays and its objective is to remove the dissolved $CO_2$ overheads and about 90% of the water through the bottom. The

alcoholic mash enters the beer column, which is operated with a reflux ratio of 3, at stage 4. A side draw at stage 8 removes a vaporized mixture with 39.4 wt% ethanol, which is then fed without condensation into the rectification column at stage 44 of 60 actual trays. There, with a reflux ration of 3.2, the ethanol is concentrated to almost azeotropic composition (92.5 wt%). To remove the remaining water, the ethanol concentrate is sent to a dehydration step realized by a delta-T molecular sieve adsorption. The regenerate of the adsorption column is recycled to the rectification column and fed at actual tray 19. After adsorption, the final ethanol product reaches a purity of 99.5 wt%. The bottom residue from the beer column is sent to a first effect evaporator and subsequent to a solid-liquid-separation step, which is described in chapter 3.3. The bottom product from rectification is sent to a water recycle.

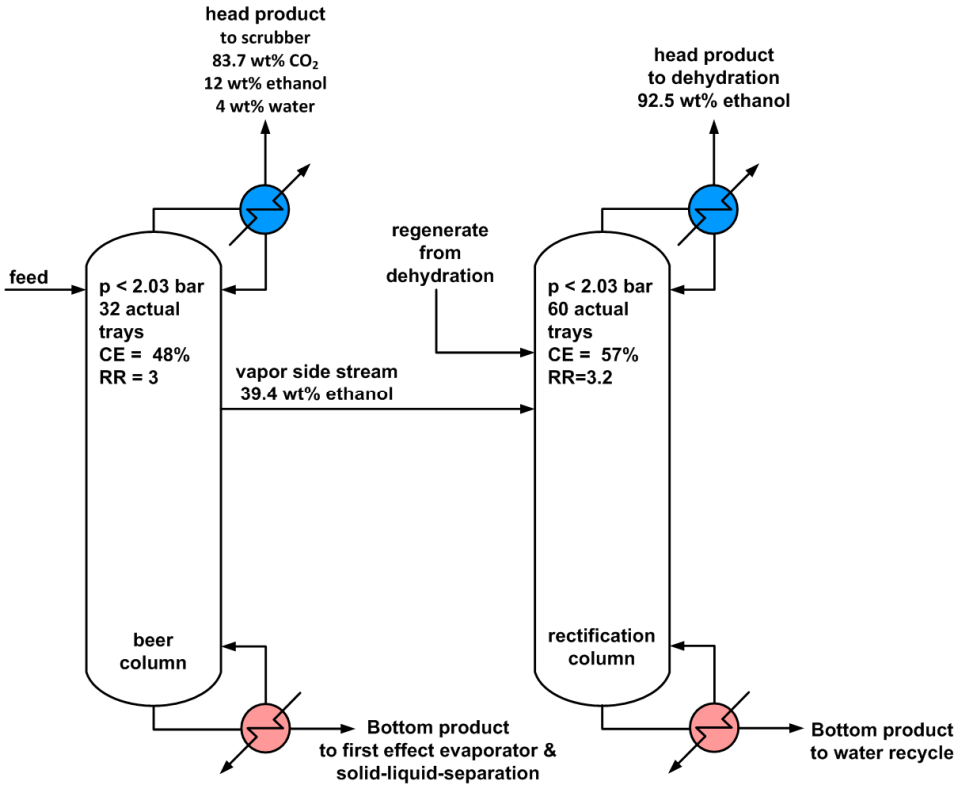


**Figure 3-4: Simplified flow sheet of the 2-column distillation configuration**

### 3.2.2.2 The 3-column distillation

This process variation was developed by the Technical University of Lund in Sweden. All subsequent information about the distillation and dehydration is taken from Sassner [2007].

The simplified process flow sheet (Figure 3-5) shows two parallel stripper columns and a rectification column that are all operated at different pressure levels. The feed is split and fed to the strippers where separation is performed at top-stage pressures of 3 bar and 1.25 bar, respectively. Both stripper columns consist of 25 actual trays, but unfortunately there is no information about the feed stages available. The resulting head products are fed to the 45 actual trays containing rectification column (top-stage pressure of 0.3 bar). The low pressure stripper column (#2) is heated by the overhead vapor from the high pressure stripper column (#1) and the overhead vapor from stripper column #2 is used as heat source for the rectification column's reboiler.

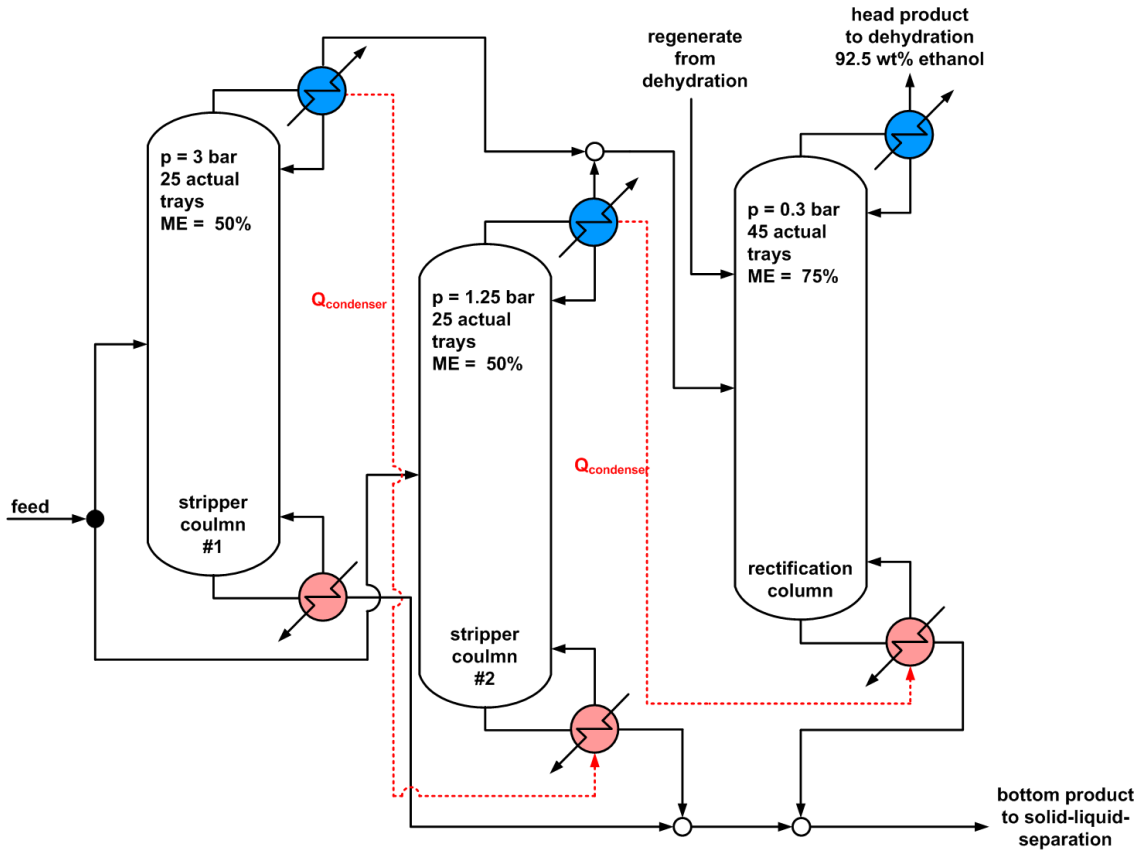


**Figure 3-5: Simplified flow sheet of the 3-column distillation configuration**

The bottom products from the stripper columns contain all the solids and a high amount of water. They are mixed with the bottom residue from the rectification column and are further processed in the solid-liquid-separation step (see chapter 3.3.). In the over-head product from the rectification column, an ethanol concentration of 92.5 wt% can be reached. For further increase, a dehydration step is necessary which is performed by pressure swing adsorption. The required product stream for regeneration of the PSA is assumed to be 20% of purified ethanol, which is returned into the rectifier. Due to this dehydration step, an ethanol purity of more than 99.8 wt% in the product can be reached. For more information about the process details see Sassner [2007, p.50 ff].

#### 3.2.2.3 Dehydration with pressure swing adsorption (PSA)

The PSA is a modern dehydration method used in all new ethanol plants [Jacques, Lyons and Kelsall, 2003]. It is a cycling batch process consisting of two molecular sieve beds used to remove the water from a vapor stream. Whilst one bed dehydrates the vapor stream, the other bed is regenerated with a small side draw from the product stream (see Figure 3-6). Contrary to the moderate pressure during regeneration, the dehydration procedure occurs at a higher pressure.

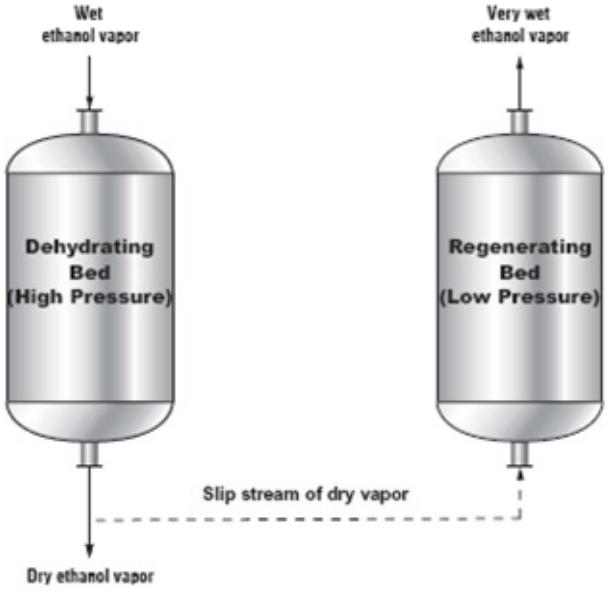


**Figure 3-6: Operation of the two bed molecular sieve dehydrator; source: [Jacues, Lyons and Kelsall, 2003, p.340]**

As adsorbent, synthetic zeolites with a pore size of 3Å (three angstroms) are used, because the water molecules with a molecule size of 2.8Å are strongly attracted into the pores while ethanol molecules with a molecule size of 4.4Å are excluded [Jacques, Lyons and Kelsall, 2003]. During the absorption of water molecules, heat is released and the bed warms up. The same amount of heat has to be supplied to regenerate the bed in order to desorb the water molecules. The net heat demand can therefore be neglected, because it is so small compared to the requirements of the distillation.

In the simulation by NREL, the PSA cycle is operated at 116°C and a pressure of 1.7 atm (1.723 bar) and designed as a conventional separator. It is assumed that 95% of the water is removed from a super heated vapor stream, together with only a small portion of ethanol, to gain a 99.5 wt% pure ethanol vapor [Aden, et al., 2002]. For comparison, the dehydration process subsequent to the 3-column distillation reaches a product with an ethanol concentration more than 99.8 wt%, whilst 20 wt% of the purified ethanol is returned into the rectifier for regenerative purposes [Sassner, 2007].

The effects of feed stream temperature change, purging time modification, feed water concentration change and the effect of the dehydrating bed to regenerating bed pressure-ratio are investigated in the work done by Simo, et al. [2008]. In that work, a PSA is modeled at 440 K (~167°C) and 379.2 kPa (~3.8 atm), and they identified a higher ethanol concentration in the product by increasing the feed temperature, extending the purging time, lowering the regeneration pressure or increasing the feed pressure. An extension of the purging duration can have a negative effect on the rectification column's separation efficiency because a higher amount of purge is recycled, which perturbs a steady operation [Simo, et al., 2008].

## 3.3 Solid-liquid-separation in the lignocellulosic ethanol production

The stillage from distillation is a mixture of liquids, soluble and insoluble solids. The latter consist of lignin, unconverted cellulose, ash, yeast and xylan. The liquid phase is mainly water and some of the organic compounds are partly dissolved in it. To produce a solid fraction with low moisture content and to ensure that most of the water can be reused in the ethanol process, a solid-liquid-separation prior to further processing steps is required [NREL, 2001]. Current technology for solid-liquid-separation includes a wide range of equipment types, like centrifuges, filter presses, belt filter presses, horizontal belt filters, Pneumapress pressure filters and extractors [NREL, 2001]. The aforementioned separator types were tested to find the best fitting variant in the ethanol process and to determine parameters for the simulation. The Pneumapress pressure filter turned out to be the best for this application among all the tested solid-liquid-separators.

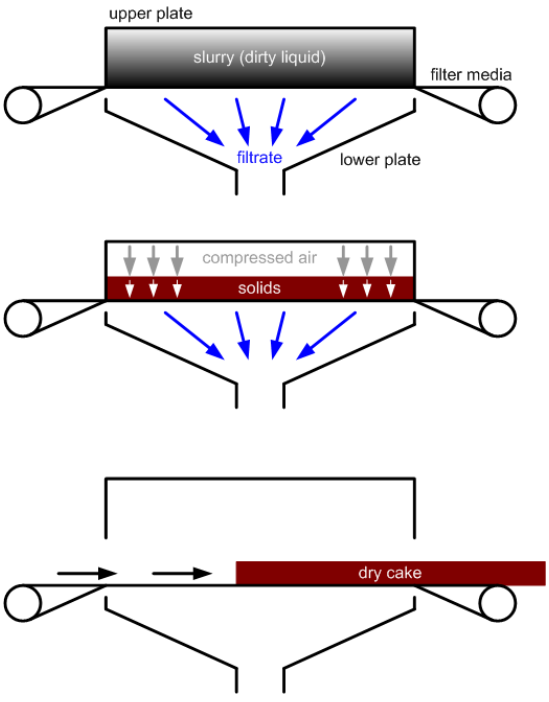


**Figure 3-7: Operating principle of a Pneumapress pressure filter; source: [NREL, 2001]**

For better understanding, the operating principle of a Pneumapress pressure filter is shown in Figure 3-7. The mixture is pumped into the filter chamber where the filter media is located.

The filtrate flows through the filter media to the lower plate. With compressed air the remaining liquid is forced trough the filter media and the solids in form of the filter cake, remain on it. The last step is the automatic discharge of the dry filter cake [NREL, 2001].

Subsequent to both distillation processes, the 2-column and the 3-column, a Pneumapress pressure filter is used. The difference is that, in the former, the distillation residue is sent to a first effect evaporator prior to the solid-liquid separation which is operated at 3.2 bar, whereas the latter foregoes this intermediate process step. Aden, et al. [2002] assumed a WIS retention of 98 wt% and in case of water and soluble solids, that are assumed to behave like the solvent, a respective portion of 10 wt% remains in the solid phase (see Table 3-2). This results into a possible cake DM up to 55%. In comparison to that, Sassner (2007) defined a WIS retention of 95 wt%, a WIS concentration in the solid residue of 40 wt% and assumed a homogeneous distribution in the liquid fraction for the water soluble components in his work.

**Table 3-2: Extract from the assumptions by NREL for each component's fraction in the solid phase on a mass basis for the solid-liquid-separation step.**

| Component | $H_2O$ | Ethanol | Soluble solids | Soluble lignin | Xylose | Glucose | Extractives | Protein | Furfural | Ash | Cellulose | Xylan | Lignin | Arabinose | Galactose | Mannose | Arabinan | Galactan | Mannan |
|---|---|---|---|---|---|---|---|---|---|---|---|---|---|---|---|---|---|---|---|
| mass fraction retaining in solid phase [wt%] | 10 | 10 | 10 | 10 | 10 | 10 | 10 | 10 | 10 | 98 | 98 | 98 | 98 | 10 | 10 | 10 | 98 | 98 | 98 |

## 3.4 Evaporation

### 3.4.1 Fundamentals of evaporation

A multistage evaporation step is one possible method to treat the liquid fraction from solid-liquid separation. Its main objective is a thermal separation of liquids to extract a solvent or obtain a concentrate [Billet, 1981]. A multistage configuration is an effective method to reduce the steam consumption compared to single stage evaporation by using the evaporated solvent from one stage as heat source for another stage at a different pressure level [Billet, 1981].

As seen in Table 3-3, increasing the number of stages results in a lower heating steam demand, which on one hand reduces the operating costs, but on the other hand increases the investment costs. The multistage evaporation system can be designed in three different variations that result from steam to concentrate's relative direction of flow. They are defined as concurrent, counter-current and co-current, where the latter is used most commonly [Billet, 1981]. In the co-current arrangement the highest pressure occurs at the first stage and is gradually decreased which results in a requirement of only one pump for the whole setup. The pressure difference is the driving force for the concentrate and the evaporated water to flow to the next stage. An aspect favoring counter-current operation is that the highly concentrated solution is evaporated at the stage with the highest temperature where the heat transfer is better compared to the co-current setup [Billet, 1981]. However, in counter-current mode, pumps for each stage are necessary, which leads to a higher failure susceptibility of the system [Billet, 1981]. In either way, the limiting factors for a multistage evaporation system are the maximum permissible heating temperature at the first stage and the last stage's lowest boiling temperature that build a total temperature difference which has to be split onto all stages [Christen, 2010].

**Table 3-3: Rule of thumb for the relative steam consumption based on the number of evaporator stages; source: [Christen, 2010]**

| Number of stages | 1 | 2 | 3 | 4 | 5 |
|---|---|---|---|---|---|
| Heating steam consumption per evaporated water on a mass basis [kg/kg] | 1.1 | 0.6 | 0.4 | 0.3 | 0.25 |

In Figure 3-8, a co-current and a counter-current setup for a 5 stage evaporation process are shown. For both configurations, the first stage is defined as the stage where primary steam enters. In the co-current setup, the feed is pumped into the first stage, at the highest pressure and highest temperature. Primary steam is provided to evaporate a certain amount of solvent which is then used as heat source for the next stage. Due to the before mentioned pressure difference ($p_1 > p_2$), the concentrate and the vapor are forced into the next stage. The vapor entering stage two evaporates a part of the solvent in the concentrate coming from stage one which is then used in stage 3. This procedure continues until stage 5 where the products, a concentrated syrup and vaporized solvent, leave the system. In contrast to that, the feed in the counter-current setup is pumped into the fifth stage, where the lowest temperature and the

lowest pressure prevail. There, a certain amount of solvent is evaporated by heat exchange between the feed and the vapor coming from stage 4. To transfer the gained concentrate to the fourth stage a pump is required, because this stage is operated at a higher pressure ($p_4 > p_5$) and higher temperature ($T_4 > T_5$). The vapor however, is forced from stage 4 to stage 5 by the before mentioned pressure difference. From here on up to the first stage, where the primary steam is fed into the system, it's the same procedure and for the five-stage counter-current evaporation system, five pumps are required in total.

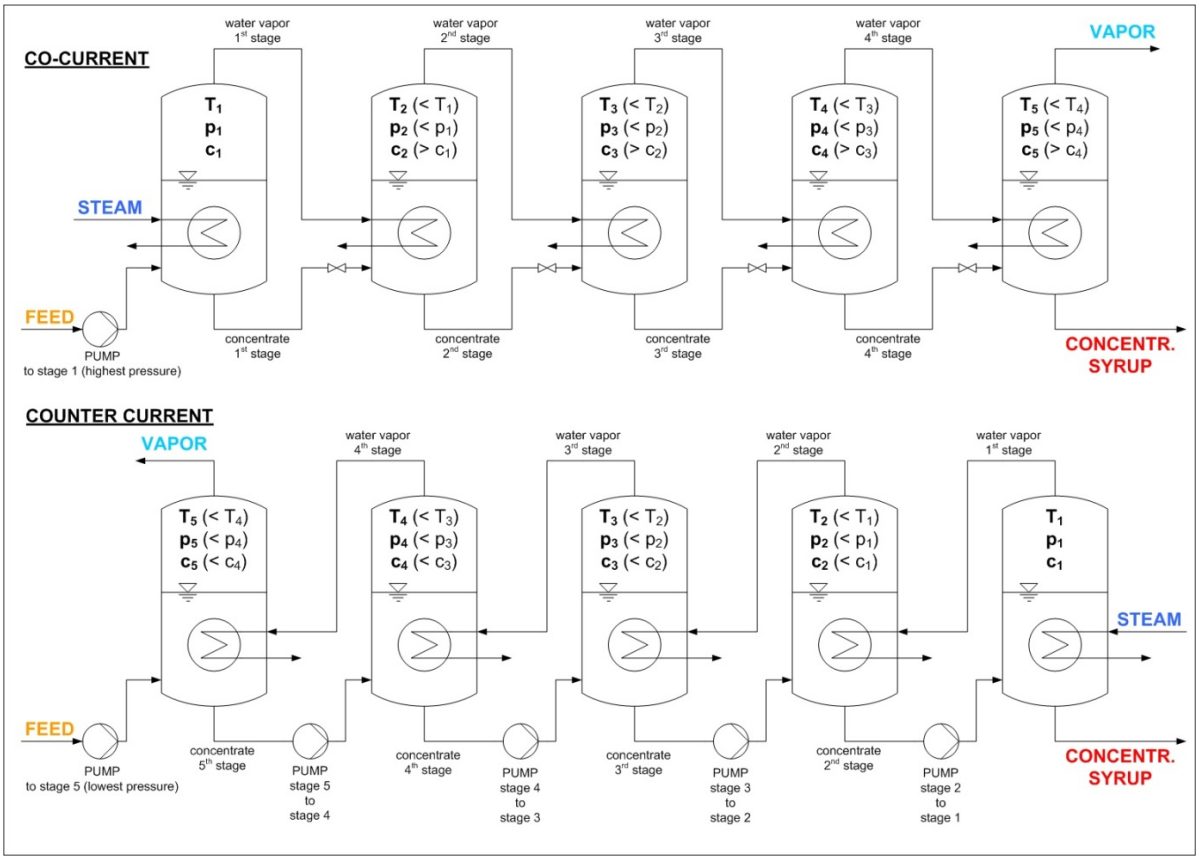


**Figure 3-8: Simplified flow sheets of 5 stage evaporation systems in a co-current and a counter current setup.**

In both setups shown in Figure 3-8, the vapor-product from the fifth stage is subsequently condensed and the resulting solvent can be reused in the process. The condensates coming from stages 1 to 5 can either be used to preheat the evaporation feed or as heat source somewhere else in the respective process. The fixed parameters in the five-stage evaporation design are the requested concentration in the syrup, primary steam conditions, the feed temperature, the pressure and boiling temperature at the first stage and the pressure and

boiling temperature at stage five. The conditions for all other stages are dependent on these parameters.

Other key factors, when designing an evaporation system for a solution, are the elevation of the boiling point and the crystallization of dissolved substances, which have to be taken into account. The latter has a huge influence on the evaporation efficiency, because crystals on the heat exchanger walls diminish the heat transfer on each stage. Furthermore, depending on the solution used, from fouling up to total blockage of the pipes may occur. The elevation of the boiling point depends on the amount of solved substances and therefore rises with concentration increase [Christen, 2010, p.372 ff].

### 3.4.2 Evaporation in lignocellulosic ethanol production

There are some differences in the process setups for evaporation described in literature [Aden, et al., 2002; Sassner, 2007]. As mentioned before, NREL positioned the first effect evaporator, which consists of two evaporation units, before the solid-liquid separation. There 24 wt% of the water entering the first stage is evaporated and the slurry is fed to the solid-liquid separation. The liquid residue enters the second effect evaporator, a single unit that removes 44 % of the entering water from concentrate. The subsequent two units form the third effect that evaporates 76 wt% of the remaining water. In total 17 wt% of the stillage end up as recycle water in the process, 10.5 wt% are in the syrup (40% DM), 61 wt% are evaporated and 11.5 wt% remain as wet cake in the pressure filter. The syrup is then sent to combustion for disposal. In all five evaporators, the ability to condense the evaporator vapor with cooling at 64°C must be secured.

The multi-stage evaporation system subsequent to the 3-column distillation, which was designed at the Technical University of Lund, uses five stages in a co-current arrangement to achieve a DM content of 60 wt% [Sassner, 2007]. Steam at a low pressure is used to heat the first stage and a pressure of 0.2 bar is set in the fifth evaporation stage. The pressure distribution over all stages is chosen so that all evaporators have the same size and the changes in heat transfer coefficient, depending on the DM content, are considered as well.

## 3.5 Biogas production

The evaporation of the liquid residue from solid-liquid separation is a process step that consumes a lot of energy. The needed steam has a high energy density (as a result of the high enthalpy of evaporation) and its only objective is to produce water vapor and syrup. A less energy consuming alternative to obtain another product would result in a better overall efficiency of the process and this is why the production of biogas draws a lot of attention.

### 3.5.1 Fundamentals of biogas-production

The biogas production is an anaerobic digestion step, which is often followed by water treatment that occurs under aerobic conditions. The former consists of four different reaction steps [Scharf, 2007; Kaltschmitt, Hartmann and Hofbauer, 2009, p.853 ff], which are shown in Figure 3-9, including the most important intermediate products formed on each step:

1. **Hydrolysis:** The carbohydrates, fats and proteins are broken down by hydrolytic bacteria into simple organic components as sugars, amino acids and fatty acids.
2. **Fermentation (or Acidogenesis, formation of acid):** The simple organic components are now accessible for fermentative bacteria, yeasts or enzymes, which convert them to hydrogen, acetic acid, carbon dioxide, alcohols and fatty acids. Hydrogen and acetic acid can be directly converted in step four, Carbone dioxide is already an end product, although some part of it will be further converted in the methanogenesis.
3. **Acetogenesis (building of acetate):** Alcohols and fatty acids are converted by acetogenic bacteria into hydrogen, acetic acid and carbon dioxide.
4. **Methanogenesis (building of methane):** The methanogenic bacteria convert the products from the previous steps into methane, carbon dioxide and water. The bacteria is really sensitive according to the pH-value, which has to be in the range of 7 [Onken and Behr, 1996]. In the methanogenesis, about 70% of the methane is produced by splitting acetic acid to carbon dioxide and methane (EQ 23). The remaining 30% result from chemical bonding of hydrogen with carbon dioxide (EQ 24).

$$CH_3COOH \rightarrow CH_4 + CO_2 \qquad \textit{EQ 23}$$

$$CO_2 + 4\,H_2 \rightarrow CH_4 + H_2O \qquad \textit{EQ 24}$$

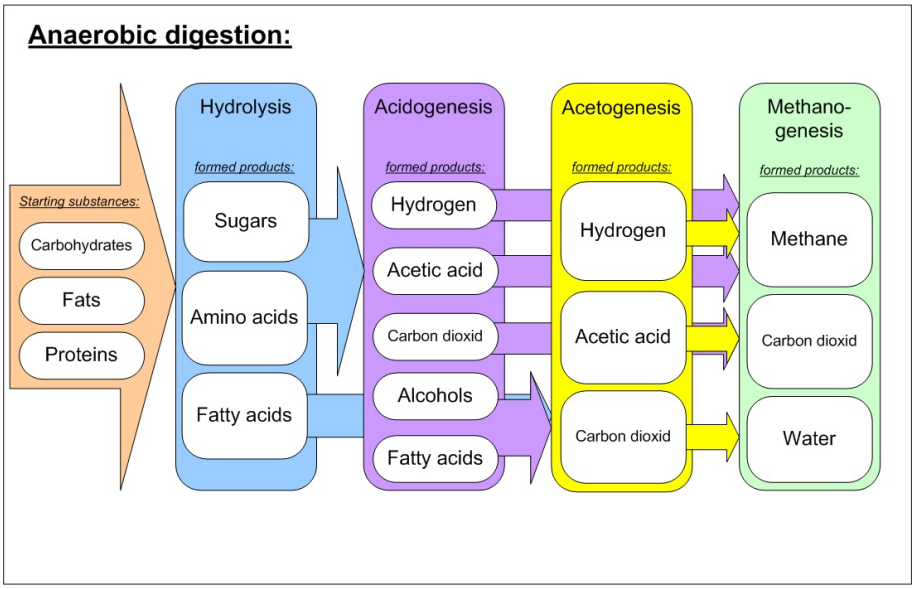


**Figure 3-9: Description of the four process steps that occur during anaerobic digestion**

The total degradation velocity is affected by the weakest link in the chain of the process, which is then the limiting factor for it [Bischofsberger, et al., 2009]. This again is influenced by the composition of the stream, where in case of streams with a high amount of solids, the hydrolysis and in case of mainly desolved organic compounds, the acetogenesis and the methanogenesis are the limiting factors [Bischofsberger, et al., 2009].

Another approach for the calculation of the possible methane yield is the empirical equation *EQ 25* for the reactions that occur in the methane fermentation [Buswell and Mueller, 1952]:

$$C_nH_aO_b + \left(n - \frac{a}{4} - \frac{b}{2}\right)H_2O \rightarrow \left(\frac{n}{2} + \frac{a}{8} - \frac{b}{4}\right)CH_4 + \left(\frac{n}{2} - \frac{a}{8} + \frac{b}{4}\right)CO_2 \qquad \textit{EQ 25}$$

## Conditions for anaerobic digestion:

As the term "anaerobic" implies, the fermentation takes place in the absence of oxygen. Some of the bacteria immediately die when they get in contact with oxygen, but the fact that they live together with facultative anaerobic bacteria from previous fermentative steps ensures some kind of resistance [Kaltschmitt, Hartmann and Hofbauer, 2009]. To establish a basis, where a high methane yield can be reached, the following conditions have to be created.

**Temperature**

The ideal temperature depends on the bacteria used in the anaerobic digestion, which prefer either mesophilic or thermophilic conditions. The former is in the range of 35 – 43 °C, whereas thermophilic bacteria require a temperature within 57 - 60 °C [Hutnan, et al., 2003; Kaltschmitt, Hartmann and Hofbauer, 2009]. Under thermophilic conditions a higher acidification rate, due to higher metabolism activity of the bacteria at higher temperature, can be reached and undesired pathogenic micro-organisms are destroyed [Bischofsberger, et al., 2009]. In Kaltschmitt's [2009] comparison of the advantages of mesophilic and thermophilic conditions for digestion, higher growing rates, shorter retention times and reduction of sludge are the main advantages of thermophilic conditions. On the other hand, less $CO_2$ and water vapor content in the biogas, a better energy balance and a wide range of organisms speak in a mesophilic conditions favor.

**pH-value**

Onken and Behr [1996] mention a pH-value for the anaerobic digestion around 7, because methanogenic bacteria require it. Furthermore, higher yields can be reached by process control (recirculation and retention of the sludge), which demands a stable composition of the waste water. As the pH-value alters during anaerobic digestion, the optimum conditions are in the range of 6.8 to 7.5 [Bischofsberger, et al., 2009]. Bischofsberger et al. [2009] suggest a pH-regulation unit before the digester in case of an alkaline or acid feed. If an adjustment of the pH-value is necessary, NaOH can be added for example [Uellendahl and Ahring, 2010].

For better understanding of the following sections, some terms have to be explained:

**VS** – volatile solids: Describes the residual material when water and the inorganic substances are extracted from the mixture. VS are the solids that have an actual availability for bioconversion [Bioconverter, 2011; Kaltschmitt, Hartmann and Hofbauer, 2009].

**HRT** – hydraulic retention time: Is defined as the ratio of the digester volume and the daily volume flow fed into the reactor. The HRT gives information about the average time a substrate remains in the digester. In equation *EQ 26*, this definition is illustrated. The HRT

has to be selected in such a way, that during constant exchange of the reactor content it is secured that not more bacteria is flushed out of it, than growing in it [Kaltschmitt, Hartmann and Hofbauer, 2009].

$$HRT = \frac{V_R}{\dot{V}_S} \qquad \textit{EQ 26}$$

$HRT$ … hydraulic retention time in d

$\dot{V}_S$ … amount of substrate fed to the digester in l/d

$V_R$ … reactor volume in l

Table 3-4 shows typical hydraulic retention times of the different digester types, whereby a wide range, starting from just a few hours up to more than 50 days, is possible.

**Table 3-4: Typical loading rates for fermentation processes (known variations in specific practical applications are given in brackets); source: [Kaltschmitt, Hartmann and Hofbauer 2009, p.872, table 16.2]**

| fermentation procedure | OLR [kg-VS/(m³*d)] | HRT [d] |
|---|---|---|
| stirred tank reactor | 2 - 4 (10) | (5) 10 - 40 (>50) |
| plug flow fermentor | 5 - 15 (20) | 10 - 40 |
| contact process | 5 - 15 | 3 - 10 |
| UASB | 5 - 15 | 0.2 - 1 (5) |
| anaerobic filter | 5 - 15 (20) | 0.5 - 8 |
| fluidized bed reactor | up to 40 | ≤ 0,15 |

**OLR** – organic loading rate: Is defined as the quotient of the organic volatile solids fed to the reactor and the effectively usable reactor volume. The OLR is often used as parameter for the system design and represents a measure for the organic material load in the reactor. Its unit is usually mass of volatile solids per digester volume and time (kg-VS/[m³*d]), but mass of chemical oxygen demand per digester volume and time (g-COD/[l*d]) is also common [Bioconverter, 2011; Kaltschmitt, Hartmann and Hofbauer, 2009].

The calculation of the OLR can be done by using equation *EQ 27*, where the load of organic dry matter $\dot{F}$ is divided by the reactor volume $V_R$ [Fachagentur Nachwachsende Rohstoffe e.V., 2006; Kaltschmitt, Hartmann and Hofbauer, 2009].

$$OLR = \frac{\dot{F}}{V_R} = \frac{\dot{m}_S \times c_S}{V_R} \qquad \textit{EQ 27}$$

$OLR$ … organic loading rate in kg-VS/(l*d)

$\dot{F}$ … load of volatile solids (VS) in kg/d

$\dot{m}_S$ … amount of substrate fed to the digester per unit of time in kg/d

$c_S$ … concentration of organic substances in %

$V_R$ … reactor volume in l

The OLR depends on the reactor type used for the fermentation process. In Table 3-4 typical loading rates for different fermentation concepts are given. It can be seen, that the OLR ranges from 2 kg-VS/(m³*d) up to 40 kg-VS/(m³*d), depending on the substrate and reactor type chosen.

With increasing organic loading rate, more substrate is fed to the digester which reduces the hydraulic retention time [Fachagentur Nachwachsende Rohstoffe e.V., 2006].

**COD** - chemical oxygen demand: Is defined as the amount of oxygen that is necessary to oxidize all soluble organic components in a stream to carbon dioxide, water and nitrous oxide [Aden, et al., 2002; Kaltschmitt, Hartmann and Hofbauer, 2009]. The COD is an estimate for the quantity of organic material in a stream, provides information about its methane potential and has the unit of a concentration. The theoretical maximum methane yield per amount of COD degraded can be calculated as following:

Since the methane yield results from the COD degraded in the process, at a prevailing anaerobic environment, the COD in the biogas is equal to the one in the process. We can proceed from the fact that methane represents the oxidable part in the biogas and equation

*EQ 28* shows that 2 moles of $O_2$ are necessary to totally oxidize 1 mole of $CH_4$. At standard conditions (0°C, 1.013 bar) 1 mol $CH_4$ equals 22.4 $l_N$ and 2 moles of $O_2$ equal 64 g $O_2$, where the latter is also defined as the COD. This results into a maximum methane yield of 0.35 $l_N$ $CH_4$ / g COD.

$$CH_4 + 2\,O_2 \rightarrow CO_2 + 2\,H_2O \qquad \textit{EQ 28}$$

**BOD** – biological oxygen demand: Describes the quantity of oxygen required for oxidation of biodegradable organic matter present in a water sample [Ramalho, 1977]. It is smaller than the respective COD, because it cannot be directly related to the composition and can therefore be assumed as 70% of the COD [Aden, et al., 2002].

**C:N:P-ratio, COD:N:P:S-ratio -** The bacteria's demand in phosphor and nitrogen is mainly dependent on the yield and the age of the sludge in the system. Kaltschmitt, Hartmann and Hofbauer [2009] indicate a C:N:P-ratio in the digester of 100-200:4:1 to obtain an unproblematic digestion. Bischofsberger, et al. [2009, p.78] on the other hand, mention a dependency of the ratio on the acidity of the feed, where acid effluents force a COD:N:P-ratio of 1000:5:1 compared to 350:5:1 for a less acidic feed, which implies that less acidic feed requires a higher amount of nutrients than acidic feed. The amount of sulfur in the digester also influences the methane yield. Therefore, Fachagentur Nachwachsende Rohstoffe e.V. [2006] indicates a C:N:P:S-ratio of 600:15:5:1, which is somewhat different to the COD:N:P:S-ratio of 300-800:5-7:1:1 by Bischofsberger, et al. [2009]. In order to obtain the right nitrogen and phosphor levels, $NH_3$ and $H_3PO_4$ are common substances for addition [Barta, Reczey and Zacchi, 2010]. Also urea, $(NH_2)_2CO_2$, is a possibility when a nitrogen increase is necessary [Bischofsberger, et al., 2009].

### 3.5.2 Biogas from lignocellulosic fermentation residues

Once the composition and the quantity of the substrate are known, the parameters for the design of an anaerobic digester have to be obtained. The COD provides information about the methane yield that is theoretically possible, which is important for the verification of the process's potential. Of course, not all organic compounds will be transformed to biogas and therefore information about the degradability of the compounds present in the stillage is necessary and has to be taken into account.

In the work of Barta, Reczey and Zacchi [2010], where the stillage of a spruce-to-ethanol process is considered for biogas generation, the degradation factors during anaerobic digestion are assumed as follows: 90% of soluble sugars, organic acids, ethanol, glycerol, enzyme and yeast are converted, 50% of all polysaccharides, extractives, degradation products and water-soluble lignin are degraded but none of the water-insoluble lignin. To ensure the appropriate levels of nitrogen (18 $g_N$/kg-COD) and phosphor (4 $g_P$/kg-COD) solutions of $NH_3$ (25%) and $H_3PO_4$ (50%) have to be added [Barta, Reczey and Zacchi, 2010]. The assumption for the organic loading rate applied to the digester is 10 kg-COD/($m^3$*day). With the assumed theoretically maximum methane yield of 0.35 $Nm^3$/kg COD removed, the production of a biogas with 50 wt% $CH_4$, 46 wt% $CO_2$ and 4 wt% $H_2O$ is assumed [Barta, Reczey and Zacchi, 2010]. The investigation of different process configurations led to results for the HRT varying between 6.2 and 9.9 days. Wingren, et al. [2008] also assume a methane yield of 0.35 $Nm^3$/kg COD consumed with 50% of the COD removed in the anaerobic digestion step and with a residence time of 20 days. Nitrogen and phosphor have to be added in this calculation as well.

In the waste water treatment process described by Aden, et al. [2002], the conversion of each organic compound to methane and carbon dioxide is set with 90%. Furthermore, a maximum methane yield of 350 l/kg-COD removed, a $CH_4$:$CO_2$ molar ratio of 3:1, a 93% removal of COD and a total conversion of sulfates to hydrogen sulfide is assumed. The digesters applied in simulation are sized for a loading rate of 12 kg-COD/($m^3$*day) and nutrients in the magnitude of 37 g/kg-COD are added [Aden, et al., 2002].

The assumptions for the degradation factors can have a huge impact on the biogas yield obtainable. On one hand a maximum gas yield and a complete degradation of the organic matter (accessible for degradation) contained in the substrate is desirable, but this is partly in contradiction with the economic targets, due to long retention times and large reactor sizes on the other hand. Therefore, a tradeoff between the degree of degradation and the economic effort has to be found.

### Experimental values for comparison

Torry-Smith, et al. [2003], for example, reached a methane yield of 529 ml-$CH_4$/g-VS, based on a substrate obtained from wet oxidized wheat straw with a COD of 27.3 g/l, an OLR of 14 g-COD/(l*d), an overall degradation factor of 84% and within a HRT of 48h.

In the work done by Uellendahl and Ahring [2010], where results for the biogas production from fermentation effluent are obtained, an UASB reactor in a pilot-scale under mesophilic conditions is used. For an OLR of 3.5 kg-VS/(m³*d), which equals 7.7 kg-COD/(m³*d) with a reduction of dissolved VS between 68% and 77%, a methane yield of 270 ml-$CH_4$/g-VS can be obtained. They also found an optimum OLR of 13.6 kg-COD/(m³*d) resulting in 700 ml-$CH_4$/g-VS. To reach these results, a hydraulic retention time of several days is necessary. These and some more experimental results are listed in Table 3-5.

**Table 3-5: Specific data from literature for the anaerobic digestion**

| raw material | reactor type | COD/ VS ratio | COD [g/l] | OLR [kg-COD /(m³*d)] | COD rem. [wt%] | HRT [d] | Source |
|---|---|---|---|---|---|---|---|
| wheat straw | n.a. | n.a | 134.9 | | 83 | 30 | [Maas, et al., 2008] |
| spruce chips | Cont. stirred tank reactor | n.a | n.a | 10 | 60% | 6,2 - 9,9 | [Barta, Reczey and Zacchi, 2010]* |
| pig manure + 25 w-% wheat straw | UASB reactor | n.a | n.a | 17.1 | 76 | 6 | [Kaparaju, et al., 2010] |
| wheat straw | UASB reactor - thermophilic cond. (53°C) | 2.2 | n.a | 6,8 | 68 - 77 | n.a | [Uellendahl and Ahring, 2010] |
| | UASB reactor - mesophilic cond. (38°C) | | n.a | 13.6 | 68 - 77 | n.a | |
| wet oxidized wheat straw | n.d. | 1.44 | 27.3 | 14 | 84 | 2 | [Torry-Smith, et al., 2003] |
| Eucalyptus | Upflow fixed film | n.a. | 22.5 | 10.7 | 86.6 | 2.1 | [Wilkie, et al., 2000] |
| | Upflow fixed film | | 22.5 | 10 | 84.4 | 2.25 | |
| | Cont. Stirred tank reactor | | 22.5 | 2.4 | 85.5 | 9.5 | |
| *Pinus radiata* | Cont. Stirred tank reactor | | 25.5 | 4 | 92 | 6.4 | |
| | UASB reactor | | 25.5 | 16 | 86 | 1.6 | |
| | UASB reactor | | 27.5 | 13.8 | 82 | 2 | |

* modeling assumptions

**Conditions for anaerobic digestion**

With an HRT of a certain amount of days set and a given amount of substrate fed to the digester, the reactor volume will increase and therefore reach a size that could not be realizable. From an economic point of view, it would be an asset to reach the highest possible methane yield at a short HRT.

Another important parameter that effects the degradation of the organic compounds is the degree of mixing in the digester. Due to the fact that a continuous process is aspired, the substrate's contact with the bacteria has to be as high as possible, during its time in the digester. The higher density of the bacteria, compared with the substrate, causes them sinking to the bottom of the digester, whereby two layers evolve – a bacteria layer and a substrate layer. This entails a contact between substrate and bacteria limited to the boundary layer. Mixing, however, increases the contact area, which results in a better degree of degradation.

**Biogas use**

In general, three possibilities for the use of biogas stand out. First of all, biogas can be used for the generation of heat and electricity in a CHP plant. Furthermore, co-firing with residues from the bioethanol process is also a possibility. And as a third possibility – upgrading, which is described subsequently.

Biogas upgrading:

The produced biogas should reach a certain quality to be interesting for upgrading or selling as a by-product. Specifications about the composition vary depending on the different directives, but as an indicator three different gas composition examples are given in Table 3-6. First of all, a biogas generated from agricultural co-fermentation plants, with a $CH_4$-content between 50 and 60 vol% is listed. Compared to that, the characteristics of a natural gas are shown and third, the demands from the ÖVGW directive G. Depending on the biogas purpose, a process step to upgrade the biogas could be necessary. But before upgrading, a cleaning step is required, because the produced biogas can also contain water, hydrogen sulfide, oxygen, siloxanes, ammonia and also some particles [Petersson, 2009]. To remove the water from the biogas, common cleaning steps are absorption (in glycol solutions), adsorption (with molecular, activated carbon or $SiO_2$), cooling or compression. For the removal of hydrogen sulfide, the adsorption on activated carbon with a defined pore size, the chemical absorption

with sodium hydroxide (NaOH) washing or $CO_2$ washing and the biological treatment by oxidation with microorganisms are appropriate separation methods [Petersson, 2009]. Besides the already mentioned adsorption with activated carbon or molecular sieves, membrane technologies can also be utilized for upgrading. To separate particles from the raw biogas, mechanical filters are often used.

**Table 3-6: Comparison of gas composition and important technical values for raw biogas, natural gas and the demands of the 31st ÖVGW Richtlinie G; source: [Bergmair, 2006]**

| | [unit] | raw biogas[a] (dry) | natural gas[b] | ÖVGW G 31 |
|---|---|---|---|---|
| **Composition:** | | | | |
| $C_xH_y$ | [vol% (dry)] | - | 0.4 | n.i. |
| $CH_4$ | [vol% (dry)] | 50 - 66 | 99 | n.i.. |
| $CO_2$ | [vol% (dry)] | 29 - 43 | 0.1 | < 2 |
| $H_2$ | [vol% (dry)] | - | - | < 4 |
| $N_2$ | [vol% (dry)] | 0.3 - 20 | 0.4 | < 5 |
| $O_2$ | [vol% (dry)] | 0.1 - 6.3 | - | < 0.5 |
| $H_2S$ | [mg/m³$_N$(dry)] | 17 - 2470 | - | < 5 |
| R-SH | [mg S/m³$_N$(dry)] | 0 - 90 | - | < 6 |
| $NH_3$ | [mg/m³$_N$(dry)] | 0.6 - 50 | - | 0 |
| siloxanes | [mg/m³$_N$(dry)] | 0 0.9 | - | 0 |
| **combustion characteristics:** | | | | |
| Wobbe-Index | [MJ/m³$_N$(dry)] | 22.7 - 33.3 | 52.9 | 47.7 - 56.5 |
| | [kWh/m³$_N$(dry)] | 6.3 - 9.3 | 14.7 | 13.3 - 15.7 |
| calorific value | [MJ/m³$_N$(dry)] | 22 - 28 | 39.6 | 38.5 - 46 |
| | [kWh/m³$_N$(dry)] | 6.1 - 7.8 | 11 | 10.7 - 12.8 |
| rel. density | - | 0.84 - 0.97 | 0.56 | 0.55 - 0.65 |

[a] Profactor Produktionsforschungs GmbH, biogas analysis of agricultural co-fermentation plants and sewage treatment plants in Upper Austria and Slovakia in 2002

[b] Analyse Salzburg AG, Österreich, January 2003

Once the biogas is cleaned, the energy density can be increased by the removal of carbon dioxide from the gas, which is also known as upgrading. A common procedure, in connection with ethanol dehydration already mentioned, is the PSA. The carbon dioxide is adsorbed under elevated pressure on zeolites or activated carbon. The presence of hydrogen sulfide or water can cause problems, the former will be irreversibly adsorbed and the latter can destroy

the structure of the adsorbent. As an alternative to the PSA, absorption methods like water scrubbing, organic physical scrubbing or chemical scrubbing are used, whereby the first mentioned is the most common technique for upgrading [Petersson, 2009]. Water scrubbing exploits the higher solubility of $CO_2$ in water compared to methane and organic physical scrubbing used the absorption affinity of $CO_2$ in an organic solvent (polyethylene or amines for example). In the chemical scrubbing procedure a chemical reaction takes place between the carbon dioxide and the amine that is present in the scrubbing solution. Common amine solutions are mono ethanol amine (MEA) and di-methyl ethanol amine (DMEA). In all three scrubbing methods, the absorption solution has to be regenerated to ensure a continuous operation of the upgrading process.

## 3.6 Fundamentals of Pinch Analysis

Pinch Analysis provides information about the potential for heat integration of a system. All streams in the system are separated either in cold or hot streams. Cold streams are heated up, whilst hot streams are used as heat source and therefore cooled down. For analysis, all hot and cold streams are plotted in a temperature-enthalpy diagram. The hot streams represent the hot composite curve (HCC) and the cold streams the cold composite curve (CCC). For more details about the construction of the composite curves see Linhoff March [1998]. The heat exchange between a hot and a cold stream only works, if the hot stream is hotter than the cold stream at any point [Smith, 2005]. This can be seen Figure 3-10, where $\Delta T_{min}$ is the minimum temperature difference between the hot and the cold stream. By changing $\Delta T_{min}$, the minimum hot utility ($Q_{Hmin}$) and the minimum cold utility ($Q_{Cmin}$) change, which in turn has an impact on the amount of heat recovered ($Q_{REC}$).

An aspect that limits $\Delta T_{min}$ downwards is its dependency on the heat transfer at that point in the process, because the smaller the $\Delta T_{min}$, the larger the required heat transfer area must be [Smith, 2005, p.361].

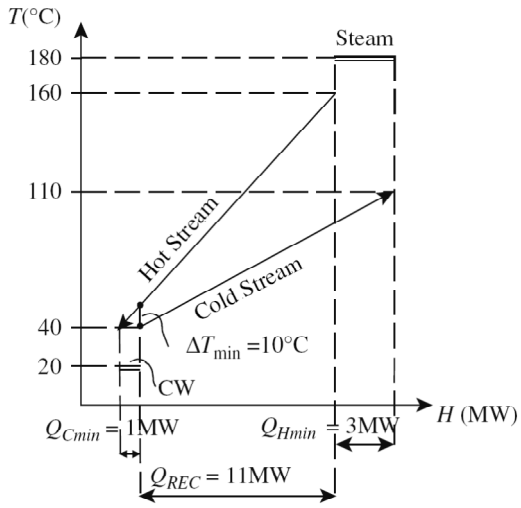


**Figure 3-10:** **Example for a heat recovery problem consisting of one hot stream and one cold stream; source: [Smith, 2005]**

The Pinch Analysis provides information about the heating requirements, the cooling requirements and the integrated heat in the considered system. Therefore, the transferred heat needs to be calculated, which can be done by using equation *EQ 29*, but it is also provided as data from the simulation in ASPEN PLUS using the adiabatic energy balance of the unit.

$$\dot{Q} = \dot{m}_{es} \times h_{es} + \dot{m}_L \times h_L - \dot{m}_F \times h_F \qquad \textit{EQ 29}$$

$\dot{Q}$ … transferred heat in kW

$\dot{m}_{es}, \dot{m}_L, \dot{m}_F$ … mass flow of evaporated solvent, concentrate and feed in kg/s

$h_{es}, h_L, h_F$ … specific enthalpy of evaporated solvent, concentrate and feed in kJ/kg

For a conventional heater, the transferred heat is calculated as shown in *EQ 30*:

$$\dot{Q} = \dot{m}_{out} \times h_{out} + \dot{m}_{in} \times h_{in} = \dot{m}_{in} \times (h_{out} - h_{in}) \qquad \textbf{EQ 30}$$

$\dot{Q}$ … transferred heat in kW

$\dot{m}_{in}, \dot{m}_{out}$ … mass flow of incoming and outgoing stream in kg/s

$h_{in}, h_{out}$ … specific enthalpy of incoming and outgoing stream in kJ/kg

To be able to analyze the process, all heat sources (hot streams) and sinks (cold streams) have to be identified. Furthermore, the related mass flows and specific heat capacities need to be determined to provide a closed mass and heat balance. In all following sections, the specific heat capacity is termed as effective heat capacity ($CP_{eff}$). Depending on the procedure in the evaporator, the effective heat capacity can be calculated with equation *EQ 31*:

$$CP_{eff} = \frac{\dot{Q}}{\dot{m}_{es} \times (T_{es} - T_F)} \qquad \textbf{EQ 31}$$

$\dot{Q}$ … transferred heat in kW

$\dot{m}_{es}$ … mass flow of evaporated solvent in kg/s

$T_{es}, T_F$ … temperature of evaporated solvent and feed in °C

The Pinch Analysis is an easy applicable method to compare the theoretical energy consumptions of different process configurations in a fast way.

## 3.7 Process-Simulation

### 3.7.1 Aspen Plus

The simulation program ASPEN Plus® by Aspen Tech, is a modeling tool for the conceptual design and optimization of chemical processes. Its main application is the stationary simulation of separation and transformation processes, by using mass and energy balances, phase equilibrium (VLE, LLE, VLLE), chemical equilibrium and reaction kinetics.

This simulation tool is a sequential-modular program, including applications of several unit operations used in chemical engineering and a wide range of thermodynamic models for property calculation. The program includes a large database of pure component and phase equilibrium data for conventional chemicals, electrolytes, solids, and polymers.

Furthermore to the general flow-sheet simulation, design specifications to reach certain targets can be set and sensitivity analysis can be performed. With the Equation Oriented (EO) modeling capability and hierarchical flow sheeting even large scale and complex processes can be simulated.

### 3.7.2 Thermodynamic model

The choice of the right thermodynamic model is important for the separation behavior and efficiency, especially in the distillation part of the simulated process. In this section, an exact calculation of the vapor-liquid-equilibrium (VLE) depends on the availability of the interaction parameters of the present components.

The non-random two-liquid model (NRTL) is one of these thermodynamic models provided by ASPEN PLUS to calculate the phase equilibrium in azeotropic separations, especially alcohol separation. This thermodynamic model is characterized by correlations between the activity coefficients and the mole fractions of the compounds, which are based on experimentally determined phase equilibrium data.

### 3.7.3 Component database

Most of the components used in the simulations are available in the standard ASPEN PLUS property database. But for some, a complete set of physical properties is determined and

entered into an in-house NREL ASPEN PLUS database [Wooley, et al., 1996]. The components glucose, xylose, cellulose, xylan, lignin, yeast and enzymes are taken from this database, which was developed by the National Renewable Energy Laboratory.

### 3.7.4 Boiling point elevation

For all simulations, a boiling point elevation is considered by ASPEN PLUS. With changing dry matter content in the solution, the impact of other substances on the boiling point increases, which is shown in Figure 3-11, where at a dry matter content of 60%, the boiling point elevation is up to 1.2°C, depending on the pressure level and compared to pure solvent. It can also be seen, that with increasing DM content and increasing pressure level the effect amplifies.

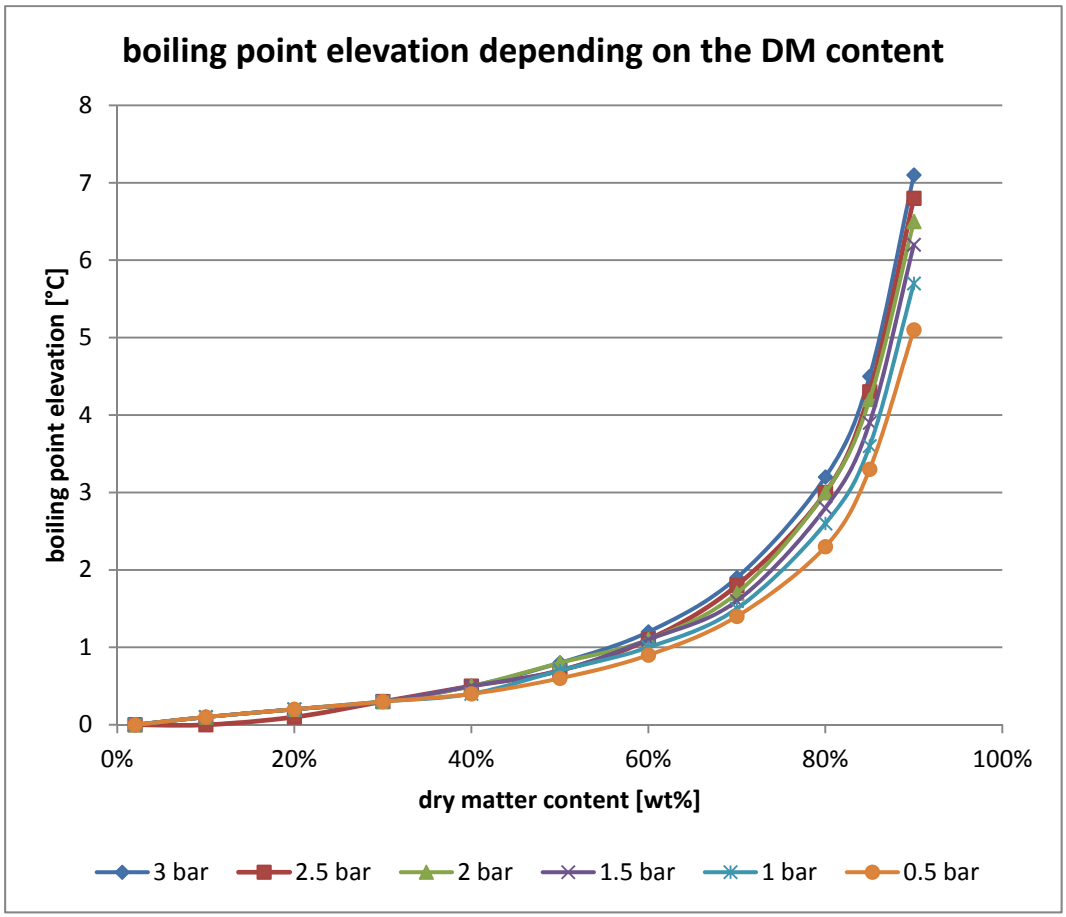


**Figure 3-11:** **Boiling point elevation of the solvent at different pressure levels, depending on the dry matter content.**

### 3.7.5 Specified components for ASPEN PLUS simulation

The different components used in the simulations are either taken from the ASPEN PLUS internal databank or the in-house NREL ASPEN PLUS database. Table 3-7 shows a complete list of the defined components, including ammonia, propionic acid, carbonic acid and hydrogen only used in the biogas simulation.

**Table 3-7: Components used in the simulations, including type and formula as stated in the ASPEN PLUS databank**

| Component ID | Type | Component name | Formula |
|---|---|---|---|
| WATER | CONV | WATER | H2O |
| ETHANOL | CONV | ETHANOL | C2H6O-2 |
| ACETAT | CONV | ACETIC-ACID | C2H4O2-1 |
| FURFURAL | CONV | FURFURAL | C5H4O2 |
| GLYCEROL | CONV | GLYCEROL | C3H8O3 |
| CO2 | CONV | CARBON-DIOXIDE | CO2 |
| CELLULOS | SOLID | CELLULOS | C6H10O5 |
| XYLAN | SOLID | XYLAN | C5H8O4 |
| LIGNIN | SOLID | LIGNIN | CXHXOX |
| XYLOSE | CONV | D-XYLOSE | C5H10O5 |
| GLUCOSE | CONV | DEXTROSE | C6H12O6 |
| YEAST | SOLID | BIOMASS | CHXNXOXSX-1 |
| ENZYMES | CONV | ZYMO | CHXOXNX |
| ASH | SOLID | SILICON-DIOXIDE | SIO2 |
| EXTRAKT | CONV | LINOLEIC-ACID | C18H32O2 |
| PROTEIN | CONV | L-GLUTAMIC-ACID | C5H9NO4 |
| O2 | CONV | OXYGEN | O2 |
| CH4 | CONV | METHANE | CH4 |
| NH3 | CONV | AMMONIA | H3N |
| C3H6O-01 | CONV | PROPIONIC-ACID | C3H6O2-1 |
| H2CO3 | CONV | CARBONIC-ACID | H2CO3 |
| H2 | CONV | HYDROGEN | H2 |

Due to the fact that some complex components exist in the system, the following simplifications have to be assumed. Cellulose is a structural polysaccharide containing a multitude of beta-linked glucose units with the molecular formula $(C_6H_{10}O_5)_n$ and is taken from the ASPEN Plus databank, where it's defined as $C_6H_{10}O_5$. The hetero-polysaccharide xylan represents the non-hydrolyzed hemi-cellulose in the feed. Silicon dioxide is defined as

the compound representing ash, based on an analysis of wheat straw ash, where $SiO_2$ is the main component with an average content of 51.51 wt% [Reisinger, et al., 2009]. For extractives, a representative component is chosen based on a study where free fatty acids, sterols, waxes, sterol esters and triglycerides were the major groups obtained [Sun and Tompkinson, 2003]. Depending on the extraction method the composition differs. Sun and Tompkinson [2003] point out that myristic acid ($C_{14}H_{28}O_2$), pentadecanoic acid ($C_{15}H_{30}O_2$), palmitic acid ($C_{16}H_{32}O_2$), linoleic acid ($C_{18}H_{32}O_2$) and oleic acid ($C_{18}H_{34}O_2$) were the major fatty acids in their analysis. Based on this information, linoleic acid is chosen to represent the extractives in this process simulation. L-Glutaminic acid is one of many proteinogenic amino acids and serves as a representative compound for all proteins in the simulation. Lignin, cellulose, yeast and enzymes, all taken from the in-house NREL ASPEN PLUS database, are defined with the respective molecular formulas $C_{7.3}H_{13.9}O_{1.3}$ , $C_6H_{10}O_5$ , $CH_{1.64}N_{0.23}O_{0.39}S_{0.0035}$ and $CH_{1.8}O_{0.5}N_{0.2}$ .

## 3.8 Conceptual design and modeling of the distillation, PSA and solid-liquid-separation in ASPEN PLUS

For the conceptual design of the two different distillation variations, the ethanol production of 100.000 t/a, with an ethanol purity higher 99.5 wt% and an ethanol recovery greater 99.9% is requested.

In the designed simulations, some of the specifications taken from literature, as described in chapter 3.2.2, had to be adapted until the simulations converged. Therefore, given parameters as reflux ratio, number of stages and feed stage were adjusted. Subsequently, the design and modeling of the two distillation variations, including PSA and solid-liquid separation unit, is described. Furthermore, chosen parameters and design specifications to maintain a convergence in the simulation are described.

### 3.8.1 The 2-column distillation

For the simulation of the distillation and dehydration process variation based on the work done by Aden, et al. [2002], which is described in section 3.2.2.1, the ASPEN PLUS operational units are arranged as seen in Figure 3-12. Therefore, two RadFrac-columns, two separators, a mixer and several heaters are applied.

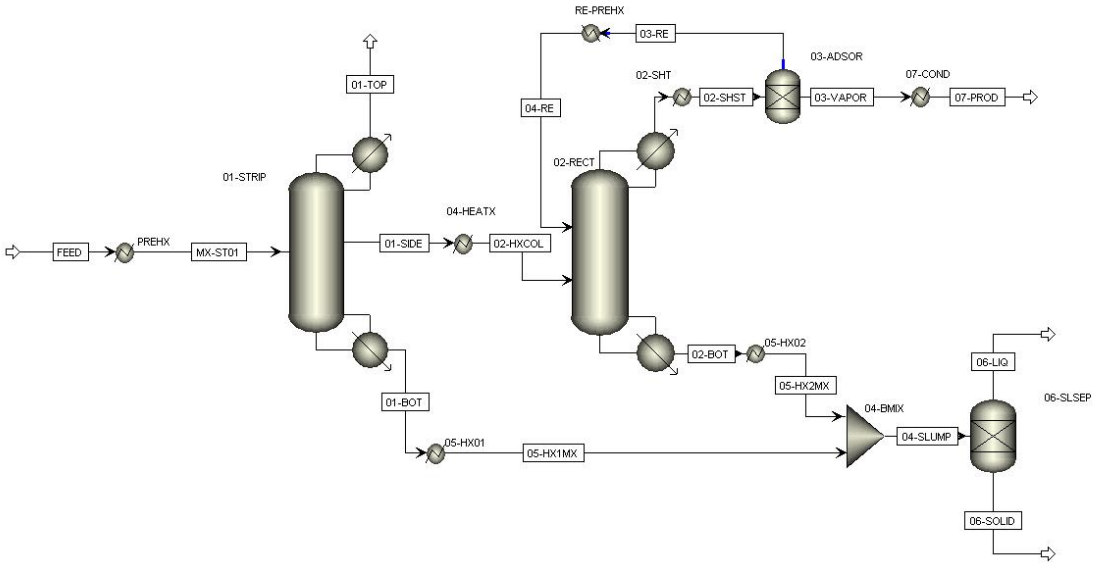


**Figure 3-12: ASPEN PLUS flow sheet of the 2-column distillation model**

The feed is preheated from 37°C to 100 °C and then fed to the stripper column *01-STRIP,* which is operated at 1.8 bar with a column pressure drop of 0.2 bar. The stripper column consists of 19 theoretical stages and the preheated alcoholic mash is fed above stage 2. There are three product streams exiting the column, *01-TOP* at the top of the column as vapor, *01-BOT* at the bottom of the column as liquid and *01-SIDE* at stage 3 as a vaporous side-draw which is then fed to the rectifier without condensation. The side stream is set as a 13.5 wt% fraction of the feed. To obtain a converging simulation some parameters given by literature are adapted, which are listed in Table 3-8.

With the following specifications set, a simulation convergence is secured:

- Reflux ratio set as 3, to ensure certain purity.
- Distillate to feed ratio set as 0.003 on a mass basis.
- A design specification to reach 35 wt% of ethanol in the side stream set as 13.5 wt% fraction of the feed.
- A design specification to obtain a 100%-recovery (-0.5%) of ethanol in the side-stream, by varying the distillate to feed ratio in the column.

**Table 3-8: Differences between the set specification and literature for the 2-column distillation setup.**

| | Simulation | Aden, et al. [2002] |
|---|---|---|
| **stripper column:** | | |
| total stages (theoretical) | 19 | 17 |
| reflux ratio | 3 | 3 |
| feed stage (theoretical) | 2 | 2 |
| ethanol content side stream | 35 wt% | 39.4 wt% |
| side stream stage (theoretical) | 3 | 4 |
| **rectification column:** | | |
| total stages (theoretical) | 20 | 34 |
| reflux ratio | 4 | 3.2 |
| feed stage (theoretical) | 11 | 25 |
| ethanol content at top | 91.4 wt% | 92.5 wt% |

The side stream *01-SIDE* is then fed into the second column, the rectifier *02-RECT*, at stage 8 of a total 15 theoretical stages. This column is operated at 1.6 bar and two product streams exit the system - the vaporous stream *02-TOP* at the top and the liquid stream *02-BOT* at the bottom. Another feed, named *03-RE*, enters the column, which is a small part of the top product and is recycle stream from the PSA column. A reflux ratio of 4 and a distillate to feed ratio approximately 0.41 (both on a mass basis) are set to obtain the ethanol-water profile as shown in Figure 3-13 and a convergence in the simulation. The feed stages for the rectification column were chosen according to this profile.

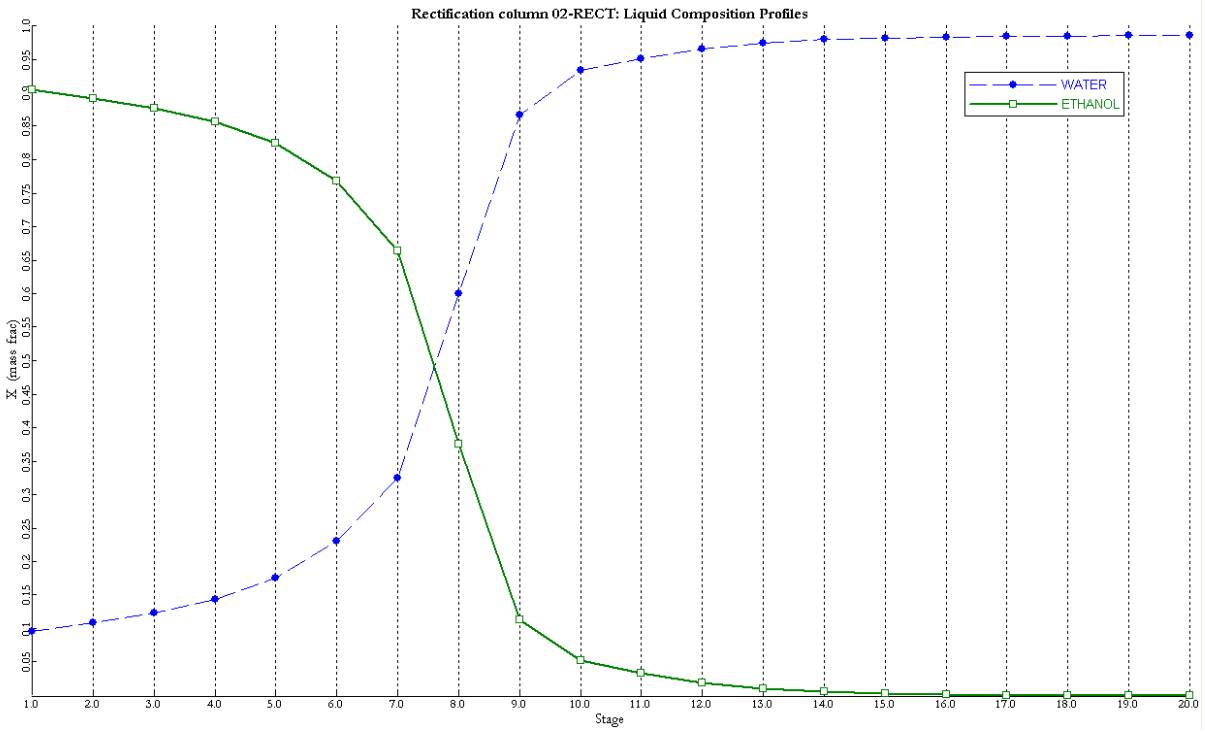


**Figure 3-13:** **Profile of the ethanol-water composition in the rectification column *02-RECT* on a mass basis in the 2-column setup.**

The overhead product *02-TOP* is superheated to 116°C and fed to the PSA-column, which is represented by a separation unit, with a pressure of 1.8 bars and split fractions for the respective components set to reach the demanded ethanol purity.

The bottom products from stripping and rectification are mixed and fed to the solid-liquid separation unit, which is operated at 3.2 bar and 40°C. There, 95% off all insoluble solids are separated and leave the unit in the *06-SOLID* stream. The split fractions of the respective components are set to reach an assumed cake dry matter of 40 wt%.

An overview about the used unit operation blocks in the ASPEN Plus simulation including the related settings and specifications is given in the appendix, section A. It can be seen, to obtain a 99.9% recovery, the set distillate to feed ratio in the stripper column changes from 0.003 to 0.00092 due to the implemented design specification.

### 3.8.2 The 3–column distillation

In the conceptual design of the distillation variation based on the work done by Sassner [2007], some major adjustments in the process setup have to be made to ensure that the simulation converges and the specifications can be achieved. As described in section 3.2.2.2, the setup consists of two stripper columns ( *01-STRIP*, *02-STRIP* ) and a rectifier unit ( *03-RECT* ) simulated with ASPEN PLUS RadFrac modeling units. Furthermore, flash drums, mixers, splitters and component separators are used in the distillation simulation. Due to separation problems with the present $CO_2$, flash drums are implemented to recover the ethanol lost as overhead vapor in the strippers. The setup differences between simulation and literature are listed in Table 3-9 and the arrangement of the units utilized in ASPEN PLUS can be seen in Figure 3-14.

**Table 3-9: Differences between the set specification and literature for the 3-column distillation setup.**

| | Simulation | Sassner [2007] |
|---|---|---|
| **stripper columns:** | | |
| pressure stripper column #1 | 3.2 bar | 3 bar |
| pressure stripper column #2 | 1 bar | 1.25 bar |
| total stages (actual) | 20 (theoretical) | 25 |
| Murfree efficiency | 50% | 50% |
| reflux ratio s.c. #1 | 2.38 | n.d.a. |
| reflux ratio s.c. #2 | 1.47 | n.d.a. |
| **rectification column:** | | |
| pressure rectification column | 0.3 bar | 0.3 bar |
| total stages (actual) | 23 (theoretical) | 45 |
| Murfree efficiency | 75% | 75% |
| reflux ratio | 2.11 | 2.4 |
| ethanol content at top | 92.4 wt% | 92.5 wt% |

*n.d.a. … no data available*

The feed is split into two streams, with 0.47 set as split fraction for the stream fed to stripper column 2 (*FTPH-02*). Both split streams are preheated, the split sent to stripper column 1 from 40°C to 130°C at 3.5 bar and the split stream sent to column 2 from 40°C to 85°C at 1.5 bar. As Table 3-9 shows, stripper column *01-STRIP* is operated at 3.2 bar, which is a slightly higher pressure than defined in literature (3 bar) to ensure the temperature difference

necessary for heat integration. In contrast to that, the chosen operational pressure of 1 bar in column *02-STRIP* is lower than the given pressure in literature (1.25 bar).

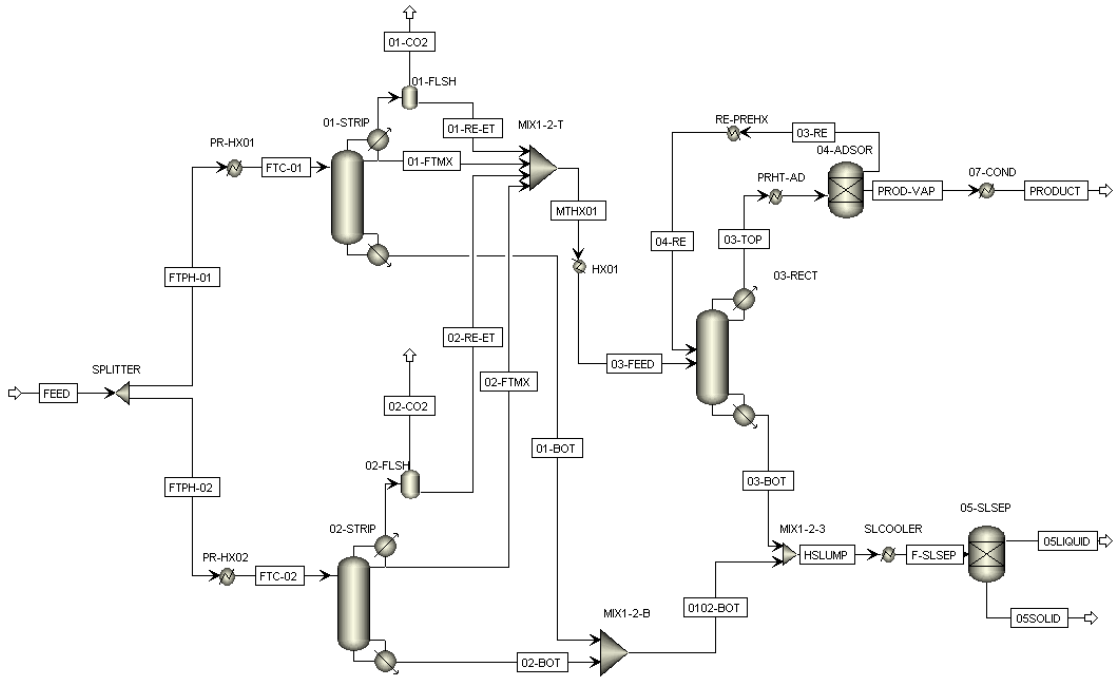


**Figure 3-14: ASPEN PLUS flow sheet of the 3-column distillation model.**

The condensers in the two stripper columns are of the partial-vapor-liquid type where most of the $CO_2$ ends up in the vaporous stream, whilst ethanol and water are condensed and result as the liquid head product. The condensation temperatures are set with 112°C and 80°C for stripper columns 1 and 2, respectively. Depending on the condensation temperature, a certain amount of ethanol remains in the vaporous stream together with the $CO_2$. This ethanol is recovered by a flash separation and is subsequently fed to the rectification column. The overhead products from both stripper columns are mixed and fed to the rectification column *03-RECT*, which is operated at 0.3 bar, with a reflux ratio of 2.1. A specified distillate rate is set to reach the targeted 92.4 wt% of ethanol. These column specifications result in a smooth ethanol-water separation curve as shown in Figure 3-15.

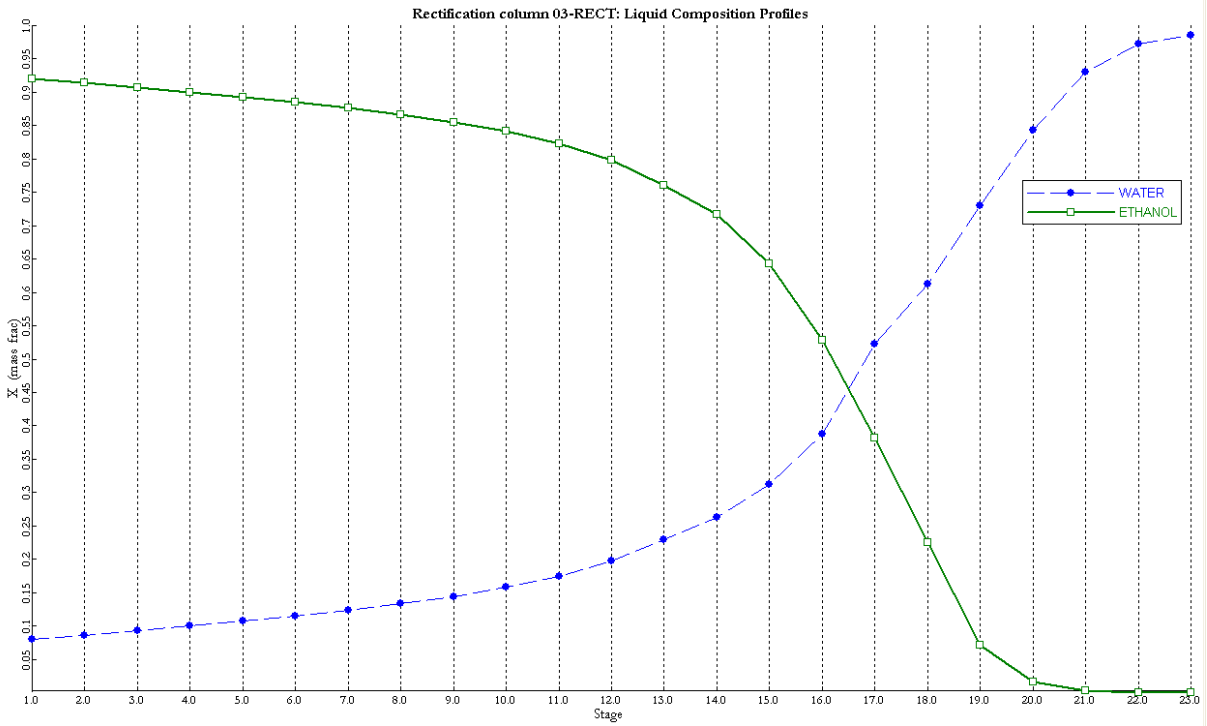


**Figure 3-15: Profile of the ethanol-water composition in the rectification column 03-RET on a mass basis in the 3-coulmn setup.**

The overhead vapor is sent to the PSA, where most of the remaining water is removed to reach an ethanol content of 99.4 wt%. The assumptions for both separator units, PSA and solid-liquid, are based on the values from Sassner [2007], but in case of the adsorption unit, a slight change of the water and ethanol split fractions is necessary to reach the targeted ethanol content in the product and to ensure a convergence in the simulation. In the solid-liquid separation unit, a final cake DM of 40 wt% will be reached.

## 3.9 Conceptual design and modeling of the multi-stage evaporation in ASPEN PLUS

As basis for the design of the multi-stage evaporation, it is assumed that the liquid residue from solid-liquid separation has a set temperature of 40°C. Before entering the first stage of the evaporator, this process stream has to be preheated to boiling temperature by an external heater.

For the simulation of a multi-stage evaporation system, the realization of a single stage in ASPEN PLUS is shown in Figure 3-16. To realize the pressure change of the feed, when

entering the evaporator-stage, a heater with a set stage pressure ($p_{stage\ x}$) and zero heat duty is implemented. The solution is then fed to a heat exchanger, where a certain amount of the solvent is evaporated, according to the heat provided by the total condensation of the steam from a previous stage (or primary steam at stage 1). The vapor liquid mixture is then separated in a flash-module, which is operated at the stage pressure, again with zero heat duty set. The evaporated solvent and the concentrated liquid are fed to the next stage, that is operated at a different pressure. The heat source enters the system at a higher temperature ($T_{stage\ x-1} > T_{stage\ x}$) and a higher pressure level ($p_{stage\ x-1} > p_{stage\ x}$), which enables the heat transfer. For simplification, losses are not considered in this system. They vary from stage to stage and depend on the pressure level, as well as on the evaporator size.

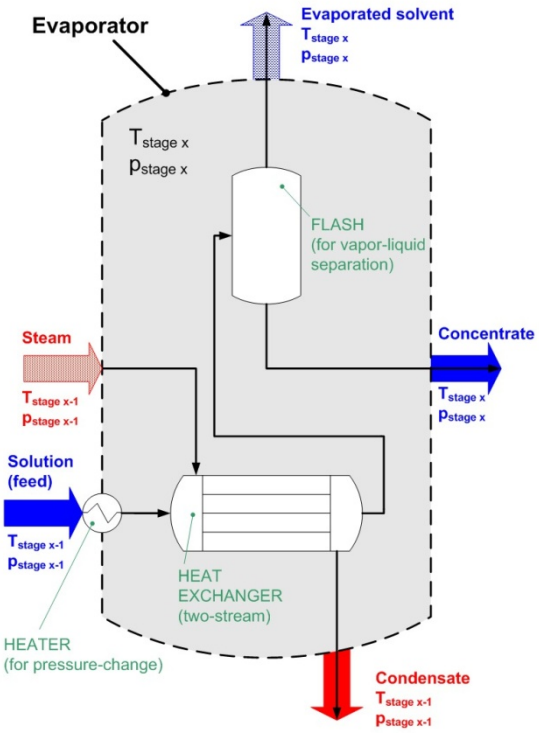


**Figure 3-16: Realization of an evaporator in ASPEN PLUS**

### 3.9.1 5-stage co-current evaporation system

The Aspen model of the 5-stage co-current evaporation system is simulated in two different executions – a *BASE CASE* and a *FLASH CASE*. To realize the 5-stage evaporation process in ASPEN PLUS, five of the single stages pictured in Figure 3-16 are conneted in series. The pressure at the first and the last stage are given as 3 bars and 0.5 bars, respectively.

Both values are taken from literature [Wingren, et al., 2008]. All remaining pressure levels are chosen according to their equal shares of the system's total temperature difference $\Delta T_{total}$ ($\Delta T_{total} = T_{boiling\ stage\ 1} - T_{boiling\ stage\ 5}$). An overview about the calculated stage temperatures ($T_S$) and the chosen pressures for simulation is given in Table 3-10.

**Table 3-10: Given and chosen temperature and pressure levels for each stage of the co-current 5-stage evaporation system**

| Stage number | $T_S$* [°C] | p** [bar] |
|---|---|---|
| **1** | 134.1 | 3 |
| **2** | 120.9 | 2 |
| **3** | 112.3 | 1.5 |
| **4** | 101.1 | 1 |
| **5** | 85.9 | 0.5 |

* calculated boiling temperature (boiling point elevation included) on each stage.
** chosen pressure for ASPEN PLUS simulation

To reach the demanded dry matter of 60 wt% (± 1%) in both cases, a design specification is implemented, that varies the amount of primary steam at the first stage.

In Figure 3-17 the *BASE CASE* is pictured, where the condensate exiting each effect is subsequently cooled down in a heat exchanger to 50°C and the resulting heat can be used as heat source, either to pre-heat the feed or some other stream in the ethanol process.

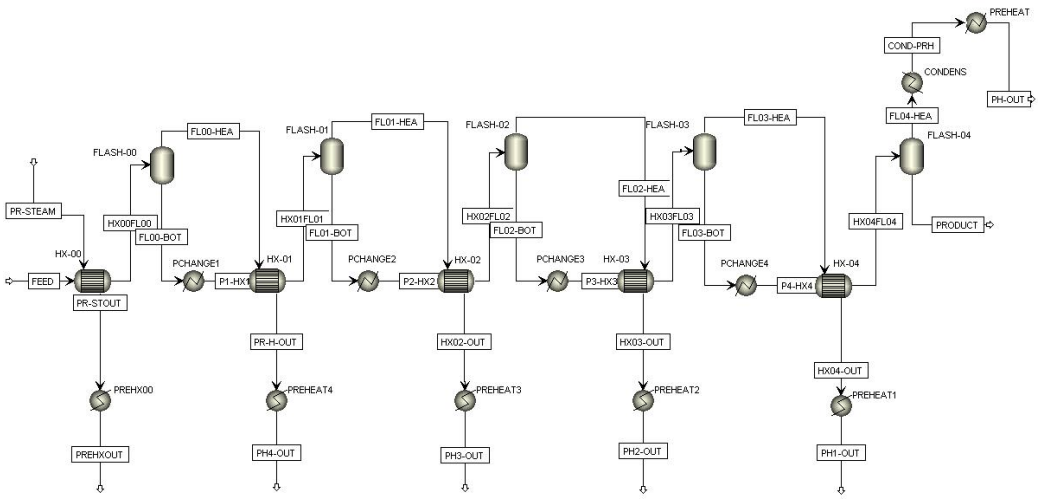


**Figure 3-17: ASPEN PLUS flow sheet of the co-current evaporation system BASE CASE**

In contrast to the *BASE CASE,* an additional flash condensate system is implemented in the *FLASH CASE* of the 5-stage evaporation arrangement. As pictured in Figure 3-18, the condensate from one effect is sent to a flash that is operated at the same pressure as the following effect. Due to this pressure difference, accompanied by a boiling point reduction in the flash, a certain amount of vapor is formed, which is subsequently mixed with the evaporated solvent at that stage. The condensate from the flash's bottom is fed to the next flash condensation unit, together with the condensate from the following evaporation effect.

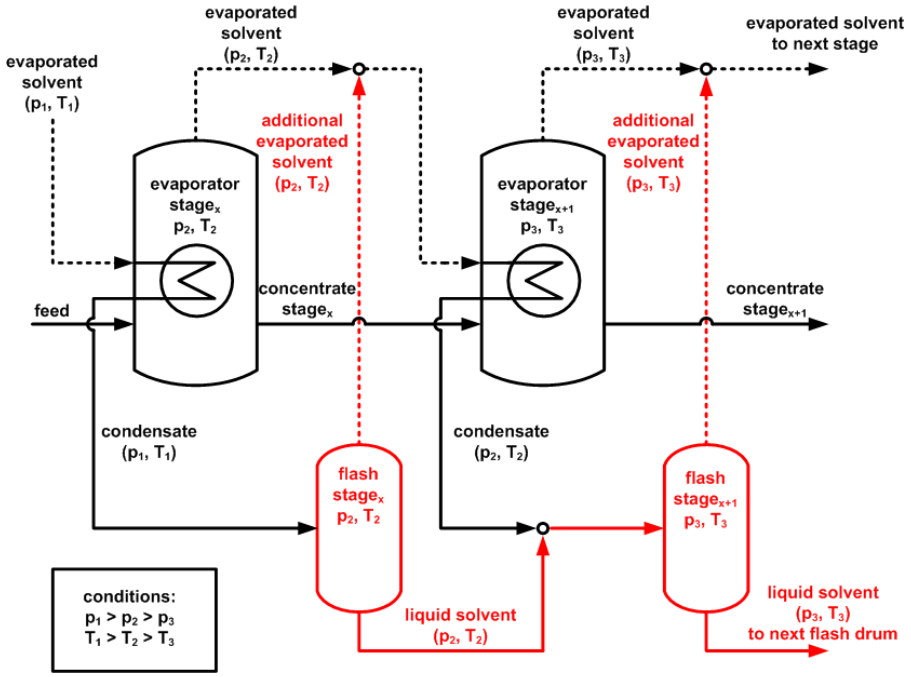


**Figure 3-18: Simplified flow sheet of the flash condensate system (red colored) implemented in the multi-stage evaporation process (black colored).**

This configuration uses the higher heat potential due to condensation, which allows the reduction of energy consumption [Westphalen and Wolf Maciel, 2000]. In Figure 3-19, the realization of the flash condensate system in ASPEN PLUS is shown. This effective utilization of the condensates, to generate additional vapor, results in one condensate stream exiting the evaporation system. This stream can be further used for preheating purposes.

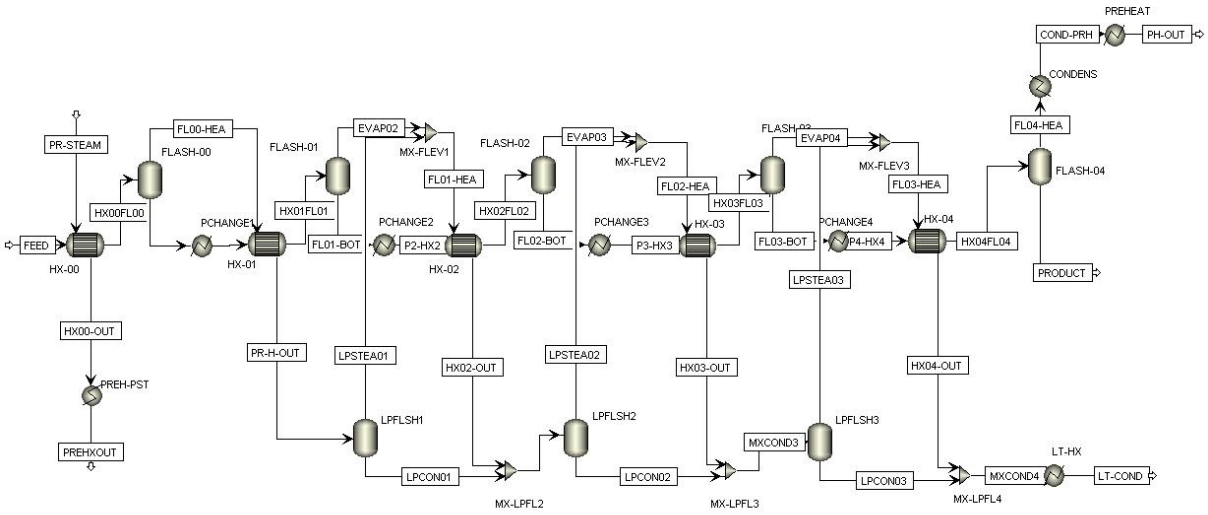


**Figure 3-19: ASPEN PLUS flow sheet of the co-current evaporation system FLASH CASE**

### 3.9.2 5-stage counter-current evaporation system

Same as the effects in the co-current 5-stage evaporation system, a single stage in the counter-current arrangement consists of several units. There is a conventional heater to create a pressure change when the feed is entering the evaporator, a heat exchanger to provide the heat transfer between the condensing vapor (hot stream) and the feed (cold stream) and a flash to separate the vaporous solvent from the liquid concentrate. All five stages are operated at different pressure levels, where the first stage pressure and the last stage pressure are given with 3 bar and 1 bar, respectively. As mentioned in section 3.4, the stage where primary steam is fed, is defined as stage 1. Therefore, the feed enters the system at stage 5 and the final concentrate exits the system at stage 1. In Table 3-11, the chosen pressure and temperature levels at each stage are shown.

**Table 3-11: Given and chosen temperature and pressure levels for each stage of the counter-current multi-stage evaporation system**

| Stage number | $T_s$* [°C] | p** [bar] |
|---|---|---|
| **1** | 142.1 | 3 |
| **2** | 129.5 | 2.5 |
| **3** | 121.4 | 2 |
| **4** | 112.1 | 1.5 |
| **5** | 100.1 | 1 |

* calculated boiling temperature (boiling point elevation included) on each stage
** chosen pressure for ASPEN PLUS simulation

Due to the fact, that the solution enters the system at the lowest pressure level and therefore lowest boiling temperature, it has to be heated until the boiling point of each stage is reached ($T_{feed,\ stage\ x} < T_{boiling,\ stage\ x}$). This means, that the heat is not only used to partly evaporate the solution, but also to preheat it from entering temperature to the boiling temperature.

Pumps are used to feed the concentrated solution to the following stage and with that, to lift the process streams to the desired pressure level of the next effect. Due to simplification, the pumps are represented by a conventional heater with the required pressure set and zero heat duty, which means that the electric power of the pumping system is not considered in the ASPEN PLUS simulation model. But this can easily be estimated by using equation *EQ 32*, where the pressure difference, the geodetic height and the efficiency of the pump are taken into account.

$$P_{el} = \left(\frac{\dot{m}_{sol} \times \Delta p}{\rho_{sol}} + \dot{m}_{sol} \times g \times H\right) \times \frac{1}{\eta} \qquad \textit{EQ 32}$$

$P_{el}$ … electric power in Watt

$\dot{m}_{sol}$ … mass flow of the solution in kg/s

$\Delta p$ … pressure difference between two stages in Pa

$\rho_{Sol}$ … density of the solution in kg/m³

$g$ … standard gravity in m/s²

$H$ … geodetic height in m

$\eta$ … efficiency of the pump

The energy demand of the pumps is very small. For example, the electric power required for pumping between stage 5 and 4 accounts for ~6 kW (with an efficiency of 0.8).

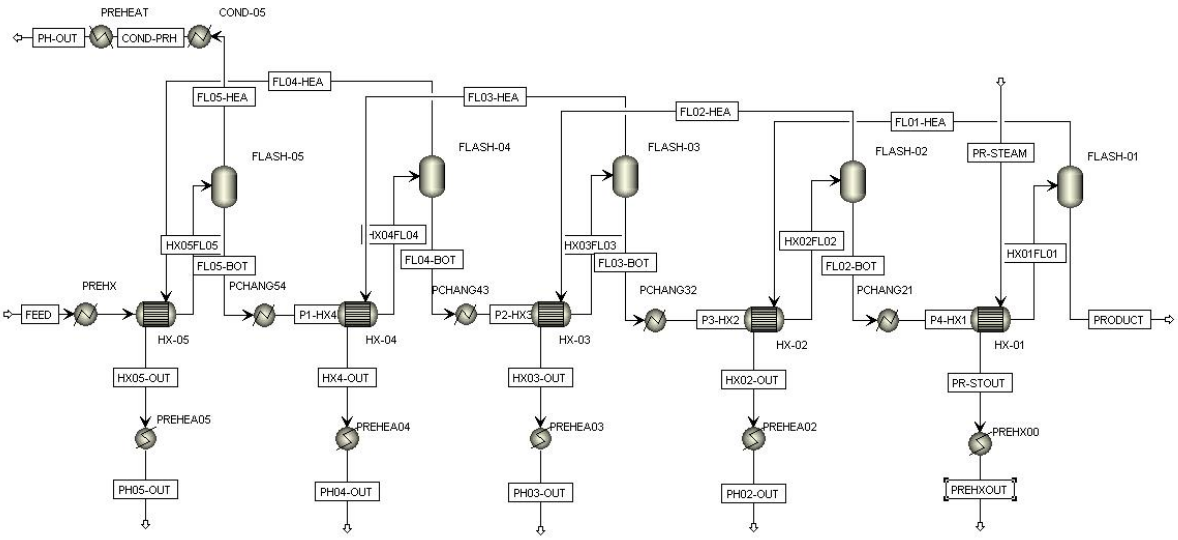


**Figure 3-20: ASPEN PLUS flow sheet of the counter-current evaporation system BASE CASE**

As for the co-current setup, a *BASE CASE* is developed, which is pictured in Figure 3-20. Again, a design specification is implemented to reach the targeted dry matter content of 60 wt% (± 1%) by variing the amount of primary steam fed. All condensates available in the *BASE CASE* are cooled down to 50°C in the heat exchangers and the thereby arising heat can either be used to preheat the feed or can be utilized in the overall prozess.

## 3.10 Conceptual design and modeling of the biogas-production in ASPEN PLUS

In the anaerobic digestion simulation, two reactor units and a conventional flash are implemented. The related ASPEN PLUS flow sheet of the biogas production process is shown in Figure 3-21. In general, the anaerobic digestion occurs in one reactor, but for a better overview, the chemical processes are split into two parts. The first reactor, named *ANAERO-D*, contains all reactions where intermediate products emerge. In the second reactor, named *METHANO*, the processes with only methane and carbon dioxide as reaction products are taken into account. For the anaerobic digestion, mesophilic conditions are chosen, with an operational temperature of 37°C and a pressure of 1 bar.

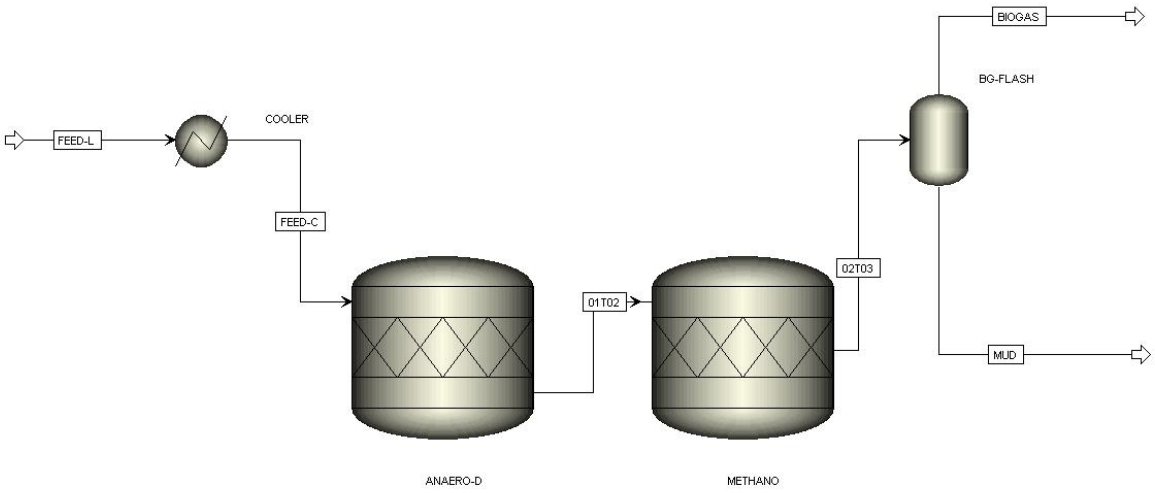


**Figure 3-21: ASPEN PLUS flow sheet of the anaerobic digestion**

The reactors designed in ASPEN PLUS are of the RStoic type, which are based on assumed fractional conversion of reactions. All reactions in the anaerobic digestion, including the conversion factor of a certain compound, are listed in Table 3-12. The residuals, including unconverted organic compounds, represent the sludge that occurs during anaerobic digestion. To separate the generated biogas, mainly containing $CH_4$ and $CO_2$, from the sludge a flash column is implemented in the simulation.

**Table 3-12: Implemented reactions in the ASPEN PLUS RStoic units for anaerobic digestion**

| Reactions | | | fractional conversion | component |
|---|---|---|---|---|
| **ANAERO-D:** | | | | |
| *protein* | | *propionic acid + carbon dioxide + ammonia + hydrogen* | | |
| $C_5H_9O_4N + 2\ H_2O$ | → | $C_3H_6O + 2\ CO_2 + NH_3 + 2\ H_2$ | 0.9 | protein |
| *ethanol* | | *acetic acid + hydrogen* | | |
| $2\ C_2H_6O + 2\ H_2O$ | → | $C_2H_4O_2 + 4\ H_2$ | 0.9 | ethanol |
| *glycerol* | | | | |
| $C_3H_8O_3$ | → | $1.75\ CH_4 + 1.25\ CO_2 + 0.5\ H_2O$ | 0.9 | glycerol |
| | | | | |
| **METHANO:** | | | | |
| *carbon dioxide* | | | | |
| $CO_2 + 4\ H_2$ | → | $CH_4 + 2\ H_2O$ | 1 | $H_2$ |
| *propionic acid* | | | | |
| $C_3H_6O + 0.5\ H_2O$ | → | $1.75\ CH_4 + 1.25\ CO_2$ | 1 | propionic acid |
| *acetic acid* | | | | |
| $C_2H_4O_2$ | → | $CH_4 + CO_2$ | 0.9 | acetic acid |
| *xylose* | | | | |
| $2\ C_5H_{10}O_5$ | → | $5\ CH_4 + 5\ CO_2$ | 0.9 | xylose |
| *furfural* | | | | |
| $C_5H_4O_2 + 3\ H_2O$ | → | $2.5\ CH_4 + 2.5\ CO_2$ | 0.9 | furfural |
| *glucose* | | | | |
| $C_6H_{12}O_6$ | → | $3\ CH_4 + 3\ CO_2$ | 0.9 | glucose |
| *extract* | | | | |
| $C_{18}H_{32}O_2 + 9\ H_2O$ | → | $12.5\ CH_4 + 5.5\ CO_2$ | 0.5 | extract |
| *xylan* | | | | |
| $C_5H_8O_4 + H_2O$ | → | $2.5\ CH_4 + 2.5\ CO_2$ | 0.5 | xylan |

For the biogas process, lignin, enzymes and cellulose are not considered in the calculation, because it is not clear how much of it actually is accessible for bioconversion - this makes the simulation somewhat conservative. The conversion rates are chosen according to Barta, Reczey and Zacchi [2010].

## 3.11 Background process

A cross-process use of possible heat sources and sinks results in a better efficiency for the overall straw to ethanol process. Figure 3-22 pictures a simplified flow sheet of this process, including pretreatment, SSF, enzyme and yeast production, the drying and co-generation process steps. The blue frame highlights the distillation, the solid-liquid separation and the further processing of the liquid stillage, which is simulated in this work. The associated cooling or heating units are colored blue or red. It can be seen, that sources of heat and sinks for heat integration exist, especially in the pretreatment section.

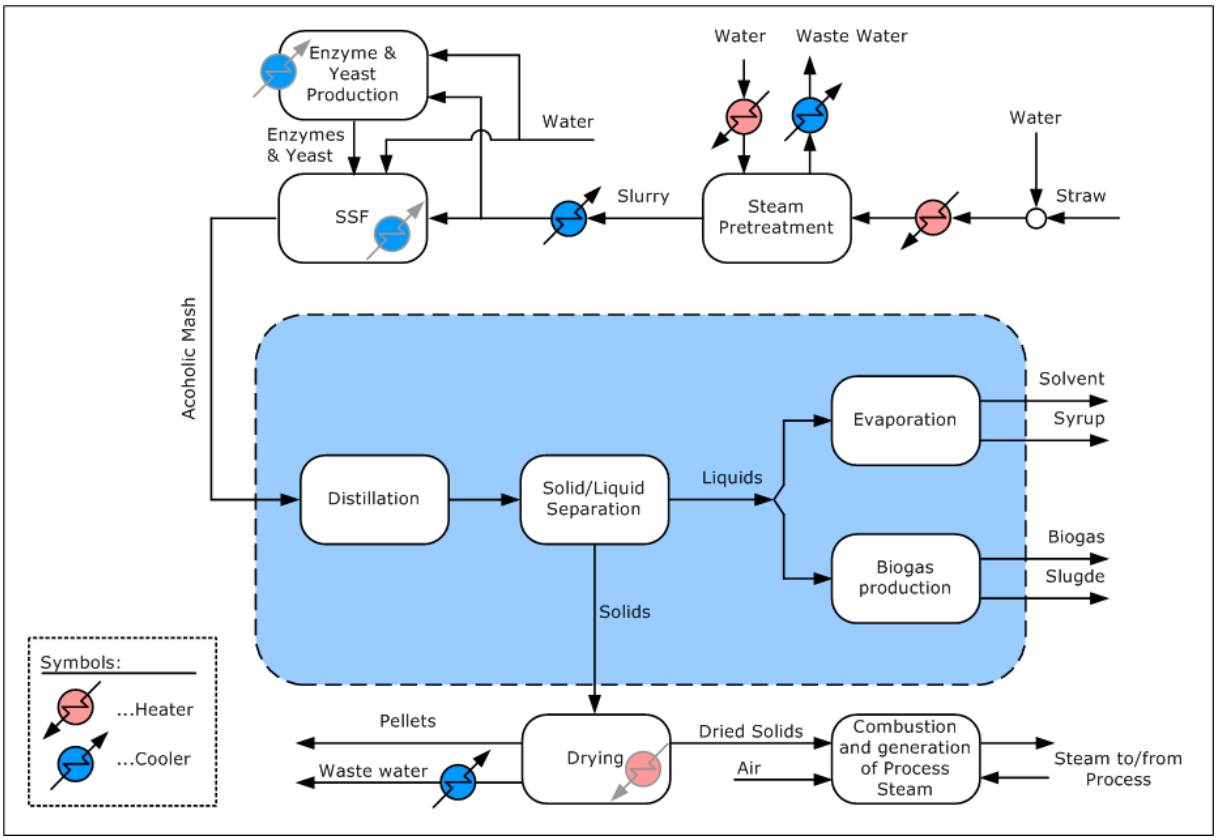


**Figure 3-22: Simplified flow sheet of the lignocellulosic ethanol process including the heat sources and sinks of the background process**

For the investigation of the different process variations from an energetic point of view, information about the background process is necessary. In Table 3-13 the process streams of the steam pretreatment, SSF, enzyme & yeast production and drying step, with the respective temperature levels, mass flows and heat are listed. This information is taken from a previous process simulation of the straw to ethanol process done by Kravanja, et al. [2011].

**Table 3-13: Given process streams for the upstream processing in the bioethanol from straw production. Data is taken from the process simulation work done by Kranvanja, et al. [2011].**

| section | name of stream part | stream type | $T_{in}$ [°C] | $T_{out}$ [°C] | mass flow [kg/s] | heat [MW] |
|---|---|---|---|---|---|---|
| Preheating straw before SP | Preheating straw for SP | cold | 23.2 | 99.0 | 57.8 | 14.09 |
| Steam pretreatment (SP) | Heat water for SP | cold | 15.0 | 211.7 | 10 | 8.49 |
| | Evaporate water for SP | cold | 211.7 | 212.7 | 10. | 19.02 |
| Drying | Superheating of drying steam | cold | 149.0 | 210.0 | 98.7 | 13.1 |
| Condense and cool steam from SP 4 bar | Condense SP 4 bar Steam | hot | 143.6 | 142.6 | 5.8 | 12.35 |
| | Cool SP 4 bar Steam | hot | 143.6 | 37.0 | 5.8 | 2.6 |
| Condense and cool steam from SP 1 bar | Condense SP 1 bar Steam | hot | 100.0 | 99.0 | 4.12 | 9.3 |
| | Cool SP 1 bar Steam | hot | 99.0 | 37.0 | 4.12 | 1.08 |
| Cooling after SP | Cool pretreated biomass | hot | 99.0 | 42.8 | 57.98 | 10.7 |
| Enzyme and yeast production | Cool reactor yeast production | hot | 31.0 | 30.0 | 9.9 | 1.6 |
| | Cool reactor enzyme production | hot | 31.0 | 30.0 | 5.4 | 0.96 |
| SSF | Cool reactor SSF | hot | 38.0 | 37.0 | 89.8 | 2.91 |

These streams are further used in the Pinch Analysis to evaluate the different process setups for downstream processing. As a result, the best fitting distillation setup in combination with a multi-stage evaporation or biogas production will be shown.

# 4 Mass and energy balance of flow sheet simulations

In the following chapters, the results from ASPEN PLUS simulation are shown. First, the focus is on the mass and heat related results of the distillation variations, followed by an analysis of the various possibilities for the 5-stage evaporation configuration, including a Pinch Analysis. The respective ASPEN PLUS flow sheets and stream tables can be found in the appendix, section C.

## 4.1 Distillation

Subsequent, the collected data from ASPEN PLUS simulation of the 2-column and 3-coulmn distillation setup is presented. These findings are further used for the Pinch Analysis of the overall process.

### 4.1.1 2-column distillation design

The conceptual design, including all process relevant temperatures and concentrations are pictured in Figure 4-1. Furthermore, the heating and cooling units with their respective heat and cooling demand are shown.

The five main streams including the feed ( *FEED* ), the ethanol product ( *07-PROD* ), the liquid ( *06-LIQ* ) and the solid reside ( *06-SOLID* ) from solid-liquid separation and the head product of the stripper column ( *01-TOP* ), are also shown and their condition and composition are listed in Table 4-1.

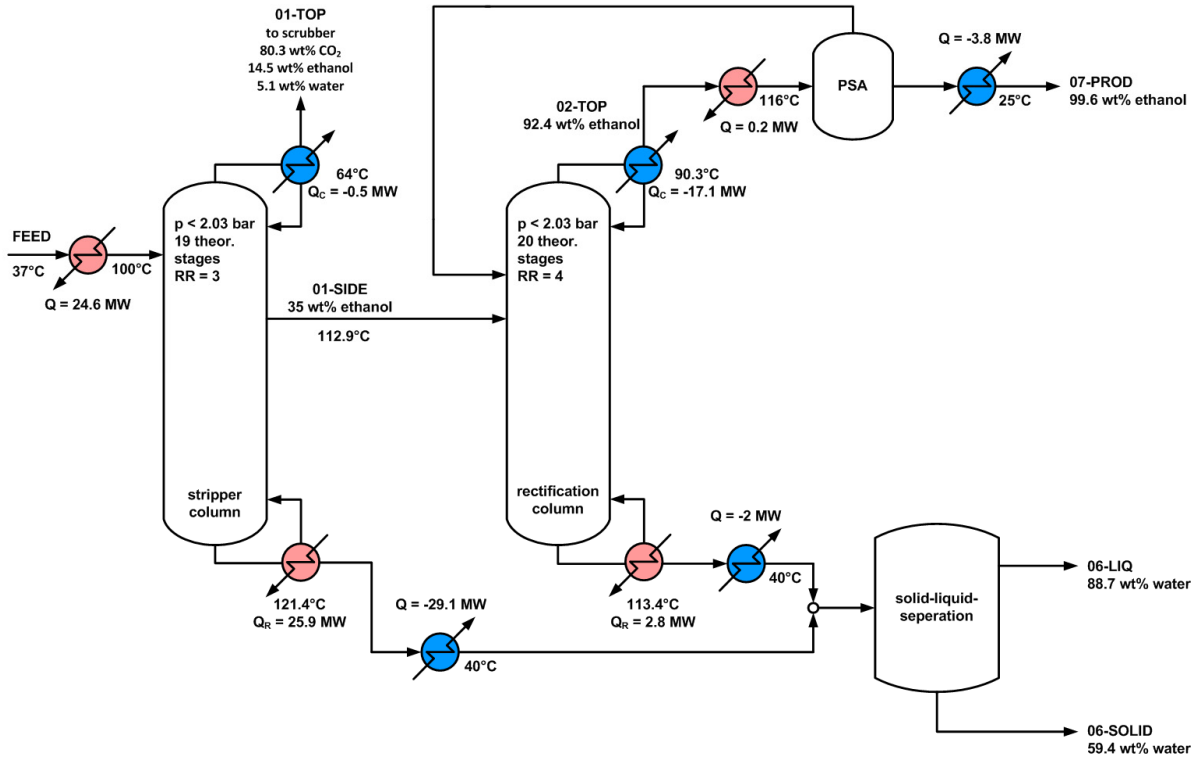


**Figure 4-1:** **Simplified flow sheet of the 2-column distillation configuration, including process simulation specific data.**

The initial stream *FEED,* as described in chapter 3.1, is preheated from 37°C to 100°C before entering the first column, which requires a heat input of 24.6 MW. This equals almost the heat duty of the separation process in the stripper column, which accounts for 25.9 MW. In the stripper column, vapor containing 80.3 wt% of $CO_2$ (95.3% of the total $CO_2$ entering the stripper), 14.5 wt% ethanol and 5.1 wt% water leaves as head product *01-TOP*. The containing ethanol can be recovered in a scrubbing step and re-circulated to the feed stream, which was not considered in this simulation.

**Table 4-1: Listing of the feed and the four product streams in terms of composition in the 2-column distillation setup**

| stream name in ASPEN flow sheet: | | FEED [1.)] | 01-TOP [2.)] | 06-LIQ [3.)] | 06-SOLID [4.)] | 07-PROD [5.)] |
|---|---|---|---|---|---|---|
| total mass flow | [kg/s] | 89.80 | 0.08 | 69.15 | 14.09 | 3.48 |
| **conditions:** | | | | | | |
| temperature | [°C] | 37 | 64 | 40 | 40 | 25 |
| pressure | [bar] | 1.013 | 1.8 | 3.2 | 3.2 | 1.013 |
| **component mass fraction:** | | | | | | |
| WATER | | 0.804 | 0.051 | 0.887 | 0.594 | 0.003 |
| ETHANOL | | 0.040 | 0.145 | 0 | 0 | 0.996 |
| ACETAT | | 0.006 | 0 | 0.008 | 0 | 0 |
| FURFURAL | | 0.003 | 0 | 0.004 | 0 | 0 |
| GLYCEROL | | 0.001 | 0 | 0.001 | 0 | 0 |
| CO2 | | 0.001 | 0.803 | 0 | 0 | 0.001 |
| CELLULOS | | 0.006 | 0 | 0 | 0.034 | 0 |
| XYLAN | | 0.003 | 0 | 0 | 0.016 | 0 |
| LIGNIN | | 0.042 | 0 | 0.003 | 0.243 | 0 |
| XYLOSE | | 0.047 | 0 | 0.058 | 0 | 0 |
| GLUCOSE | | 0 | 0 | 0 | 0 | 0 |
| YEAST | | 0.006 | 0 | 0 | 0.032 | 0 |
| ENZYMES | | 0.002 | 0 | 0.002 | 0 | 0 |
| ASH | | 0.014 | 0 | 0.001 | 0.081 | 0 |
| EXTRAKT | | 0.018 | 0 | 0.023 | 0 | 0 |
| PROTEIN | | 0.009 | 0 | 0.012 | 0 | 0 |

[1.)] alcoholoic mash, fed to the stripper column
[2.)] head product from stripper column
[3.)] liquid residue from solid-liquid separation
[4.)] solid residue from solid liquid separation
[5.)] final ethanol product

The side stream *01-SIDE*, a vaporous product with an ethanol content of 35 wt%, is sent to the rectification column. There, with a reboiler duty of 2.8 MW, ethanol is separated from water, to reach an ethanol concentration of 92.4 wt% at the top of the column. A rectifier condenser duty of 17.1 MW is needed. The head product *02-TOP* is superheated from 90.3°C to 116°C, before it is sent to the PSA. For superheating 0.2 MW have to be provided, which can either be primary steam or in the course of a heat integration. The resulting vaporous ethanol product, containing 99.6 wt% of ethanol, is condensed and cooled to 25°C which requires 3.8 MW of cooling duty.

The bottom products from both columns are cooled down, the respective cooling duties and mass flows, as well as the temperature levels, are listed in Table 4-2. Subsequent to cooling, these streams are mixed and the resulting stream, named distillation stillage, is sent to solid-liquid-separation. The solid residue *06-SOLID* with a WIS content of 40.6%, is separated from the liquid fraction *06-LIQ*. The latter has a water content higher than 88 wt%, a WIS content of 0.7 wt% and a water soluble solids (WSS) content of 9.3 wt%. The composition of the stream *06-LIQ* is subsequently used as initial value for the simulations of biogas-production and the multi-stage evaporation system.

In Table 4-2, all the before mentioned distillation relevant heat sources and sinks are listed. The overall heat and cooling demands account for 53.6 MW and 52.4 MW, respectively. The data obtained will be used in chapter 5 for the Pinch Analysis.

**Table 4-2: Heating and cooling requirement in the 2-column distillation variation, including temperature levels and respective mass flow.**

| name of stream | stream type | $T_{in}$ [°C] | | $T_{out}$ [°C] | mass flow [kg/s] | heat [MW] |
|---|---|---|---|---|---|---|
| preheating of the feed | sink | 37.0 | → | 100.0 | 86.8 | 24.6 |
| superheating before PSA | sink | 90.3 | → | 116.0 | 4.5 | 0.2 |
| reboiler stripper column | sink | boiling at 121.4°C | | | - | 25.9 |
| reboiler rectification column | sink | boiling at 113.4°C | | | - | 2.8 |
| condenser stripper column | heat source | condensation at 64°C | | | - | -0.5 |
| condenser rectification column | heat source | condensation at 90.3°C | | | - | -17.1 |
| cooling stripper bottom | heat source | 121.4 | → | 40.0 | 76.8 | -29.1 |
| cooling rectifier bottom | heat source | 113.4 | → | 40.0 | 6.4 | -2.0 |
| condensation and cooling EtOH product | heat source | 116.0 | → | 25.0 | 3.5 | -3.8 |

### 4.1.2 3-column distillation design

Figure 4-2 shows a simplified flow sheet of the 3-column distillation configuration, with the process relevant temperatures, heating and cooling duties and stream concentrations.

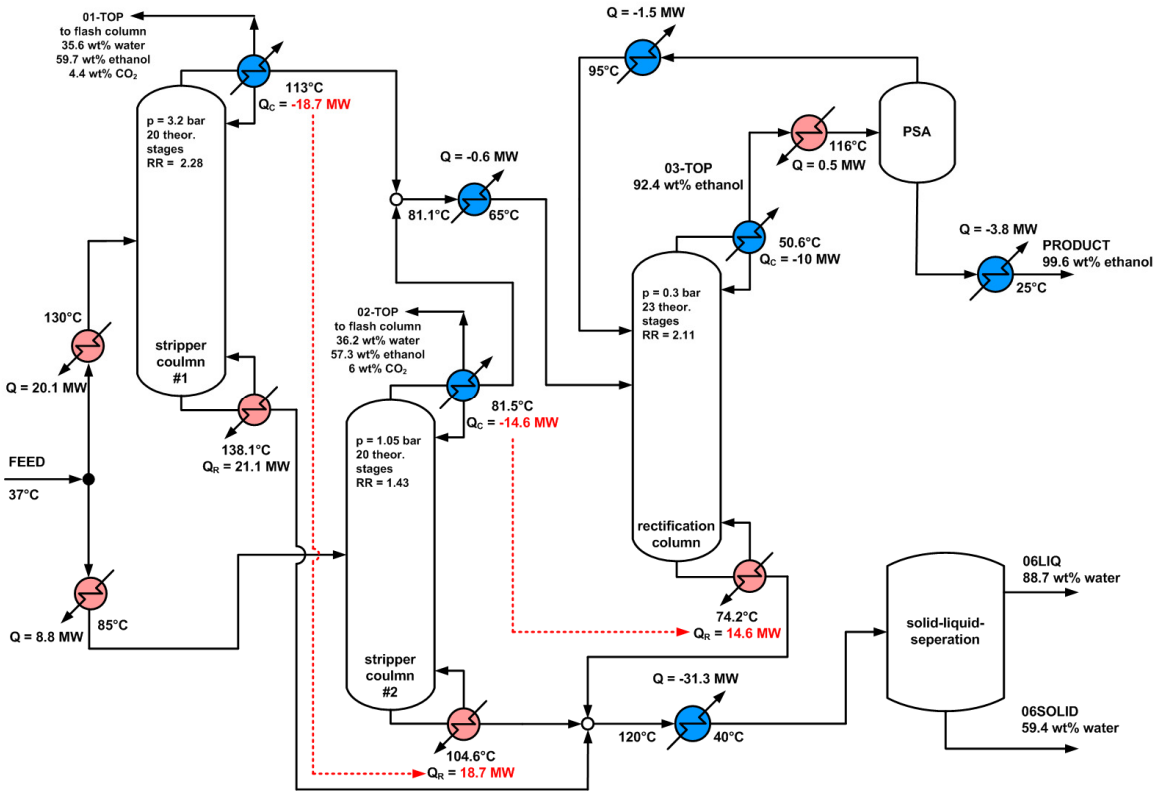


**Figure 4-2: Simplified flow sheet of the 3-column distillation configuration, including process simulation specific data.**

As Figure 4-2 shows, the alcoholic mash is split in two streams, with 3.21 kg/s sent to stripper column #1 and 3.03 kg/s fed to stripper column #2. Preheating to 130°C and 85°C requires 20.1 MW and 8.8 MW, respectively. In both stripper columns the condensers are operated as partial-vapor-liquid condensers, as a result two head products are gained, a liquid stream *01-FTMX* (*02-FTMX* in the second stripper) and a vaporous stream *01-TOP* (*02-TOP*). The vapor contains almost all $CO_2$ fed to the column, but also a large amount of water and ethanol. The ethanol is recovered in a flash column, which is not pictured in Figure 4-2, and then mixed with the liquid head product from the stripper column. An ethanol loss due to flash separation cannot be avoided, but with 0.72 g/s in *01-FLSH* and 1.3 g/s in *02-FLSH*, it is kept within its limits. Another option would be a scrubbing step to recover the ethanol and

return it to the feed, which was not considered in this simulation. Due to condensation, 18.7 MW of heat at 113°C are available in stripper column #1, which is utilized to heat the reboiler of stripper column #2 at 104.6°C. With the 14.6 MW of heat gained in the condenser of stripper column #2, at a temperature of 81.5°C, the rectifier is heated. The reboiler in the rectification column is operated at 74.2°C. Additionally to the ethanol water mixture from the stripper columns the rectifier is fed with the recycle stream from the PSA.

**Table 4-3: Listing of the feed, three product streams and the stripper column head products in terms of composition in the 3-column distillation setup**

| stream name in ASPEN flow sheet: | FEED [1.] | 01-CO2 [2.] | 01-FTMX [3.] | 02-CO2 [4.] | 02-FTMX [5.] | 05LIQUID [6.] | 05SOLID [7.] | PRODUCT [8.] |
|---|---|---|---|---|---|---|---|---|
| total mass flow [kg/s] | 86.80 | 0.02 | 3.03 | 0.03 | 3.21 | 69.16 | 14.10 | 3.50 |
| **conditions** | | | | | | | | |
| temperature [°C] | 37 | 37 | 113 | 25 | 81.5 | 40 | 40 | 25 |
| pressure [bar] | 1.013 | 3 | 3.2 | 1 | 1.05 | 3.2 | 3.2 | 1.013 |
| **component mass fraction** | | | | | | | | |
| WATER | 0.804 | 0.007 | 0.544 | 0.01 | 0.574 | 0.887 | 0.594 | 0.002 |
| ETHANOL | 0.040 | 0.029 | 0.45 | 0.044 | 0.416 | 0 | 0 | 0.994 |
| ACETAT | 0.006 | 0 | 0.002 | 0 | 0.002 | 0.008 | 0 | 0 |
| FURFURAL | 0.003 | 0 | 0.002 | 0 | 0.006 | 0.004 | 0 | 0 |
| GLYCEROL | 0.001 | 0 | 0 | 0 | 0 | 0.001 | 0 | 0 |
| CO2 | 0.001 | 0.964 | 0 | 0.945 | 0 | 0 | 0 | 0.005 |
| CELLULOS | 0.006 | 0 | 0 | 0 | 0 | 0 | 0.034 | 0 |
| XYLAN | 0.003 | 0 | 0 | 0 | 0 | 0 | 0.016 | 0 |
| LIGNIN | 0.042 | 0 | 0 | 0 | 0 | 0.003 | 0.243 | 0 |
| XYLOSE | 0.047 | 0 | 0 | 0 | 0 | 0.058 | 0 | 0 |
| GLUCOSE | 0 | 0 | 0 | 0 | 0 | 0 | 0 | 0 |
| YEAST | 0.006 | 0 | 0 | 0 | 0 | 0 | 0.033 | 0 |
| ENZYMES | 0.002 | 0 | 0 | 0 | 0 | 0.002 | 0 | 0 |
| ASH | 0.014 | 0 | 0 | 0 | 0 | 0.001 | 0.081 | 0 |
| EXTRAKT | 0.018 | 0 | 0.002 | 0 | 0.002 | 0.023 | 0 | 0 |
| PROTEIN | 0.009 | 0 | 0 | 0 | 0 | 0.012 | 0 | 0 |

1.) feed fed to stripper column #1
2.) vaporous head product of stripper column #1, containing mainly $CO_2$ and EtOH
3.) liquid head product of stripper column #1, containing mainly $H_2O$ and EtOH
4.) vaporous head product from stripper column #2, containing mainly $CO_2$ and EtOH
5.) liquid head product of stripper column #1, containing mainly $H_2O$ and EtOH
6.) liquid residue from solid-liquid separation
7.) solid residue from solid liquid separation
8.) final ethanol product

The head product of the rectification column *03-TOP* contains 92.4 wt% of ethanol and during partial condensation 10 MW of cooling duty are required. The vaporous stream *02-TOP* is superheated from 50.6°C to 116°C, which requires 0.5 MW of heat, before it is sent to PSA. There, the vaporous product with a final ethanol concentration of 99.6 wt% is gained, subsequently condensed and cooled to 25°C. The PSA recycle stream, is also condensed and fed to the rectifier.

The bottom products from both stripper columns and the rectification column are mixed and cooled from 120.6 °C to 40°C, pressurized up to 3.2 bars and sent to the solid-liquid separation. The solid residue ( *05SOLID* ) from solid-liquid separation has a WIS content of 40.4 wt%, the liquid product ( *05LIQUID* ) contains 0.4 wt% WIS and 9.5 wt% WSS. All components, except fractions of $CO_2$, ethanol and water, end up either in the *05SOLID* or *05LIQUID* stream.

The operational condition and composition of the feed and the five products is listed in Table 4-3.

**Table 4-4: Listing of the feed and the four product streams in terms of composition in the 3-column distillation setup**

| name of stream | stream type | $T_{in}$ [°C] | | $T_{out}$ [°C] | mass flow [kg/s] | heat [MW] |
|---|---|---|---|---|---|---|
| preheating of the feed #1 | sink | 37 | → | 130 | 46.0 | 20.1 |
| preheating of the feed #2 | sink | 37 | → | 85 | 40.8 | 8.8 |
| superheating before PSA | sink | 50.6 | → | 116 | 4.7 | 0.5 |
| reboiler stripper column #1 | sink | boiling at 138.1 | | | - | 21.1 |
| reboiler stripper column #2 | sink | boiling at 104.6 | | | - | 18.7* |
| reboiler rectification column | sink | boiling at 74.2 | | | - | 14.6* |
| condenser stripper column #1 | heat source | condensation at 113 | | | - | -18.7* |
| condenser stripper column #2 | heat source | condensation at 81.5 | | | - | -14.6* |
| condenser rectification column | heat source | condensation at 50.6 | | | - | -10.0 |
| cool slump | heat source | 120.6 | → | 40 | 83.3 | -31.3 |
| cool re-circulation | heat source | 116 | → | 95 | 1.2 | -1.5 |
| cool feed rectifier | heat source | 81.1 | → | 65 | 7.5 | -0.6 |
| condensation EtOH product | heat source | 116 | → | 25 | 3.5 | -3.8 |

* heat integration as shown in Figure 4-2

In Table 4-4 the heating and cooling duties, as shown in Figure 4-2, are listed. Furthermore, the respective mass flows and temperature levels are stated. The reboiler duty of stripper column #2 and of the rectification column are not considered for the overall heat demand, because this heat requirement is covered by the respective condensation heat of stripper columns #1 and #2.

Of totally 50.5 MW heat, this 3-column distillation variation requires 28.9 MW of it for preheating. The cooling demand accounts for 47.3 MW.

### 4.1.3 Comparison of the different configurations

For comparison of the two different distillation configurations, a final ethanol content of 99.6 wt% is maintained. Furthermore, with 99.98% in both configurations, the demanded 99.9% in ethanol recovery are surpassed as shown in Table 4-5.

**Table 4-5: Comparison of the 2-column and 3-column distillation variation**

| | [unit] | 2-column distillation | 3-column distillation |
|---|---|---|---|
| ethanol content in the final product | [%] | 99.6% | 99.6% |
| ethanol recovery | [%] | 99.98% | 99.98% |
| total heat demand | [MW] | 53.6 | 50.5 |
| total cooling demand | [MW] | 52.4 | 47.3 |
| specific energy requirement (only distillation columns) | [MJ/kg] | 8.3 | 6.0 |
| specific energy requirement (including preheating) | [MJ/kg] | 15.4 | 14.4 |

The specific energy requirement in Table 4-5 is calculated as the quotient of the energy requirement and the amount of anhydrous ethanol produced. If the preheating section is left out, the energy requirement in the 2-column setup accounts for 8.3 $MJ/kg_{EtOH}$ and in the 3-column setup 6 $MJ/kg_{EtOH}$. This is compared with results for different technologies from literature in Figure 4-3. Both values are in the literatures range and with the set specifications in the simulated 3-column configuration an even lower result than given by literature (7 $MJ/kg_{EtOH}$ ; [Galbe, et al., 2007]) can be reached. In Figure 4-3, the required energy to produce one kilogram of anhydrous ethanol, depending on the ethanol concentration in the

fermentation broth, is plotted. The results for the 2-column distillation model are close to the values reached by Jaques, Lyons and Kelsall [2003], which describe the practical minimum for a one stripper and one rectifier system.

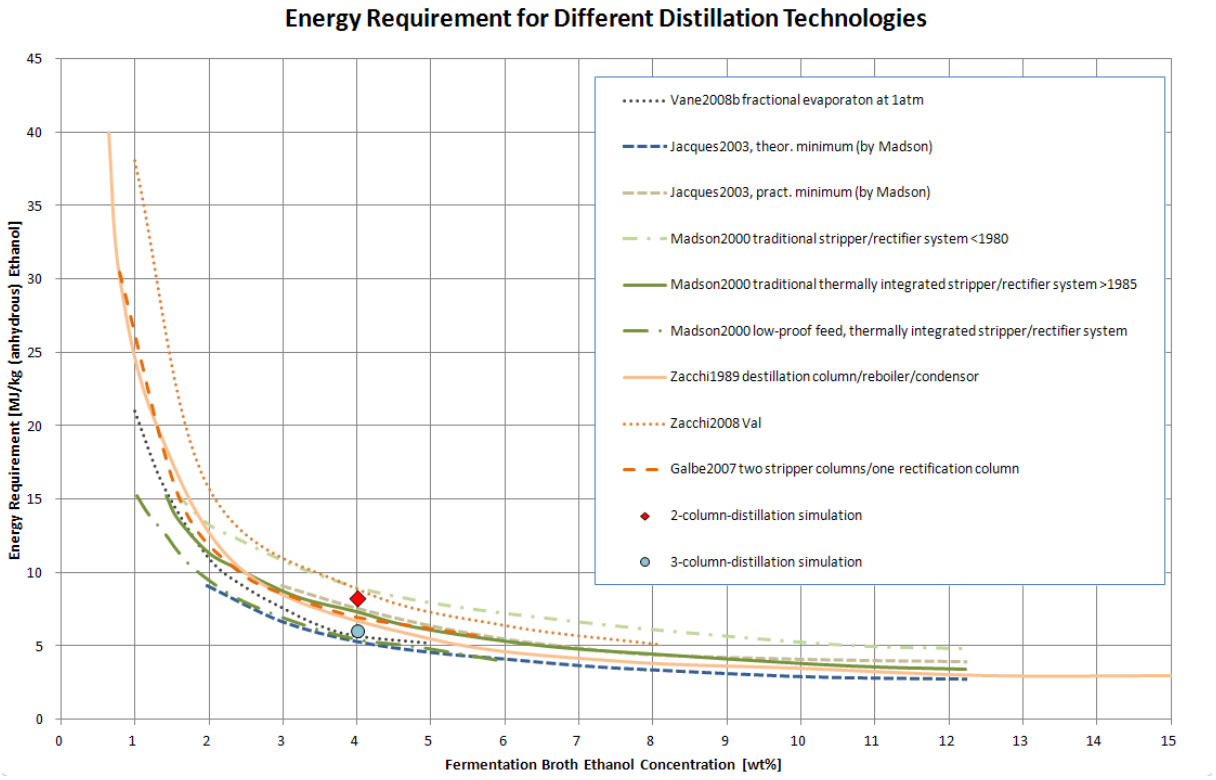


**Figure 4-3:** **Comparison of energy requirements for different distillation technologies including this work's NREL and LUND destillation variation; [Galbe, et al., 2007; Jacques, Lyons and Kelsall, 2003; Madson and Lococo, 2000; Vane, 2008; Zacchi and Axelsson, 1989]**

Additionally, the specific energy requirement for the two different distillation setups considering preheating is listed in Table 4-5. This results in 15.4 MJ/$kg_{EtOH}$ and 14.4 MJ/$kg_{EtOH}$ for the 2-column and the 3-column setup, respectively.

Not only the consideration of the heating demand is of great interest, also the cooling demand can have a large impact on the efficiency of the process. The cooling demand accounts for 52.4 MW and 47.3 MW for the 2-column and the 3-column setup, respectively. These two values only provide information about the total heat that has to be removed, but for comparison the temperature levels and mass flows have also to be considered.

Due to the heat integration in the 3-column configuration, the overall heat demand is reduced, because only the reboiler of the first distillation column has to be heated by utility and only the condensation heat from the rectification column has to be removed. This reflects in the higher difference between the two systems when only the distillation columns are taken into account, compared to the smaller difference with the preheating considered. The heating and cooling demand has to be provided either by utility (process steam and cooling water) or by heat integration of the overall process.

## 4.2 5-stage evaporation system

The simulations of the different 5-stage evaporation configurations were done for the liquid stream resulting from solid-liquid separation of both, the 2-column and the 3-column distillation setup. Because the composition of these streams is very similar, only the results for the 2-column setup are presented. For the Pinch Analysis, also only the evaporation unit results based on the 2-column distillation configuration are used.

To evaluate the evaporation section, three different systems are investigated:

- co-current base case
- co-current flash case (base case with implemented flash condensate system)
- counter-current base case

The target of all evaporation systems is a DM content of 60% in the syrup.

A detailed listing of streams, simulation units, simulation results and flow sheets for the different configurations can be seen in the appendix, section C.

### 4.2.1 Co-current BASE CASE configuration

As Table 4-7 shows, to preheat the feed from 40°C to boiling temperature at 3 bar, 26.8 MW of heat have to be provided. Furthermore, 9.7 kg/s of primary steam are needed to evaporate the solvent at the first stage of the 5 stage evaporation system, which equals 20.8 MW of heat. In the following 4 stages, respective 20.8 MW, 24.4 MW, 26.2 MW and 27.9 MW of heat are transferred to evaporate the solvent, which is listed in Table 4-6.

With increasing stage number, the transferred heat increases accompanied by an increase in amount of solvent evaporated. This is due to the assumption of no heat losses in the system and the partial evaporation of the solvent when entering the evaporation stage operated at a lower pressure.

**Table 4-6: Heat transferred at each stage of the co-current BASE CASE configuration**

| stage nr. | heat transferred [MW] |
|---|---|
| 1 | 20.8 |
| 2 | 20.8 |
| 3 | 24.4 |
| 4 | 26.2 |
| 5 | 27.9 |

At stage five, the biggest fraction of solvent is separated under vacuum conditions, which accounts for 13.3 kg/s. At this stage, also a large amount of acetate (29.5 wt% of total acetate) and extractives (27.7 wt% of total extractives) turns into the vaporous phase. The simulation shows, the higher the pressure at an evaporation stage, the less acetate and extractives are evaporated. Contrary to that, most of the ethanol (68.8 wt% of total ethanol) and furfurals (50 wt% of total furfurals) are already evaporated at the first stage.

**Table 4-7: Heat sources and sinks in the co-current BASE CASE configuration**

| name of stream | stream type | $T_{in}$ [°C] | | $T_{out}$ [°C] | mass flow [kg/s] | heat [MW] |
|---|---|---|---|---|---|---|
| feed preheating | cold | 40.0 | → | 134.0 | 69.1 | 26.8 |
| evaporation first stage | cold | 134.0 | → | 134.1 | 9.8 | 20.8 |
| cool condensate 1st stage | hot | 143.7 | → | 50.0 | 9.7 | -4.1 |
| cool condensate 2nd stage | hot | 133.2 | → | 50.0 | 9.8 | -3.6 |
| cool condensate 3rd stage | hot | 120.1 | → | 50.0 | 11.2 | -3.4 |
| cool condensate 4th stage | hot | 111.3 | → | 50.0 | 11.9 | -3.1 |
| cool condensate 5th stage | hot | 99.7 | → | 50.0 | 12.6 | -2.6 |
| condensation vapor 5th stage | hot | 85.9 | → | 81.4 | 13.3 | -29.5 |
| cool solvent 5th stage | hot | 81.4 | → | 50.0 | 13.3 | -1.7 |

In Table 4-7 the potential cooling demand is represented by the condensate streams from each stage, including the condensation of the evaporated solvent at the last stage, accounting for almost 48 MW of heating demand. With the respective mass flows and temperature levels given, the condensate streams from stages 1 to 4 can be utilized as heat sources to preheat the feed or in the overall process. As a vacuum pump is utilized to create the 0.5 bar at the last stage, the heat from condensation and cooling is not available for heat integration. The overall cooling demand of this setup accounts for 47.9 MW.

The final syrup contains 40 wt% water, 39 wt% xylose, 7.7 wt% protein, 7.3 wt% extractives, 1.7 wt% lignin, 1.5 wt% enzymes and small fractions of acetate, glycerol, cellulose, xylan, furfurals, yeast and ash.

### 4.2.2 Co-current FLASH CASE configuration

An option to reduce the heat demand in the co-current mode is the implementation of a flash condensate system, as described in chapter 3.9.1. The heat needed for preheating is the same as in the base case, but the primary steam demand in this system accounts only for 9.2 kg/s. In Table 4-8 the heat transferred at each stage is listed and it can be seen that it increases much more than in the base case configuration. This is caused by the additionally evaporated solvent in the flash columns.

**Table 4-8: Heat transferred at each stage of the co-current FLASH CASE configuration**

| stage nr. | heat transferred [MW] |
|---|---|
| 1 | 19.7 |
| 2 | 19.7 |
| 3 | 23.8 |
| 4 | 26.6 |
| 5 | 30.1 |

In contrast to the base case, the condensate streams from each stage are further used in the flash system, which result in one large stream that has to be cooled from 99.5°C to 50°C. All

heat sources and sinks in this system are listed in Table 4-9. Due to less primary steam needed, less heat is required to cool the condensate from the first stage.

Same as in the base case, the heat available due to condensation and cooling of the solvent at the 5th stage cannot be utilized for heat integration. These cooling requirements have to be provided by utility.

**Table 4-9: Heat sources and sinks in the co-current FLASH CASE configuration**

| name of stream | stream type | $T_{in}$ [°C] | | $T_{out}$ [°C] | mass flow [kg/s] | heat [MW] |
|---|---|---|---|---|---|---|
| feed preheating | cold | 40.0 | → | 134.0 | 69.1 | 26.8 |
| evaporation first stage | cold | 134.0 | → | 134.1 | 9.3 | 19.7 |
| cool condensate 1st stage | hot | 143.7 | → | 50.0 | 9.2 | -3.9 |
| cool condensate from flash system | hot | 99.5 | → | 50.0 | 44.5 | -9.2 |
| condensation vapor 5th stage | hot | 85.9 | → | 81.4 | 14.3 | -31.7 |
| cool solvent 5th stage | hot | 81.4 | → | 50 | 14.3 | -1.8 |

The final concentrate contains 40 wt% water, 38.9 wt% xylose, 7.7 wt% protein, 7.2 wt% extractives, 1.7 wt% lignin, 1.5 wt% enzymes and small fractions of acetate, glycerol, cellulose, xylan, furfurals, yeast and ash.

### 4.2.3 Counter-current BASE CASE configuration

In contrast to the two co-current configurations, the simulation of the counter-current evaporation system only converged when the feed was not preheated by an external heater. Therefore, the analysis of the counter-current setup is done with the preheating section left out. This entails a higher heat demand in the 5th stage, where the feed enters the system, because the solvent has to be heated to boiling temperature at the respective stage before it can be evaporated. The results for heat demand cannot be compared with the co-current cases, but they give an insight into the general behavior of the counter-current evaporation system.

**Table 4-10: Heat transferred at each stage of the counter-current BASE CASE configuration with preheating left out.**

| stage nr. | heat transferred [MW] |
|---|---|
| 1 | 36.0 |
| 2 | 34.5 |
| 3 | 32.7 |
| 4 | 30.1 |
| 5 | 26.0 |

The transferred heat in the counter-current setup decreases from stage 1 to stage 5, because the biggest amount of solvent has to be evaporated at the first stage, which is shown in Table 4-10. What points out in the counter current configuration is that at stage five only 2.7 kg/s of solvent are evaporated. At this stage most of the heat is used to preheat the feed to boiling temperature. This is far lower than the before mentioned values and the 13.8 kg/s and 11.8 kg/s from stages three and four, which goes hand in hand with the decreasing transferred heat.

It can be seen from the simulation's mass balance, that at the first stage 33.6 wt% of total acetate and 31.2 wt% of total extractives are evaporated. Furthermore, 45 wt% of furfurals and 48.5 wt% of ethanol end up in the vaporous stream of stage 4, whilst 34 wt% of ethanol are evaporated at the last stage.

**Table 4-11: Heat sources and sinks in the counter-current BASE CASE configuration, preheating left out**

| name of stream | stream type | $T_{in}$ [°C] | | $T_{out}$ [°C] | mass flow [kg/s] | heat [MW] |
|---|---|---|---|---|---|---|
| heating first stage | cold | 129.5 | → | 141.1 | 16.4 | 0.4 |
| evaporation first stage | cold | 141.1 | → | 142.1 | 16.4 | 35.5 |
| cool condensate 1st stage | hot | 143.7 | → | 50.0 | 16.8 | -7.1 |
| cool condensate 2nd stage | hot | 133.7 | → | 50 | 16.4 | -5.9 |
| cool condensate 3rd stage | hot | 127.5 | → | 50 | 15.2 | -5.1 |
| cool condensate 4th stage | hot | 120.2 | → | 50 | 13.8 | -4.2 |
| cool condensate 5th stage | hot | 111.1 | → | 50 | 11.8 | -3.1 |
| condensation vapor 5th stage | hot | 100.1 | → | 99 | 2.7 | -6.0 |
| cool solvent 5th stage | hot | 99 | → | 50 | 2.7 | -0.6 |

In Table 4-11 the requirements for heating and cooling in the counter current application are listed, including the respective temperature levels and mass flows. The results for the total heat and cooling demand are 35.9 MW and 32 MW, respectively. These streams could also be utilized for heat integration in the overall lignocellulosic ethanol process.

### 4.2.4 Comparison of co-current and counter current configurations

With a heating demand of 46.5 MW, the implementation of a flash condensate system into the co-current 5-stage evaporation system has not the desired impact to justify the additional equipment necessary. As shown in Table 4-12, the cooling demand can be slightly reduced by 1.3 MW. A comparison with the counter-current setup is not so easy, because preheating was not considered in the simulation setup of the counter-current evaporation system. Still, the results obtained from the simulation can be used as "worst case" of this setup, because preheating before entering the evaporator will only lead to a decrease in heating and cooling demand.

**Table 4-12: Comparison of heating demand, cooling demand and integrated heat for co-current BASE CASE, FLASH CASE and the counter-curent BASE CASE**

| | heating demand [MW] | cooling demand [MW] | heat integration [MW] |
|---|---|---|---|
| co-current BASE CASE | 47.1 | 47.9 | 99.3 |
| co-current FLASH CASE | 46.5 | 46.6 | 100.2 |
| counter-current BASE CASE* | 35.9 | 31.9 | 123.3 |

* no preheating before entering evaporator

The specific heat demand, defined as the ratio of amount of steam used and the amount of solvent evaporated, is used to compare the different configurations. In literature, a specific heat demand of 0.25 $kg_{steam}/kg_{evap.solvent}$ for a 5-stage evaporation system is stated, which is also listed in Table 3-3 [Christen, 2010]. For the three different 5-stage evaporation systems, an even lower specific heat demand can be reached, as Table 4-13 shows. These low values are achieved, because the evaporation system has no heat losses on the one hand and on the other

hand the heat demand needed to preheat the feed from 40°C to boiling point is not considered. Taking the latter into account, results in a dramatically increase in the specific heat demand. The co-current base case and flash case change from 0.165 to 0.408 $kg_{steam}/kg_{evap.solvent}$ and from 0.150 to 0.391 $kg_{steam}/kg_{evap.solvent}$, respectively.

For the counter-current setup only the result for the specific heat demand based on a feed temperature of 40°C is available. Compared to the two co-current setups, the counter-current simulation accounts for 0.280 $kg_{steam}/kg_{evap.solvent}$, which is the lowest value.

Another important factor for the evaluation of the 5-stage evaporation configurations is the amount of evaporated solvent at the last stage. A practical rule indicates, the less evaporated solvent from the last stage is sent to the condenser, the more efficient the evaporation system works – from en energetic point of view [Westphalen and Wolf Maciel, 2000]. The counter-current setup shows by far the best result, accounting for 2.7 kg/s of evaporated solvent compared to 13.3 and 14.3 kg/s for the co-current base case and flash case.

**Table 4-13: Difference in specific heat demand and primary steam demand for the simulated evaporation variations co- and counter current.**

| | [unit] | co-current BASE CASE | co-current FLASH CASE | counter-current BASE CASE |
|---|---|---|---|---|
| **specific heat demand (excl. preheating to boiling point)** | [kg steam/kg evap. solvent] | 0.165 | 0.150 | n.a. |
| **specific heat demand (feed temperature = 40°C)** | [kg steam/kg evap. solvent] | 0.408 | 0.391 | 0.280 |
| **primary steam demand** | [kg/s] | 9.7* | 9.2* | (16.8**) |
| **amount of evaporated solvent at the last stage** | [kg/s] | 13.3 | 14.3 | 2.7 |

* based on the values for specific heat demand excluding the preheating of the feed to boiling point
** based on the value for specific heat demand including the preheating of the feed from 40°C to boiling point

As Westphalen and Wolf Maciel [2000] mention, the amount of evaporated solvent increases through the effects in a co-current configuration, because the evaporation is assisted by the sensible heat of the liquid streams. Contrary, when utilizing a counter-current setup, the amount of evaporated solvent decreases through the effects, due to the increase of the liquid temperature (sensible heat) until boiling temperature, which consumes a certain amount of heat.

The utilization of a flash condensation system results in a small reduction of heating and cooling demand, but increases the amount of evaporated solvent at the last stage. Based on

the results from simulation, the statement by Westphalen and Wolf Maciel [2000] can be confirmed. Still, the savings in primary steam are so low, that the additional equipment is not profitable. Implementing a flash condensate system makes sense, when higher concentrations are demanded, because a higher amount of evaporated solvent results in a higher amount of additional steam due to flash evaporation.

In nowadays industry, not only multi-stage evaporation systems are used to decrease the steam consumption. An alternative to that is the thermal compression process, where part from the vapor is compressed to a higher pressure and fed into the same evaporator as heat source [Billet 1981, p.25]. The compression can either take place thermally by using an injector or mechanically by using a turbo compressor.

For a more detailed look at the energetic differences of the different configurations and the potential for heat integration, a Pinch Analysis will provide needed information.

### 4.2.5 Principles for the Pinch-Analysis of the 5-stage evaporation system

For an energetic evaluation of the different evaporation configurations, the Pinch Analysis method is used. This allows a simple and fast way to determine the heat and cooling demand, as well as the integration factor of the evaporation systems considered.

There are certain assumptions that have to be made, when using the Pinch Analysis for the simulated evaporation systems.

Primary steam needs to be provided at a temperature higher 144°C and 4 bar, because the boiling temperature in the first stage of the co-current setup is 134°C and a minimum temperature difference of 10°C must be maintained. Due to the fact, that the exhaust vapor from one effect is used as heat source at the next stage, the primary steam describes the main heating requirement in the system. The Pinch Analysis is done for the *BASE CASE* of the two different configurations, where the condensate in each stage subsequently is cooled down to 50 °C, as well as for the *FLASH CASE* of the co-current setup.

In Pinch Analysis, only streams with a constant mass flow rate can be used, which has to be considered when separating the streams at each stage. To picture this problem, a closer look at the procedures in each evaporation stage is shown in Figure 4-4.

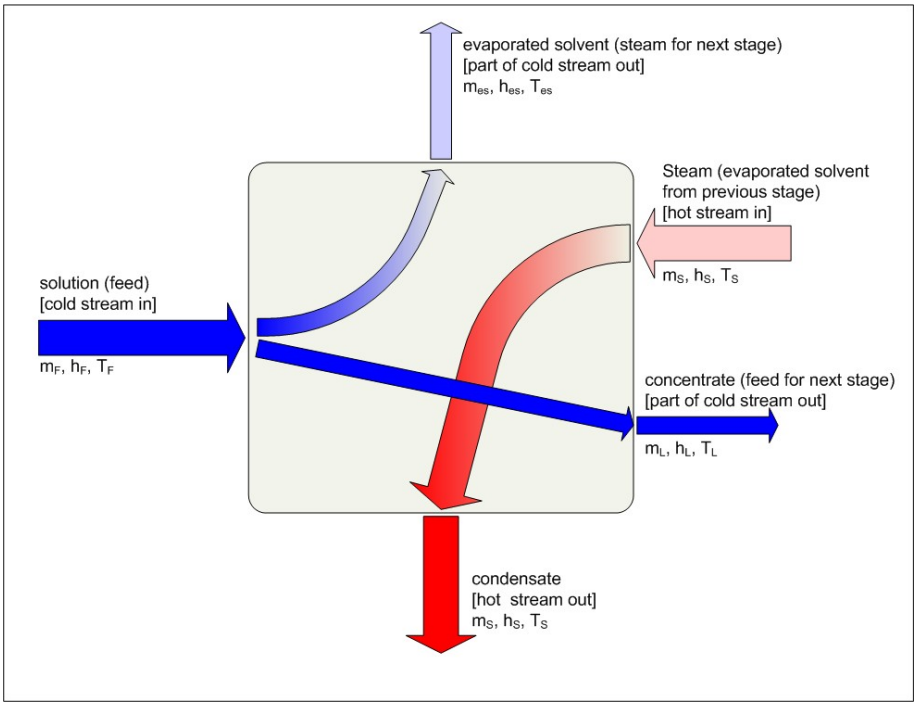


**Figure 4-4:** **Illustration of the procedures occurring at one effect of the multistage-evaporation system**

Due to the condensation of the hot steam, the feed is heated up and partly evaporated, which divides it into two parts – the vapor fraction and the liquid fraction.

The effective heat capacity is calculated by using equation *EQ 33* which considers the required heat up from feed temperature ($T_F$) to boiling temperature ($T_{boiling} = T_{es}$) and the heat for partly evaporation of the solvent ($\Delta h_{evap}$).

$$CP_{eff} = \frac{\frac{\dot{Q}}{\dot{m}_{es}} - \Delta h_{evap}}{(T_{es} - T_F)} \qquad \textit{EQ 33}$$

$T_{es}, T_F$ … temperature of evaporated solvent and feed in °C

$CP_{eff}$ … effective heat capacity in kJ/(kg*K)

$\Delta h_{evap}$ … enthalpy of vaporization in kJ/kg

$\dot{Q}$ … transferred heat in kW

$\dot{m}_{es}$ … mass flow of evaporated solvent in kg/s

The procedure of combined heat up and subsequent evaporation is shown in Figure 4-5 and emerges in every stage of the counter-current configuration, as well as in the first stage of the co-current setup.

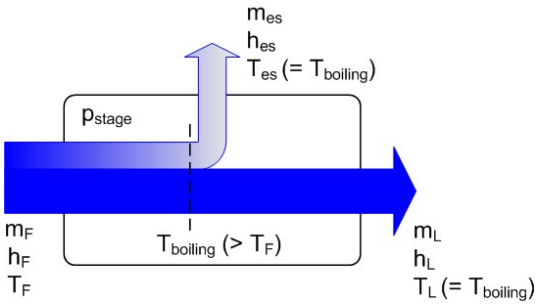


**Figure 4-5: Schematic representation of the procedures in a single stage, when the feed has to be heated up to boiling temperature**

### 4.2.6 Pinch Analysis of 5-stage evaporation systems

Primary steam and the steam formed in the last stage are not considered as sources of heat in the Pinch Analysis. The former is defined as a hot utility in the process, which should be reduced. For the analysis, transferred heat, mass flow, inlet temperature and outlet temperature are taken from the ASPEN PLUS simulation.

For the Pinch Analysis, three different minimum temperature differences $\Delta T_{min}$ are chosen, 8°C, 5°C and 3°C. In the co-current configurations, preheating to boiling temperature before entering the first stage is not considered. For the co-current base case with a minimum temperature difference of 8°C the resulting red colored hot composite curve (HCC) and the blue colored cold composite curve (CCC) are plotted in Figure 4-6. The green colored area shows the section, where heat is recovered in the process due to heat transfer between hot and cold process streams. The horizontal gaps between the HCC and the CCC at 40°C and 144°C are the respective cold and hot utility demands. In this case, the former accounts for 28.6 MW and the latter for 28.9 MW.

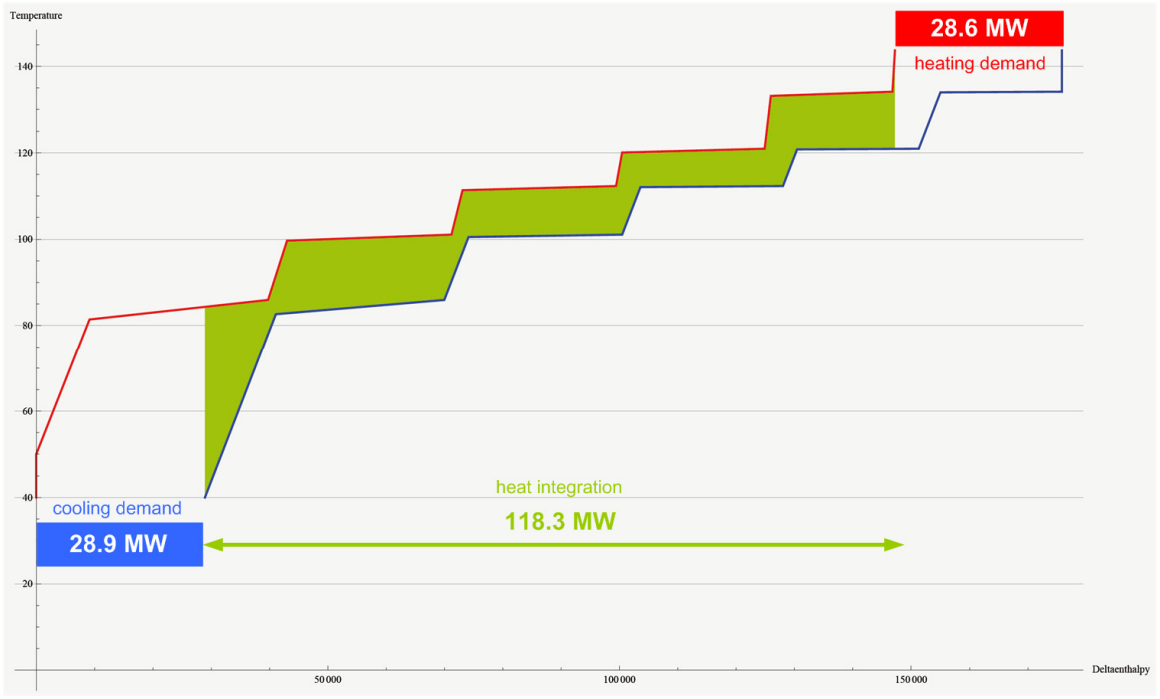


**Figure 4-6: HCC and CCC of the co-current setup with a minimum temperature difference dT = 8°C**

The related grand composite curve (GCC) diagram for this particular case is shown in Figure 4-7, with the temperatures of the utility levels and process streams shifted by $\Delta T_{min}/2$ (see also Linnhoff March [1998]). The GCC provides information about the heating and cooling demand at the different temperature levels of the system.

As pictured in Figure 4-7, the Pinch Point is located at a temperature of 82°C, which describes the point where $\Delta T_{min}$ is observed. At the top of the GCC, the thermodynamically minimum hot utility is represented by the red bar, which accounts for the previous mentioned 28.6 MW and will be provided by middle pressure (MP) steam at 144°C. The blue bar at the bottom (28.9 MW) characterizes the thermodynamically minimum cold utility of the system, which will be covered by cooling water. As expected, with an integrated heat of 118.3 MW, a very high degree of energy integration can be reached by this system.

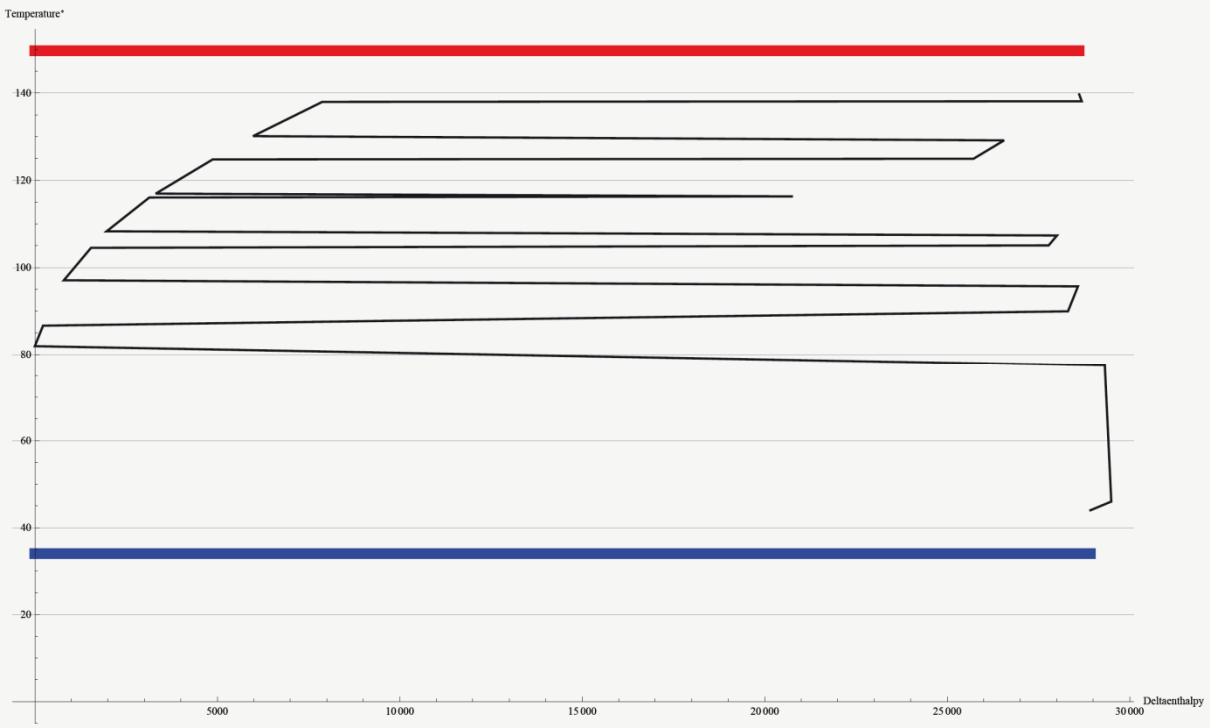


**Figure 4-7: GCC of the co-current setup with a minimum temperature difference dT = 10°C**

The associated GCC, HCC and CCC diagrams for all other process variations with the respective minimum temperature differences can be found in the Appendix, in section D.

### 4.2.7 Interpretation of the Pinch Analysis

In Figure 4-8 and Figure 4-9 the effect of changing the minimum temperature difference for the respective evaporation setups compared to the results from simulation are shown. The respective stage to stage temperature differences for the simulation are given in Table 3-10 in chapter 3.9.1 and vary between 8.6°C and 15.2°C. By changing the temperature minimum, the utility demand (hot and cold) is minimized, which results in a heat integration increase. For the base case of the co-current setup, Figure 4-8 shows that the simulation results are much higher than the case with a minimum temperature difference of 8°C, with a hot and cold utility difference by respectively 18.5 MW and 19 MW. Decreasing $\Delta T_{min}$ to 5°C or 3°C reduces the heat and cooling just slightly.

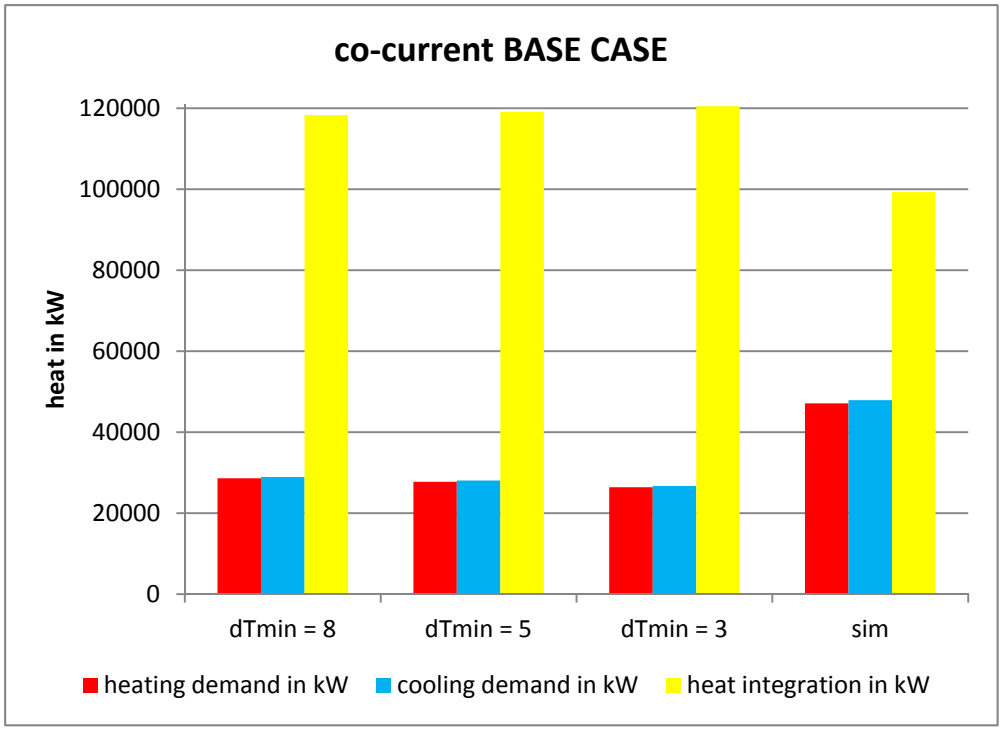


**Figure 4-8:** **Comparison of heating demand, cooling demand and amount of heat integrated in three minimum temperature difference cases (8°C, 5°C, 3°C) and the results from the ASPEN PLUS simulation for the co-current setup**

The effects of a minimum temperature difference change in the co-current setup with additional evaporation of condensate in flash drums, is pictured in Figure 4-9. With 46.5 MW of heating demand and 46.6 MW of cooling demand, the simulation values for this case are a

little bit lower than the simulation values from the base case configuration. The temperature differences between the stages, taken from simulation of the flash case configuration, are the same as for the base case and listed in Table 3-10. The diagram shows that with a minimum temperature difference of 8°C a reduction in heat and cooling demand by 15.7 MW can be reached. A further decrease to 5°C and 3°C results in heating demand savings by respective 0.8 MW and 3.7 MW, accompanied by cooling demand savings of respective 0.9 MW and 3.4 MW.

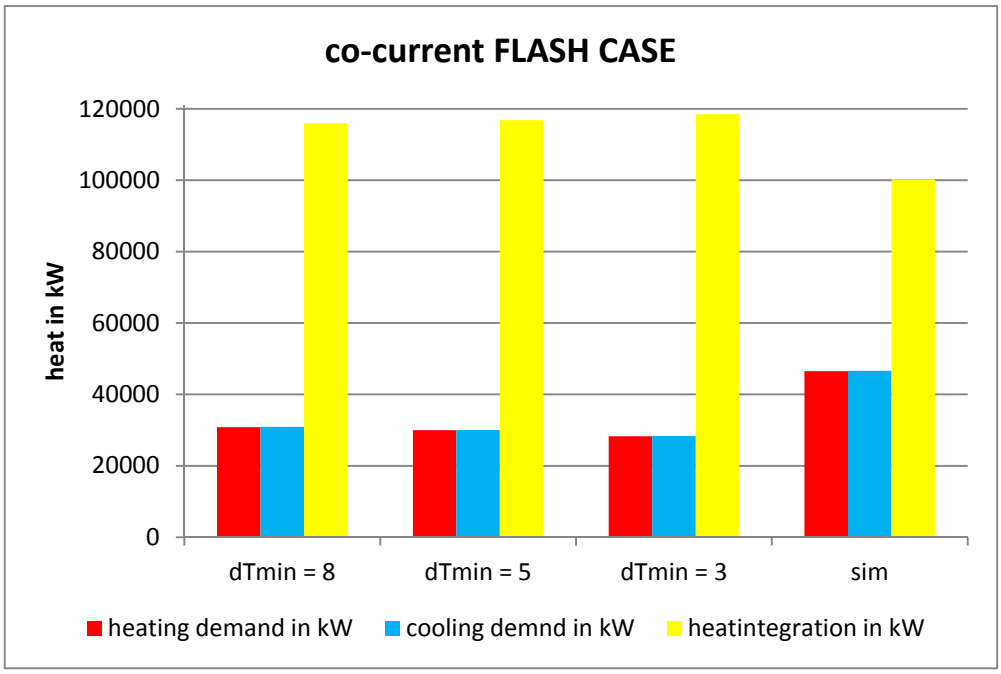


**Figure 4-9:** **Comparison of heating demand, cooling demand and amount of heat integrated in three minimum temperature difference cases (8°C, 5°C, 3°C) and the results from ASPEN PLUS simulation for the co-current setup with implemented flash condensate system.**

In Table 4-14, the results for heating demand, cooling demand and heat integration of the two different configurations are listed. It can be seen, that a change of the minimum temperature difference has a larger impact for the co-current base case than for the co-current flash case.

**Table 4-14: Comparison of heating demand, cooling demand and heat integration for different $dT_{min}$ in the co-current base case and flash case setup.**

| case | | $\Delta T_{min}$ [°C] | heating demand [kW] | cooling demand [kW] | heat integration [kW] |
|---|---|---|---|---|---|
| co-current | BASE CASE | $dT_{min}$ = 8 | 28.6 | 28.9 | 118.3 |
| | | $dT_{min}$ = 5 | 27.8 | 28.1 | 119.2 |
| | | $dT_{min}$ = 3 | 26.4 | 26.7 | 120.5 |
| | | ASPEN sim. | 47.1 | 47.9 | 99.3 |
| | FLASH CASE | $dT_{min}$ = 8 | 30.8 | 30.9 | 116.0 |
| | | $dT_{min}$ = 5 | 30.0 | 30.0 | 116.8 |
| | | $dT_{min}$ = 3 | 28.3 | 28.4 | 118.5 |
| | | ASPEN sim. | 46.5 | 46.6 | 100.2 |

The large differences in heating and cooling demand between the results from the simulation and Pinch Analysis are traced back to the fact that in the simulation, preheating of the feed to boiling temperature is taken into account. The utilization of the condensates from each evaporation stage for feed preheating provides a high potential for energy recovery.

## 4.3 Biogas-production

The 69.1 kg/s of liquid reside coming from solid-liquid separation has a COD of 154 g/l. With the defined reactions and the respective conversion rates, as described in chapter 3.10 and a resulting COD removal of 72%, 6.78 kg/s of biogas will be gained. The composition of the biogas is given in Table 4-15 and it can be assumed that the volume fraction is equal to the mole fraction, resulting in 49.9 vol% of $CH_4$ and 43.7 vol% of $CO_2$.

**Table 4-15: Composition of the biogas produced in the ASPEN PLUS simulation**

| component | mass fraction [kg/kg] | mole fraction [kmol/kmol] |
|---|---|---|
| $CH_4$ | 0.282 | 0.499 |
| $CO_2$ | 0.678 | 0.437 |
| $H_2O$ | 0.039 | 0.062 |
| $NH_3$ | 0.001 | 0.002 |

For comparison, the theoretical possible methane yield is calculated according to Buswell and Mueller [1952] by using *EQ 25* from chapter 3.5.2 for all organic compounds except lignin and ash. The resulting value for $CH_4$ and $CO_2$ content compared to the results from the ASPEN PLUS simulation are listed in Table 4-16. The difference in biogas yield results from the difference in conversion rates for the components. The Buswell equation calculates the theoretically possible maximum methane yield, assuming a total conversion of each organic component. In the ASPEN PLUS simulation different conversion factors for the respective components are applied, as they are listed in Table 3-12 in chapter 3.10.

**Table 4-16: Comparison of theoretically possible biogas yield according to Buswell and Mueller [1958] and the results gained from the ASPEN PLUS simulation.**

| calc. method | biogas yield | | | | | | | |
|---|---|---|---|---|---|---|---|---|
| | $CH_4$ | | | | $CO_2$ | | | |
| | mass flow [kg/s] | mole flow [kmol/s] | mass fraction [kg/kg] | mole fraction [kmol/kmol] | mass flow [kg/s] | mole flow [kmol/s] | mass fraction [kg/kg] | mole fraction [kmol/kmol] |
| Buswell | 2.825 | 0.176 | 0.282 | 0.499 | 5.886 | 0.134 | 0.678 | 0.437 |
| ASPEN PLUS simulation | 1.911 | 0.119 | 0.294 | 0.534 | 4.592 | 0.104 | 0.706 | 0.466 |

The composition of the theoretically possible biogas, with 57 vol% methane and 43 vol% of carbon dioxide, varies a little bit from the simulation result.

With 6.78 kg/s of biogas produced, a mass fraction of 0.282 and a lower heating value of methane of 50.1 MJ/kg, an energy potential of 95.7 MW is calculated. Theoretically, an energy potential of 141.5 MW could be obtained, as listed in Table 4-17.

**Table 4-17: Energy content of the biogas**

| calculation method | energy content [MW] |
|---|---|
| Buswell | 141.5 |
| ASPEN PLUS simulation | 95.7 |

### 4.3.1 Reactor dimension

For a rough estimation of the digester size, an organic loading rate of 15 g-COD/(l*d) is chosen. This value is based on the findings from literature, as listed in Table 3-5 in chapter 3.5.2. With a calculated chemical oxygen demand of 153.26 g-COD/l and the volume flow rate taken from ASPEN PLUS simulation, the required reactor volume results in 63285 m³. As Table 4-18 shows, with a reactor volume of that size, the required hydraulic retention time accounts for 10.2 days.

**Table 4-18: Assumptions and results for the design of the anaerobic digester**

| reactor sizing | | |
|---|---|---|
| **assumptions** | | |
| COD | [g/l] | 153.26 |
| Volume flow of substrate | [m³/h] | 258.076 |
| OLR | [g-COD/(l*d)] | 15 |
| **results** | | |
| Reactor volume | [m³] | 63285 |
| HRT | [d] | 10.2 |

Compared to a reactor volume of 22600 m³, as it is needed in the upstream process for the ethanol conversion, the calculated 63285 m³ are very high [Kravanja, et al., 2011]. This can be considered as the major drawback of the biogas production. To reduce the digester volume, faster and more efficient conversions are needed, as it is the case with high performance reactors.

# 5 Energy integration of the process variants in context with the background process

The different configurations for the down stream process in the ethanol production from lignocellulosic material are evaluated using Pinch Analysis to determine the energy demand of the overall process. Furthermore, the appropriate distillation setup for biogas and evaporation should be found. Therefore, the data from the ASPEN PLUS simulation of the four different configurations, together with the data from the background process is analyzed. The four configurations, also pictured in Figure 5-1, are as follows:

**A.)** Background process + 2-column distillation + 5-stage evaporation

**B.)** Background process + 3-column distillation + 5-stage evaporation

**C.)** Background process + 2-column distillation + biogas production

**D.)** Background process + 3-column distillation + biogas production

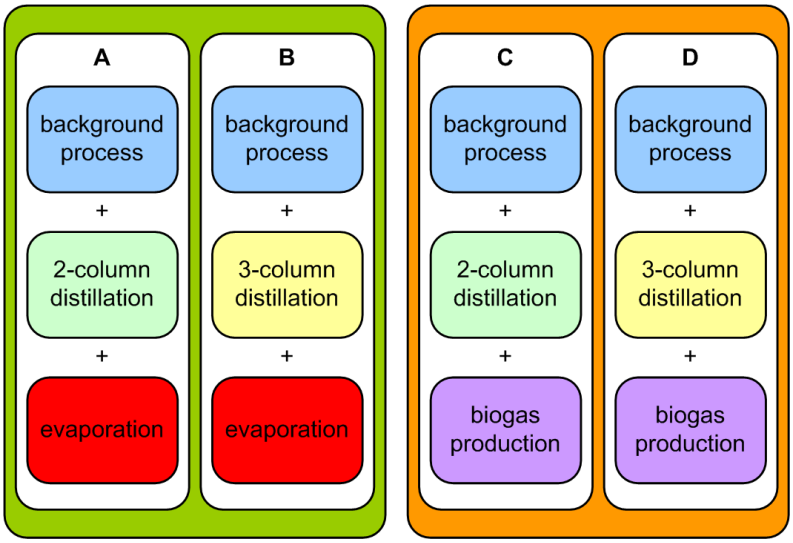


**Figure 5-1: Process configuration variations for energetic comparison**

**Background process:**

The data taken into account for the background process, which is described in chapter 3.11, is based on previous simulation work [Kravanja, et al., 2011]. In Table 5-1 all Pinch Analysis relevant streams for the background process are listed, including the preheating and the steam pretreatment of the straw, the condensation and cooling of steam at different pressure levels, the enzyme production and SSF, as well as the streams in the drying section of the process. All streams are defined by the inlet and outlet temperature, the mass flow and the transferred heat. The stream type gives information, whether the stream is a sink (cold) or a heat source (hot).

**Table 5-1: Pinch Analysis specific streams for the background process.**

| name of stream part | stream type | $T_{in}$ [°C] | $T_{out}$ [°C] | mass flow [kg/s] | heat [MW] |
|---|---|---|---|---|---|
| **Preheat straw for SE** | | | | | |
| Preheat straw for SE | cold | 23.15 | 99 | 57.8 | 14.1 |
| **Steam pretreatment** | | | | | |
| Heat water for SE | cold | 15 | 211.7 | 10.06 | 8.5 |
| Evaporate water for SE | cold | 211.7 | 212.7 | 10.06 | 19.02 |
| **Superheat drying steam** | | | | | |
| Superheat drying steam | cold | 149 | 210 | 98.7 | 13.1 |
| **Condense and cool steam from SE 4 bar** | | | | | |
| Condense SE 4 bar steam | hot | 143.6 | 142.6 | 5.8 | 12.4 |
| Cool SE 4 bar steam | hot | 143.6 | 37 | 5.8 | 2.6 |
| **Condense and cool steam from SE 1 bar** | | | | | |
| Condense SE 1 bar steam | hot | 99.96 | 98.96 | 4.12 | 9.3 |
| Cool SE 1 bar steam | hot | 98.96 | 37 | 4.12 | 1.08 |
| **Cool pretreated biomass** | | | | | |
| Cool pretreated biomass | hot | 99 | 42.8 | 57.98 | 10.7 |
| **Enzyme production and SSF** | | | | | |
| Cool reactor yeast production | hot | 31 | 30 | 9.9 | 1.6 |
| Cool reactor enzyme production | hot | 31 | 30 | 5.4 | 0.96 |
| Cool reactor SSF | hot | 38 | 37 | 89.8 | 2.9 |
| **Condense and cool secondary steam from dryer** | | | | | |
| Cool secondary steam dryer | hot | 149 | 145.37 | 5.8 | 0.05 |
| Condense secondary steam | hot | 145.37 | 144.37 | 5.8 | 12.3 |
| Cool secondary steam condensate | hot | 145.37 | 37 | 5.8 | 2.6 |

**Distillation:**

The considered process streams for the distillation section are based on the mass and energy balance results from the ASPEN PLUS simulations in chapter 4.1. For the Pinch Analysis the streams of the respective configuration have to be distinguished. This is can be seen in Table 5-2, where all relevant streams for the 2-column distillation and all relevant streams for the 3-column distillation are listed separately.

**Table 5-2: Pinch Analysis specific process streams for the distillation section**

| name of stream part | stream type | $T_{in}$ [°C] | $T_{out}$ [°C] | mass flow [kg/s] | heat [MW] |
|---|---|---|---|---|---|
| **2-column distillation:** | | | | | |
| Preheating of the feed | cold | 37 | 100 | 89.8 | 24.6 |
| Superheating before PSA | cold | 90.3 | 116 | 4.46 | 0.2 |
| Reboiler stripper column | cold | 120.9 | 121.9 | 76.82 | 25.9 |
| Reboiler rectification column | cold | 112.9 | 113.9 | 6.42 | 2.8 |
| Condenser stripper column | hot | 64.5 | 63.5 | 0.08 | 0.46 |
| Condenser rectification column | hot | 90.8 | 89.8 | 4.46 | 17.07 |
| Cooling stripper bottom | hot | 121.4 | 40 | 76.82 | 29.1 |
| Cooling rectifier bottom | hot | 113.4 | 40 | 6.42 | 2.03 |
| Condensation EtOH product | hot | 116 | 25 | 3.48 | 3.8 |
| **3-column distillation:** | | | | | |
| Preheating of the feed #1 | cold | 37 | 130 | 46.01 | 20.1 |
| Preheating of the feed #2 | cold | 37 | 85 | 40.8 | 8.8 |
| Superheating before PSA | cold | 50.6 | 116 | 4.7 | 0.5 |
| Reboiler stripper column #1 | cold | 137.6 | 138.6 | 42.17 | 21.1 |
| Reboiler stripper column #2 | cold | 104.1 | 105.1 | 37.06 | 18.7 |
| Reboiler rectification column | cold | 73.7 | 74.7 | 4.02 | 14.6 |
| Condenser stripper column #1 | hot | 113.5 | 112.5 | 3.03 | 18.7 |
| Condenser stripper column #2 | hot | 82 | 81 | 3.21 | 14.6 |
| Condenser rectification column | hot | 51.1 | 50.1 | 4.7 | 10.04 |
| Cooling slump | hot | 120.6 | 40 | 83.26 | 31.3 |
| Cooling re-circulation | hot | 116 | 95 | 1.2 | 1.5 |
| Cooling feed of the rectifier | hot | 81.1 | 65 | 7.52 | 0.65 |
| Condensation EtOH product | hot | 116 | 25 | 3.5 | 3.8 |

**5-stage evaporation:**

To consider the 5-stage evaporation in the process configurations A and B, the data from the co-current base case setup in chapter 4.2.1 is taken. The respective streams with temperature levels, mass flows and heat demand are listed in Table 5-3.

**Table 5-3: Pinch Analysis specific process streams for the evaporation section**

| name of stream part | stream type | $T_{in}$ [°C] | $T_{out}$ [°C] | mass flow [kg/s] | heat [MW] |
|---|---|---|---|---|---|
| **Evaporation** | | | | | |
| Feed preheating | cold | 40 | 134 | 69.15 | 26.8 |
| Evaporation first stage | cold | 134 | 134.1 | 9.78 | 20.8 |
| Cooling condensate 1st stage | hot | 143.7 | 50 | 9.72 | 4.1 |
| Cooling condensate 2nd stage | hot | 133.2 | 50 | 9.78 | 3.6 |
| Cooling condensate 3rd stage | hot | 120.1 | 50 | 11.20 | 3.4 |
| Cooling condensate 4th stage | hot | 111.3 | 50 | 11.91 | 3.1 |
| Cooling condensate 5th stage | hot | 99.7 | 50 | 12.58 | 2.6 |
| Condensation vapor 5th stage | hot | 86 | 81.4 | 13.31 | 29.5 |
| Cooling solvent 5th stage | hot | 81.4 | 50 | 13.31 | 1.7 |

The Pinch Analysis in chapter 4.2.6 shows that the co-current configuration of the multi-stage evaporation is internally well integrated and is therefore seen as a black box in the analysis of the overall process.

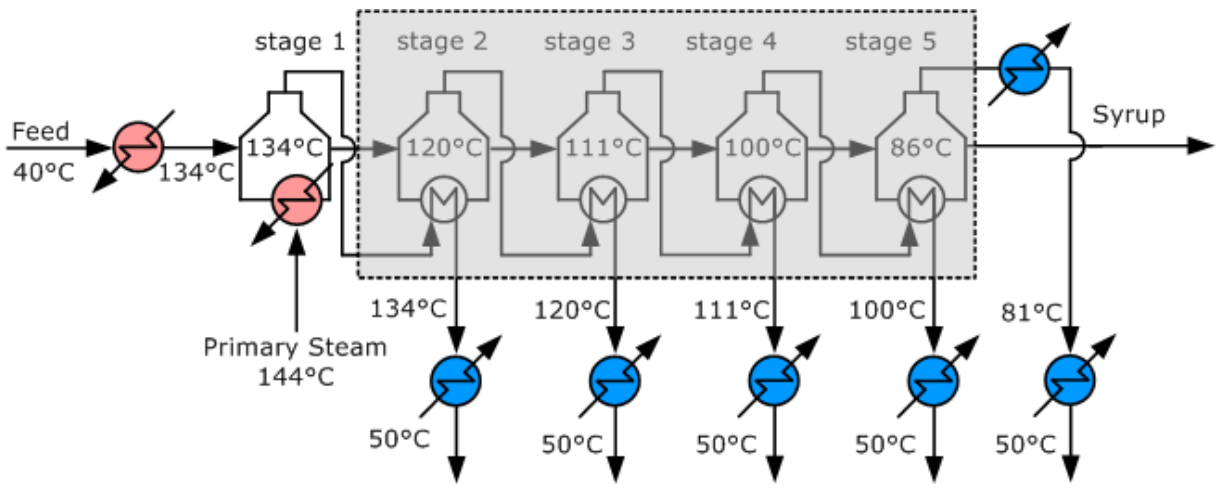


**Figure 5-2: Streams from evaporation considered for Pinch Analysis of the overall process configurations**

As a result only the preheating of the feed and the evaporation at the first stage has to be considered as heat sinks, which is shown in Figure 5-2. Furthermore, the cooling of the condensate streams from each stage and the condensation of the vaporous solvent from the fifth stage are accounted as heat sources.

**Biogas production:**

In the configurations including the biogas production (C and D), only streams from the background process and the distillation section are taken into account. The anaerobic digestion is assumed to have no heating and cooling demand, because there is no detailed information about it. Digester size, heat losses and heat of reaction have to be known for a reasonable approach.

The temperature of the stream entering the digester is 40°C, which corresponds to operational conditions of the biogas production, where mesophilic conditions (37°C) for the anaerobic digestion are assumed and the heat losses are partly balanced by the heat of reaction. The energy demand of the fermentor will be very small compared to the energy intensive steam pretreatment, distillation, evaporation and drying [P. Kravanja, personal comunication, 2011].

For the Pinch Analysis of the different overall process configurations a minimum temperature difference $\Delta T_{min}$ = 7°C is chosen.

# 6 Results & Discussion

The results obtained from Pinch Analysis are listed in Table 6-1. The concepts including evaporation are compared with each other, same as the concepts including biogas. A crosswise comparison of evaporation and biogas concepts is pointless, because the latter has lower energy consumption in principle. For the calculation of the minimum energy consumption, the required heat demand for the overall process is taken into account.

If a 5-stage evaporation system is utilized for stillage treatment, the 3-column distillation concept requires less heating and cooling demand, with savings of 3.7 MW in hot utility and 5.7 MW in cold utility.

**Table 6-1: Comparison of heating demand, cooling demand and integrated heat for the different process configurations.**

| | [unit] | 5-stage evaporation | | biogas production | | |
|---|---|---|---|---|---|---|
| | | 2-column distillation | 3-column distillation | 2-column distillation | 3-column distillation | 3-column distillation |
| Set $dT_{min}$ in Pinch Analysis | [°C] | 7 | 7 | 7 | 7 | 5 |
| Heating demand | [MW] | 64.0 | 60.3 | 38.8 | 46.8 | 35.2 |
| Cooling demand | [MW] | 64.8 | 59.1 | 39.3 | 45.4 | 33.7 |
| Heat integration | [MW] | 91.9 | 125.9 | 69.5 | 91.7 | 103.4 |
| Pinch point | [°C] | 116.4 | 116.6 | 116.4 | 141.1 | 142.9 |
| Minimum energy consumption per kg of ethanol | [MJ/$kg_{EtOH}$] | 18.4 | 17.2 | 11.1 | 13.4 | 10.0 |
| **variant** | | **A** | **B** | **C** | **D** | |

The Pinch Analysis for the processes including biogas production, with a set minimum temperature difference of 7°C, results in a lower heating and cooling demand for the 2-column distillation concept. The grand composite curve of the biogas concept including a 3-column distillation (Figure 6-1), with a respective heating and cooling demand of 46.8 MW and 45.4 MW, shows that the two streams very close to the pinch point could not be integrated due to a too small temperature difference and this causes additional heating and cooling. One of them represents the heat needed by the reboiler of the stripper column operated at 3 bar. The temperature level of the reboiler is just slightly higher than the temperature level of the steam provided by the background process.

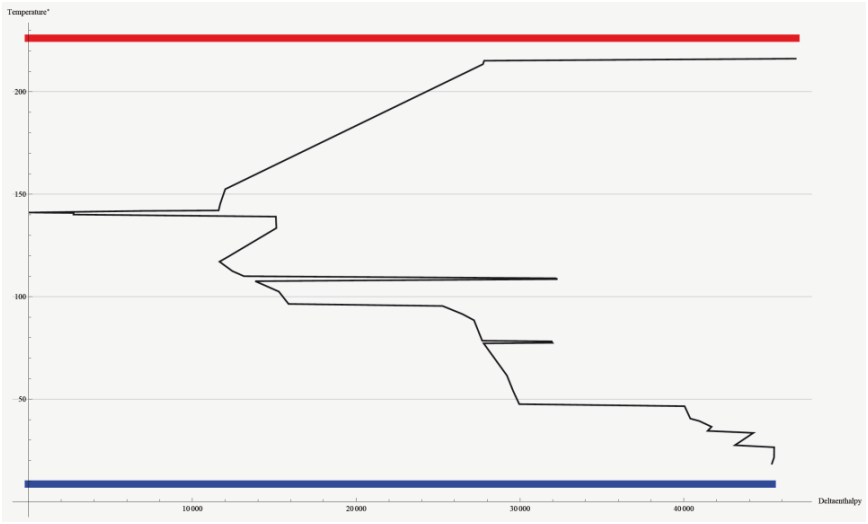


**Figure 6-1: GCC of the process including 3-column distillation and subsequent biogas production**

These additional energy requirements are reduced by changing the minimum temperature difference to 5°C, as shown in Figure 6-2. With 35.2 MW and 33.7 MW, the respective heat and cooling demand results in a better concept than the combination of biogas with a 2-column distillation. An investigation of the process streams showed, that the two process streams causing this problem are the secondary steam at 4 bar and the reboiler of the stripper column, with a respective outlet temperature of 142.6°C and 138.6°C.

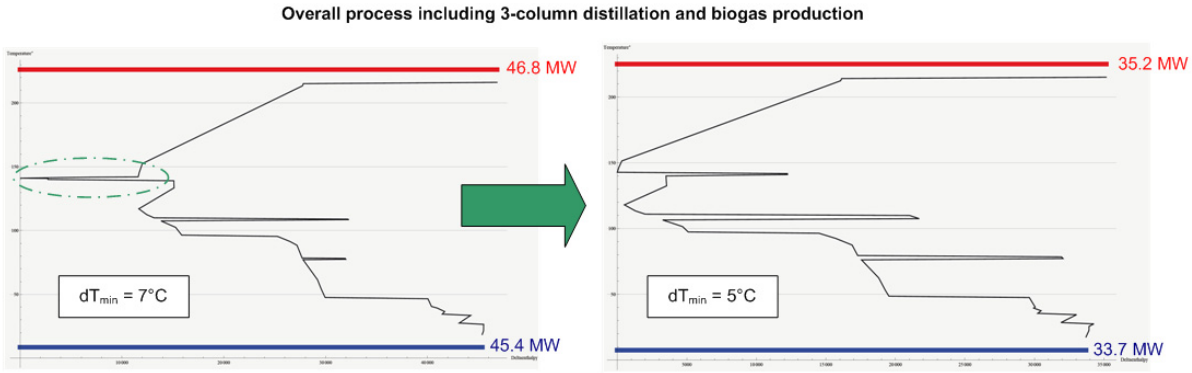


**Figure 6-2:** **Effect on energy requirements by changing the minimum temperature difference in the Pinch Analysis.**

Maintaining the necessary minimum temperature difference can make this heat feasible, either by providing the secondary steam at a higher pressure or by lowering the operational pressure of the stripper column.

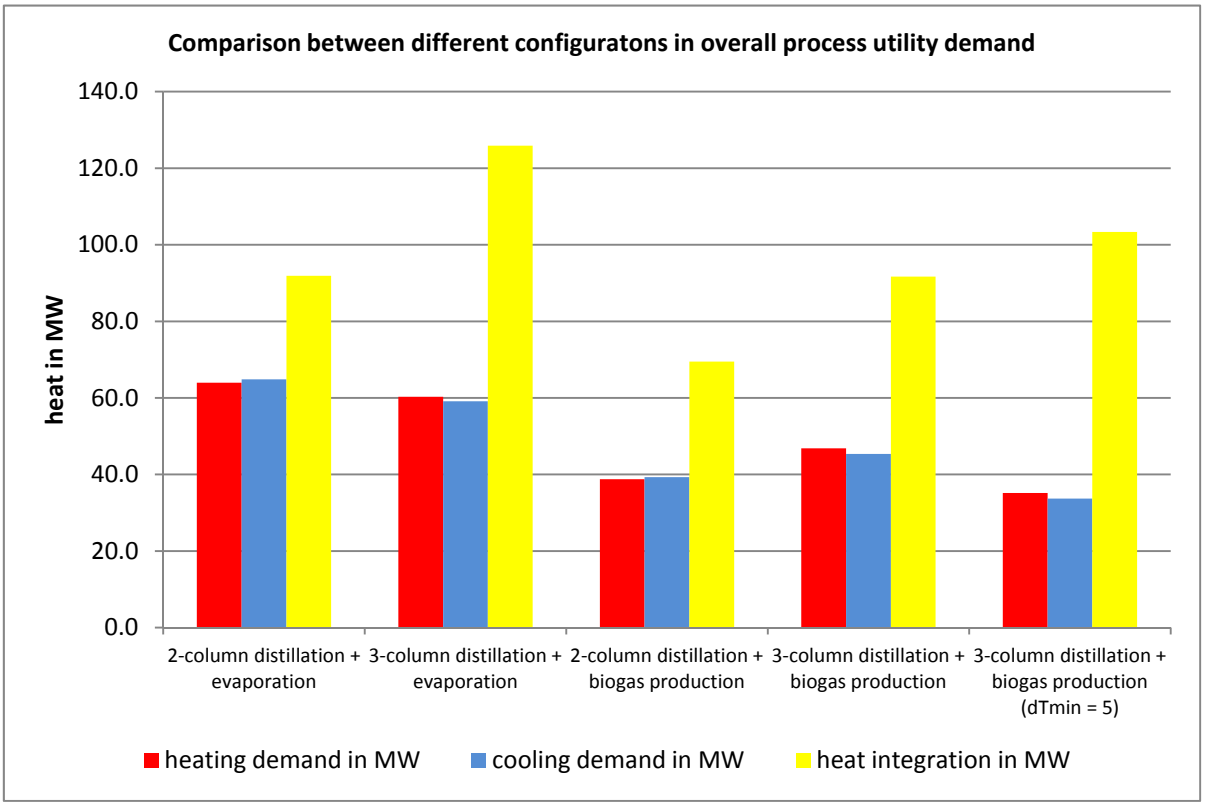


**Figure 6-3:** **Comparison of the different configurations by heating demand, cooling demand and heat integration**

The evaluation of the four different concepts, which is pictured in Figure 6-3, shows that the configurations B and D are preferable for the respective stillage treatment by evaporation and biogas production. In both variants the 3-column distillation concept is utilized. It is questionable if the moderate savings in heating and cooling demand justify the additional expenses in equipment. A techno-economic evaluation of the process variants is needed to answer this question.

As Figure 6-3 shows, the highest heat integration could be achieved in the combination of 3-column distillation with the 5-stage evaporation system. The respective hot and cold composite curves of this configuration are pictured in Figure 6-4.

The hot and cold composite curves, as well as the grant composite curves for the evaluated process variants can be found in the appendix, section D.

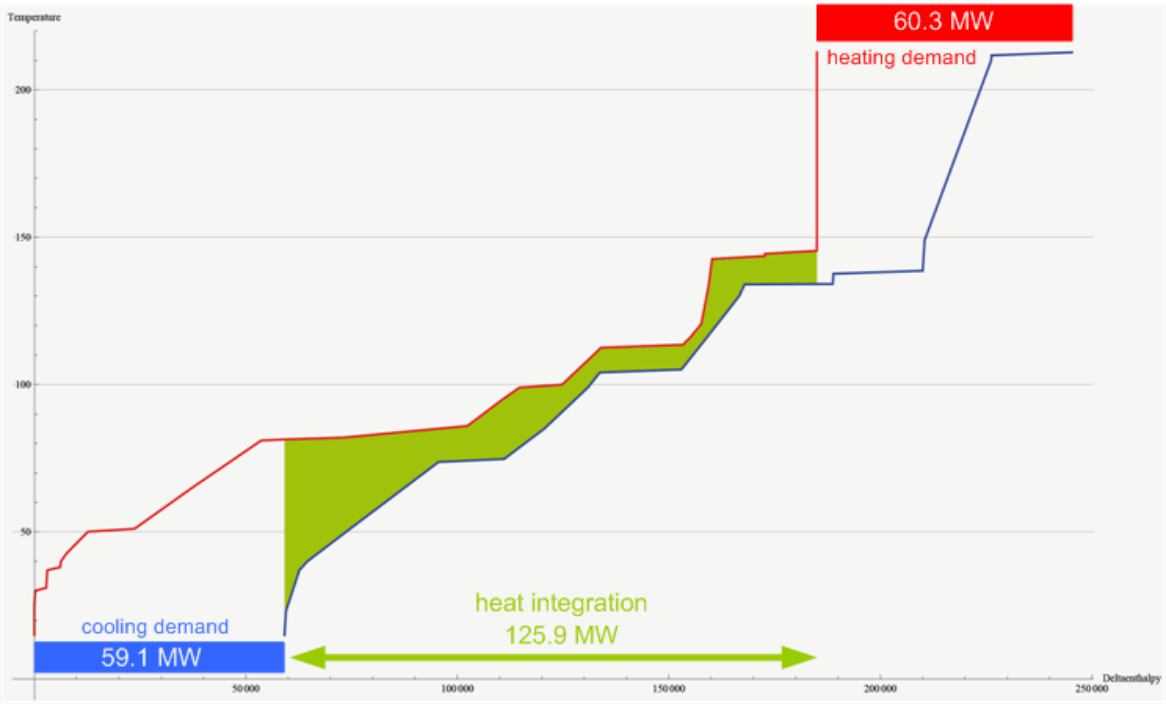


**Figure 6-4: HCC and CCC of the overall process including 3-column distillation with subsequent evaporation of the stillage**

Another option to reduce the energy requirements of the different concepts is the implementation of a heat pump. The grand composite curve of variant A, as pictured in Figure 6-5, shows the possible application area for the heat pump. The heat pump should be integrated across the pinch, which is at 116°C in this case, to pump the heat from the part

below the pinch to the part above the pinch. The heat below 116°C can be seen as a heat source and heat available above 116°C can be seen as a heat sink.

The heat pump's performance depends on its coefficient of performance ($COP_{HP}$), which is defined as the useful energy delivered to the process divided by the power expended to produce this useful energy [Smith 2005, p.382].

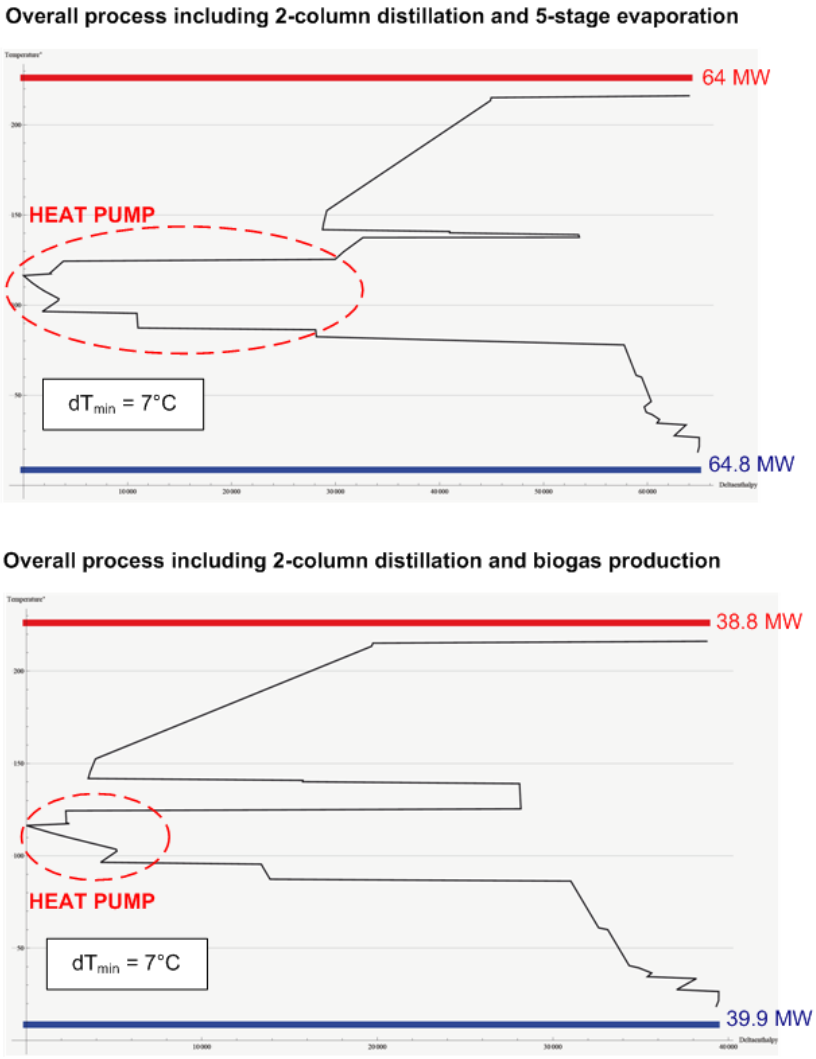


**Figure 6-5: Possibilities for heat pump implementation in variant A and C.**

To utilize a heat pump in variant A, as shown in the upper picture of Figure 6-5, the heat source at 85°C could be used as heat sink at 125°C by means of electricity used in the heat

pump. For a temperature difference of 40°C and with a $COP_{HP}$ of 3, the electric power of 10 MW would be necessary in the heat pump [Modarresi, personal comunication, 2011]. At that high temperature level, conventional heat pumps cannot be utilized, but there are some high temperature applications available. The profitability along with the feasibility depends on the additional costs for the heat pump, the electric power needed and the resulting reduction in heat and cooling demand.

# 7 Conclusion & Perspective

In the overall ethanol from lignocellulosic biomass process, the downstream section accounts for more than 60% of the total energy demand. Furthermore, the energy demand of the distillation section varies between 31% and 34%, depending on the configuration used. Whether in a 2-column or a 3-column configuration, the distillation is the standard technology used for continuous separation of ethanol from mixtures. This makes the optimization and integration of the distillation section so important. For an ethanol product capacity of 100,000 t/a, the 3-column distillation configuration has turned out to be better suitable for both, the 5-stage evaporation and the biogas production. Owing to the internal heat integration of the two distillation columns and the rectification column, savings in heating and cooling demand, compared to the same configuration with no heat integration, of respective 33.3 MW and 39.8 MW are achieved. The savings, compared to the 2-column configuration, are 3.1 MW and 5.1 MW for hot and cold utility requirements. It is therefore questionable, if the additional expenses in equipment pay off.

Besides the energy intensive distillation, also the treatment of the distillation stillage can have an impact on the overall heating and cooling demand of the process. In case of a multi-stage evaporation system, additional 47.6 MW and 49.9 MW for hot and cold utility are estimated, which is based on the process simulation of the co-current 5-stage evaporation. Even though the simulation in counter-current mode could not be utilized for further analysis, this evaporation setup suggests a less energy intensive behavior. A further development of this simulation will be necessary to confirm or refute this suggestion. Another possibility to reduce the hot and cold utility demand of an evaporation system is the implementation of a flash condensate system. The simulation showed a slightly reduction, but it can be suggested that it won't be enough to be profitable.

The combination and integration of the background process with the 3-column distillation and a 5-stage evaporation results in a heat integration potential of 125.9 MW, which is based

on the Pinch Analysis with a minimum temperature difference of 7°C. This displays the importance of an overall heat integration in the lignocelluloses to ethanol process.

By replacing the evaporation system with an anaerobic digester, the energy demand will be reduced by one third and biogas as a second product will be available. Based on the simulation, 6.78 kg/s of biogas with a methane content of 50 vol% can be produced, which would require a reactor size greater 63000 m³ with a HRT of more than 10 days, based on the set specifications. Compared a reactor volume of 22600 m³ needed for ethanol conversion in the upstream process, the biogas reactor needs to be 2.8 times bigger. Still, the amount of biogas accounts for 95.7 MW compared to the 93.8 MW energy content in the 3.5 kg/s of produced bioethanol.

It can be seen that the overall process heat demand could be easily covered by biogas. Generally, this is done by the utilization of the dried solid residues from solid-liquid separation, with an energy content of 121 MW (based on the lower heating value). Thus, biogas can be upgraded and utilized as an additional product. With these actions, an energy self–sufficiency can be achieved. Furthermore, a reduction of GHG emissions is in the favor of a combined production of bioethanol and biogas.

# Bibliography

Aden, A., et al. (2002), *Lignocellulosic Biomass to Ethanol Process Design and Economics Utilizing Co-Current Dilute Acid Prehydrolysis and Enzymatic Hydrolysis for Corn Stover - NREL/TP-510-32438*. National Renewable Energy Laboratory (NREL), Storming Media.

Balat, M. and Balat H. (2009), Recent trends in global production and utilization of bio-ethanol fuel, *Applied Energy*, 86: 2273-2282.

Barta, Z., Reczey, K., and Zacchi, G. (2010), Techno-economic evaluation of stillage treatment with anaerobic digestion in a softwood-to-ethanol process, *Biotechnology for Biofuels*, 3: 21.

Bergmair, J. (2006), *Biomethan - Aufbereitung von Biogas zur Einspeisung in das Salzburger Gasnetz*, BMVIT, Schriftreihe 8.

Billet, R. (1981), *Verdampfung und ihre technischen Anwendungen*, Weinheim, Wiley-VCH.

Bioconverter (2011), www.bioconverter.com/technology/primer.htm (accessed October 20, 2011).

Bischofsberger, W. et al. (2009), *Anaerobtechnik*. 2., vollst. überarb. A., Berlin, Springer.

Buswell, A. M., and Mueller, H. F. (1952), Mechanism of Methane Fermentation, *Industrial and Engineerign Chemistry*, 44: 550-552.

Cardona, C. A., and Sanchez, O. J. (2007), Fuel ethanol production: Process design trends and integration opportunities, *Bioresource Technology*, 98: 2415-2457.

Christen, D. S. (2010), *Praxiswissen der chemischen Verfahrenstechnik, Kapitel 13 - Verdampfen*, Berlin Heidelberg, Springer-Verlag.

Directive 2009/28/EC of the European Parliament and of the Council (2009), http://eur-lex.europa.eu/LexUriServ/LexUriServ.do?uri=OJ:L:2009:140:0016:0062:en:PDF (accessed 10 10, 2011).

Edwards, R., et al. (2007), Well-to-Wheels Analysis of Future Automotive Fuels and Powertrains in the European Context.

Eisentraut, A. (2010), Sustainable Production of SECOND -Generation Biofuels, IEA International Energy Agency.

European Biomas Industry Association (2008), Bioethanol Production and Use, http://www.erec.org/fileadmin/erec_docs/Projcet_Documents/RESTMAC/Brochure5_Bioethanol_low_res.pdf (accessed August 20, 2011).

Fachagentur Nachwachsende Rohstoffe e.V. (2006), Handreichung Biogasgewinnung und –nutzung, Gülzow.

Farrell, A. E., et al. (2006), Ethanol Can Contribute to Energy and Environmental Goals, *Science*, 311: 506-508.

Fulton, L., et al. (2004), *Biofuels for Transport - An International Perspective,* edited by the International Energy Agency. OECD.

Galbe, M., and Zacchi, G. (2002), A review of the production of ethanol from softwood, *Applied Microbiology and Biotechnology*, 59: 618-628.

Galbe, M., et al. (2007), Process engineering economics of bioethanol production, *Advances in Biochemical Engineering / Biotechnology*, 108: 303-327.

Global Renewable Fuels Alliance (2011), www.globalrfa.org/pr_021111.php (accessed May 9, 2011).

Gmehling, J., and Brehm, A. (1996), *Grundoperationen - Lehrbuch der technischen Chemie, Band 2.* Stuttgart, New York, Georg Thieme Verlag.

Hahn-Hägerdal, B., et al. (2006), Bio-ethanol – the fuel of tomorrow from the residues of today, *Trends in Biotechnology*, 24: 549-556.

Houghton, J. T., et al. (2001), *Climate Change 2001: The Scientific Basis*, Cambridge: The Press Syndicate of the University of Cambridge.

Hutnan, M., et al. (2003), Anaerobic Treatment of Wheat Stillage, *Chem. Biochem. Eng. Q. 17 (3)*, May 22, 2003: 233-241.

IEA (2011), Oil Market Report, International Energy Agency.

Jacques, K. A., Lyons T. P., and Kelsall D. R. (2003), *The Alcohol Textbook*, 4th edition, Nottingham University Press.

Kaltschmitt, M., Hartmann, H., and Hofbauer, H. (2009), *Energie aus Biomasse.*, Berlin Heidelberg, Springer-Verlag.

Kaparaju, P., et al. (2010), Optimization of biogas production from wheat straw stillage in UASB reactor, *Applied Energy*, 87: 3779-3783.

Kim, T. H (2004), *Doctoral Thesis: Bioconversion of Lignocellulosic Material into Ethanol: Pretreatment, Enzymatic Hydrolysis and Ethanol Fermentation*, Auburn University.

Kravanja, P., and Friedl A.. (2011), Process Simulation of Ethanol from Straw – Validation of scenarios for Austria, *Chemical Engineering Transactions*, 25: 863-868.

Kravanja, P. (2011), personal comunication, Vienna, December 22, 2011.

Kravanja, P., et al. (2011), Perspectives for the production of bioethanol from wood and straw in Austria: technical, economic, and ecological aspects, *Clean Technologies and Environmental Policy*, 1-15.

Larson, E. D. (2006), A review of life-cycle analysis studies on liquid biofuel systems for the transport sector, *Energy for Sustainable Development*, 10: 109-126.

Linnhoff March (1998), Introduction to Pinch Technology, Northwich.

Lurgi GmbH (2011), Bioethanol, www.lurgi.com/website/fileadmin/user_upload/1_PDF/1_Broshures_Flyer/englisch/0304e_BioEthanol.pdf (accessed Februar 9, 2011).

Maas, R., et al. (2008), Pilot-scale conversion of lime-treated wheat straw into bioethanol: quality assessment of bioethanol and valorization of side streams by anaerobic digestion and combustion, *Biotechnology for Biofuels*, 1: 14.

Madson, P, and Lococo, D (2000), Recovery of volatile products from dilute high-fouling process streams, *Applied Biochemistry and Biotechnology*, 84-86: 1049-1061.

Modarresi, A. (2011), personal communication, Vienna, December 22.

NREL, Harris Group (2001), LIQUID/SOLID Separation Report 99-10600/14. National Renewable Energy Laboratory, Golden, Colorado.

Olofsson, K., et al. (2008), A short review on SSF - an interesting process option for ethanol production from lignocellulosic feedstocks, *Biotechnology for Biofuels*, 1: 7.

Onken, U., and Behr A. (1996), *Chemische Prozesskunde, Lehrbuch der technischen Chemie, Band3*, New York, Georg Thieme Verlag Stuttgart.

Petersson, A. (2009), Biogas upgrading technologies – developments and innovations, IEA International Energy Agency.

Ramalho, R. S. (1977), *Introduction to Wastewater Treatment Processes*, New York, Academic Press.

Reisinger, K., et al. (2009), BIOBIB - A Database for biofuels.

Renewable Fuels Association (2011), http://www.ethanolrfa.org/pages/statistics#E (accessed May 12, 2011).

Roehr, M. (2001), *The Biotechnology of Ethanol: Classical and Future Applications*, Wiley-VCH.

Sassner, P. (2007), *Doctoral Thesis: Lignocellulosic ethanol production based on steam pretreatment and SSF*, Lund University.

Scharf, P. (2007), *Master Thesis: Producing biogas out of wastewater.* Vienna.

Schmitz, N. (2003), Bioethanol in Deutschland, FNR, Münster, Landwirtschaftsverlag GmbH.

Schmitz, N. (2006), Marktanalyse - Nachwachsende Rohstoffe, Fachagentur Nachwachsende Rohstoffe e. V.

Simo, M., et al. (2008), Simulation of pressure swing adsorption in fuel ethanol production process, *Computers and Chemical Engineering*, 32:1635-1649.

Slade, R., et al. (2009). The commercial performance of cellulosic ethanol supply-chains in Europe, *Biotechnology for Biofuels*, 2:3.

Smith, R. M. (2005), *Chemical Process: Design and Integration,* 2nd edition, John Wiley & Sons.

Sun, R. C., and Tompkinson J. (2003), Comparative study of organic solvent and water-soluble lipophilic extractives from wheat straw I: yield and chemical composition, *Journal of Wood Science*, 49: 47-52.

Torry-Smith, M., et al. (2003), Purification of bioethanol effluent in an UASB reactor system with simultaneous biogas formation, *Biotechnology and Bioengineering*, 84: 7-12.

Uellendahl, H., and Ahring, B. K. (2010), Anaerobic digestion as final step of a cellulosic ethanol biorefinery: Biogas production from fermentation effluent in a UASB reactor - pilot-scale results, *Biotechnology and Bioengineering*, 107: 59-64.

Vane, L. M. (2008), Separation technologies for the recovery and dehydration of alcohols from fermentation broths, *Biofuels, Bioproducts and Biorefining*, 2: 553-588.

Westphalen, D. L., and Wolf Maciel M. R. (2000), Pinch analysis of evaporation systems, *Brazilian Journal of Chemical Engineering*, 17: 525-538.

Wilkie, A. C., et al. (2000), Stillage characterization and anaerobic treatment of ethanol stillage from conventional and cellulosic feedstocks, *Biomass and Bioenergy*, 19: 63-102.

Wingren, A., et al. (2008), Energy considerations for a SSF-based softwood ethanol plant, *Bioresource Technology*, 99: 2121-2131.

Winter, R., et al. (2011), Biofuels in the transport sector 2011 - Summary of the data for the Republic of Austria pursuant to Article 4(1) of Directive 2003/30/EC for the reporting year 2010, Federal Ministry for Agriculture, Forestry, the Environment and Water Management.

Wooley, R. J., et al. (1996), *Development of an ASPEN PLUS physical property database for biofuels components,* National Renewable Energy Laboratory (NREL).

Zacchi, G., and Axelsson A. (1989), Economic evaluation of preconcentration in production of ethanol from dilute sugar solutions, *Biotechnology and Bioengineering*, 34: 223-233.

# Appendix

# A. ASPEN PLUS simulation settings

## 2-column distillation

**Table A-1: ASPEN PLUS Unit Operation Blocks used in the 2-column distillation model**

| Unit operation | Name | ASPEN PLUS "block" | Comments / specifications |
|---|---|---|---|
| Stripper Column, 1.8 bar | 01-STRIP | RadFrac | Convergence: Standard<br>19 theoretical stages,<br>top stage p = 1.8 bar,<br>DF = 0.003 (0.00092*) on a mass basis,<br>RR = 3 on a mass basis,<br>condenser type: Partial-Vapor |
| Recification Column, 1.6 bar | 02-RECT | RadFrac | Convergence: Standard<br>20 theoretical stages,<br>top stage p = 1.6 bar,<br>DF = 0.41 on a mass basis,<br>RR = 4 on a mass basis,<br>condenser type: Partial-Vapor |
| Pressure Swing Adsorption | 03-ADSOR | Sep | p = 1.8 bar |
| Solid-Liquid-Separation | 06-SLSEP | Sep2 | Simplified simulation of the Pneumapress® Filter |
| Heaters/Coolers | 02-SHT | Heater | T = 116°C, p = 1.8 bar |
| | 04-HEATX | Heater | HD = 0 Watt, p = 1.8 bar |
| | 05-HX01 | Heater | T = 40°C, p = 3.2 bar |
| | 05-HX02 | Heater | T = 40°C, p = 3.2 bar |
| | 07-COND | Heater | T = 25°C, p = 1.013 bar |
| | PREHX | Heater | T = 100°C, p = 3.0 bar |
| | RE-PREHX | Heater | VF = 0, P = 1.8 bar |
| Mixers | 04-BMIX | Mixer | |

* Calculated values due to design specification
RR…reflux ratio, p…pressure, T…temperature, HD…heat duty, CT…condenser temperature, VF…vapor fraction, DF…distillate to feed ratio

### 3-column distillation

**Table A-2: ASPEN PLUS unit operation blocks used in the 3-column distillation model**

| Unit operation | Name | ASPEN PLUS "block" | Comments / specifications |
|---|---|---|---|
| Stripper Column, 3.2 bar | 01-STRIP | RadFrac | Convergence: Azeotropic<br>20 theoretical stages, top stage p = 3.2 bar,<br>PD = 0.1 bar, feed on stage 2<br>DR = 13810 kg/h,<br>RR = 2.38 on a mass basis,<br>condenser type: Partial-Vapor-Liquid,<br>CT = 113°C |
| Stripper Column, 1.0 bar | 02-STRIP | RadFrac | Convergence: Azeotropic<br>20 theoretical stages, top stage p = 1.05 bar,<br>PD = 0.1 bar, feed on stage 2<br>DR = 13450 kg/h,<br>RR = 1.47 on a mass basis,<br>condenser type: Partial-Vapor-Liquid,<br>CT* = 81.5°C |
| Recification Column, 0.3 bar | 03-RECT | RadFrac | Convergence: Standard<br>22 theoretical stages, top stage p = 0.3 bar,<br>PD = 0.075 bar,<br>DR = 16925 kg/h,<br>RR = 2.11 on a mass basis,<br>condenser type: Partial-Vapor |
| PSA | 04-ADSOR | Sep | p = 1.8 bar |
| Solid-Liquid-Separation | 05-SLSEP | Sep2 | simplified simulation of the Pneumapress® Filter |
| Splitter | SPLITTER | FSplit | split fraction of stream "FTPH-02" = 0.47 |
| Heaters/Coolers | PR-HX01 | Heater | T = 130°C, p = 3.5 bar |
| | PR-HX02 | Heater | T = 85°C, p = 1.5 bar |
| | HX01 | Heater | T = 65°C, p = 1.05 bar |
| | RE-PREHX | Heater | VF = 0, p = 1.8 bar |
| | PRHT-AD | Heater | T = 116°C, p = 1.8 bar |
| | 07-COND | Heater | T = 25°C, p = 1.013 bar |
| | SLCOOLER | Heater | T = 40°C, p = 3.2 bar |
| Mixers | MIX1-2-T | Mixer | p = 1.05 bar |
| | MIX1-2-B | Mixer | |
| | MIX1-2-3 | Mixer | p = 3.2 bar |
| Ethanol Recovery Flash Drums | 01-FLSH | Flash2 | T = 37°C, p = 3.0 bar |
| | 02-FLSH | Flash2 | T = 25°C, p = 1.0 bar |

RR…reflux ratio, DR…distillate rate, p…pressure, T…temperature, HD…heat duty, CT…condenser temperature, PD…pressure drop, VF…vapor fraction

## 5-stage evaporation system

**Table A-3: ASPEN PLUS unit operation blocks used in the 5-stage evaporation co-current BASE CASE model**

| Unit operation | Name | ASPEN PLUS "block" | Comments / specifications |
|---|---|---|---|
| Preheater | FEED-PHX | Heater | p = 3 bar, VF = 0 |
| Evaporator 1st stage | HX-00 | HeatX | outlet hot stream VF = 0, hot side outlet p = 4 bar, cold side outlet p = 3 bar |
| | FLASH-00 | Flash | p = 3 bar, HD = 0 |
| | PREHX00 | Heater | p = 4 bar, T = 50°C |
| Evaporator 2nd stage | PCHANGE1 | Heater | p = 2 bar, HD = 0 |
| | HX-01 | HeatX | outlet hot stream VF = 0, hot side outlet p = 3 bar, cold side outlet p = 2 bar |
| | FLASH-01 | Flash | p = 2 bar, HD = 0 |
| | PREHEAT4 | Heater | p = 3 bar, T = 50°C |
| Evaporator 3rd stage | PCHANGE2 | Heater | p = 1.5 bar, HD = 0 |
| | HX-02 | HeatX | outlet hot stream VF = 0, hot side outlet p = 2 bar, cold side outlet p = 1.5 bar |
| | FLASH-02 | Flash | p = 1.5 bar, HD = 0 |
| | PREHEAT3 | Heater | p = 2 bar, T = 50°C |
| Evaporator 4th stage | PCHANGE3 | Heater | p = 1 bar, HD = 0 |
| | HX-03 | HeatX | outlet hot stream VF = 0, hot side outlet p = 1.5 bar, cold side outlet p = 1 bar |
| | FLASH-03 | Flash | p = 1 bar, HD = 0 |
| | PREHEAT2 | Heater | p = 1.5 bar, T = 50°C |
| Evaporator 5th stage | PCHANGE4 | Heater | p = 0.5 bar, HD = 0 |
| | HX-04 | HeatX | outlet hot stream VF = 0, hot side outlet p = 1 bar, cold side outlet p = 0.5 bar |
| | FLASH-04 | Flash | p = 0.5 bar, HD = 0 |
| | PREHEAT1 | Heater | p = 1 bar, T = 50°C |
| | CONDENS | Heater | p = 0.5 bar, VF = 0 |
| | PREHEAT | Heater | p = 0.5 bar, T = 50°C |

p…pressure, T…temperature, HD…heat duty, VF…vapor fraction

**Table A-4: ASPEN PLUS unit operation blocks used in the 5-stage evaporation co-current FLASH CASE model**

| Unit operation | Name | ASPEN PLUS "block" | Comments / specifications |
|---|---|---|---|
| Preheater | FEED-PHX | Heater | p = 3 bar, VF = 0 |
| Evaporator 1st stage | HX-00 | HeatX | outlet hot stream VF = 0, hot side outlet p = 4 bar, cold side outlet p = 3 bar |
| | FLASH-00 | Flash | p = 3 bar, HD = 0 |
| | PREH-PST | Heater | p = 4 bar, T = 50°C |
| Evaporator 2nd stage | PCHANGE1 | Heater | p = 2 bar, HD = 0 |
| | HX-01 | HeatX | outlet hot stream VF = 0, hot side outlet p = 3 bar, cold side outlet p = 2 bar |
| | FLASH-01 | Flash | p = 2 bar, HD = 0 |
| | LPFLSH1 | Flash | p = 2 bar, VF = 0 |
| Evaporator 3rd stage | PCHANGE2 | Heater | p = 1.5 bar, HD = 0 |
| | HX-02 | HeatX | outlet hot stream VF = 0, hot side outlet p = 2 bar, cold side outlet p = 1.5 bar |
| | FLASH-02 | Flash | p = 1.5 bar, HD = 0 |
| | LPFLSH2 | Flash | p = 1.5 bar, VF = 0 |
| Evaporator 4th stage | PCHANGE3 | Heater | p = 1 bar, HD = 0 |
| | HX-03 | HeatX | outlet hot stream VF = 0, hot side outlet p = 1.5 bar, cold side outlet p = 1 bar |
| | FLASH-03 | Flash | p = 1 bar, HD = 0 |
| | LPFLSH3 | Flash | p = 1 bar, VF = 0 |
| Evaporator 5th stage | PCHANGE4 | Heater | p = 0.5 bar, HD = 0 |
| | HX-04 | HeatX | outlet hot stream VF = 0, hot side outlet p = 1 bar, cold side outlet p = 0.5 bar |
| | FLASH-04 | Flash | p = 0.5 bar, HD = 0 |
| | LT-HX | Heater | p = 1 bar, T = 50°C |
| | CONDENS | Heater | p = 0.5 bar, VF = 0 |
| | PREHEAT | Heater | p = 0.5 bar, T = 50°C |

p…pressure, T…temperature, HD…heat duty, VF…vapor fraction

**Table A-5: ASPEN PLUS unit operation blocks used in the 5-stage evaporation counter-current BASE CASE model**

| Unit operation | Name | ASPEN PLUS "block" | Comments / specifications |
|---|---|---|---|
| Preheater | PREHX | Heater | p = 1 bar, T = 40°C |
| Evaporator 1st stage | PCHANG21 | Heater | p = 3 bar, HD = 0 |
| | HX-01 | HeatX | outlet hot stream VF = 0,<br>hot side outlet p = 4 bar,<br>cold side outlet p = 3 bar |
| | FLASH-01 | Flash | p = 3 bar, HD = 0 |
| | PREHX00 | Heater | p = 4 bar, T = 50°C |
| Evaporator 2nd stage | PCHANG32 | Heater | p = 2.5 bar, HD = 0 |
| | HX-02 | HeatX | outlet hot stream VF = 0,<br>hot side outlet p = 3 bar,<br>cold side outlet p = 2.5 bar |
| | FLASH-02 | Flash | p = 2.5 bar, HD = 0 |
| | PREHEA02 | Heater | p = 3 bar, T = 50°C |
| Evaporator 3rd stage | PCHANG43 | Heater | p = 2 bar, HD = 0 |
| | HX-03 | HeatX | outlet hot stream VF = 0,<br>hot side outlet p = 2.5 bar,<br>cold side outlet p = 2 bar |
| | FLASH-03 | Flash | p = 2 bar, HD = 0 |
| | PREHEA03 | Heater | p = 2.5 bar, T = 50°C |
| Evaporator 4th stage | PCHANG54 | Heater | p = 1.5 bar, HD = 0 |
| | HX-04 | HeatX | outlet hot stream VF = 0,<br>hot side outlet p = 2 bar,<br>cold side outlet p = 1.5 bar |
| | FLASH-04 | Flash | p = 1.5 bar, HD = 0 |
| | PREHEA04 | Heater | p = 2 bar, T = 50°C |
| Evaporator 5th stage | HX-05 | HeatX | outlet hot stream VF = 0,<br>hot side outlet p = 1.5 bar,<br>cold side outlet p = 1 bar |
| | FLASH-05 | Flash | p = 1 bar, HD = 0 |
| | PREHEA05 | Heater | p = 1.5 bar, T = 50°C |
| | COND-05 | Heater | p = 1 bar, VF = 0 |
| | PREHEAT | Heater | p = 1 bar, T = 50°C |

p…pressure, T…temperature, HD…heat duty, VF…vapor fraction

**Table A-6: ASPEN PLUS Unit Operation Blocks used in the biogas model**

| Unit operation | Name | ASPEN PLUS "block" | Comments / specifications |
|---|---|---|---|
| Cooling | COOLER | Heater | p = 1 bar, T = 37°C |
| Fermentor | BG-FLASH | Flash | p = 1 atm, HD = 0 |
| | ANAERO-D | Rstoic | p = 1 bar, T = 37°C |
| | METHANO | Rstoic | p = 1 bar, T = 37°C |

p…pressure, T…temperature, HD…heat duty, VF…vapor fraction

# B. ASPEN PLUS design specifications

**Table B-1: Design specifications applied in the ASPEN PLUS simulation models**

| Simulation model | Specification name | Specification (target) | Manipulated variables |
|---|---|---|---|
| 2-column distillation | 01-RECOV | Ratio of ethanol mass flow in stream 01-SIDE to FEED is 1 (tolerance = 0.005) | Distillate to feed ratio of block 01-STRIP<br>lower: 0.001,<br>upper: 0.005 |
| Evaporation co-current BASE CASE | EKONZ | Mass fraction of water in the stream PRODUCT is 0.4 (tolerance = 0.001) | Mass flow of stream PR-STEAM<br>lower: 26000 kg/h,<br>upper: 35000 kg/h |
| Evaporation co-current FLASH CASE | EKONZ | Mass fraction of water in the stream PRODUCT is 0.4 (tolerance = 0.01) | Mass flow of stream PR-STEAM<br>lower: 20000 kg/h,<br>upper: 40000 kg/h |
| Evaporation counter-current BASE CASE | EINDAMPF | Mass fraction of water in the stream PRODUCT is 0.4 (tolerance = 0.05) | Mass flow of stream PR-STEAM<br>lower: 59000 kg/h,<br>upper: 60500 kg/h |

# C. ASPEN PLUS flow sheets and process streams

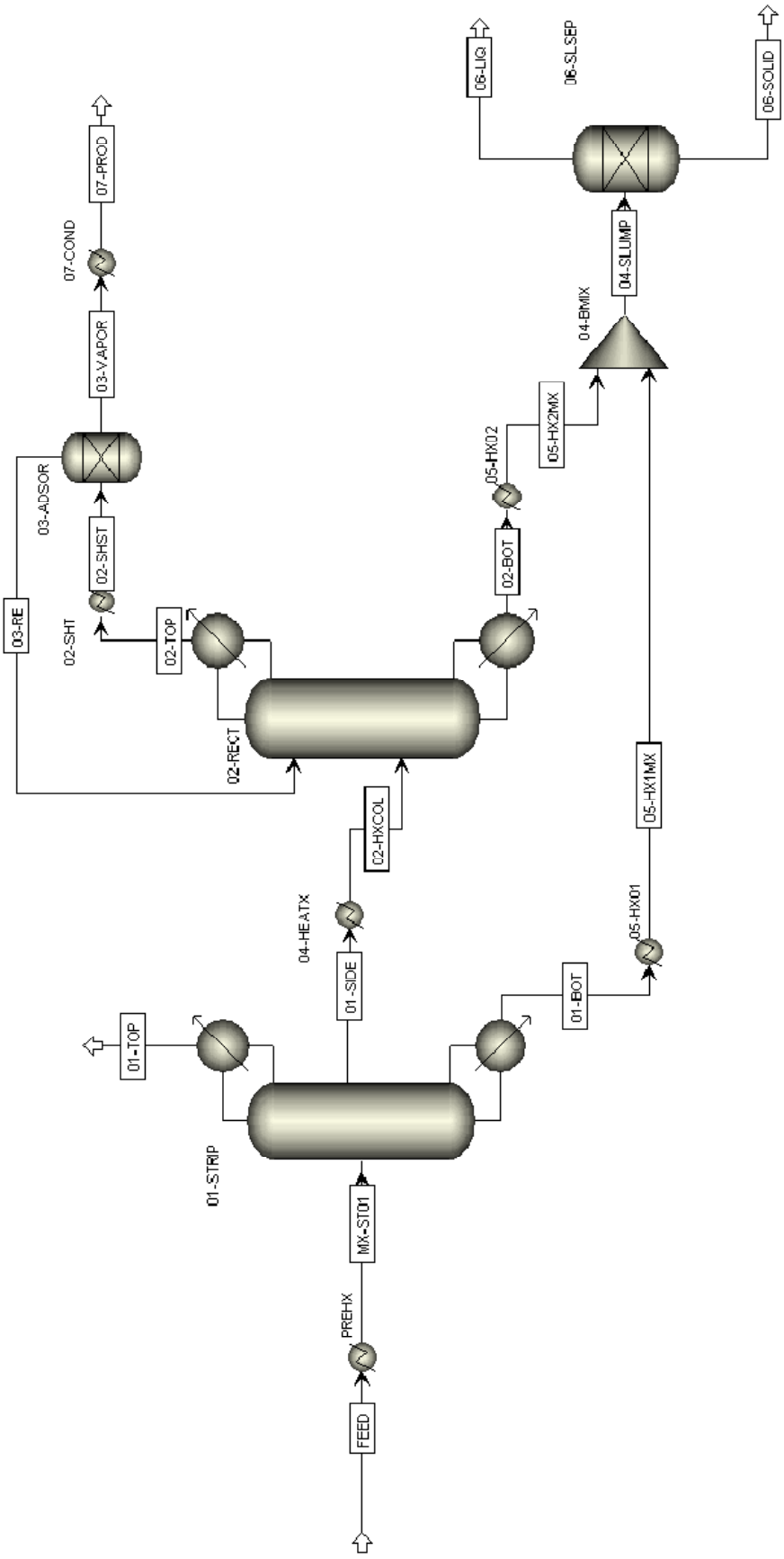


**Figure C-1: ASPEN PLUS flow sheet of the 2-column distillation model**

**Table C-1: ASPEN PLUS simulation process streams of the 2-column distillation model**

| Stream name | | 01-BOT | 01-SIDE | 01-TOP | 02-BOT | 02-HXCOL | 02-SHST | 02-TOP | 03-RE | 03-VAPOR | 04-SLUMP | 05-HX1MX | 05-HX2MX | 06-LIQ | 06-SOLID | 07-PROD | FEED | MX-ST01 |
|---|---|---|---|---|---|---|---|---|---|---|---|---|---|---|---|---|---|---|
| **Temperature** | [°C] | 121.4 | 112.9 | 64 | 113.4 | 112.9 | 116 | 90.3 | 116 | 116 | 40 | 40 | 40 | 40 | 40 | 25 | 37 | 100 |
| **Pressure** | [bar] | 2 | 1.822 | 1.8 | 1.6 | 1.8 | 1.8 | 1.6 | 1.8 | 1.8 | 3.2 | 3.2 | 3.2 | 3.2 | 3.2 | 1.013 | 1.013 | 3 |
| **Vapor fraction** | [1] | 0 | 1 | 1 | 0 | 1 | 1 | 1 | 1 | 1 | 0 | 0 | 0 | 0 | 0 | 0 | 0 | 0 |
| **Total mole flow** | [kmol/h] | 13141.4 | 1542.0 | 7.0 | 1268.6 | 1542.0 | 395.3 | 395.3 | 122.0 | 273.4 | 14410.0 | 13141.4 | 1268.6 | 12481.0 | 1929.0 | 273.4 | 14690.3 | 14690.3 |
| **Total mass flow** | [kg/h] | 276541.6 | 35651.8 | 286.7 | 23121.9 | 35651.8 | 16067.7 | 16067.7 | 3537.9 | 12529.9 | 299663.5 | 276541.6 | 23121.9 | 248925.8 | 50737.7 | 12529.9 | 312480.0 | 312480.0 |
| **Component mass flow** | | | | | | | | | | | | | | | | | | |
| WATER | [kg/h] | 228237.8 | 22834.6 | 14.7 | 22793.3 | 22834.6 | 1377.3 | 1377.3 | 1336.0 | 41.3 | 251031.0 | 228237.8 | 22793.3 | 220907.3 | 30123.7 | 41.3 | 251087.1 | 251087.1 |
| ETHANOL | [kg/h] | 2.0 | 12478.1 | 41.6 | 0.9 | 12478.1 | 14679.1 | 14679.1 | 2201.9 | 12477.2 | 2.9 | 2.0 | 0.9 | 2.9 | 0.0 | 12477.2 | 12521.7 | 12521.7 |
| ACETAT | [kg/h] | 1875.5 | 90.3 | 0.0 | 90.3 | 90.3 | 0.0 | 0.0 | 0.0 | 0.0 | 1965.8 | 1875.5 | 90.3 | 1965.8 | 0.0 | 0.0 | 1965.8 | 1965.8 |
| FURFURAL | [kg/h] | 781.1 | 145.9 | 0.1 | 145.9 | 145.9 | 0.0 | 0.0 | 0.0 | 0.0 | 927.0 | 781.1 | 145.9 | 927.0 | 0.0 | 0.0 | 927.1 | 927.1 |
| GLYCEROL | [kg/h] | 264.7 | 0.0 | 0.0 | 0.0 | 0.0 | 0.0 | 0.0 | 0.0 | 0.0 | 264.7 | 264.7 | 0.0 | 264.7 | 0.0 | 0.0 | 264.7 | 264.7 |
| CO2 | [kg/h] | 0.0 | 11.4 | 230.2 | 0.0 | 11.4 | 11.4 | 11.4 | 0.0 | 11.4 | 0.0 | 0.0 | 0.0 | 0.0 | 0.0 | 11.4 | 241.5 | 241.5 |
| CELLULOS | [kg/h] | 1794.9 | 1.6 | 0.0 | 1.6 | 1.6 | 0.0 | 0.0 | 0.0 | 0.0 | 1796.4 | 1794.9 | 1.6 | 89.8 | 1706.6 | 0.0 | 1796.4 | 1796.4 |
| XYLAN | [kg/h] | 856.8 | 0.0 | 0.0 | 0.0 | 0.0 | 0.0 | 0.0 | 0.0 | 0.0 | 856.8 | 856.8 | 0.0 | 42.8 | 814.0 | 0.0 | 856.8 | 856.8 |
| LIGNIN | [kg/h] | 12979.5 | 0.0 | 0.0 | 0.0 | 0.0 | 0.0 | 0.0 | 0.0 | 0.0 | 12979.5 | 12979.5 | 0.0 | 649.0 | 12330.5 | 0.0 | 12979.5 | 12979.5 |
| XYLOSE | [kg/h] | 14558.8 | 0.0 | 0.0 | 0.0 | 0.0 | 0.0 | 0.0 | 0.0 | 0.0 | 14558.8 | 14558.8 | 0.0 | 14558.8 | 0.0 | 0.0 | 14558.8 | 14558.8 |
| GLUCOSE | [kg/h] | 0.0 | 0.0 | 0.0 | 0.0 | 0.0 | 0.0 | 0.0 | 0.0 | 0.0 | 0.0 | 0.0 | 0.0 | 0.0 | 0.0 | 0.0 | 0.0 | 0.0 |
| YEAST | [kg/h] | 1739.6 | 0.0 | 0.0 | 0.0 | 0.0 | 0.0 | 0.0 | 0.0 | 0.0 | 1739.6 | 1739.6 | 0.0 | 87.0 | 1652.6 | 0.0 | 1739.6 | 1739.6 |
| ENZYMES | [kg/h] | 561.5 | 0.0 | 0.0 | 0.0 | 0.0 | 0.0 | 0.0 | 0.0 | 0.0 | 561.5 | 561.5 | 0.0 | 561.5 | 0.0 | 0.0 | 561.5 | 561.5 |
| ASH | [kg/h] | 4326.6 | 0.0 | 0.0 | 0.0 | 0.0 | 0.0 | 0.0 | 0.0 | 0.0 | 4326.6 | 4326.6 | 0.0 | 216.3 | 4110.3 | 0.0 | 4326.6 | 4326.6 |
| EXTRAKT | [kg/h] | 5678.5 | 89.9 | 0.0 | 89.9 | 89.9 | 0.0 | 0.0 | 0.0 | 0.0 | 5768.4 | 5678.5 | 89.9 | 5768.4 | 0.0 | 0.0 | 5768.4 | 5768.4 |
| PROTEIN | [kg/h] | 2884.5 | 0.0 | 0.0 | 0.0 | 0.0 | 0.0 | 0.0 | 0.0 | 0.0 | 2884.5 | 2884.5 | 0.0 | 2884.5 | 0.0 | 0.0 | 2884.5 | 2884.5 |
| **Mass fraction** | | | | | | | | | | | | | | | | | | |
| WATER | [1] | 0.825 | 0.64 | 0.051 | 0.986 | 0.64 | 0.086 | 0.086 | 0.378 | 0.003 | 0.838 | 0.825 | 0.986 | 0.887 | 0.594 | 0.003 | 0.804 | 0.804 |
| ETHANOL | [1] | 0 | 0.35 | 0.145 | 0 | 0.35 | 0.914 | 0.914 | 0.622 | 0.996 | 0 | 0 | 0 | 0 | 0 | 0.996 | 0.04 | 0.04 |
| ACETAT | [1] | 0.007 | 0.003 | 0 | 0.004 | 0.003 | 0 | 0 | 0 | 0 | 0.007 | 0.007 | 0.004 | 0.008 | 0 | 0 | 0.006 | 0.006 |
| FURFURAL | [1] | 0.003 | 0.004 | 0 | 0.006 | 0.004 | 0 | 0 | 0 | 0 | 0.003 | 0.003 | 0.006 | 0.004 | 0 | 0 | 0.003 | 0.003 |
| GLYCEROL | [1] | 0.001 | 0 | 0 | 0 | 0 | 0 | 0 | 0 | 0 | 0.001 | 0.001 | 0 | 0.001 | 0 | 0 | 0.001 | 0.001 |
| CO2 | [1] | 0 | 0 | 0.803 | 0 | 0 | 0.001 | 0.001 | 0 | 0.001 | 0 | 0 | 0 | 0 | 0 | 0.001 | 0.001 | 0.001 |
| CELLULOS | [1] | 0.006 | 0 | 0 | 0 | 0 | 0 | 0 | 0 | 0 | 0.006 | 0.006 | 0 | 0 | 0.034 | 0 | 0.006 | 0.006 |
| XYLAN | [1] | 0.003 | 0 | 0 | 0 | 0 | 0 | 0 | 0 | 0 | 0.003 | 0.003 | 0 | 0 | 0.016 | 0 | 0.003 | 0.003 |
| LIGNIN | [1] | 0.047 | 0 | 0 | 0 | 0 | 0 | 0 | 0 | 0 | 0.043 | 0.047 | 0 | 0.003 | 0.243 | 0 | 0.042 | 0.042 |
| XYLOSE | [1] | 0.053 | 0 | 0 | 0 | 0 | 0 | 0 | 0 | 0 | 0.049 | 0.053 | 0 | 0.058 | 0 | 0 | 0.047 | 0.047 |
| GLUCOSE | [1] | 0 | 0 | 0 | 0 | 0 | 0 | 0 | 0 | 0 | 0 | 0 | 0 | 0 | 0 | 0 | 0 | 0 |
| YEAST | [1] | 0.006 | 0 | 0 | 0 | 0 | 0 | 0 | 0 | 0 | 0.006 | 0.006 | 0 | 0 | 0.033 | 0 | 0.006 | 0.006 |
| ENZYMES | [1] | 0.002 | 0 | 0 | 0 | 0 | 0 | 0 | 0 | 0 | 0.002 | 0.002 | 0 | 0.002 | 0 | 0 | 0.002 | 0.002 |
| ASH | [1] | 0.016 | 0 | 0 | 0 | 0 | 0 | 0 | 0 | 0 | 0.014 | 0.016 | 0 | 0.001 | 0.081 | 0 | 0.014 | 0.014 |
| EXTRAKT | [1] | 0.021 | 0.003 | 0 | 0.004 | 0.003 | 0 | 0 | 0 | 0 | 0.019 | 0.021 | 0.004 | 0.023 | 0 | 0 | 0.018 | 0.018 |
| PROTEIN | [1] | 0.01 | 0 | 0 | 0 | 0 | 0 | 0 | 0 | 0 | 0.01 | 0.01 | 0 | 0.012 | 0 | 0 | 0.009 | 0.009 |

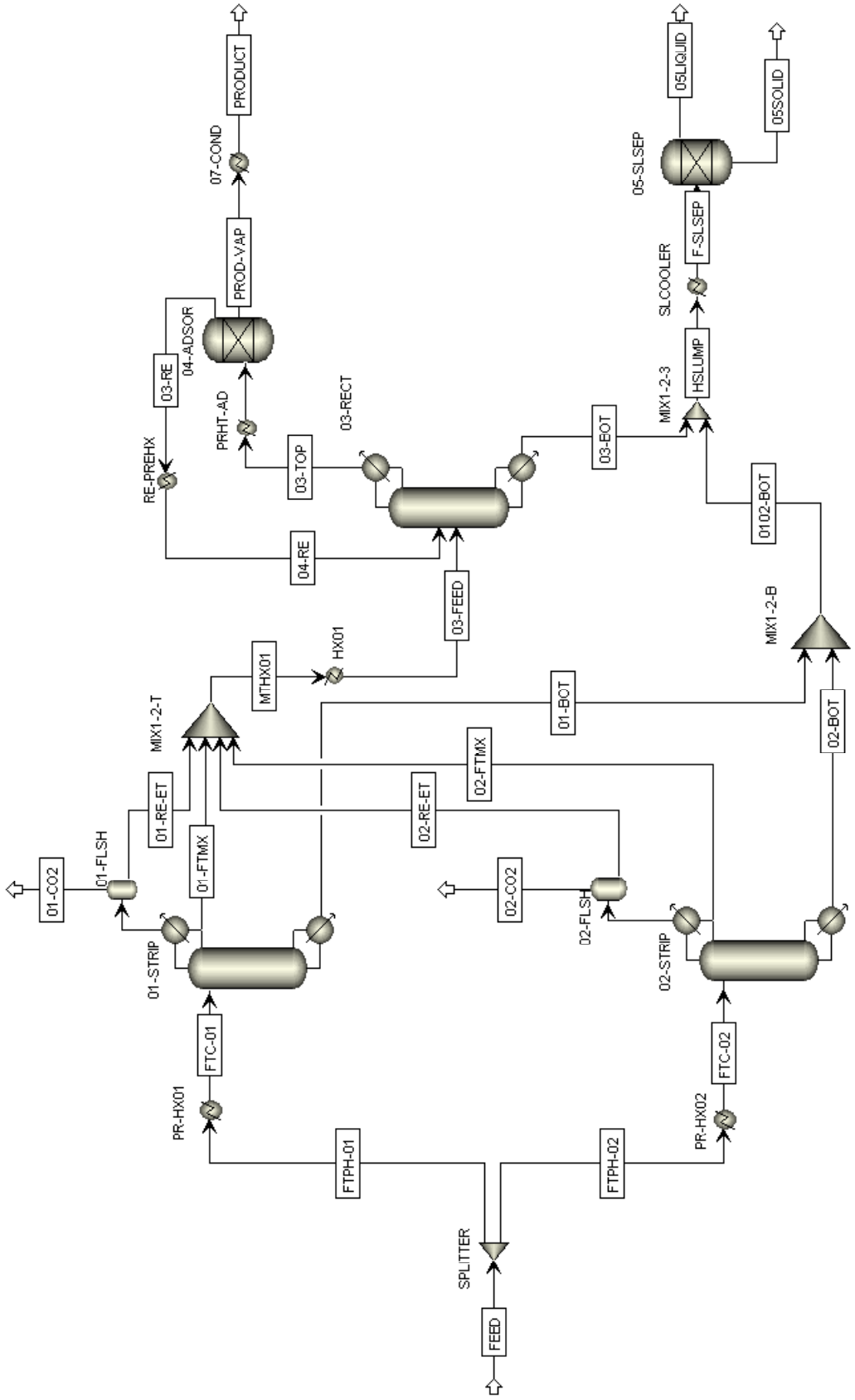


**Figure C-2: ASPEN PLUS flow sheet of the 3-column distillation model**

**Table C-2: ASPEN PLUS simulation process streams of the 3-column distillation model (part 1)**

| Stream name | | 01-BOT | 01-CO2 | 01-FTMX | 01-RE-ET | 01-TOP | 02-BOT | 02-CO2 | 02-FTMX | 02-RE-ET | 02-TOP | 03-BOT | 03-FEED | 03-RE | 03-TOP | 04-ETVAP | … |
|---|---|---|---|---|---|---|---|---|---|---|---|---|---|---|---|---|---|
| **Temperature** | [°C] | 138.1 | 37 | 113 | 37 | 113 | 104.6 | 25 | 81.5 | 25 | 81.5 | 74.2 | 65 | 116 | 50.6 | 116 | … |
| **Pressure** | [bar] | 3.3 | 3 | 3.2 | 3 | 3.2 | 1.15 | 1 | 1.05 | 1 | 1.05 | 0.375 | 1.05 | 1.8 | 0.3 | 1.8 | … |
| **Vapor fraction** | [1] | 0 | 1 | 0 | 0 | 1 | 0 | 1 | 0 | 0 | 1 | 0 | 0.001 | 1 | 1 | 1 | … |
| **Total mole flow** | [kmol/h] | 7252.0 | 2.0 | 436.7 | 95.8 | 97.9 | 6367.0 | 2.4 | 474.2 | 61.5 | 63.9 | 794.0 | 1068.3 | 134.6 | 408.9 | 408.9 | … |
| **Total mass flow** | [kg/h] | 151819.7 | 88.4 | 10911.3 | 2810.3 | 2898.7 | 133429.1 | 105.4 | 11567.3 | 1777.3 | 1882.7 | 14471.3 | 27066.2 | 4330.0 | 16925.0 | 16925.0 | … |
| **Component mass flow** | | | | | | | | | | | | | | | | | |
| WATER | [kg/h] | 126118.9 | 0.6 | 5936.6 | 1032.4 | 1033.0 | 110699.5 | 1.1 | 6641.1 | 680.0 | 681.1 | 14265.6 | 14290.1 | 1201.6 | 1226.1 | 1226.1 | … |
| ETHANOL | [kg/h] | 0.4 | 2.6 | 4906.0 | 1728.2 | 1730.7 | 0.7 | 4.7 | 4806.4 | 1074.0 | 1078.6 | 0.9 | 12514.5 | 3128.4 | 15642.1 | 15642.1 | … |
| ACETAT | [kg/h] | 1017.8 | 0.0 | 21.4 | 2.8 | 2.8 | 897.0 | 0.0 | 25.1 | 2.0 | 2.0 | 51.2 | 51.2 | 0.0 | 0.0 | 0.0 | … |
| FURFURAL | [kg/h] | 463.4 | 0.0 | 24.5 | 3.5 | 3.5 | 359.9 | 0.0 | 69.0 | 6.9 | 6.9 | 103.9 | 103.9 | 0.0 | 0.0 | 0.0 | … |
| GLYCEROL | [kg/h] | 140.3 | 0.0 | 0.0 | 0.0 | 0.0 | 124.4 | 0.0 | 0.0 | 0.0 | 0.0 | 0.0 | 0.0 | 0.0 | 0.0 | 0.0 | … |
| CO2 | [kg/h] | 0.0 | 85.2 | 1.8 | 41.0 | 126.2 | 0.0 | 99.6 | 1.2 | 12.8 | 112.3 | 0.0 | 56.8 | 0.0 | 56.8 | 56.8 | … |
| CELLULOS | [kg/h] | 951.7 | 0.0 | 0.5 | 0.1 | 0.1 | 844.1 | 0.0 | 0.3 | 0.0 | 0.0 | 0.9 | 0.9 | 0.0 | 0.0 | 0.0 | … |
| XYLAN | [kg/h] | 454.2 | 0.0 | 0.0 | 0.0 | 0.0 | 402.7 | 0.0 | 0.0 | 0.0 | 0.0 | 0.0 | 0.0 | 0.0 | 0.0 | 0.0 | … |
| LIGNIN | [kg/h] | 6879.8 | 0.0 | 0.0 | 0.0 | 0.0 | 6100.9 | 0.0 | 0.0 | 0.0 | 0.0 | 0.0 | 0.0 | 0.0 | 0.0 | 0.0 | … |
| XYLOSE | [kg/h] | 7716.9 | 0.0 | 0.0 | 0.0 | 0.0 | 6843.2 | 0.0 | 0.0 | 0.0 | 0.0 | 0.0 | 0.0 | 0.0 | 0.0 | 0.0 | … |
| GLUCOSE | [kg/h] | 0.0 | 0.0 | 0.0 | 0.0 | 0.0 | 0.0 | 0.0 | 0.0 | 0.0 | 0.0 | 0.0 | 0.0 | 0.0 | 0.0 | 0.0 | … |
| YEAST | [kg/h] | 922.1 | 0.0 | 0.0 | 0.0 | 0.0 | 817.7 | 0.0 | 0.0 | 0.0 | 0.0 | 0.0 | 0.0 | 0.0 | 0.0 | 0.0 | … |
| ENZYMES | [kg/h] | 297.6 | 0.0 | 0.0 | 0.0 | 0.0 | 263.9 | 0.0 | 0.0 | 0.0 | 0.0 | 0.0 | 0.0 | 0.0 | 0.0 | 0.0 | … |
| ASH | [kg/h] | 2293.3 | 0.0 | 0.0 | 0.0 | 0.0 | 2033.7 | 0.0 | 0.0 | 0.0 | 0.0 | 0.0 | 0.0 | 0.0 | 0.0 | 0.0 | … |
| EXTRAKT | [kg/h] | 3034.5 | 0.0 | 20.6 | 2.4 | 2.4 | 2685.5 | 0.0 | 24.2 | 1.7 | 1.7 | 48.9 | 48.9 | 0.0 | 0.0 | 0.0 | … |
| PROTEIN | [kg/h] | 1528.9 | 0.0 | 0.0 | 0.0 | 0.0 | 1355.8 | 0.0 | 0.0 | 0.0 | 0.0 | 0.0 | 0.0 | 0.0 | 0.0 | 0.0 | … |
| **Mass fraction** | | | | | | | | | | | | | | | | | |
| WATER | [1] | 0.831 | 0.007 | 0.544 | 0.367 | 0.356 | 0.83 | 0.01 | 0.574 | 0.383 | 0.362 | 0.986 | 0.528 | 0.278 | 0.072 | 0.072 | … |
| ETHANOL | [1] | 0 | 0.029 | 0.45 | 0.615 | 0.597 | 0 | 0.044 | 0.416 | 0.604 | 0.573 | 0 | 0.462 | 0.722 | 0.924 | 0.924 | … |
| ACETAT | [1] | 0.007 | 0 | 0.002 | 0.001 | 0.001 | 0.007 | 0 | 0.002 | 0.001 | 0.001 | 0.004 | 0.002 | 0 | 0 | 0 | … |
| FURFURAL | [1] | 0.003 | 0 | 0.002 | 0.001 | 0.001 | 0.003 | 0 | 0.006 | 0.004 | 0.004 | 0.007 | 0.004 | 0 | 0 | 0 | … |
| GLYCEROL | [1] | 0.001 | 0 | 0 | 0 | 0 | 0.001 | 0 | 0 | 0 | 0 | 0 | 0 | 0 | 0 | 0 | … |
| CO2 | [1] | 0 | 0.964 | 0 | 0.015 | 0.044 | 0 | 0.945 | 0 | 0.007 | 0.06 | 0 | 0.002 | 0 | 0.003 | 0.003 | … |
| CELLULOS | [1] | 0.006 | 0 | 0 | 0 | 0 | 0.006 | 0 | 0 | 0 | 0 | 0 | 0 | 0 | 0 | 0 | … |
| XYLAN | [1] | 0.003 | 0 | 0 | 0 | 0 | 0.003 | 0 | 0 | 0 | 0 | 0 | 0 | 0 | 0 | 0 | … |
| LIGNIN | [1] | 0.045 | 0 | 0 | 0 | 0 | 0.046 | 0 | 0 | 0 | 0 | 0 | 0 | 0 | 0 | 0 | … |
| XYLOSE | [1] | 0.051 | 0 | 0 | 0 | 0 | 0.051 | 0 | 0 | 0 | 0 | 0 | 0 | 0 | 0 | 0 | … |
| GLUCOSE | [1] | 0 | 0 | 0 | 0 | 0 | 0 | 0 | 0 | 0 | 0 | 0 | 0 | 0 | 0 | 0 | … |
| YEAST | [1] | 0.006 | 0 | 0 | 0 | 0 | 0.006 | 0 | 0 | 0 | 0 | 0 | 0 | 0 | 0 | 0 | … |
| ENZYMES | [1] | 0.002 | 0 | 0 | 0 | 0 | 0.002 | 0 | 0 | 0 | 0 | 0 | 0 | 0 | 0 | 0 | … |
| ASH | [1] | 0.015 | 0 | 0 | 0 | 0 | 0.015 | 0 | 0 | 0 | 0 | 0 | 0 | 0 | 0 | 0 | … |
| EXTRAKT | [1] | 0.02 | 0 | 0.002 | 0.001 | 0.001 | 0.02 | 0 | 0.002 | 0.001 | 0.001 | 0.003 | 0.002 | 0 | 0 | 0 | … |
| PROTEIN | [1] | 0.01 | 0 | 0 | 0 | 0 | 0.01 | 0 | 0 | 0 | 0 | 0 | 0 | 0 | 0 | 0 | … |

**Table C-3: ASPEN PLUS simulation process streams of the 3-column distillation model (part 2)**

| Stream name | | … | 04-RE | 05LIQUID | 05SOLID | 0102-BOT | F-SLSEP | FEED | FTC-01 | FTC-02 | FTPH-01 | FTPH-02 | HSLUMP | MTHX01 | PROD-VAP | PRODUCT |
|---|---|---|---|---|---|---|---|---|---|---|---|---|---|---|---|---|
| **Temperature** | [°C] | … | 95 | 40 | 40 | 104.6 | 40 | 37 | 130 | 85 | 37 | 37 | 120.6 | 81.1 | 116 | 25 |
| **Pressure** | [bar] | … | 1.8 | 3.2 | 3.2 | 1.15 | 3.2 | 1.013 | 3.5 | 1.5 | 1.013 | 1.013 | 3.2 | 1.05 | 1.8 | 1.013 |
| **Vapor fraction** | [1] | … | 0 | 0 | 0 | 0.046 | 0 | 0 | 0.002 | 0 | 0 | 0 | 0 | 0.016 | 1 | 0 |
| **Total mole flow** | [kmol/h] | … | 134.6 | 12483.6 | 1929.4 | 13619.0 | 14413.0 | 14691.7 | 7786.6 | 6905.1 | 7786.6 | 6905.1 | 14413.0 | 1068.3 | 274.3 | 274.3 |
| **Total mass flow** | [kg/h] | … | 4330.0 | 248974.1 | 50746.0 | 285248.8 | 299720.1 | 312508.8 | 165629.7 | 146879.1 | 165629.7 | 146879.1 | 299720.1 | 27066.2 | 12594.9 | 12594.9 |
| **Component mass flow** | | | | | | | | | | | | | | | | |
| WATER | [kg/h] | … | 1201.6 | 220953.9 | 30130.1 | 236818.4 | 251084.0 | 251110.2 | 133088.4 | 118021.8 | 133088.4 | 118021.8 | 251084.0 | 14290.1 | 24.5 | 24.5 |
| ETHANOL | [kg/h] | … | 3128.4 | 1.9 | 0.0 | 1.1 | 1.9 | 12522.9 | 6637.1 | 5885.7 | 6637.1 | 5885.7 | 1.9 | 12514.5 | 12513.7 | 12513.7 |
| ACETAT | [kg/h] | … | 0.0 | 1966.0 | 0.0 | 1914.8 | 1966.0 | 1966.0 | 1042.0 | 924.0 | 1042.0 | 924.0 | 1966.0 | 51.2 | 0.0 | 0.0 |
| FURFURAL | [kg/h] | … | 0.0 | 927.2 | 0.0 | 823.3 | 927.2 | 927.2 | 491.4 | 435.8 | 491.4 | 435.8 | 927.2 | 103.9 | 0.0 | 0.0 |
| GLYCEROL | [kg/h] | … | 0.0 | 264.7 | 0.0 | 264.7 | 264.7 | 264.7 | 140.3 | 124.4 | 140.3 | 124.4 | 264.7 | 0.0 | 0.0 | 0.0 |
| CO2 | [kg/h] | … | 0.0 | 0.0 | 0.0 | 0.0 | 0.0 | 241.6 | 128.0 | 113.5 | 128.0 | 113.5 | 0.0 | 56.8 | 56.8 | 56.8 |
| CELLULOS | [kg/h] | … | 0.0 | 89.8 | 1706.8 | 1795.8 | 1796.6 | 1796.6 | 952.2 | 844.4 | 952.2 | 844.4 | 1796.6 | 0.9 | 0.0 | 0.0 |
| XYLAN | [kg/h] | … | 0.0 | 42.8 | 814.1 | 856.9 | 856.9 | 856.9 | 454.2 | 402.7 | 454.2 | 402.7 | 856.9 | 0.0 | 0.0 | 0.0 |
| LIGNIN | [kg/h] | … | 0.0 | 649.0 | 12331.6 | 12980.7 | 12980.7 | 12980.7 | 6879.8 | 6100.9 | 6879.8 | 6100.9 | 12980.7 | 0.0 | 0.0 | 0.0 |
| XYLOSE | [kg/h] | … | 0.0 | 14560.1 | 0.0 | 14560.1 | 14560.1 | 14560.1 | 7716.9 | 6843.2 | 7716.9 | 6843.2 | 14560.1 | 0.0 | 0.0 | 0.0 |
| GLUCOSE | [kg/h] | … | 0.0 | 0.0 | 0.0 | 0.0 | 0.0 | 0.0 | 0.0 | 0.0 | 0.0 | 0.0 | 0.0 | 0.0 | 0.0 | 0.0 |
| YEAST | [kg/h] | … | 0.0 | 87.0 | 1652.8 | 1739.7 | 1739.7 | 1739.7 | 922.1 | 817.7 | 922.1 | 817.7 | 1739.7 | 0.0 | 0.0 | 0.0 |
| ENZYMES | [kg/h] | … | 0.0 | 561.6 | 0.0 | 561.6 | 561.6 | 561.6 | 297.6 | 263.9 | 297.6 | 263.9 | 561.6 | 0.0 | 0.0 | 0.0 |
| ASH | [kg/h] | … | 0.0 | 216.4 | 4110.6 | 4327.0 | 4327.0 | 4327.0 | 2293.3 | 2033.7 | 2293.3 | 2033.7 | 4327.0 | 0.0 | 0.0 | 0.0 |
| EXTRAKT | [kg/h] | … | 0.0 | 5768.9 | 0.0 | 5720.0 | 5768.9 | 5768.9 | 3057.5 | 2711.4 | 3057.5 | 2711.4 | 5768.9 | 48.9 | 0.0 | 0.0 |
| PROTEIN | [kg/h] | … | 0.0 | 2884.8 | 0.0 | 2884.8 | 2884.8 | 2884.8 | 1528.9 | 1355.8 | 1528.9 | 1355.8 | 2884.8 | 0.0 | 0.0 | 0.0 |
| **Mass fraction** | | | | | | | | | | | | | | | | |
| WATER | [1] | … | 0.278 | 0.887 | 0.594 | 0.83 | 0.838 | 0.804 | 0.804 | 0.804 | 0.804 | 0.804 | 0.838 | 0.528 | 0.002 | 0.002 |
| ETHANOL | [1] | … | 0.722 | 0 | 0 | 0 | 0 | 0.04 | 0.04 | 0.04 | 0.04 | 0.04 | 0 | 0.462 | 0.994 | 0.994 |
| ACETAT | [1] | … | 0 | 0.008 | 0 | 0.007 | 0.007 | 0.006 | 0.006 | 0.006 | 0.006 | 0.006 | 0.007 | 0.002 | 0 | 0 |
| FURFURAL | [1] | … | 0 | 0.004 | 0 | 0.003 | 0.003 | 0.003 | 0.003 | 0.003 | 0.003 | 0.003 | 0.003 | 0.004 | 0 | 0 |
| GLYCEROL | [1] | … | 0 | 0.001 | 0 | 0.001 | 0.001 | 0.001 | 0.001 | 0.001 | 0.001 | 0.001 | 0.001 | 0 | 0 | 0 |
| CO2 | [1] | … | 0 | 0 | 0 | 0 | 0 | 0.001 | 0.001 | 0.001 | 0.001 | 0.001 | 0 | 0.002 | 0.005 | 0.005 |
| CELLULOS | [1] | … | 0 | 0 | 0.034 | 0.006 | 0.006 | 0.006 | 0.006 | 0.006 | 0.006 | 0.006 | 0.006 | 0 | 0 | 0 |
| XYLAN | [1] | … | 0 | 0 | 0.016 | 0.003 | 0.003 | 0.003 | 0.003 | 0.003 | 0.003 | 0.003 | 0.003 | 0 | 0 | 0 |
| LIGNIN | [1] | … | 0 | 0.003 | 0.243 | 0.046 | 0.043 | 0.042 | 0.042 | 0.042 | 0.042 | 0.042 | 0.043 | 0 | 0 | 0 |
| XYLOSE | [1] | … | 0 | 0.058 | 0 | 0.051 | 0.049 | 0.047 | 0.047 | 0.047 | 0.047 | 0.047 | 0.049 | 0 | 0 | 0 |
| GLUCOSE | [1] | … | 0 | 0 | 0 | 0 | 0 | 0 | 0 | 0 | 0 | 0 | 0 | 0 | 0 | 0 |
| YEAST | [1] | … | 0 | 0 | 0.033 | 0.006 | 0.006 | 0.006 | 0.006 | 0.006 | 0.006 | 0.006 | 0.006 | 0 | 0 | 0 |
| ENZYMES | [1] | … | 0 | 0.002 | 0 | 0.002 | 0.002 | 0.002 | 0.002 | 0.002 | 0.002 | 0.002 | 0.002 | 0 | 0 | 0 |
| ASH | [1] | … | 0 | 0.001 | 0.081 | 0.015 | 0.014 | 0.014 | 0.014 | 0.014 | 0.014 | 0.014 | 0.014 | 0 | 0 | 0 |
| EXTRAKT | [1] | … | 0 | 0.023 | 0 | 0.02 | 0.019 | 0.018 | 0.018 | 0.018 | 0.018 | 0.018 | 0.019 | 0.002 | 0 | 0 |
| PROTEIN | [1] | … | 0 | 0.012 | 0 | 0.01 | 0.01 | 0.009 | 0.009 | 0.009 | 0.009 | 0.009 | 0.01 | 0 | 0 | 0 |

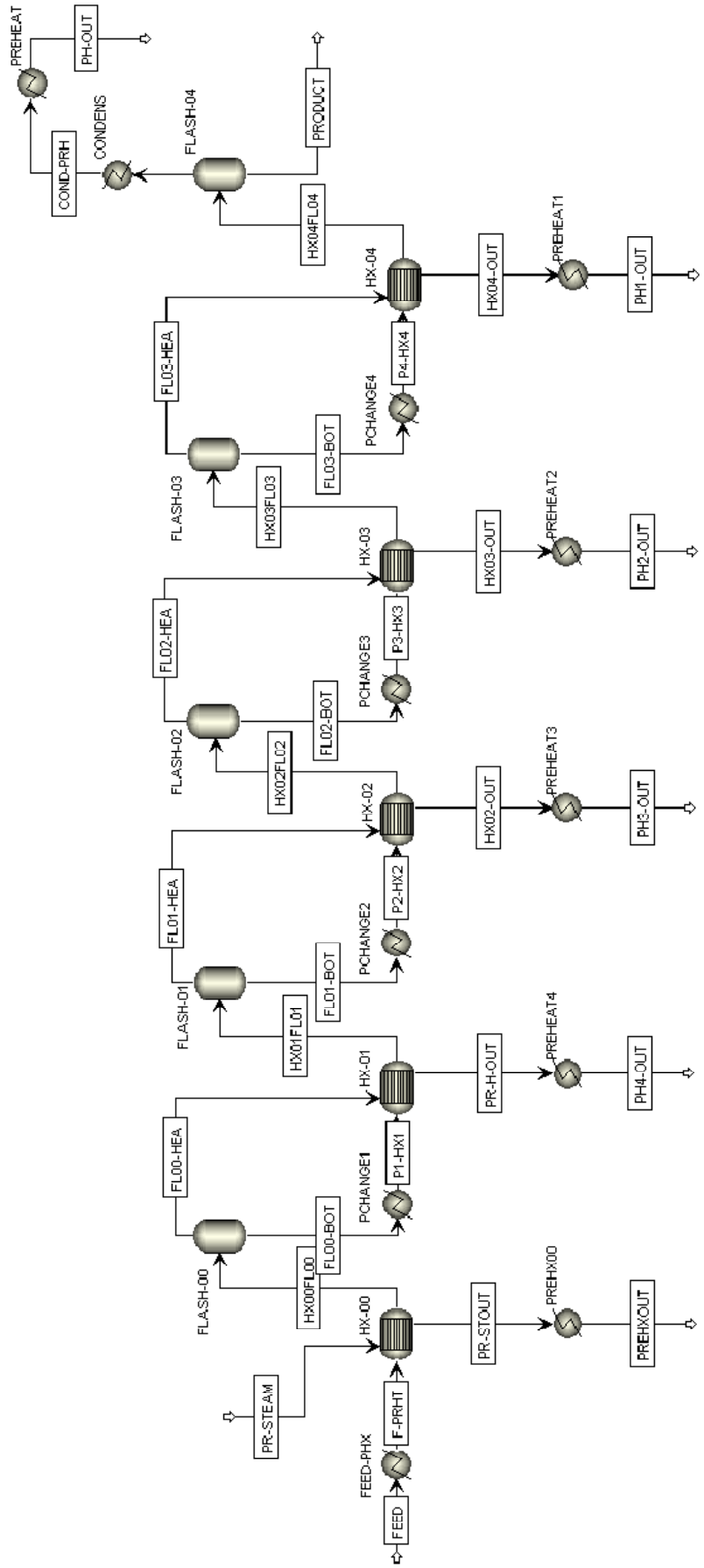


**Figure C-3: ASPEN PLUS flow sheet of the 5-stage co-current evaporation BASE CASE model**

**Table C-4: ASPEN PLUS simulation process streams of the 5-stage evaporation co-current BASE CASE model based on the 2-column dist. results (part 1)**

| Stream name | | COND-PRH | F-PRHT | FEED | FL00-BOT | FL00-HEA | FL01-BOT | FL01-HEA | FL02-BOT | FL02-HEA | FL03-BOT | FL03-HEA | FL04-HEA | HX00FL00 | HX01FL01 | HX02-OUT | HX02FL02 | HX03-OUT | … |
|---|---|---|---|---|---|---|---|---|---|---|---|---|---|---|---|---|---|---|---|
| **Temperature** | [°C] | 81.4 | 134 | 40 | 134.1 | 134.1 | 120.9 | 120.9 | 112.3 | 112.3 | 101.1 | 101.1 | 85.9 | 134.1 | 120.9 | 120.1 | 112.3 | 111.3 | … |
| **Pressure** | [bar] | 0.5 | 3 | 3.2 | 3 | 3 | 2 | 2 | 1.5 | 1.5 | 1 | 1 | 0.5 | 3 | 2 | 2 | 1.5 | 1.5 | … |
| **Vapor fraction** | [1] | 0 | 0 | 0 | 0 | 1 | 0 | 1 | 0 | 1 | 0 | 1 | 1 | 0.153 | 0.209 | 0 | 0.28 | 0 | … |
| **Total mole flow** | [kmol/h] | 2553.9 | 12481.0 | 12481.0 | 10565.3 | 1915.7 | 8362.0 | 2203.3 | 6018.9 | 2343.1 | 3553.6 | 2465.3 | 2553.9 | 12481.0 | 10565.3 | 2203.3 | 8362.0 | 2343.1 | … |
| **Total mass flow** | [kg/h] | 47924.1 | 248925.8 | 248925.8 | 213737.5 | 35188.2 | 173409.3 | 40328.2 | 130548.9 | 42860.4 | 85277.6 | 45271.3 | 47924.1 | 248925.8 | 213737.5 | 40328.2 | 173409.3 | 42860.4 | … |
| **Component mass flow** | | | | | | | | | | | | | | | | | | | |
| WATER | [kg/h] | 45729.1 | 220907.3 | 220907.3 | 186548.2 | 34359.2 | 146992.2 | 39556.0 | 104912.7 | 42079.4 | 60658.3 | 44254.4 | 45729.1 | 220907.3 | 186548.2 | 39556.0 | 146992.2 | 42079.4 | … |
| ETHANOL | [kg/h] | 0.0 | 2.9 | 2.9 | 0.9 | 2.0 | 0.2 | 0.7 | 0.0 | 0.2 | 0.0 | 0.0 | 0.0 | 2.9 | 0.9 | 0.7 | 0.2 | 0.2 | … |
| ACETAT | [kg/h] | 580.0 | 1965.8 | 1965.8 | 1790.7 | 175.1 | 1563.1 | 227.6 | 1281.3 | 281.8 | 910.7 | 370.6 | 580.0 | 1965.8 | 1790.7 | 227.6 | 1563.1 | 281.8 | … |
| FURFURAL | [kg/h] | 12.1 | 927.0 | 927.0 | 463.9 | 463.1 | 186.6 | 277.3 | 60.3 | 126.4 | 14.3 | 46.0 | 12.1 | 927.0 | 463.9 | 277.3 | 186.6 | 126.4 | … |
| GLYCEROL | [kg/h] | 0.1 | 264.7 | 264.7 | 264.7 | 0.0 | 264.6 | 0.0 | 264.6 | 0.0 | 264.6 | 0.0 | 0.1 | 264.7 | 264.7 | 0.0 | 264.6 | 0.0 | … |
| CO2 | [kg/h] | 0.0 | 0.0 | 0.0 | 0.0 | 0.0 | 0.0 | 0.0 | 0.0 | 0.0 | 0.0 | 0.0 | 0.0 | 0.0 | 0.0 | 0.0 | 0.0 | 0.0 | … |
| CELLULOS | [kg/h] | 1.6 | 89.8 | 89.8 | 89.6 | 0.3 | 89.3 | 0.3 | 88.9 | 0.4 | 88.3 | 0.5 | 1.6 | 89.8 | 89.6 | 0.3 | 89.3 | 0.4 | … |
| XYLAN | [kg/h] | 0.0 | 42.8 | 42.8 | 42.8 | 0.0 | 42.8 | 0.0 | 42.8 | 0.0 | 42.8 | 0.0 | 0.0 | 42.8 | 42.8 | 0.0 | 42.8 | 0.0 | … |
| LIGNIN | [kg/h] | 0.0 | 649.0 | 649.0 | 649.0 | 0.0 | 649.0 | 0.0 | 649.0 | 0.0 | 649.0 | 0.0 | 0.0 | 649.0 | 649.0 | 0.0 | 649.0 | 0.0 | … |
| XYLOSE | [kg/h] | 0.0 | 14558.8 | 14558.8 | 14558.8 | 0.0 | 14558.8 | 0.0 | 14558.8 | 0.0 | 14558.8 | 0.0 | 0.0 | 14558.8 | 14558.8 | 0.0 | 14558.8 | 0.0 | … |
| GLUCOSE | [kg/h] | 0.0 | 0.0 | 0.0 | 0.0 | 0.0 | 0.0 | 0.0 | 0.0 | 0.0 | 0.0 | 0.0 | 0.0 | 0.0 | 0.0 | 0.0 | 0.0 | 0.0 | … |
| YEAST | [kg/h] | 0.0 | 87.0 | 87.0 | 87.0 | 0.0 | 87.0 | 0.0 | 87.0 | 0.0 | 87.0 | 0.0 | 0.0 | 87.0 | 87.0 | 0.0 | 87.0 | 0.0 | … |
| ENZYMES | [kg/h] | 0.0 | 561.5 | 561.5 | 561.5 | 0.0 | 561.5 | 0.0 | 561.5 | 0.0 | 561.5 | 0.0 | 0.0 | 561.5 | 561.5 | 0.0 | 561.5 | 0.0 | … |
| ASH | [kg/h] | 0.0 | 216.3 | 216.3 | 216.3 | 0.0 | 216.3 | 0.0 | 216.3 | 0.0 | 216.3 | 0.0 | 0.0 | 216.3 | 216.3 | 0.0 | 216.3 | 0.0 | … |
| EXTRAKT | [kg/h] | 1601.2 | 5768.4 | 5768.4 | 5579.8 | 188.6 | 5313.4 | 266.3 | 4941.2 | 372.2 | 4341.5 | 599.7 | 1601.2 | 5768.4 | 5579.8 | 266.3 | 5313.4 | 372.2 | … |
| PROTEIN | [kg/h] | 0.0 | 2884.5 | 2884.5 | 2884.5 | 0.0 | 2884.5 | 0.0 | 2884.5 | 0.0 | 2884.4 | 0.0 | 0.0 | 2884.5 | 2884.5 | 0.0 | 2884.5 | 0.0 | … |
| **Mass fraction** | | | | | | | | | | | | | | | | | | | |
| WATER | [1] | 0.954 | 0.887 | 0.887 | 0.873 | 0.976 | 0.848 | 0.981 | 0.804 | 0.982 | 0.711 | 0.978 | 0.954 | 0.887 | 0.873 | 0.981 | 0.848 | 0.982 | … |
| ETHANOL | [1] | 0 | 0 | 0 | 0 | 0 | 0 | 0 | 0 | 0 | 0 | 0 | 0 | 0 | 0 | 0 | 0 | 0 | … |
| ACETAT | [1] | 0.012 | 0.008 | 0.008 | 0.008 | 0.005 | 0.009 | 0.006 | 0.01 | 0.007 | 0.011 | 0.008 | 0.012 | 0.008 | 0.008 | 0.006 | 0.009 | 0.007 | … |
| FURFURAL | [1] | 0 | 0.004 | 0.004 | 0.002 | 0.013 | 0.001 | 0.007 | 0 | 0.003 | 0 | 0.001 | 0 | 0.004 | 0.002 | 0.007 | 0.001 | 0.003 | … |
| GLYCEROL | [1] | 0 | 0.001 | 0.001 | 0.001 | 0 | 0.002 | 0 | 0.002 | 0 | 0.003 | 0 | 0 | 0.001 | 0.001 | 0 | 0.002 | 0 | … |
| CO2 | [1] | 0 | 0 | 0 | 0 | 0 | 0 | 0 | 0 | 0 | 0 | 0 | 0 | 0 | 0 | 0 | 0 | 0 | … |
| CELLULOS | [1] | 0 | 0 | 0 | 0 | 0 | 0.001 | 0 | 0.001 | 0 | 0.001 | 0 | 0 | 0 | 0 | 0 | 0.001 | 0 | … |
| XYLAN | [1] | 0 | 0 | 0 | 0 | 0 | 0 | 0 | 0 | 0 | 0.001 | 0 | 0 | 0 | 0 | 0 | 0 | 0 | … |
| LIGNIN | [1] | 0 | 0.003 | 0.003 | 0.003 | 0 | 0.004 | 0 | 0.005 | 0 | 0.008 | 0 | 0 | 0.003 | 0.003 | 0 | 0.004 | 0 | … |
| XYLOSE | [1] | 0 | 0.058 | 0.058 | 0.068 | 0 | 0.084 | 0 | 0.112 | 0 | 0.171 | 0 | 0 | 0.058 | 0.068 | 0 | 0.084 | 0 | … |
| GLUCOSE | [1] | 0 | 0 | 0 | 0 | 0 | 0 | 0 | 0 | 0 | 0 | 0 | 0 | 0 | 0 | 0 | 0 | 0 | … |
| YEAST | [1] | 0 | 0 | 0 | 0 | 0 | 0.001 | 0 | 0.001 | 0 | 0.001 | 0 | 0 | 0 | 0 | 0 | 0.001 | 0 | … |
| ENZYMES | [1] | 0 | 0.002 | 0.002 | 0.003 | 0 | 0.003 | 0 | 0.004 | 0 | 0.007 | 0 | 0 | 0.002 | 0.003 | 0 | 0.003 | 0 | … |
| ASH | [1] | 0 | 0.001 | 0.001 | 0.001 | 0 | 0.001 | 0 | 0.002 | 0 | 0.003 | 0 | 0 | 0.001 | 0.001 | 0 | 0.001 | 0 | … |
| EXTRAKT | [1] | 0.033 | 0.023 | 0.023 | 0.026 | 0.005 | 0.031 | 0.007 | 0.038 | 0.009 | 0.051 | 0.013 | 0.033 | 0.023 | 0.026 | 0.007 | 0.031 | 0.009 | … |
| PROTEIN | [1] | 0 | 0.012 | 0.012 | 0.013 | 0 | 0.017 | 0 | 0.022 | 0 | 0.034 | 0 | 0 | 0.012 | 0.013 | 0 | 0.017 | 0 | … |

**Table C-5: ASPEN PLUS simulation process streams of the 5-stage evaporation co-current BASE CASE model based on the 2-column dist. results (part 2)**

| Stream name | | … | HX03FL03 | HX04-OUT | HX04FL04 | P1-HX1 | P2-HX2 | P3-HX3 | P4-HX4 | PH-OUT | PH1-OUT | PH2-OUT | PH3-OUT | PH4-OUT | PR-H-OUT | PR-STEAM | PR-STOUT | PREHXOUT | PRODUCT |
|---|---|---|---|---|---|---|---|---|---|---|---|---|---|---|---|---|---|---|---|
| **Temperature** | [°C] | … | 101.1 | 99.7 | 85.9 | 120.8 | 112 | 100.5 | 82.7 | 50 | 50 | 50 | 50 | 50 | 133.2 | 144 | 143.7 | 50 | 85.9 |
| **Pressure** | [bar] | … | 1 | 1 | 0.5 | 2 | 1.5 | 1 | 0.5 | 0.5 | 1 | 1.5 | 2 | 3 | 3 | 4 | 4 | 4 | 0.5 |
| **Vapor fraction** | [1] | … | 0.41 | 0 | 0.719 | 0.03 | 0.02 | 0.026 | 0.04 | 0 | 0 | 0 | 0 | 0 | 0 | 1 | 0 | 0 | 0 |
| **Total mole flow** | [kmol/h] | … | 6018.9 | 2465.3 | 3553.6 | 10565.3 | 8362.0 | 6018.9 | 3553.6 | 2553.9 | 2465.3 | 2343.1 | 2203.3 | 1915.7 | 1915.7 | 1942.8 | 1942.8 | 1942.8 | 999.7 |
| **Total mass flow** | [kg/h] | … | 130548.9 | 45271.3 | 85277.6 | 213737.5 | 173409.3 | 130548.9 | 85277.6 | 47924.1 | 45271.3 | 42860.4 | 40328.2 | 35188.2 | 35188.2 | 35000.0 | 35000.0 | 35000.0 | 37353.5 |
| **Component mass flow** | | | | | | | | | | | | | | | | | | | |
| WATER | [kg/h] | … | 104912.7 | 44254.4 | 60658.3 | 186548.2 | 146992.2 | 104912.7 | 60658.3 | 45729.1 | 44254.4 | 42079.4 | 39556.0 | 34359.2 | 34359.2 | 35000.0 | 35000.0 | 35000.0 | 14929.2 |
| ETHANOL | [kg/h] | … | 0.0 | 0.0 | 0.0 | 0.9 | 0.2 | 0.0 | 0.0 | 0.0 | 0.0 | 0.2 | 0.7 | 2.0 | 2.0 | 0.0 | 0.0 | 0.0 | 0.0 |
| ACETAT | [kg/h] | … | 1281.3 | 370.6 | 910.7 | 1790.7 | 1563.1 | 1281.3 | 910.7 | 580.0 | 370.6 | 281.8 | 227.6 | 175.1 | 175.1 | 0.0 | 0.0 | 0.0 | 330.8 |
| FURFURAL | [kg/h] | … | 60.3 | 46.0 | 14.3 | 463.9 | 186.6 | 60.3 | 14.3 | 12.1 | 46.0 | 126.4 | 277.3 | 463.1 | 463.1 | 0.0 | 0.0 | 0.0 | 2.2 |
| GLYCEROL | [kg/h] | … | 264.6 | 0.0 | 264.6 | 264.7 | 264.6 | 264.6 | 264.6 | 0.1 | 0.0 | 0.0 | 0.0 | 0.0 | 0.0 | 0.0 | 0.0 | 0.0 | 264.5 |
| CO2 | [kg/h] | … | 0.0 | 0.0 | 0.0 | 0.0 | 0.0 | 0.0 | 0.0 | 0.0 | 0.0 | 0.0 | 0.0 | 0.0 | 0.0 | 0.0 | 0.0 | 0.0 | 0.0 |
| CELLULOS | [kg/h] | … | 88.9 | 0.5 | 88.3 | 89.6 | 89.3 | 88.9 | 88.3 | 1.6 | 0.5 | 0.4 | 0.3 | 0.3 | 0.3 | 0.0 | 0.0 | 0.0 | 86.8 |
| XYLAN | [kg/h] | … | 42.8 | 0.0 | 42.8 | 42.8 | 42.8 | 42.8 | 42.8 | 0.0 | 0.0 | 0.0 | 0.0 | 0.0 | 0.0 | 0.0 | 0.0 | 0.0 | 42.8 |
| LIGNIN | [kg/h] | … | 649.0 | 0.0 | 649.0 | 649.0 | 649.0 | 649.0 | 649.0 | 0.0 | 0.0 | 0.0 | 0.0 | 0.0 | 0.0 | 0.0 | 0.0 | 0.0 | 649.0 |
| XYLOSE | [kg/h] | … | 14558.8 | 0.0 | 14558.8 | 14558.8 | 14558.8 | 14558.8 | 14558.8 | 0.0 | 0.0 | 0.0 | 0.0 | 0.0 | 0.0 | 0.0 | 0.0 | 0.0 | 14558.8 |
| GLUCOSE | [kg/h] | … | 0.0 | 0.0 | 0.0 | 0.0 | 0.0 | 0.0 | 0.0 | 0.0 | 0.0 | 0.0 | 0.0 | 0.0 | 0.0 | 0.0 | 0.0 | 0.0 | 0.0 |
| YEAST | [kg/h] | … | 87.0 | 0.0 | 87.0 | 87.0 | 87.0 | 87.0 | 87.0 | 0.0 | 0.0 | 0.0 | 0.0 | 0.0 | 0.0 | 0.0 | 0.0 | 0.0 | 87.0 |
| ENZYMES | [kg/h] | … | 561.5 | 0.0 | 561.5 | 561.5 | 561.5 | 561.5 | 561.5 | 0.0 | 0.0 | 0.0 | 0.0 | 0.0 | 0.0 | 0.0 | 0.0 | 0.0 | 561.5 |
| ASH | [kg/h] | … | 216.3 | 0.0 | 216.3 | 216.3 | 216.3 | 216.3 | 216.3 | 0.0 | 0.0 | 0.0 | 0.0 | 0.0 | 0.0 | 0.0 | 0.0 | 0.0 | 216.3 |
| EXTRAKT | [kg/h] | … | 4941.2 | 599.7 | 4341.5 | 5579.8 | 5313.4 | 4941.2 | 4341.5 | 1601.2 | 599.7 | 372.2 | 266.3 | 188.6 | 188.6 | 0.0 | 0.0 | 0.0 | 2740.3 |
| PROTEIN | [kg/h] | … | 2884.5 | 0.0 | 2884.4 | 2884.5 | 2884.5 | 2884.5 | 2884.4 | 0.0 | 0.0 | 0.0 | 0.0 | 0.0 | 0.0 | 0.0 | 0.0 | 0.0 | 2884.4 |
| **Mass fraction** | | | | | | | | | | | | | | | | | | | |
| WATER | [1] | … | 0.804 | 0.978 | 0.711 | 0.873 | 0.848 | 0.804 | 0.711 | 0.954 | 0.978 | 0.982 | 0.981 | 0.976 | 0.976 | 1 | 1 | 1 | 0.4 |
| ETHANOL | [1] | … | 0 | 0 | 0 | 0 | 0 | 0 | 0 | 0 | 0 | 0 | 0 | 0 | 0 | 0 | 0 | 0 | 0 |
| ACETAT | [1] | … | 0.01 | 0.008 | 0.011 | 0.008 | 0.009 | 0.01 | 0.011 | 0.012 | 0.008 | 0.007 | 0.006 | 0.005 | 0.005 | 0 | 0 | 0 | 0.009 |
| FURFURAL | [1] | … | 0 | 0.001 | 0 | 0.002 | 0.001 | 0 | 0 | 0 | 0.001 | 0.003 | 0.007 | 0.013 | 0.013 | 0 | 0 | 0 | 0 |
| GLYCEROL | [1] | … | 0.002 | 0 | 0.003 | 0.001 | 0.002 | 0.002 | 0.003 | 0 | 0 | 0 | 0 | 0 | 0 | 0 | 0 | 0 | 0.007 |
| CO2 | [1] | … | 0 | 0 | 0 | 0 | 0 | 0 | 0 | 0 | 0 | 0 | 0 | 0 | 0 | 0 | 0 | 0 | 0 |
| CELLULOS | [1] | … | 0.001 | 0 | 0.001 | 0 | 0.001 | 0.001 | 0.001 | 0 | 0 | 0 | 0 | 0 | 0 | 0 | 0 | 0 | 0.002 |
| XYLAN | [1] | … | 0 | 0 | 0.001 | 0 | 0 | 0 | 0.001 | 0 | 0 | 0 | 0 | 0 | 0 | 0 | 0 | 0 | 0.001 |
| LIGNIN | [1] | … | 0.005 | 0 | 0.008 | 0.003 | 0.004 | 0.005 | 0.008 | 0 | 0 | 0 | 0 | 0 | 0 | 0 | 0 | 0 | 0.017 |
| XYLOSE | [1] | … | 0.112 | 0 | 0.171 | 0.068 | 0.084 | 0.112 | 0.171 | 0 | 0 | 0 | 0 | 0 | 0 | 0 | 0 | 0 | 0.39 |
| GLUCOSE | [1] | … | 0 | 0 | 0 | 0 | 0 | 0 | 0 | 0 | 0 | 0 | 0 | 0 | 0 | 0 | 0 | 0 | 0 |
| YEAST | [1] | … | 0.001 | 0 | 0.001 | 0 | 0.001 | 0.001 | 0.001 | 0 | 0 | 0 | 0 | 0 | 0 | 0 | 0 | 0 | 0.002 |
| ENZYMES | [1] | … | 0.004 | 0 | 0.007 | 0.003 | 0.003 | 0.004 | 0.007 | 0 | 0 | 0 | 0 | 0 | 0 | 0 | 0 | 0 | 0.015 |
| ASH | [1] | … | 0.002 | 0 | 0.003 | 0.001 | 0.001 | 0.002 | 0.003 | 0 | 0 | 0 | 0 | 0 | 0 | 0 | 0 | 0 | 0.006 |
| EXTRAKT | [1] | … | 0.038 | 0.013 | 0.051 | 0.026 | 0.031 | 0.038 | 0.051 | 0.033 | 0.013 | 0.009 | 0.007 | 0.005 | 0.005 | 0 | 0 | 0 | 0.073 |
| PROTEIN | [1] | … | 0.022 | 0 | 0.034 | 0.013 | 0.017 | 0.022 | 0.034 | 0 | 0 | 0 | 0 | 0 | 0 | 0 | 0 | 0 | 0.077 |

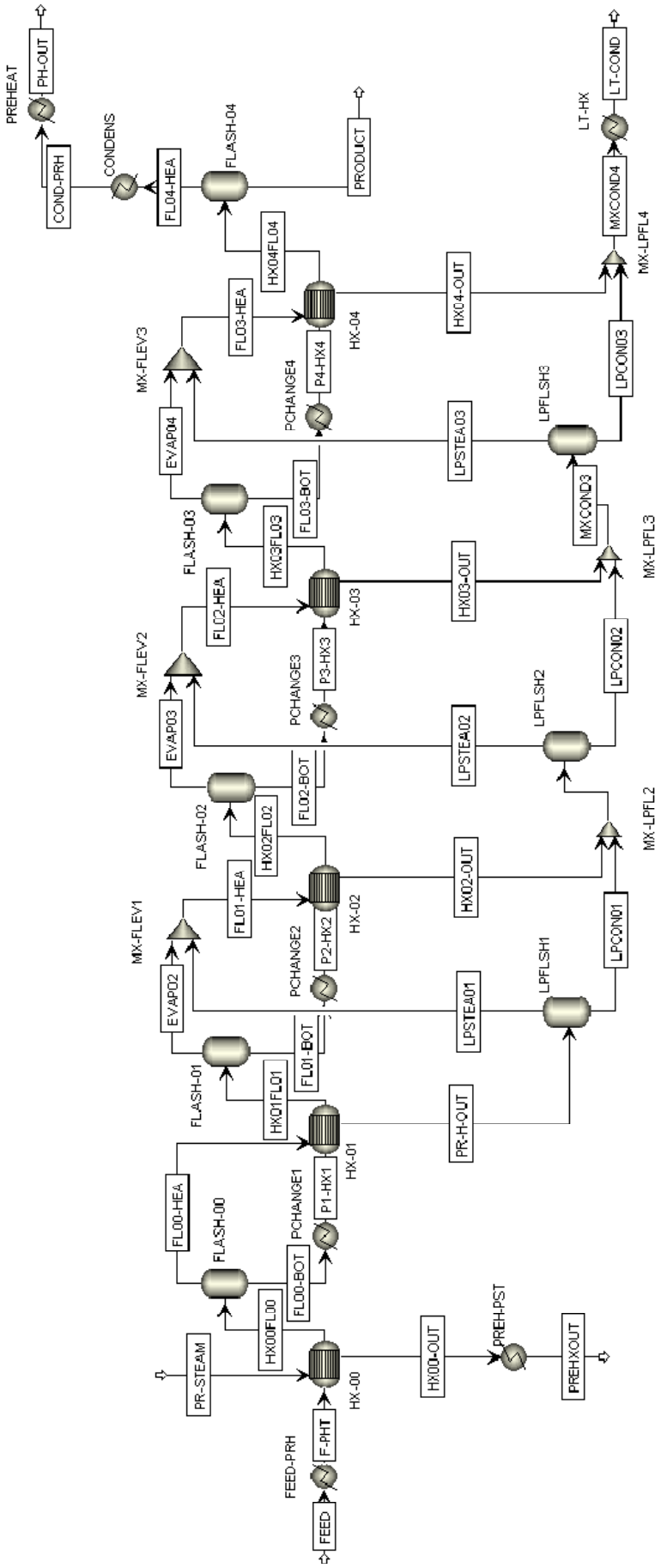


**Figure C-4: ASPEN PLUS flow sheet of the 5-stage evaporation co-current FLASH CASE model**

**Table C-6: ASPEN PLUS simulation process streams of the 5-stage evaporation co-current FLASH CASE model based on the 2-column dist. results (part 1)**

| Stream name | | COND-PRH | EVAP02 | EVAP03 | EVAP04 | F-PHT | FEED | FL00-BOT | FL00-HEA | FL01-BOT | FL01-HEA | FL02-BOT | FL02-HEA | FL03-BOT | FL03-HEA | FL04-HEA | HX00-OUT | HX00FL00 | HX01FL01 | HX02-OUT | HX02FL02 | HX03-OUT | HX03FL03 | ... |
|---|---|---|---|---|---|---|---|---|---|---|---|---|---|---|---|---|---|---|---|---|---|---|---|---|
| **Temperature** | [°C] | 81.4 | 120.9 | 112.3 | 101 | 134 | 40 | 134.1 | 134.1 | 120.9 | 120.9 | 112.3 | 112.2 | 101 | 100.9 | 85.9 | 143.7 | 134.1 | 120.9 | 120 | 112.3 | 111.3 | 101 | ... |
| **Pressure** | [bar] | 0.5 | 2 | 1.5 | 1 | 3 | 3.2 | 3 | 3 | 2 | 2 | 1.5 | 1.5 | 1 | 1 | 0.5 | 4 | 3 | 2 | 2 | 1.5 | 1.5 | 1 | ... |
| **Vapor fraction** | [1] | 0 | 1 | 1 | 1 | 0 | 0 | 0 | 1 | 0 | 1 | 0 | 1 | 0 | 1 | 1 | 0 | 0.146 | 0.198 | 0 | 0.269 | 0 | 0.401 | ... |
| **Total mole flow** | [kmol/h] | 2743.7 | 2107.6 | 2304.7 | 2505.1 | 12481.0 | 12481.0 | 10665.6 | 1815.4 | 8557.9 | 2160.4 | 6253.2 | 2377.5 | 3748.1 | 2652.2 | 2743.7 | 1842.2 | 12481.0 | 10665.6 | 2160.4 | 8557.9 | 2377.5 | 6253.2 | ... |
| **Total mass flow** | [kg/h] | 51454.8 | 38581.6 | 42152.8 | 45976.0 | 248925.8 | 248925.8 | 215572.7 | 33353.1 | 176991.1 | 39595.7 | 134838.3 | 43537.6 | 88862.2 | 48741.1 | 51454.8 | 33188.1 | 248925.8 | 215572.7 | 39595.7 | 176991.1 | 43537.6 | 134838.3 | ... |
| **Component mass flow** | | | | | | | | | | | | | | | | | | | | | | | | |
| WATER | [kg/h] | 49132.8 | 37836.4 | 41390.9 | 44971.9 | 220907.3 | 220907.3 | 188347.9 | 32559.4 | 150511.4 | 38770.8 | 109120.5 | 42684.5 | 64148.6 | 47595.6 | 49132.8 | 33188.1 | 220907.3 | 188347.9 | 38770.8 | 150511.4 | 42684.5 | 109120.5 | ... |
| ETHANOL | [kg/h] | 0.0 | 0.7 | 0.2 | 0.0 | 2.9 | 2.9 | 0.9 | 2.0 | 0.2 | 1.2 | 0.0 | 0.7 | 0.0 | 0.7 | 0.0 | 0.0 | 2.9 | 0.9 | 1.2 | 0.2 | 0.7 | 0.0 | ... |
| ACETAT | [kg/h] | 614.9 | 215.6 | 272.9 | 368.9 | 1965.8 | 1965.8 | 1800.6 | 165.2 | 1585.0 | 218.1 | 1312.1 | 276.7 | 943.3 | 377.4 | 614.9 | 0.0 | 1965.8 | 1800.6 | 218.1 | 1585.0 | 276.7 | 1312.1 | ... |
| FURFURAL | [kg/h] | 13.6 | 278.5 | 133.2 | 50.5 | 927.0 | 927.0 | 478.1 | 448.8 | 199.6 | 354.2 | 66.4 | 218.7 | 15.9 | 179.2 | 13.6 | 0.0 | 927.0 | 478.1 | 354.2 | 199.6 | 218.7 | 66.4 | ... |
| GLYCEROL | [kg/h] | 0.1 | 0.0 | 0.0 | 0.0 | 264.7 | 264.7 | 264.7 | 0.0 | 264.6 | 0.0 | 264.6 | 0.0 | 264.6 | 0.0 | 0.1 | 0.0 | 264.7 | 264.7 | 0.0 | 264.6 | 0.0 | 264.6 | ... |
| CO2 | [kg/h] | 0.0 | 0.0 | 0.0 | 0.0 | 0.0 | 0.0 | 0.0 | 0.0 | 0.0 | 0.0 | 0.0 | 0.0 | 0.0 | 0.0 | 0.0 | 0.0 | 0.0 | 0.0 | 0.0 | 0.0 | 0.0 | 0.0 | ... |
| CELLULOS | [kg/h] | 1.7 | 0.3 | 0.4 | 0.5 | 89.8 | 89.8 | 89.6 | 0.2 | 89.3 | 0.3 | 88.9 | 0.4 | 88.4 | 0.5 | 1.7 | 0.0 | 89.8 | 89.6 | 0.3 | 89.3 | 0.4 | 88.9 | ... |
| XYLAN | [kg/h] | 0.0 | 0.0 | 0.0 | 0.0 | 42.8 | 42.8 | 42.8 | 0.0 | 42.8 | 0.0 | 42.8 | 0.0 | 42.8 | 0.0 | 0.0 | 0.0 | 42.8 | 42.8 | 0.0 | 42.8 | 0.0 | 42.8 | ... |
| LIGNIN | [kg/h] | 0.0 | 0.0 | 0.0 | 0.0 | 649.0 | 649.0 | 649.0 | 0.0 | 649.0 | 0.0 | 649.0 | 0.0 | 649.0 | 0.0 | 0.0 | 0.0 | 649.0 | 649.0 | 0.0 | 649.0 | 0.0 | 649.0 | ... |
| XYLOSE | [kg/h] | 0.0 | 0.0 | 0.0 | 0.0 | 14558.8 | 14558.8 | 14558.8 | 0.0 | 14558.8 | 0.0 | 14558.8 | 0.0 | 14558.8 | 0.0 | 0.0 | 0.0 | 14558.8 | 14558.8 | 0.0 | 14558.8 | 0.0 | 14558.8 | ... |
| GLUCOSE | [kg/h] | 0.0 | 0.0 | 0.0 | 0.0 | 0.0 | 0.0 | 0.0 | 0.0 | 0.0 | 0.0 | 0.0 | 0.0 | 0.0 | 0.0 | 0.0 | 0.0 | 0.0 | 0.0 | 0.0 | 0.0 | 0.0 | 0.0 | ... |
| YEAST | [kg/h] | 0.0 | 0.0 | 0.0 | 0.0 | 87.0 | 87.0 | 87.0 | 0.0 | 87.0 | 0.0 | 87.0 | 0.0 | 87.0 | 0.0 | 0.0 | 0.0 | 87.0 | 87.0 | 0.0 | 87.0 | 0.0 | 87.0 | ... |
| ENZYMES | [kg/h] | 0.0 | 0.0 | 0.0 | 0.0 | 561.5 | 561.5 | 561.5 | 0.0 | 561.5 | 0.0 | 561.5 | 0.0 | 561.5 | 0.0 | 0.0 | 0.0 | 561.5 | 561.5 | 0.0 | 561.5 | 0.0 | 561.5 | ... |
| ASH | [kg/h] | 0.0 | 0.0 | 0.0 | 0.0 | 216.3 | 216.3 | 216.3 | 0.0 | 216.3 | 0.0 | 216.3 | 0.0 | 216.3 | 0.0 | 0.0 | 0.0 | 216.3 | 216.3 | 0.0 | 216.3 | 0.0 | 216.3 | ... |
| EXTRAKT | [kg/h] | 1691.6 | 250.1 | 355.2 | 584.2 | 5768.4 | 5768.4 | 5591.0 | 177.3 | 5341.0 | 251.0 | 4985.8 | 356.7 | 4401.6 | 587.7 | 1691.6 | 0.0 | 5768.4 | 5591.0 | 251.0 | 5341.0 | 356.7 | 4985.8 | ... |
| PROTEIN | [kg/h] | 0.0 | 0.0 | 0.0 | 0.0 | 2884.5 | 2884.5 | 2884.5 | 0.0 | 2884.5 | 0.0 | 2884.5 | 0.0 | 2884.5 | 0.0 | 0.0 | 0.0 | 2884.5 | 2884.5 | 0.0 | 2884.5 | 0.0 | 2884.5 | ... |
| **Mass fraction** | | | | | | | | | | | | | | | | | | | | | | | | |
| WATER | [1] | 0.955 | 0.981 | 0.982 | 0.978 | 0.887 | 0.887 | 0.874 | 0.976 | 0.85 | 0.979 | 0.809 | 0.98 | 0.722 | 0.976 | 0.955 | 1 | 0.887 | 0.874 | 0.979 | 0.85 | 0.98 | 0.809 | ... |
| ETHANOL | [1] | 0 | 0 | 0 | 0 | 0 | 0 | 0 | 0 | 0 | 0 | 0 | 0 | 0 | 0 | 0 | 0 | 0 | 0 | 0 | 0 | 0 | 0 | ... |
| ACETAT | [1] | 0.012 | 0.006 | 0.006 | 0.008 | 0.008 | 0.008 | 0.008 | 0.005 | 0.009 | 0.006 | 0.01 | 0.006 | 0.011 | 0.008 | 0.012 | 0 | 0.008 | 0.008 | 0.006 | 0.009 | 0.006 | 0.01 | ... |
| FURFURAL | [1] | 0 | 0.007 | 0.003 | 0.001 | 0.004 | 0.004 | 0.002 | 0.013 | 0.001 | 0.009 | 0 | 0.005 | 0 | 0.004 | 0 | 0 | 0.004 | 0.002 | 0.009 | 0.001 | 0.005 | 0 | ... |
| GLYCEROL | [1] | 0 | 0 | 0 | 0 | 0.001 | 0.001 | 0.001 | 0 | 0.001 | 0 | 0.002 | 0 | 0.003 | 0 | 0 | 0 | 0.001 | 0.001 | 0 | 0.001 | 0 | 0.002 | ... |
| CO2 | [1] | 0 | 0 | 0 | 0 | 0 | 0 | 0 | 0 | 0 | 0 | 0 | 0 | 0 | 0 | 0 | 0 | 0 | 0 | 0 | 0 | 0 | 0 | ... |
| CELLULOS | [1] | 0 | 0 | 0 | 0 | 0 | 0 | 0 | 0 | 0.001 | 0 | 0.001 | 0 | 0.001 | 0 | 0 | 0 | 0 | 0 | 0 | 0.001 | 0 | 0.001 | ... |
| XYLAN | [1] | 0 | 0 | 0 | 0 | 0 | 0 | 0 | 0 | 0 | 0 | 0 | 0 | 0 | 0 | 0 | 0 | 0 | 0 | 0 | 0 | 0 | 0 | ... |
| LIGNIN | [1] | 0 | 0 | 0 | 0 | 0.003 | 0.003 | 0.003 | 0 | 0.004 | 0 | 0.005 | 0 | 0.007 | 0 | 0 | 0 | 0.003 | 0.003 | 0 | 0.004 | 0 | 0.005 | ... |
| XYLOSE | [1] | 0 | 0 | 0 | 0 | 0.058 | 0.058 | 0.068 | 0 | 0.082 | 0 | 0.108 | 0 | 0.164 | 0 | 0 | 0 | 0.058 | 0.068 | 0 | 0.082 | 0 | 0.108 | ... |
| GLUCOSE | [1] | 0 | 0 | 0 | 0 | 0 | 0 | 0 | 0 | 0 | 0 | 0 | 0 | 0 | 0 | 0 | 0 | 0 | 0 | 0 | 0 | 0 | 0 | ... |
| YEAST | [1] | 0 | 0 | 0 | 0 | 0 | 0 | 0 | 0 | 0 | 0 | 0.001 | 0 | 0.001 | 0 | 0 | 0 | 0 | 0 | 0 | 0 | 0 | 0.001 | ... |
| ENZYMES | [1] | 0 | 0 | 0 | 0 | 0.002 | 0.002 | 0.003 | 0 | 0.003 | 0 | 0.004 | 0 | 0.006 | 0 | 0 | 0 | 0.002 | 0.003 | 0 | 0.003 | 0 | 0.004 | ... |
| ASH | [1] | 0 | 0 | 0 | 0 | 0.001 | 0.001 | 0.001 | 0 | 0.001 | 0 | 0.002 | 0 | 0.002 | 0 | 0 | 0 | 0.001 | 0.001 | 0 | 0.001 | 0 | 0.002 | ... |
| EXTRAKT | [1] | 0.033 | 0.006 | 0.008 | 0.013 | 0.023 | 0.023 | 0.026 | 0.005 | 0.03 | 0.006 | 0.037 | 0.008 | 0.05 | 0.012 | 0.033 | 0 | 0.023 | 0.026 | 0.006 | 0.03 | 0.008 | 0.037 | ... |
| PROTEIN | [1] | 0 | 0 | 0 | 0 | 0.012 | 0.012 | 0.013 | 0 | 0.016 | 0 | 0.021 | 0 | 0.032 | 0 | 0 | 0 | 0.012 | 0.013 | 0 | 0.016 | 0 | 0.021 | ... |

**Table C-7: ASPEN PLUS simulation process streams of the 5-stage evaporation co-current FLASH CASE model based on the 2-column dist. results (part 2)**

| Stream name | | … | HX04-OUT | HX04FL04 | LPCON01 | LPCON02 | LPCON03 | LPSTEA01 | LPSTEA02 | LPSTEA03 | LT-COND | MXCOND2 | MXCOND3 | MXCOND4 | P1-HX1 | P2-HX2 | P3-HX3 | P4-HX4 | PH-OUT | PR-H-OUT | PR-STEAM | PREHXOUT | PRODUCT |
|---|---|---|---|---|---|---|---|---|---|---|---|---|---|---|---|---|---|---|---|---|---|---|---|
| **Temperature** | [°C] | … | 99.6 | 85.9 | 119.9 | 111.1 | 99.5 | 119.9 | 111.1 | 99.5 | 50 | 119.9 | 111.2 | 99.5 | 120.8 | 112 | 100.5 | 82.6 | 50 | 133.1 | 144 | 50 | 85.9 |
| **Pressure** | [bar] | … | 1 | 0.5 | 2 | 1.5 | 1 | 2 | 1.5 | 1 | 1 | 2 | 1.5 | 1 | 2 | 1.5 | 1 | 0.5 | 0.5 | 3 | 4 | 4 | 0.5 |
| **Vapor fraction** | [1] | … | 0 | 0.732 | 0 | 0 | 0 | 1 | 1 | 1 | 0 | 0 | 0 | 0 | 0.03 | 0.02 | 0.025 | 0.04 | 0 | 0 | 1 | 0 | 0 |
| **Total mole flow** | [kmol/h] | … | 2652.2 | 3748.1 | 1762.7 | 3850.3 | 6080.7 | 52.7 | 72.8 | 147.1 | 8732.9 | 3923.1 | 6227.8 | 8732.9 | 10665.6 | 8557.9 | 6253.2 | 3748.1 | 2743.7 | 1815.4 | 1842.2 | 1842.2 | 1004.4 |
| **Total mass flow** | [kg/h] | … | 48741.1 | 88862.2 | 32339.0 | 70549.9 | 111322.4 | 1014.0 | 1384.8 | 2765.1 | 160063.5 | 71934.7 | 114087.5 | 160063.5 | 215572.7 | 176991.1 | 134838.3 | 88862.2 | 51454.8 | 33353.1 | 33188.1 | 33188.1 | 37407.4 |
| **Component mass flow** | | | | | | | | | | | | | | | | | | | | | | | |
| WATER | [kg/h] | … | 47595.6 | 64148.6 | 31625.0 | 69102.3 | 109163.1 | 934.4 | 1293.5 | 2623.7 | 156758.7 | 70395.9 | 111786.8 | 156758.7 | 188347.9 | 150511.4 | 109120.5 | 64148.6 | 49132.8 | 32559.4 | 33188.1 | 33188.1 | 15015.8 |
| ETHANOL | [kg/h] | … | 0.7 | 0.0 | 1.4 | 2.2 | 2.2 | 0.5 | 0.5 | 0.7 | 2.9 | 2.7 | 2.9 | 2.9 | 0.9 | 0.2 | 0.0 | 0.0 | 0.0 | 2.0 | 0.0 | 0.0 | 0.0 |
| ACETAT | [kg/h] | … | 377.4 | 943.3 | 162.7 | 377.0 | 645.1 | 2.5 | 3.8 | 8.5 | 1022.5 | 380.8 | 653.7 | 1022.5 | 1800.6 | 1585.0 | 1312.1 | 943.3 | 614.9 | 165.2 | 0.0 | 0.0 | 328.3 |
| FURFURAL | [kg/h] | … | 179.2 | 15.9 | 373.2 | 641.9 | 731.9 | 75.6 | 85.4 | 128.7 | 911.1 | 727.4 | 860.6 | 911.1 | 478.1 | 199.6 | 66.4 | 15.9 | 13.6 | 448.8 | 0.0 | 0.0 | 2.3 |
| GLYCEROL | [kg/h] | … | 0.0 | 264.6 | 0.0 | 0.0 | 0.0 | 0.0 | 0.0 | 0.0 | 0.1 | 0.0 | 0.0 | 0.1 | 264.7 | 264.6 | 264.6 | 264.6 | 0.1 | 0.0 | 0.0 | 0.0 | 264.5 |
| CO2 | [kg/h] | … | 0.0 | 0.0 | 0.0 | 0.0 | 0.0 | 0.0 | 0.0 | 0.0 | 0.0 | 0.0 | 0.0 | 0.0 | 0.0 | 0.0 | 0.0 | 0.0 | 0.0 | 0.0 | 0.0 | 0.0 | 0.0 |
| CELLULOS | [kg/h] | … | 0.5 | 88.4 | 0.2 | 0.5 | 0.9 | 0.0 | 0.0 | 0.0 | 1.4 | 0.5 | 0.9 | 1.4 | 89.6 | 89.3 | 88.9 | 88.4 | 1.7 | 0.2 | 0.0 | 0.0 | 86.7 |
| XYLAN | [kg/h] | … | 0.0 | 42.8 | 0.0 | 0.0 | 0.0 | 0.0 | 0.0 | 0.0 | 0.0 | 0.0 | 0.0 | 0.0 | 42.8 | 42.8 | 42.8 | 42.8 | 0.0 | 0.0 | 0.0 | 0.0 | 42.8 |
| LIGNIN | [kg/h] | … | 0.0 | 649.0 | 0.0 | 0.0 | 0.0 | 0.0 | 0.0 | 0.0 | 0.0 | 0.0 | 0.0 | 0.0 | 649.0 | 649.0 | 649.0 | 649.0 | 0.0 | 0.0 | 0.0 | 0.0 | 649.0 |
| XYLOSE | [kg/h] | … | 0.0 | 14558.8 | 0.0 | 0.0 | 0.0 | 0.0 | 0.0 | 0.0 | 0.0 | 0.0 | 0.0 | 0.0 | 14558.8 | 14558.8 | 14558.8 | 14558.8 | 0.0 | 0.0 | 0.0 | 0.0 | 14558.8 |
| GLUCOSE | [kg/h] | … | 0.0 | 0.0 | 0.0 | 0.0 | 0.0 | 0.0 | 0.0 | 0.0 | 0.0 | 0.0 | 0.0 | 0.0 | 0.0 | 0.0 | 0.0 | 0.0 | 0.0 | 0.0 | 0.0 | 0.0 | 0.0 |
| YEAST | [kg/h] | … | 0.0 | 87.0 | 0.0 | 0.0 | 0.0 | 0.0 | 0.0 | 0.0 | 0.0 | 0.0 | 0.0 | 0.0 | 87.0 | 87.0 | 87.0 | 87.0 | 0.0 | 0.0 | 0.0 | 0.0 | 87.0 |
| ENZYMES | [kg/h] | … | 0.0 | 561.5 | 0.0 | 0.0 | 0.0 | 0.0 | 0.0 | 0.0 | 0.0 | 0.0 | 0.0 | 0.0 | 561.5 | 561.5 | 561.5 | 561.5 | 0.0 | 0.0 | 0.0 | 0.0 | 561.5 |
| ASH | [kg/h] | … | 0.0 | 216.3 | 0.0 | 0.0 | 0.0 | 0.0 | 0.0 | 0.0 | 0.0 | 0.0 | 0.0 | 0.0 | 216.3 | 216.3 | 216.3 | 216.3 | 0.0 | 0.0 | 0.0 | 0.0 | 216.3 |
| EXTRAKT | [kg/h] | … | 587.7 | 4401.6 | 176.4 | 425.9 | 779.1 | 0.9 | 1.5 | 3.5 | 1366.8 | 427.4 | 782.6 | 1366.8 | 5591.0 | 5341.0 | 4985.8 | 4401.6 | 1691.6 | 177.3 | 0.0 | 0.0 | 2710.0 |
| PROTEIN | [kg/h] | … | 0.0 | 2884.5 | 0.0 | 0.0 | 0.0 | 0.0 | 0.0 | 0.0 | 0.1 | 0.0 | 0.0 | 0.1 | 2884.5 | 2884.5 | 2884.5 | 2884.5 | 0.0 | 0.0 | 0.0 | 0.0 | 2884.4 |
| **Mass fraction** | | | | | | | | | | | | | | | | | | | | | | | |
| WATER | [1] | … | 0.976 | 0.722 | 0.978 | 0.979 | 0.981 | 0.921 | 0.934 | 0.949 | 0.979 | 0.979 | 0.98 | 0.979 | 0.874 | 0.85 | 0.809 | 0.722 | 0.955 | 0.976 | 1 | 1 | 0.401 |
| ETHANOL | [1] | … | 0 | 0 | 0 | 0 | 0 | 0.001 | 0 | 0 | 0 | 0 | 0 | 0 | 0 | 0 | 0 | 0 | 0 | 0 | 0 | 0 | 0 |
| ACETAT | [1] | … | 0.008 | 0.011 | 0.005 | 0.005 | 0.006 | 0.003 | 0.003 | 0.003 | 0.006 | 0.005 | 0.006 | 0.006 | 0.008 | 0.009 | 0.01 | 0.011 | 0.012 | 0.005 | 0 | 0 | 0.009 |
| FURFURAL | [1] | … | 0.004 | 0 | 0.012 | 0.009 | 0.007 | 0.075 | 0.062 | 0.047 | 0.006 | 0.01 | 0.008 | 0.006 | 0.002 | 0.001 | 0 | 0 | 0 | 0.013 | 0 | 0 | 0 |
| GLYCEROL | [1] | … | 0 | 0.003 | 0 | 0 | 0 | 0 | 0 | 0 | 0 | 0 | 0 | 0 | 0.001 | 0.001 | 0.002 | 0.003 | 0 | 0 | 0 | 0 | 0.007 |
| CO2 | [1] | … | 0 | 0 | 0 | 0 | 0 | 0 | 0 | 0 | 0 | 0 | 0 | 0 | 0 | 0 | 0 | 0 | 0 | 0 | 0 | 0 | 0 |
| CELLULOS | [1] | … | 0 | 0.001 | 0 | 0 | 0 | 0 | 0 | 0 | 0 | 0 | 0 | 0 | 0 | 0.001 | 0.001 | 0.001 | 0 | 0 | 0 | 0 | 0.002 |
| XYLAN | [1] | … | 0 | 0 | 0 | 0 | 0 | 0 | 0 | 0 | 0 | 0 | 0 | 0 | 0 | 0 | 0 | 0 | 0 | 0 | 0 | 0 | 0.001 |
| LIGNIN | [1] | … | 0 | 0.007 | 0 | 0 | 0 | 0 | 0 | 0 | 0 | 0 | 0 | 0 | 0.003 | 0.004 | 0.005 | 0.007 | 0 | 0 | 0 | 0 | 0.017 |
| XYLOSE | [1] | … | 0 | 0.164 | 0 | 0 | 0 | 0 | 0 | 0 | 0 | 0 | 0 | 0 | 0.068 | 0.082 | 0.108 | 0.164 | 0 | 0 | 0 | 0 | 0.389 |
| GLUCOSE | [1] | … | 0 | 0 | 0 | 0 | 0 | 0 | 0 | 0 | 0 | 0 | 0 | 0 | 0 | 0 | 0 | 0 | 0 | 0 | 0 | 0 | 0 |
| YEAST | [1] | … | 0 | 0.001 | 0 | 0 | 0 | 0 | 0 | 0 | 0 | 0 | 0 | 0 | 0 | 0 | 0.001 | 0.001 | 0 | 0 | 0 | 0 | 0.002 |
| ENZYMES | [1] | … | 0 | 0.006 | 0 | 0 | 0 | 0 | 0 | 0 | 0 | 0 | 0 | 0 | 0.003 | 0.003 | 0.004 | 0.006 | 0 | 0 | 0 | 0 | 0.015 |
| ASH | [1] | … | 0 | 0.002 | 0 | 0 | 0 | 0 | 0 | 0 | 0 | 0 | 0 | 0 | 0.001 | 0.001 | 0.002 | 0.002 | 0 | 0 | 0 | 0 | 0.006 |
| EXTRAKT | [1] | … | 0.012 | 0.05 | 0.005 | 0.006 | 0.007 | 0.001 | 0.001 | 0.001 | 0.009 | 0.006 | 0.007 | 0.009 | 0.026 | 0.03 | 0.037 | 0.05 | 0.033 | 0.005 | 0 | 0 | 0.072 |
| PROTEIN | [1] | … | 0 | 0.032 | 0 | 0 | 0 | 0 | 0 | 0 | 0 | 0 | 0 | 0 | 0.013 | 0.016 | 0.021 | 0.032 | 0 | 0 | 0 | 0 | 0.077 |

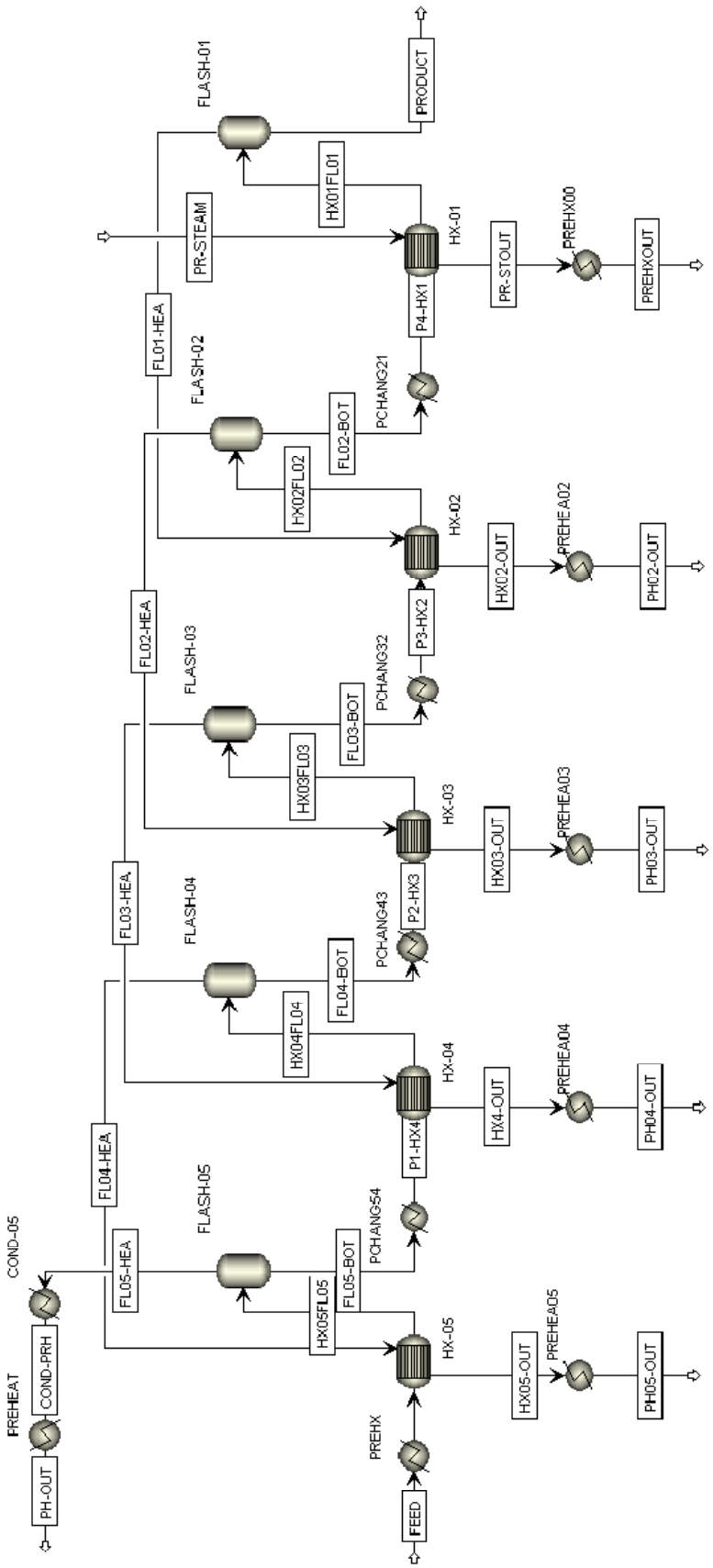


**Figure C-5: ASPEN PLUS flow sheet of the 5-stage counter-current BASE CASE evaporation model**

**Table C-8: ASPEN PLUS simulation process streams of the 5-stage evaporation counter-current BASE CASE model based on the 2-column dist. results (part 1)**

| Stream name | | COND-PRH | FEED | FL01-HEA | FL02-BOT | FL02-HEA | FL03-BOT | FL03-HEA | FL04-BOT | FL04-HEA | FL05-BOT | FL05-HEA | HX01FL01 | HX02-OUT | HX02FL02 | HX03-OUT | HX03FL03 | HX04FL04 | … |
|---|---|---|---|---|---|---|---|---|---|---|---|---|---|---|---|---|---|---|---|
| **Temperature** | [°C] | 99 | 40 | 142.1 | 129.5 | 129.5 | 121.4 | 121.4 | 112.1 | 112.1 | 100.1 | 100.1 | 142.1 | 133.7 | 129.5 | 127.5 | 121.4 | 112.1 | … |
| **Pressure** | [bar] | 1 | 3.2 | 3 | 2.5 | 2.5 | 2 | 2 | 1.5 | 1.5 | 1 | 1 | 3 | 3 | 2.5 | 2.5 | 2 | 1.5 | … |
| **Vapor fraction** | [1] | 0 | 0 | 1 | 0 | 1 | 0 | 1 | 0 | 1 | 0 | 1 | 0.742 | 0 | 0.412 | 0 | 0.273 | 0.189 | … |
| **Total mole flow** | [kmol/h] | 531.9 | 12829.1 | 3162.8 | 4264.3 | 2987.8 | 7252.2 | 2719.4 | 9971.7 | 2325.5 | 12297.2 | 531.9 | 4264.3 | 3162.8 | 7252.2 | 2987.8 | 9971.7 | 12297.2 | … |
| **Total mass flow** | [kg/h] | 9817.4 | 255573.5 | 59153.0 | 98665.8 | 54752.1 | 153420.3 | 49712.9 | 203133.2 | 42622.0 | 245756.1 | 9817.4 | 98665.8 | 59153.0 | 153420.3 | 54752.1 | 203133.2 | 245756.1 | … |
| **Component mass flow** | | | | | | | | | | | | | | | | | | | |
| WATER | [kg/h] | 9526.5 | 225891.4 | 56659.0 | 72140.0 | 53651.3 | 125793.7 | 48839.4 | 174633.1 | 41731.0 | 216364.9 | 9526.5 | 72140.0 | 56659.0 | 125793.7 | 53651.3 | 174633.1 | 216364.9 | … |
| ETHANOL | [kg/h] | 5.6 | 16.6 | 0.1 | 0.1 | 0.5 | 0.5 | 2.4 | 2.9 | 8.0 | 10.9 | 5.6 | 0.1 | 0.1 | 0.5 | 0.5 | 2.9 | 10.9 | … |
| ACETAT | [kg/h] | 46.9 | 1965.8 | 661.4 | 1002.4 | 400.0 | 1402.3 | 294.7 | 1697.1 | 221.8 | 1918.9 | 46.9 | 1002.4 | 661.4 | 1402.3 | 400.0 | 1697.1 | 1918.9 | … |
| FURFURAL | [kg/h] | 190.9 | 924.4 | 23.8 | 30.4 | 80.8 | 111.2 | 206.4 | 317.6 | 415.8 | 733.4 | 190.9 | 30.4 | 23.8 | 111.2 | 80.8 | 317.6 | 733.4 | … |
| GLYCEROL | [kg/h] | 0.0 | 264.7 | 0.4 | 264.6 | 0.1 | 264.6 | 0.0 | 264.7 | 0.0 | 264.7 | 0.0 | 264.6 | 0.4 | 264.6 | 0.1 | 264.7 | 264.7 | … |
| CO2 | [kg/h] | 0.0 | 0.0 | 0.0 | 0.0 | 0.0 | 0.0 | 0.0 | 0.0 | 0.0 | 0.0 | 0.0 | 0.0 | 0.0 | 0.0 | 0.0 | 0.0 | 0.0 | … |
| CELLULOS | [kg/h] | 0.0 | 89.8 | 5.5 | 88.2 | 1.0 | 89.1 | 0.4 | 89.6 | 0.2 | 89.8 | 0.0 | 88.2 | 5.5 | 89.1 | 1.0 | 89.6 | 89.8 | … |
| XYLAN | [kg/h] | 0.0 | 42.8 | 0.0 | 42.8 | 0.0 | 42.8 | 0.0 | 42.8 | 0.0 | 42.8 | 0.0 | 42.8 | 0.0 | 42.8 | 0.0 | 42.8 | 42.8 | … |
| LIGNIN | [kg/h] | 0.0 | 649.0 | 0.1 | 649.0 | 0.0 | 649.0 | 0.0 | 649.0 | 0.0 | 649.0 | 0.0 | 649.0 | 0.1 | 649.0 | 0.0 | 649.0 | 649.0 | … |
| XYLOSE | [kg/h] | 0.0 | 14558.8 | 0.0 | 14558.8 | 0.0 | 14558.8 | 0.0 | 14558.8 | 0.0 | 14558.8 | 0.0 | 14558.8 | 0.0 | 14558.8 | 0.0 | 14558.8 | 14558.8 | … |
| GLUCOSE | [kg/h] | 0.0 | 0.0 | 0.0 | 0.0 | 0.0 | 0.0 | 0.0 | 0.0 | 0.0 | 0.0 | 0.0 | 0.0 | 0.0 | 0.0 | 0.0 | 0.0 | 0.0 | … |
| YEAST | [kg/h] | 0.0 | 1739.6 | 0.3 | 1739.5 | 0.0 | 1739.6 | 0.0 | 1739.6 | 0.0 | 1739.6 | 0.0 | 1739.5 | 0.3 | 1739.6 | 0.0 | 1739.6 | 1739.6 | … |
| ENZYMES | [kg/h] | 0.0 | 561.5 | 0.1 | 561.5 | 0.0 | 561.5 | 0.0 | 561.5 | 0.0 | 561.5 | 0.0 | 561.5 | 0.1 | 561.5 | 0.0 | 561.5 | 561.5 | … |
| ASH | [kg/h] | 0.0 | 216.3 | 0.0 | 216.3 | 0.0 | 216.3 | 0.0 | 216.3 | 0.0 | 216.3 | 0.0 | 216.3 | 0.0 | 216.3 | 0.0 | 216.3 | 216.3 | … |
| EXTRAKT | [kg/h] | 47.4 | 5768.4 | 1802.0 | 4487.9 | 618.4 | 5106.3 | 369.5 | 5475.8 | 245.2 | 5721.0 | 47.4 | 4487.9 | 1802.0 | 5106.3 | 618.4 | 5475.8 | 5721.0 | … |
| PROTEIN | [kg/h] | 0.0 | 2884.5 | 0.4 | 2884.4 | 0.1 | 2884.5 | 0.0 | 2884.5 | 0.0 | 2884.5 | 0.0 | 2884.4 | 0.4 | 2884.5 | 0.1 | 2884.5 | 2884.5 | … |
| **Mass fraction** | | | | | | | | | | | | | | | | | | | |
| WATER | [1] | 0.97 | 0.884 | 0.958 | 0.731 | 0.98 | 0.82 | 0.982 | 0.86 | 0.979 | 0.88 | 0.97 | 0.731 | 0.958 | 0.82 | 0.98 | 0.86 | 0.88 | … |
| ETHANOL | [1] | 0.001 | 0 | 0 | 0 | 0 | 0 | 0 | 0 | 0 | 0 | 0.001 | 0 | 0 | 0 | 0 | 0 | 0 | … |
| ACETAT | [1] | 0.005 | 0.008 | 0.011 | 0.01 | 0.007 | 0.009 | 0.006 | 0.008 | 0.005 | 0.008 | 0.005 | 0.01 | 0.011 | 0.009 | 0.007 | 0.008 | 0.008 | … |
| FURFURAL | [1] | 0.019 | 0.004 | 0 | 0 | 0.001 | 0.001 | 0.004 | 0.002 | 0.01 | 0.003 | 0.019 | 0 | 0 | 0.001 | 0.001 | 0.002 | 0.003 | … |
| GLYCEROL | [1] | 0 | 0.001 | 0 | 0.003 | 0 | 0.002 | 0 | 0.001 | 0 | 0.001 | 0 | 0.003 | 0 | 0.002 | 0 | 0.001 | 0.001 | … |
| CO2 | [1] | 0 | 0 | 0 | 0 | 0 | 0 | 0 | 0 | 0 | 0 | 0 | 0 | 0 | 0 | 0 | 0 | 0 | … |
| CELLULOS | [1] | 0 | 0 | 0 | 0.001 | 0 | 0.001 | 0 | 0 | 0 | 0 | 0 | 0.001 | 0 | 0.001 | 0 | 0 | 0 | … |
| XYLAN | [1] | 0 | 0 | 0 | 0 | 0 | 0 | 0 | 0 | 0 | 0 | 0 | 0 | 0 | 0 | 0 | 0 | 0 | … |
| LIGNIN | [1] | 0 | 0.003 | 0 | 0.007 | 0 | 0.004 | 0 | 0.003 | 0 | 0.003 | 0 | 0.007 | 0 | 0.004 | 0 | 0.003 | 0.003 | … |
| XYLOSE | [1] | 0 | 0.057 | 0 | 0.148 | 0 | 0.095 | 0 | 0.072 | 0 | 0.059 | 0 | 0.148 | 0 | 0.095 | 0 | 0.072 | 0.059 | … |
| GLUCOSE | [1] | 0 | 0 | 0 | 0 | 0 | 0 | 0 | 0 | 0 | 0 | 0 | 0 | 0 | 0 | 0 | 0 | 0 | … |
| YEAST | [1] | 0 | 0.007 | 0 | 0.018 | 0 | 0.011 | 0 | 0.009 | 0 | 0.007 | 0 | 0.018 | 0 | 0.011 | 0 | 0.009 | 0.007 | … |
| ENZYMES | [1] | 0 | 0.002 | 0 | 0.006 | 0 | 0.004 | 0 | 0.003 | 0 | 0.002 | 0 | 0.006 | 0 | 0.004 | 0 | 0.003 | 0.002 | … |
| ASH | [1] | 0 | 0.001 | 0 | 0.002 | 0 | 0.001 | 0 | 0.001 | 0 | 0.001 | 0 | 0.002 | 0 | 0.001 | 0 | 0.001 | 0.001 | … |
| EXTRAKT | [1] | 0.005 | 0.023 | 0.03 | 0.045 | 0.011 | 0.033 | 0.007 | 0.027 | 0.006 | 0.023 | 0.005 | 0.045 | 0.03 | 0.033 | 0.011 | 0.027 | 0.023 | … |
| PROTEIN | [1] | 0 | 0.011 | 0 | 0.029 | 0 | 0.019 | 0 | 0.014 | 0 | 0.012 | 0 | 0.029 | 0 | 0.019 | 0 | 0.014 | 0.012 | … |

**Table C-9: ASPEN PLUS simulation process streams of the 5-stage evaporation counter-current BASE CASE model based on the 2-column dist. results (part 2)**

| Stream name | | … | HX4-OUT | HX05-OUT | HX05FL05 | P1-HX4 | P2-HX3 | P3-HX2 | P4-HX1 | PH-OUT | PH02-OUT | PH03-OUT | PH04-OUT | PH05-OUT | PHX-HX05 | PR-STEAM | PR-STOUT | PREHXOUT | PRODUCT |
|---|---|---|---|---|---|---|---|---|---|---|---|---|---|---|---|---|---|---|---|
| **Temperature** | [°C] | … | 120.2 | 111.1 | 100.1 | 100.1 | 112.1 | 121.4 | 129.5 | 50 | 50 | 50 | 50 | 50 | 40 | 144 | 143.7 | 50 | 142.1 |
| **Pressure** | [bar] | … | 2 | 1.5 | 1 | 1.5 | 2 | 2.5 | 3 | 1 | 3 | 2.5 | 2 | 1.5 | 1 | 4 | 4 | 4 | 3 |
| **Vapor fraction** | [1] | … | 0 | 0 | 0.041 | 0 | 0 | 0 | 0 | 0 | 0 | 0 | 0 | 0 | 0 | 1 | 0 | 0 | 0 |
| **Total mole flow** | [kmol/h] | … | 2719.4 | 2325.5 | 12829.1 | 12297.2 | 9971.7 | 7252.2 | 4264.3 | 531.9 | 3162.8 | 2987.8 | 2719.4 | 2325.5 | 12829.1 | 3358.3 | 3358.3 | 3358.3 | 1101.5 |
| **Total mass flow** | [kg/h] | … | 49712.9 | 42622.0 | 255573.5 | 245756.1 | 203133.2 | 153420.3 | 98665.8 | 9817.4 | 59153.0 | 54752.1 | 49712.9 | 42622.0 | 255573.5 | 60500.0 | 60500.0 | 60500.0 | 39512.8 |
| **Component mass flow** | | | | | | | | | | | | | | | | | | | |
| WATER | [kg/h] | … | 48839.4 | 41731.0 | 225891.4 | 216364.9 | 174633.1 | 125793.7 | 72140.0 | 9526.5 | 56659.0 | 53651.3 | 48839.4 | 41731.0 | 225891.4 | 60500.0 | 60500.0 | 60500.0 | 15481.0 |
| ETHANOL | [kg/h] | … | 2.4 | 8.0 | 16.6 | 10.9 | 2.9 | 0.5 | 0.1 | 5.6 | 0.1 | 0.5 | 2.4 | 8.0 | 16.6 | 0.0 | 0.0 | 0.0 | 0.0 |
| ACETAT | [kg/h] | … | 294.7 | 221.8 | 1965.8 | 1918.9 | 1697.1 | 1402.3 | 1002.4 | 46.9 | 661.4 | 400.0 | 294.7 | 221.8 | 1965.8 | 0.0 | 0.0 | 0.0 | 341.0 |
| FURFURAL | [kg/h] | … | 206.4 | 415.8 | 924.4 | 733.4 | 317.6 | 111.2 | 30.4 | 190.9 | 23.8 | 80.8 | 206.4 | 415.8 | 924.4 | 0.0 | 0.0 | 0.0 | 6.6 |
| GLYCEROL | [kg/h] | … | 0.0 | 0.0 | 264.7 | 264.7 | 264.7 | 264.6 | 264.6 | 0.0 | 0.4 | 0.1 | 0.0 | 0.0 | 264.7 | 0.0 | 0.0 | 0.0 | 264.1 |
| CO2 | [kg/h] | … | 0.0 | 0.0 | 0.0 | 0.0 | 0.0 | 0.0 | 0.0 | 0.0 | 0.0 | 0.0 | 0.0 | 0.0 | 0.0 | 0.0 | 0.0 | 0.0 | 0.0 |
| CELLULOS | [kg/h] | … | 0.4 | 0.2 | 89.8 | 89.8 | 89.6 | 89.1 | 88.2 | 0.0 | 5.5 | 1.0 | 0.4 | 0.2 | 89.8 | 0.0 | 0.0 | 0.0 | 82.6 |
| XYLAN | [kg/h] | … | 0.0 | 0.0 | 42.8 | 42.8 | 42.8 | 42.8 | 42.8 | 0.0 | 0.0 | 0.0 | 0.0 | 0.0 | 42.8 | 0.0 | 0.0 | 0.0 | 42.8 |
| LIGNIN | [kg/h] | … | 0.0 | 0.0 | 649.0 | 649.0 | 649.0 | 649.0 | 649.0 | 0.0 | 0.1 | 0.0 | 0.0 | 0.0 | 649.0 | 0.0 | 0.0 | 0.0 | 648.9 |
| XYLOSE | [kg/h] | … | 0.0 | 0.0 | 14558.8 | 14558.8 | 14558.8 | 14558.8 | 14558.8 | 0.0 | 0.0 | 0.0 | 0.0 | 0.0 | 14558.8 | 0.0 | 0.0 | 0.0 | 14558.8 |
| GLUCOSE | [kg/h] | … | 0.0 | 0.0 | 0.0 | 0.0 | 0.0 | 0.0 | 0.0 | 0.0 | 0.0 | 0.0 | 0.0 | 0.0 | 0.0 | 0.0 | 0.0 | 0.0 | 0.0 |
| YEAST | [kg/h] | … | 0.0 | 0.0 | 1739.6 | 1739.6 | 1739.6 | 1739.6 | 1739.5 | 0.0 | 0.3 | 0.0 | 0.0 | 0.0 | 1739.6 | 0.0 | 0.0 | 0.0 | 1739.3 |
| ENZYMES | [kg/h] | … | 0.0 | 0.0 | 561.5 | 561.5 | 561.5 | 561.5 | 561.5 | 0.0 | 0.1 | 0.0 | 0.0 | 0.0 | 561.5 | 0.0 | 0.0 | 0.0 | 561.4 |
| ASH | [kg/h] | … | 0.0 | 0.0 | 216.3 | 216.3 | 216.3 | 216.3 | 216.3 | 0.0 | 0.0 | 0.0 | 0.0 | 0.0 | 216.3 | 0.0 | 0.0 | 0.0 | 216.3 |
| EXTRAKT | [kg/h] | … | 369.5 | 245.2 | 5768.4 | 5721.0 | 5475.8 | 5106.3 | 4487.9 | 47.4 | 1802.0 | 618.4 | 369.5 | 245.2 | 5768.4 | 0.0 | 0.0 | 0.0 | 2685.9 |
| PROTEIN | [kg/h] | … | 0.0 | 0.0 | 2884.5 | 2884.5 | 2884.5 | 2884.5 | 2884.4 | 0.0 | 0.4 | 0.1 | 0.0 | 0.0 | 2884.5 | 0.0 | 0.0 | 0.0 | 2884.0 |
| **Mass fraction** | | | | | | | | | | | | | | | | | | | |
| WATER | [1] | … | 0.982 | 0.979 | 0.884 | 0.88 | 0.86 | 0.82 | 0.731 | 0.97 | 0.958 | 0.98 | 0.982 | 0.979 | 0.884 | 1 | 1 | 1 | 0.392 |
| ETHANOL | [1] | … | 0 | 0 | 0 | 0 | 0 | 0 | 0 | 0.001 | 0 | 0 | 0 | 0 | 0 | 0 | 0 | 0 | 0 |
| ACETAT | [1] | … | 0.006 | 0.005 | 0.008 | 0.008 | 0.008 | 0.009 | 0.01 | 0.005 | 0.011 | 0.007 | 0.006 | 0.005 | 0.008 | 0 | 0 | 0 | 0.009 |
| FURFURAL | [1] | … | 0.004 | 0.01 | 0.004 | 0.003 | 0.002 | 0.001 | 0 | 0.019 | 0 | 0.001 | 0.004 | 0.01 | 0.004 | 0 | 0 | 0 | 0 |
| GLYCEROL | [1] | … | 0 | 0 | 0.001 | 0.001 | 0.001 | 0.002 | 0.003 | 0 | 0 | 0 | 0 | 0 | 0.001 | 0 | 0 | 0 | 0.007 |
| CO2 | [1] | … | 0 | 0 | 0 | 0 | 0 | 0 | 0 | 0 | 0 | 0 | 0 | 0 | 0 | 0 | 0 | 0 | 0 |
| CELLULOS | [1] | … | 0 | 0 | 0 | 0 | 0 | 0.001 | 0.001 | 0 | 0 | 0 | 0 | 0 | 0 | 0 | 0 | 0 | 0.002 |
| XYLAN | [1] | … | 0 | 0 | 0 | 0 | 0 | 0 | 0 | 0 | 0 | 0 | 0 | 0 | 0 | 0 | 0 | 0 | 0.001 |
| LIGNIN | [1] | … | 0 | 0 | 0.003 | 0.003 | 0.003 | 0.004 | 0.007 | 0 | 0 | 0 | 0 | 0 | 0.003 | 0 | 0 | 0 | 0.016 |
| XYLOSE | [1] | … | 0 | 0 | 0.057 | 0.059 | 0.072 | 0.095 | 0.148 | 0 | 0 | 0 | 0 | 0 | 0.057 | 0 | 0 | 0 | 0.368 |
| GLUCOSE | [1] | … | 0 | 0 | 0 | 0 | 0 | 0 | 0 | 0 | 0 | 0 | 0 | 0 | 0 | 0 | 0 | 0 | 0 |
| YEAST | [1] | … | 0 | 0 | 0.007 | 0.007 | 0.009 | 0.011 | 0.018 | 0 | 0 | 0 | 0 | 0 | 0.007 | 0 | 0 | 0 | 0.044 |
| ENZYMES | [1] | … | 0 | 0 | 0.002 | 0.002 | 0.003 | 0.004 | 0.006 | 0 | 0 | 0 | 0 | 0 | 0.002 | 0 | 0 | 0 | 0.014 |
| ASH | [1] | … | 0 | 0 | 0.001 | 0.001 | 0.001 | 0.001 | 0.002 | 0 | 0 | 0 | 0 | 0 | 0.001 | 0 | 0 | 0 | 0.005 |
| EXTRAKT | [1] | … | 0.007 | 0.006 | 0.023 | 0.023 | 0.027 | 0.033 | 0.045 | 0.005 | 0.03 | 0.011 | 0.007 | 0.006 | 0.023 | 0 | 0 | 0 | 0.068 |
| PROTEIN | [1] | … | 0 | 0 | 0.011 | 0.012 | 0.014 | 0.019 | 0.029 | 0 | 0 | 0 | 0 | 0 | 0.011 | 0 | 0 | 0 | 0.073 |

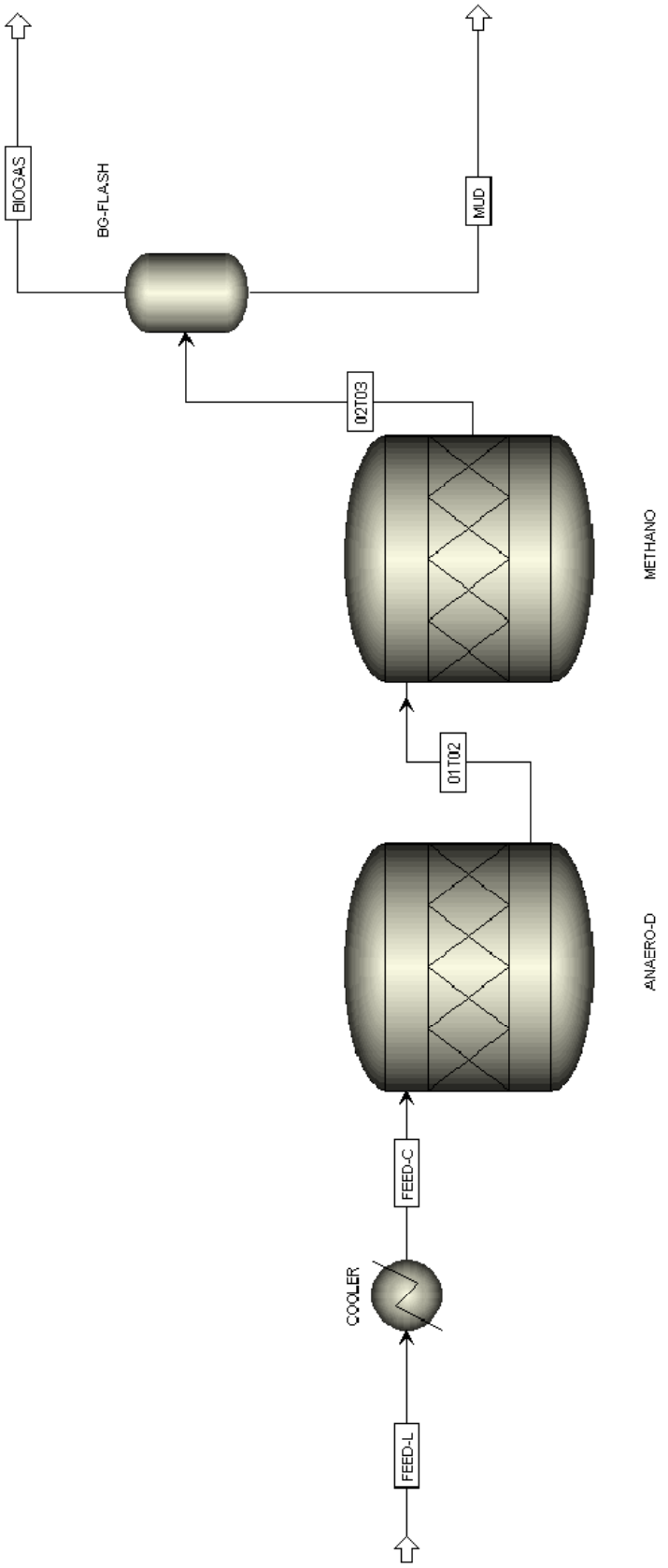


**Figure C-6: ASPEN PLUS flow sheet of the biogas model**

**Table C-10: ASPEN PLUS simulation process streams of the biogas model based on the 2-column dist. results**

| Stream name | | 01T02 | 02T03 | BIOGAS | FEED-C | FEED-L | MUD |
|---|---|---|---|---|---|---|---|
| **Temperature** | [°C] | 37 | 37 | 37 | 37 | 40 | 37 |
| **Pressure** | [bar] | 1 | 1 | 1.01 | 1 | 1 | 1.01 |
| **Vapor fraction** | [1] | 0.006 | 0.066 | 1 | 0 | 0 | 0 |
| **Total mole flow** | [kmol/h] | 12540.5 | 13019.3 | 859.7 | 12481.0 | 12481.0 | 12159.6 |
| **Total mass flow** | [kg/h] | 248925.8 | 248925.8 | 24409.5 | 248925.8 | 248925.8 | 224516.3 |
| **Component mass flow** | | | | | | | |
| WATER | [kg/h] | 220293.8 | 218314.2 | 963.1 | 220907.3 | 220907.3 | 217351.0 |
| ETHANOL | [kg/h] | 0.3 | 0.3 | 0.0 | 2.9 | 2.9 | 0.3 |
| ACETAT | [kg/h] | 1969.2 | 196.9 | 0.5 | 1965.8 | 1965.8 | 196.4 |
| FURFURAL | [kg/h] | 927.0 | 92.7 | 2.1 | 927.0 | 927.0 | 90.6 |
| GLYCEROL | [kg/h] | 26.5 | 26.5 | 0.0 | 264.7 | 264.7 | 26.5 |
| CO2 | [kg/h] | 1695.4 | 16640.3 | 16531.6 | 0.0 | 0.0 | 108.7 |
| CELLULOS | [kg/h] | 89.8 | 89.8 | 0.0 | 89.8 | 89.8 | 89.8 |
| XYLAN | [kg/h] | 42.8 | 21.4 | 0.0 | 42.8 | 42.8 | 21.4 |
| LIGNIN | [kg/h] | 649.0 | 649.0 | 0.0 | 649.0 | 649.0 | 649.0 |
| XYLOSE | [kg/h] | 14558.8 | 1455.9 | 0.0 | 14558.8 | 14558.8 | 1455.9 |
| GLUCOSE | [kg/h] | 0.0 | 0.0 | 0.0 | 0.0 | 0.0 | 0.0 |
| YEAST | [kg/h] | 87.0 | 87.0 | 0.0 | 87.0 | 87.0 | 87.0 |
| ENZYMES | [kg/h] | 561.5 | 561.5 | 0.0 | 561.5 | 561.5 | 561.5 |
| ASH | [kg/h] | 216.3 | 216.3 | 0.0 | 216.3 | 216.3 | 216.3 |
| EXTRAKT | [kg/h] | 5768.4 | 2884.2 | 2.3 | 5768.4 | 5768.4 | 2881.8 |
| PROTEIN | [kg/h] | 288.5 | 288.5 | 0.0 | 2884.5 | 2884.5 | 288.5 |
| O2 | [kg/h] | 0.0 | 0.0 | 0.0 | 0.0 | 0.0 | 0.0 |
| CH4 | [kg/h] | 72.6 | 7100.9 | 6878.3 | 0.0 | 0.0 | 222.5 |
| NH3 | [kg/h] | 300.5 | 300.5 | 31.4 | 0.0 | 0.0 | 269.1 |
| C3H6O-01 | [kg/h] | 1307.1 | 0.0 | 0.0 | 0.0 | 0.0 | 0.0 |
| H2CO3 | [kg/h] | 0.0 | 0.0 | 0.0 | 0.0 | 0.0 | 0.0 |
| H2 | [kg/h] | 71.4 | 0.0 | 0.0 | 0.0 | 0.0 | 0.0 |
| **Mass fraction** | | | | | | | |
| WATER | [1] | 0.885 | 0.877 | 0.039 | 0.887 | 0.887 | 0.968 |
| ETHANOL | [1] | 0 | 0 | 0 | 0 | 0 | 0 |
| ACETAT | [1] | 0.008 | 0.001 | 0 | 0.008 | 0.008 | 0.001 |
| FURFURAL | [1] | 0.004 | 0 | 0 | 0.004 | 0.004 | 0 |
| GLYCEROL | [1] | 0 | 0 | 0 | 0.001 | 0.001 | 0 |
| CO2 | [1] | 0.007 | 0.067 | 0.677 | 0 | 0 | 0 |
| CELLULOS | [1] | 0 | 0 | 0 | 0 | 0 | 0 |
| XYLAN | [1] | 0 | 0 | 0 | 0 | 0 | 0 |
| LIGNIN | [1] | 0.003 | 0.003 | 0 | 0.003 | 0.003 | 0.003 |
| XYLOSE | [1] | 0.058 | 0.006 | 0 | 0.058 | 0.058 | 0.006 |
| GLUCOSE | [1] | 0 | 0 | 0 | 0 | 0 | 0 |
| YEAST | [1] | 0 | 0 | 0 | 0 | 0 | 0 |
| ENZYMES | [1] | 0.002 | 0.002 | 0 | 0.002 | 0.002 | 0.003 |
| ASH | [1] | 0.001 | 0.001 | 0 | 0.001 | 0.001 | 0.001 |
| EXTRAKT | [1] | 0.023 | 0.012 | 0 | 0.023 | 0.023 | 0.013 |
| PROTEIN | [1] | 0.001 | 0.001 | 0 | 0.012 | 0.012 | 0.001 |
| O2 | [1] | 0 | 0 | 0 | 0 | 0 | 0 |
| CH4 | [1] | 0 | 0.029 | 0.282 | 0 | 0 | 0.001 |
| NH3 | [1] | 0.001 | 0.001 | 0.001 | 0 | 0 | 0.001 |
| C3H6O-01 | [1] | 0.005 | 0 | 0 | 0 | 0 | 0 |
| H2CO3 | [1] | 0 | 0 | 0 | 0 | 0 | 0 |
| H2 | [1] | 0 | 0 | 0 | 0 | 0 | 0 |

# D. PINCH ANALYSIS

# CCC, GCC and HCC of the multi-stage evaporation system

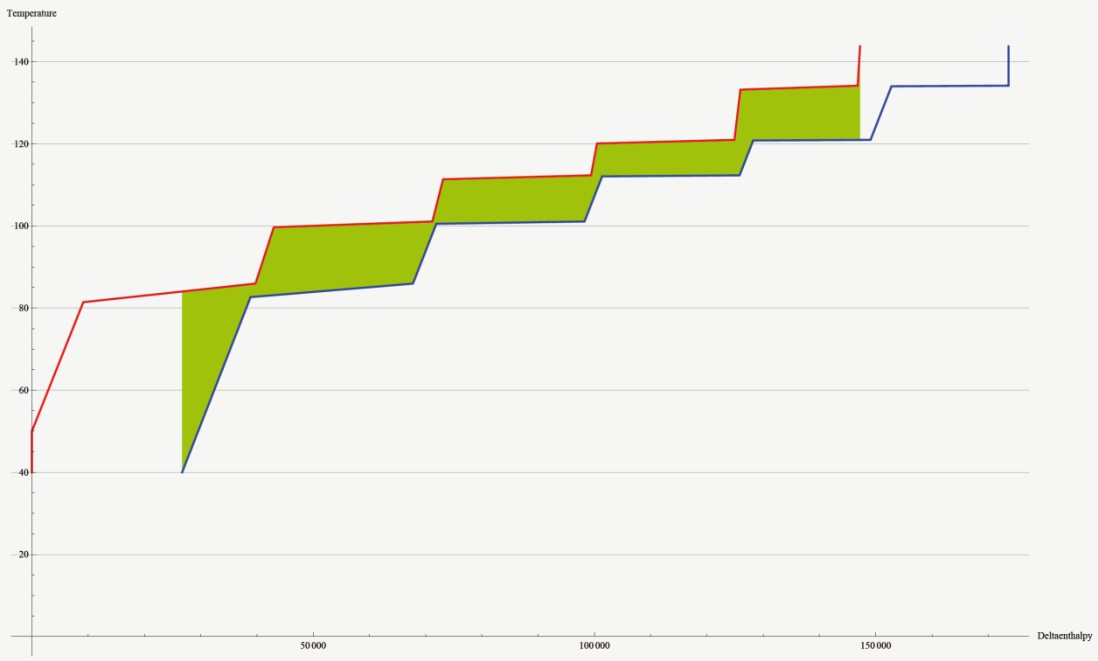


**Figure D-1:** **CCC and HCC of the co-current 5-stage evaporation system with a minimum temperature difference of 3°C**

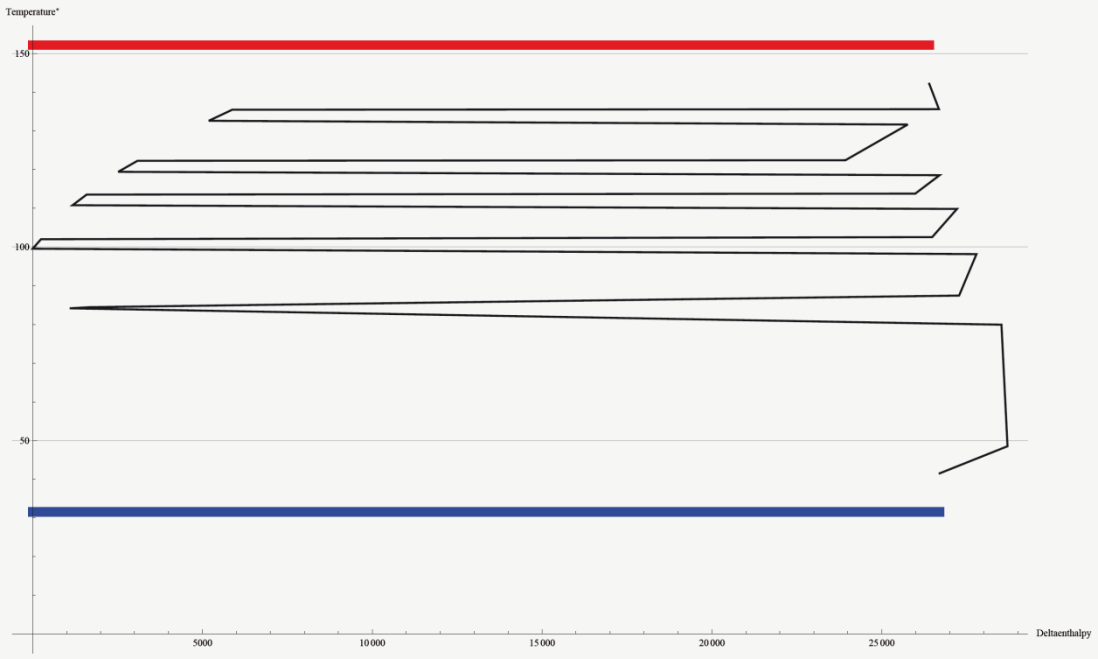


**Figure D-2:** **GCC of the co-current 5-stage evaporation system with a minimum temperature difference of 3°C**

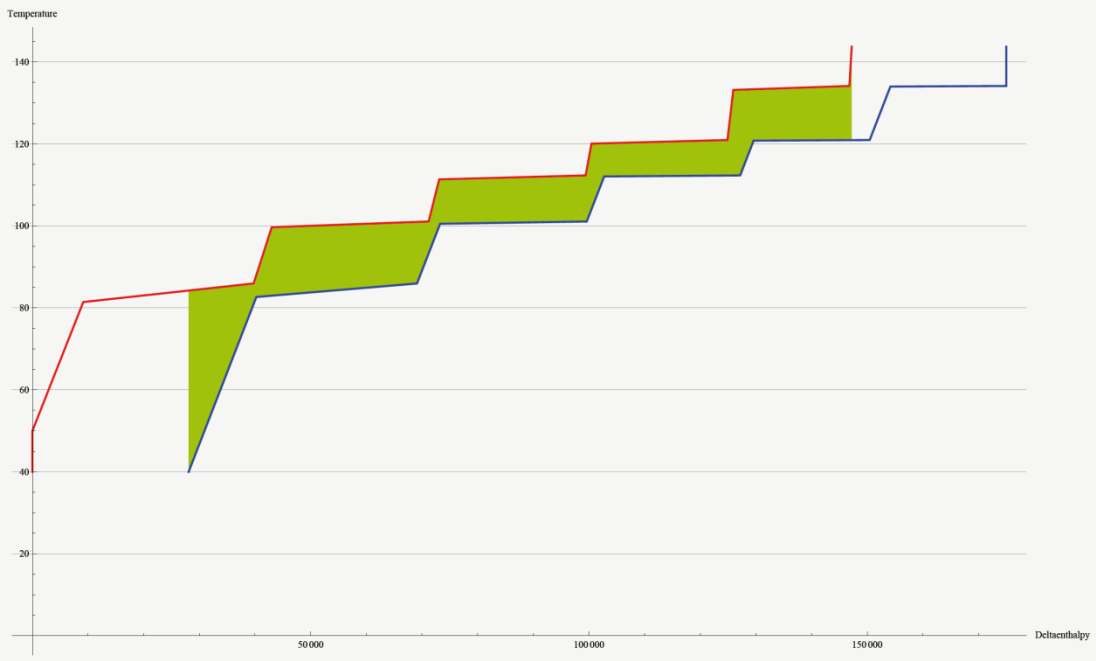


**Figure D-3:** **CCC and HCC of the co-current 5-stage evaporation system with a minimum temperature difference of 5°C**

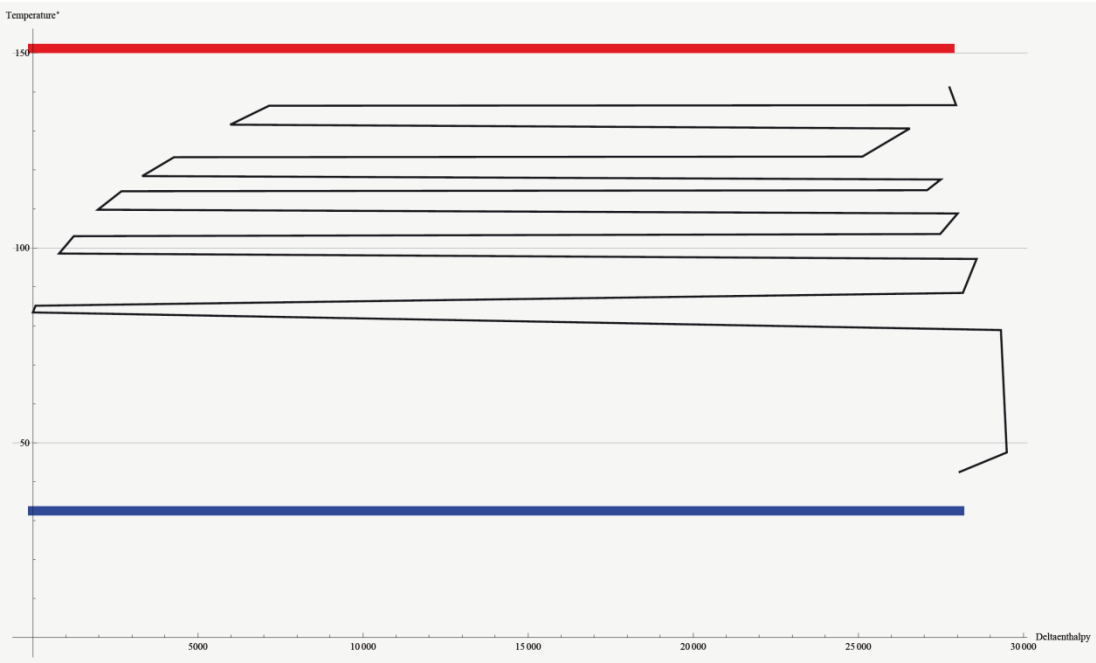


**Figure D-4:** **GCC of the co-current 5-stage evaporation system with a minimum temperature difference of 5°C**

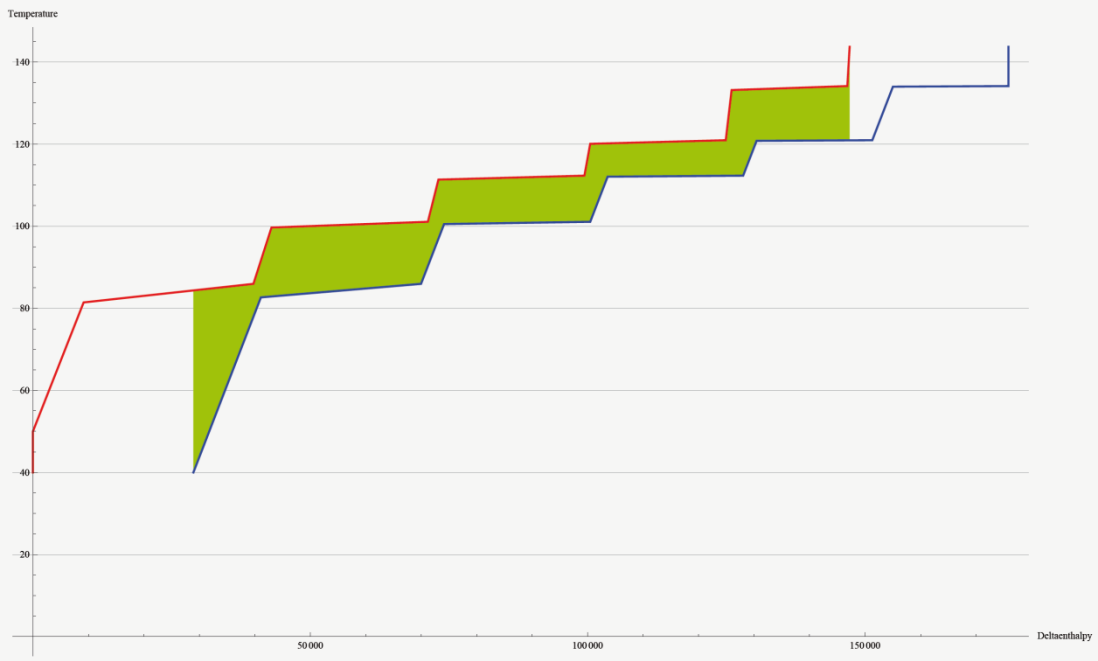


**Figure D-5:** **CCC and HCC of the co-current 5-stage evaporation system with a minimum temperature difference of 8°C**

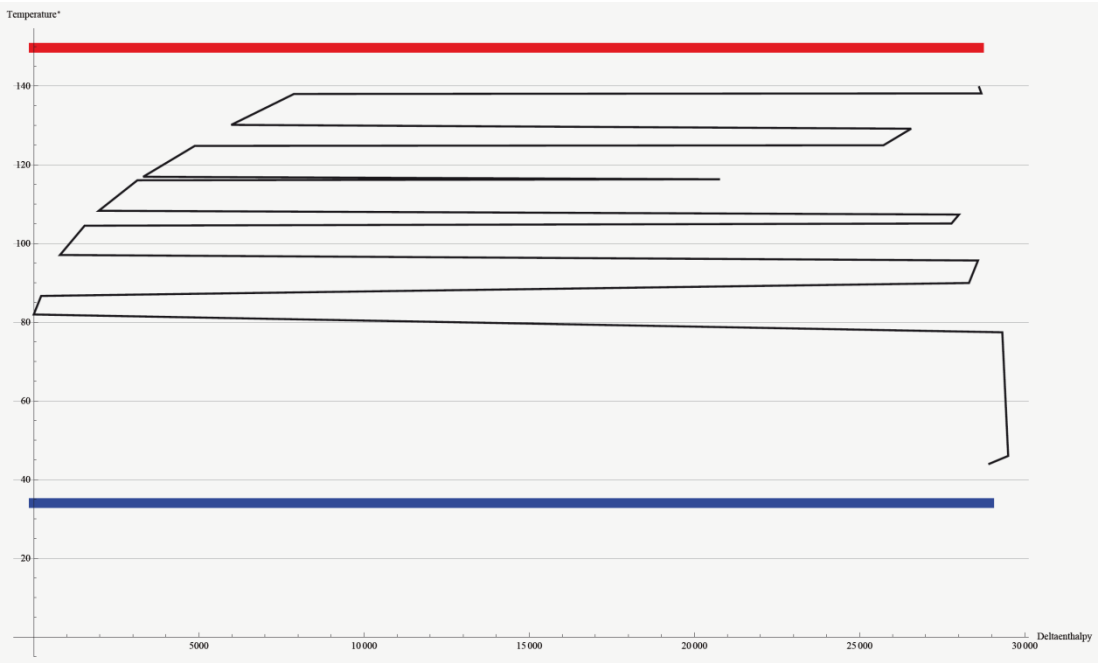


**Figure D-6:** **GCC of the co-current 5-stage evaporation system with a minimum temperature difference of 8°C**

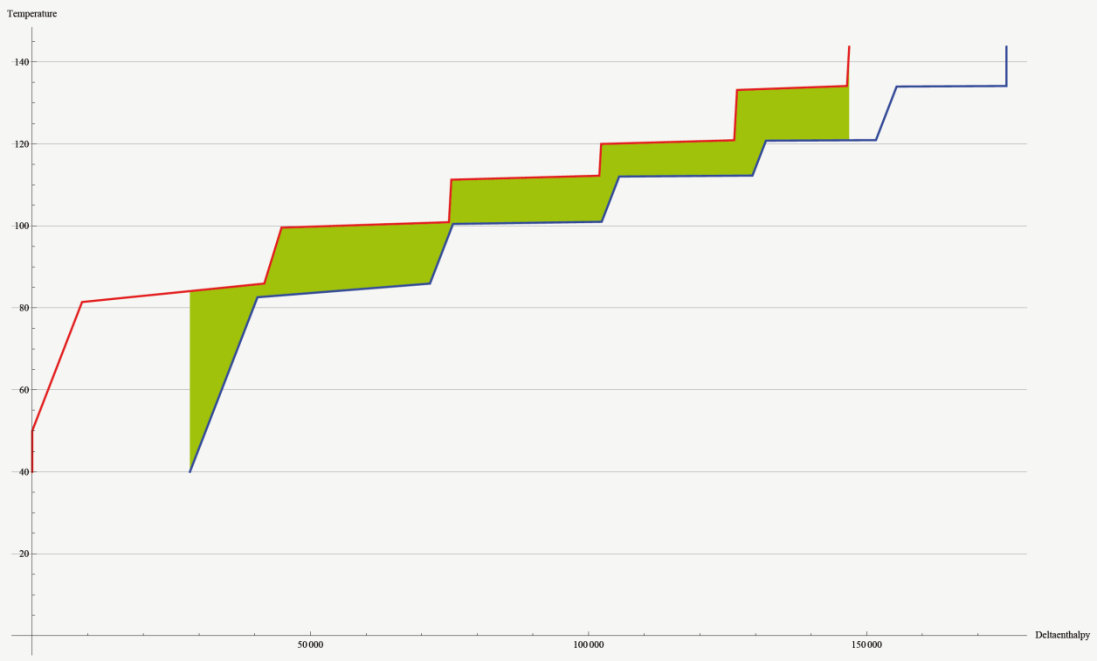


**Figure D-7:** **CCC and HCC of the co-current 5-stage evaporation, including a flash condensate system, with a minimum temperature difference of 3°C**

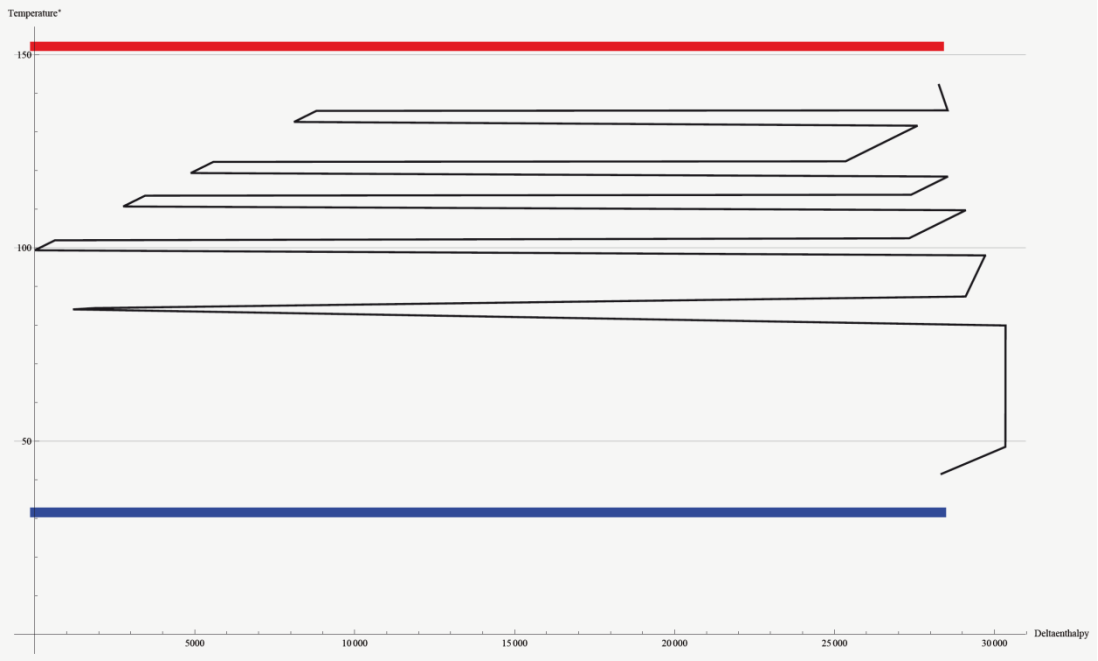


**Figure D-8:** **GCC of the co-current 5-stage evaporation, including a flash condensate system, with a minimum temperature difference of 3°C**

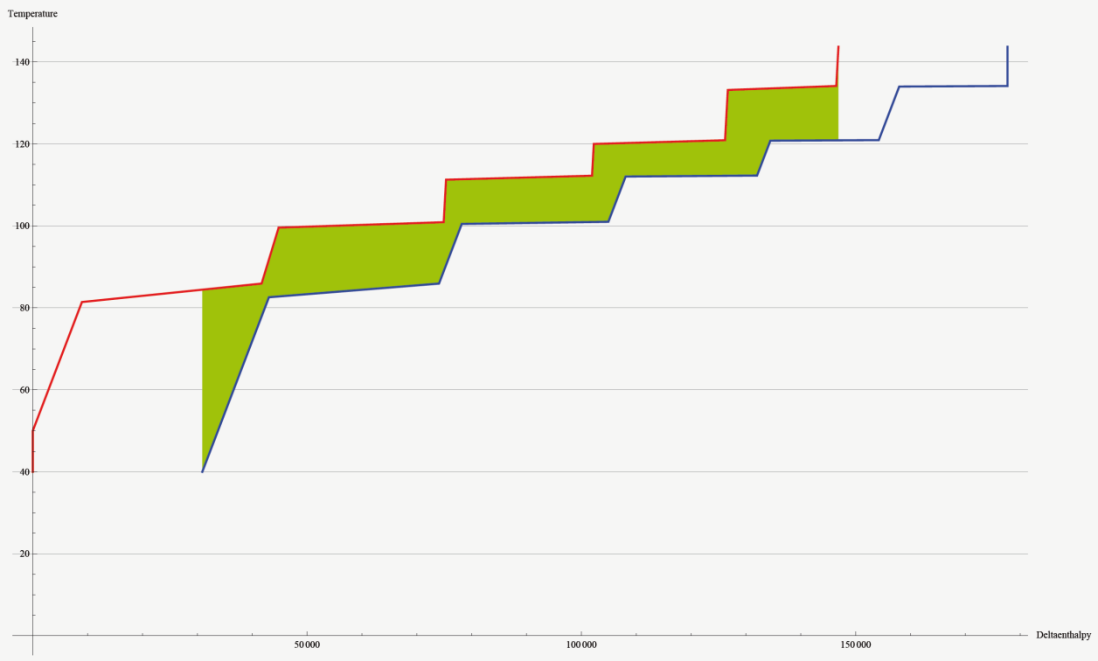


**Figure D-9:** **CCC and HCC of the co-current 5-stage evaporation, including a flash condensate system, with a minimum temperature difference of 5°C**

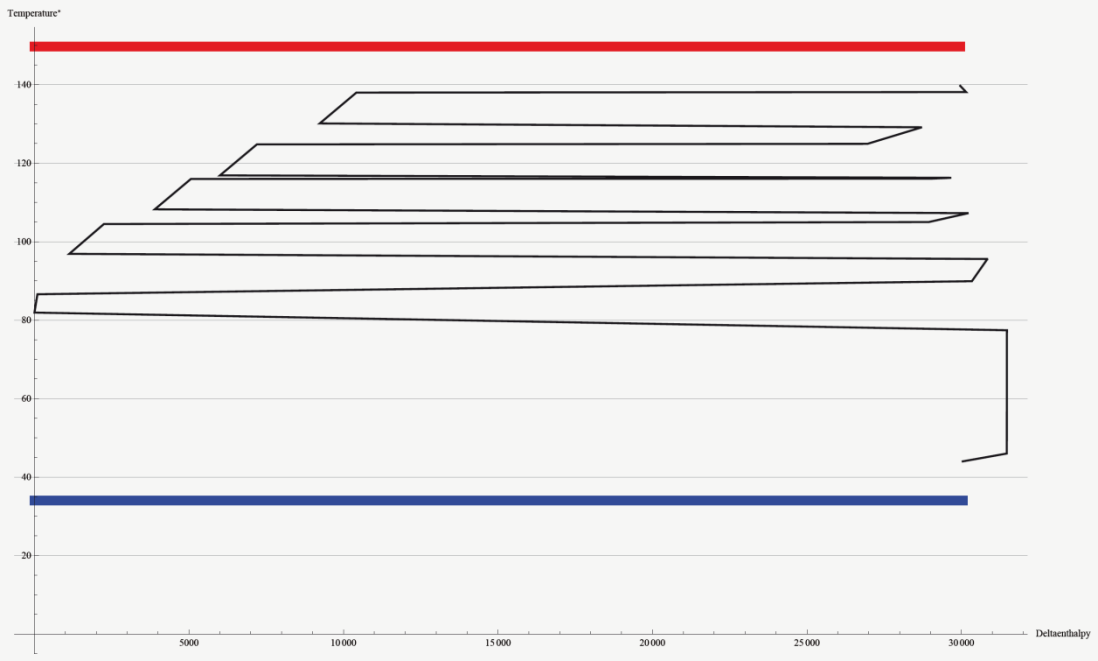


**Figure D-10:** **GCC of the co-current 5-stage evaporation, including a flash condensate system, with a minimum temperature difference of 5°C**

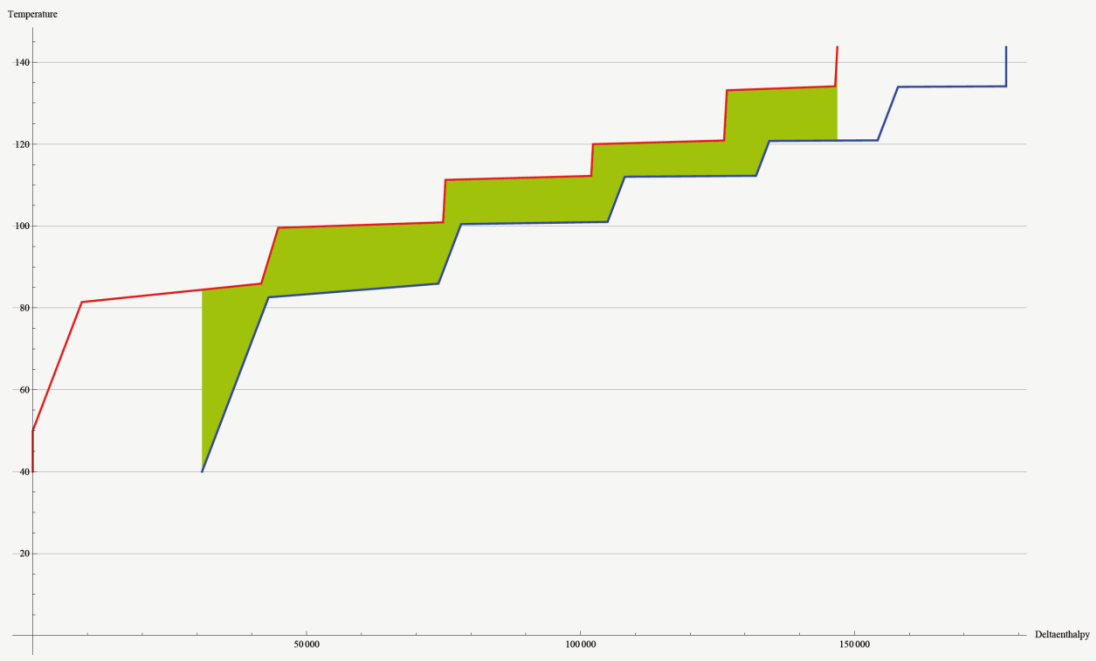


**Figure D-11:** **CCC and HCC of the co-current 5-stage evaporation, including a flash condensate system, with a minimum temperature difference of 8°C**

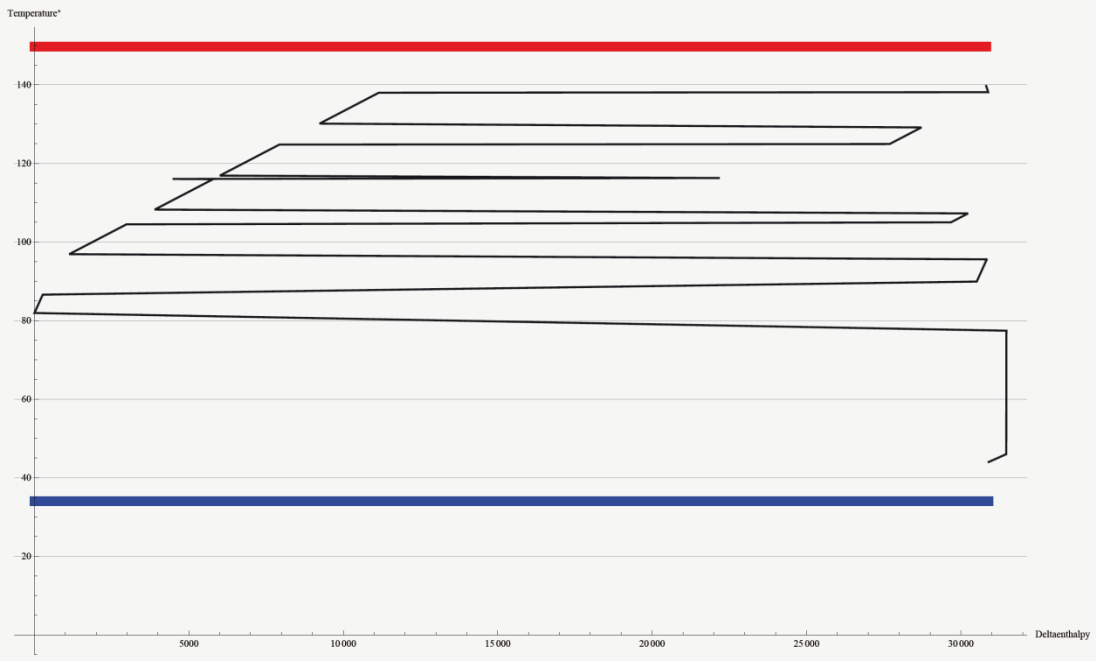


**Figure D-12:** **GCC of the co-current 5-stage evaporation, including a flash condensate system, with a minimum temperature difference of 8°C**

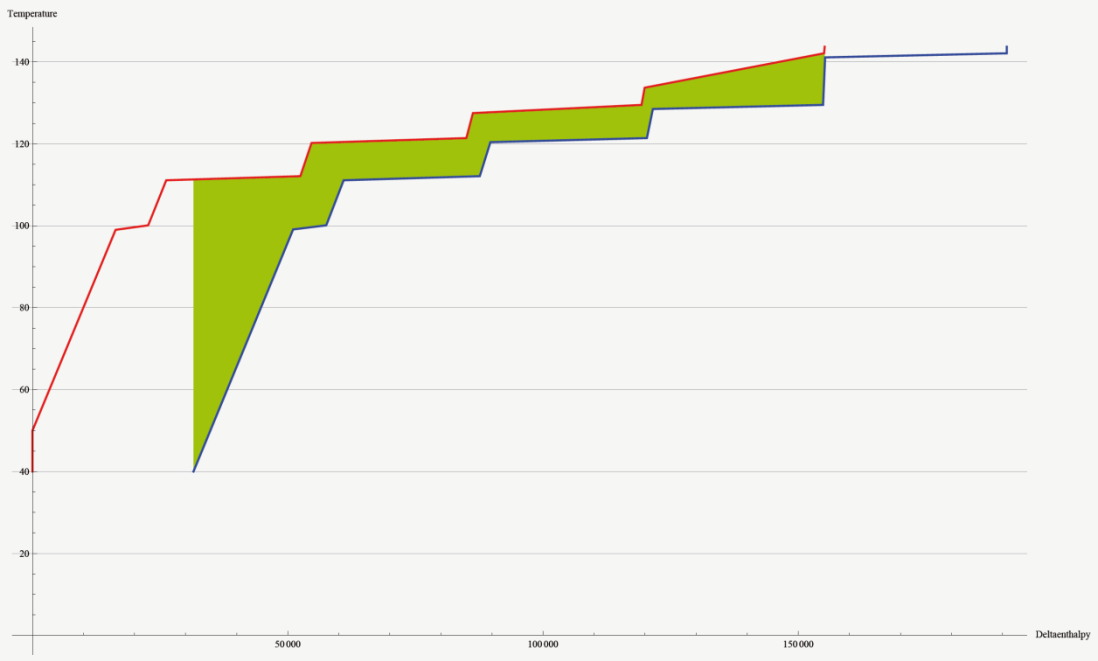


**Figure D-13:** **CCC and HCC of the counter-current 5-stage evaporation system with a minimum temperature difference of 3°C**

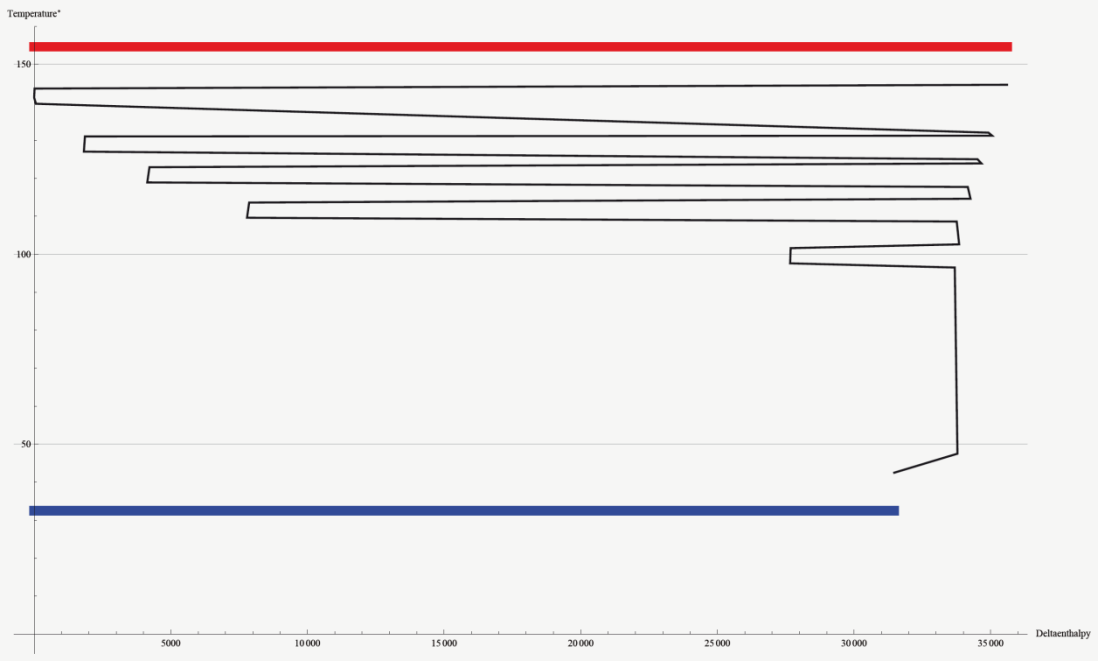


**Figure D-14:** **GCC of the counter-current 5-stage evaporation system with a minimum temperature difference of 3°C**

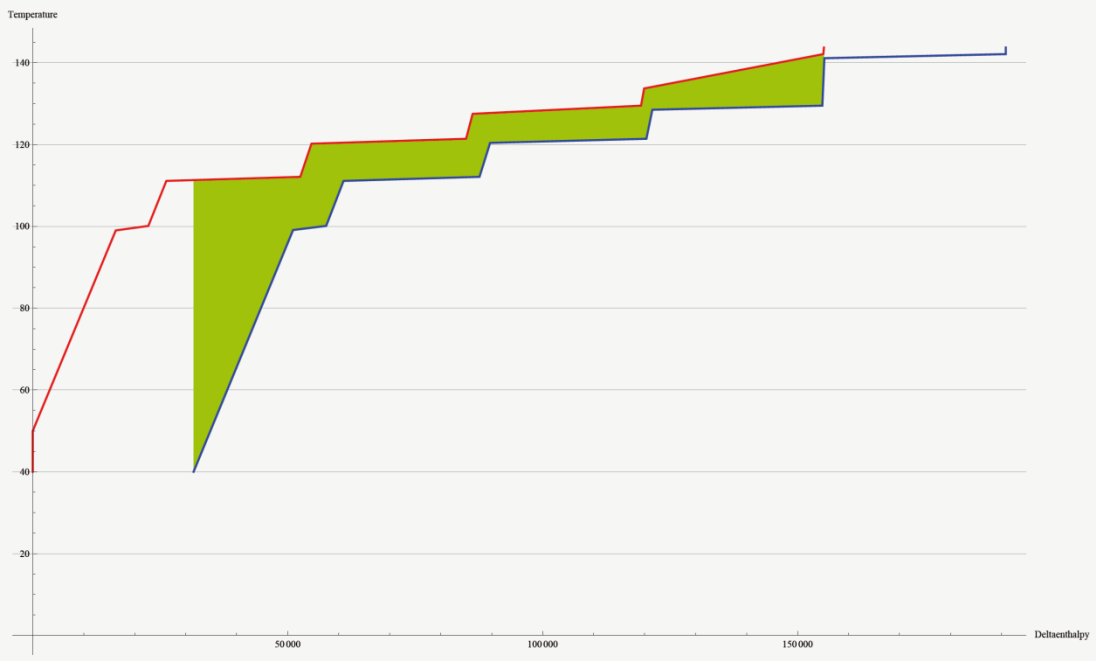


**Figure D-15:** **CCC and HCC of the counter-current 5-stage evaporation system with a minimum temperature difference of 5°C**

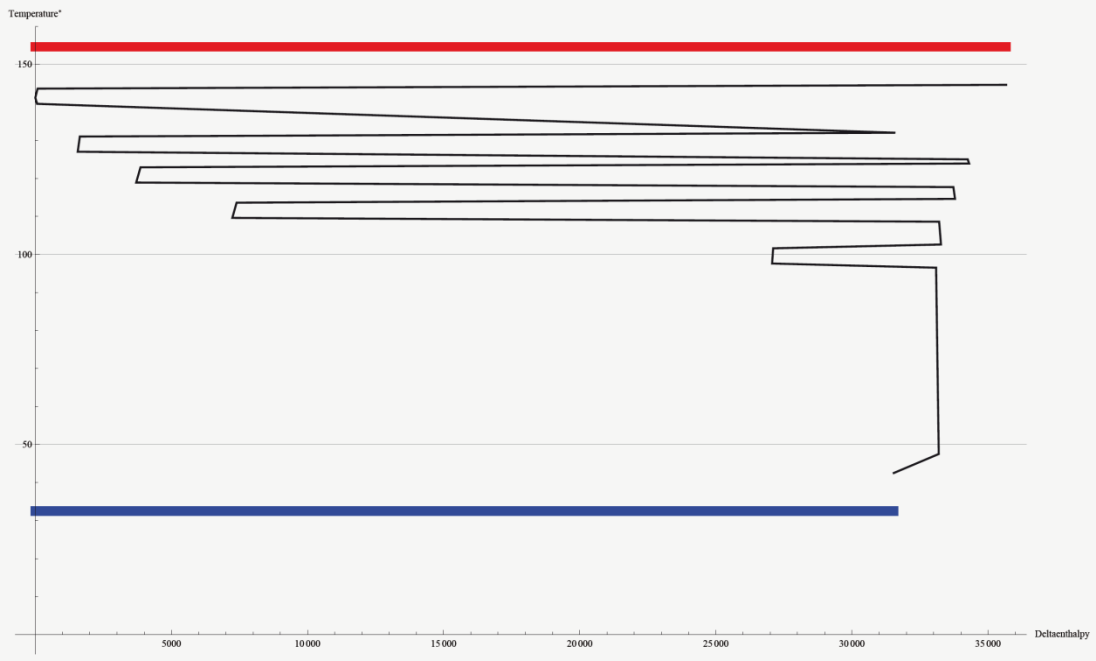


**Figure D-16:** **GCC of the counter-current 5-stage evaporation system with a minimum temperature difference of 5°C**

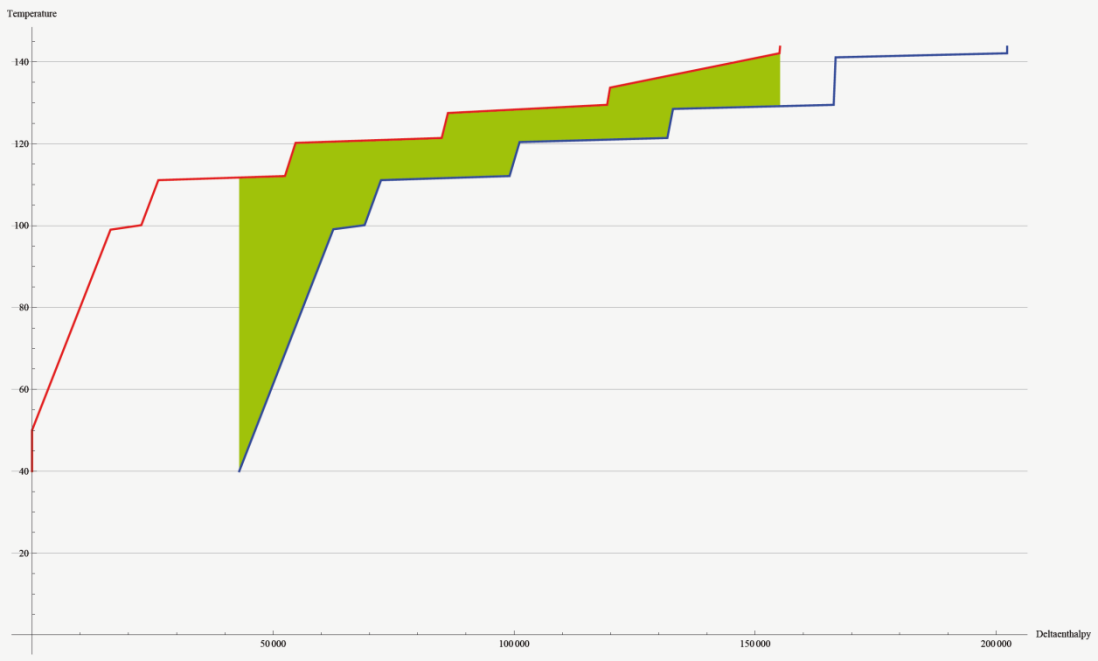


**Figure D-17:** **CCC and HCC of the counter-current 5-stage evaporation system with a minimum temperature difference of 8°C**

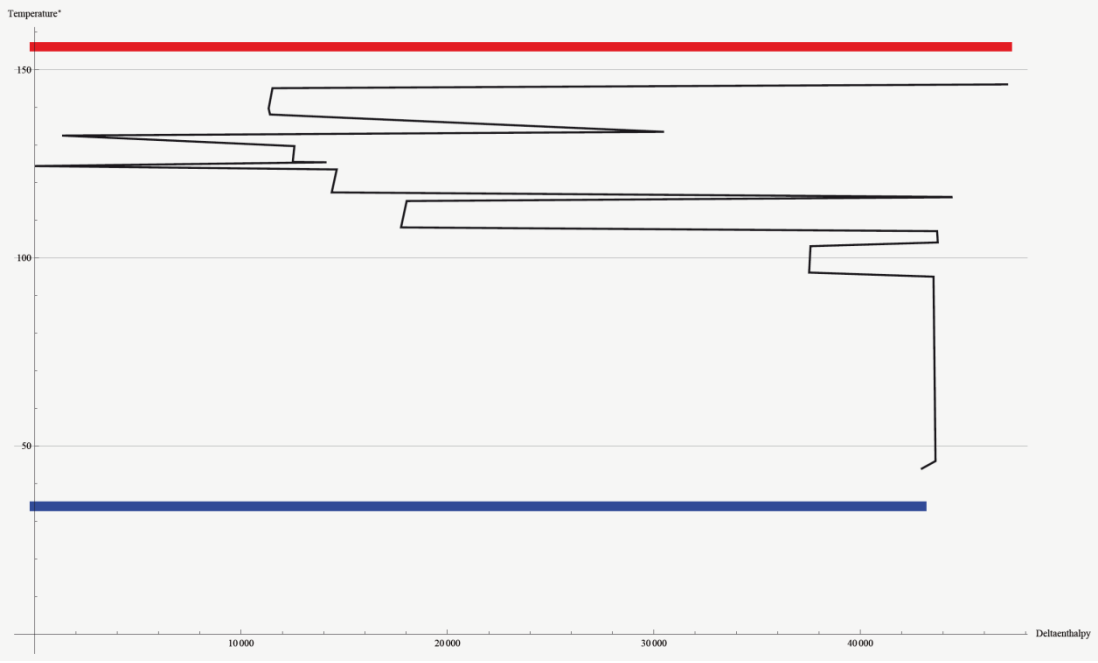


**Figure D-18:** **GCC of the counter-current 5-stage evaporation system with a minimum temperature difference of 8°C**

## CCC, GCC and HCC of the overall process

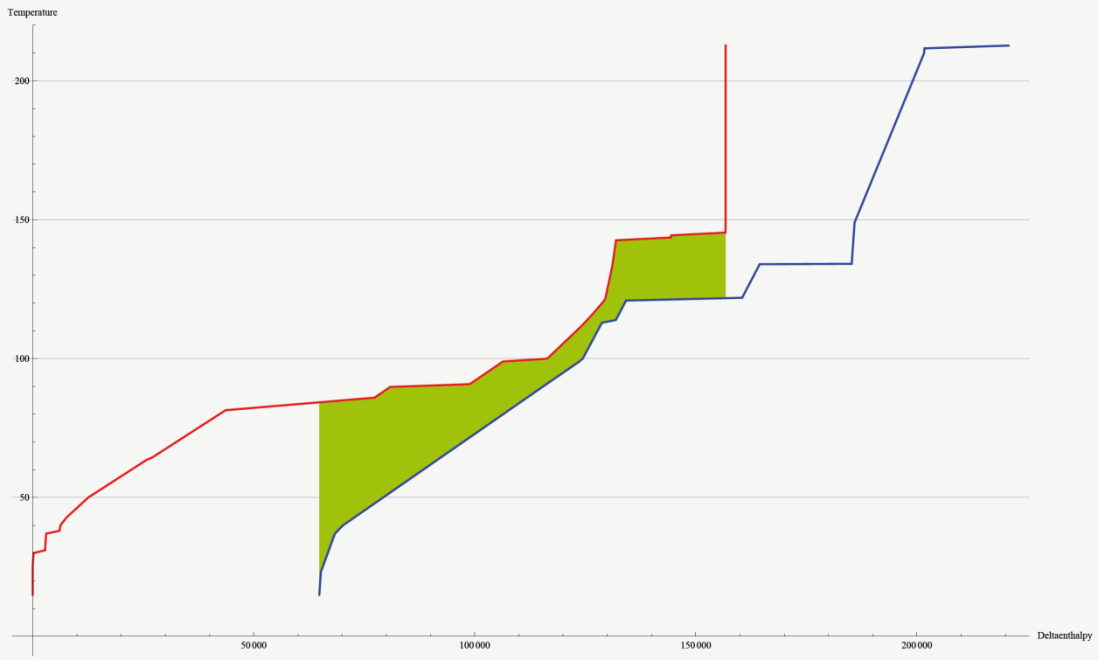


**Figure D-19:** **CCC and HCC of the overall bioethanol process including a 2-column distillation and a multi-stage evaporation with a minimum temperature difference of 7°C**

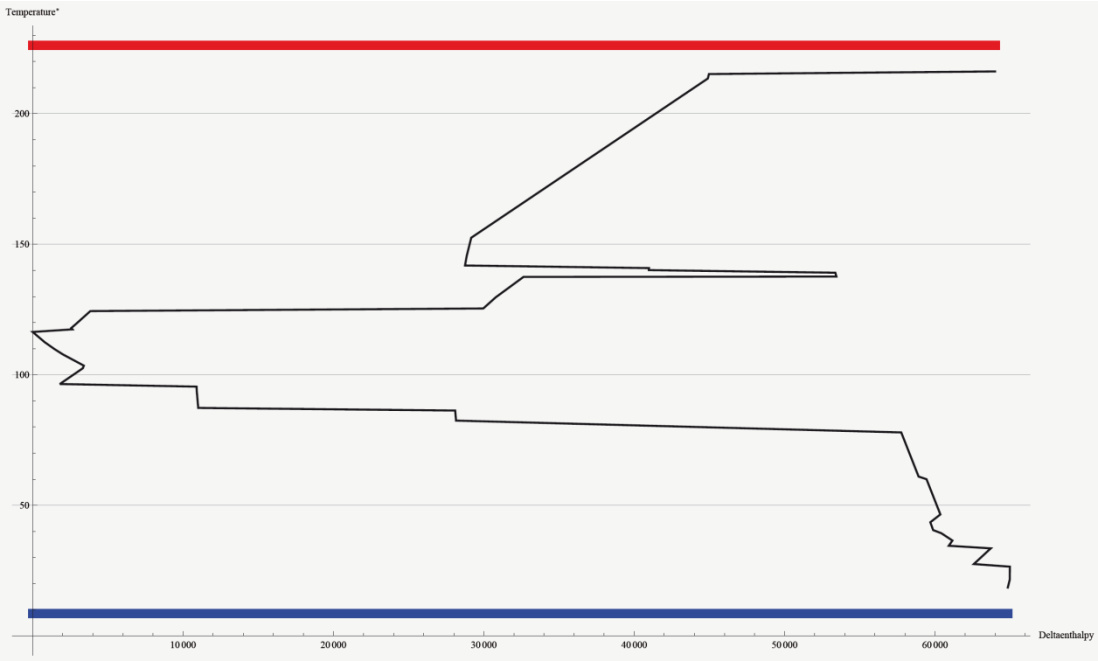


**Figure D-20:** **GCC of the overall bioethanol process including a 2-column distillation and a multi-stage evaporation with a minimum temperature difference of 7°C**

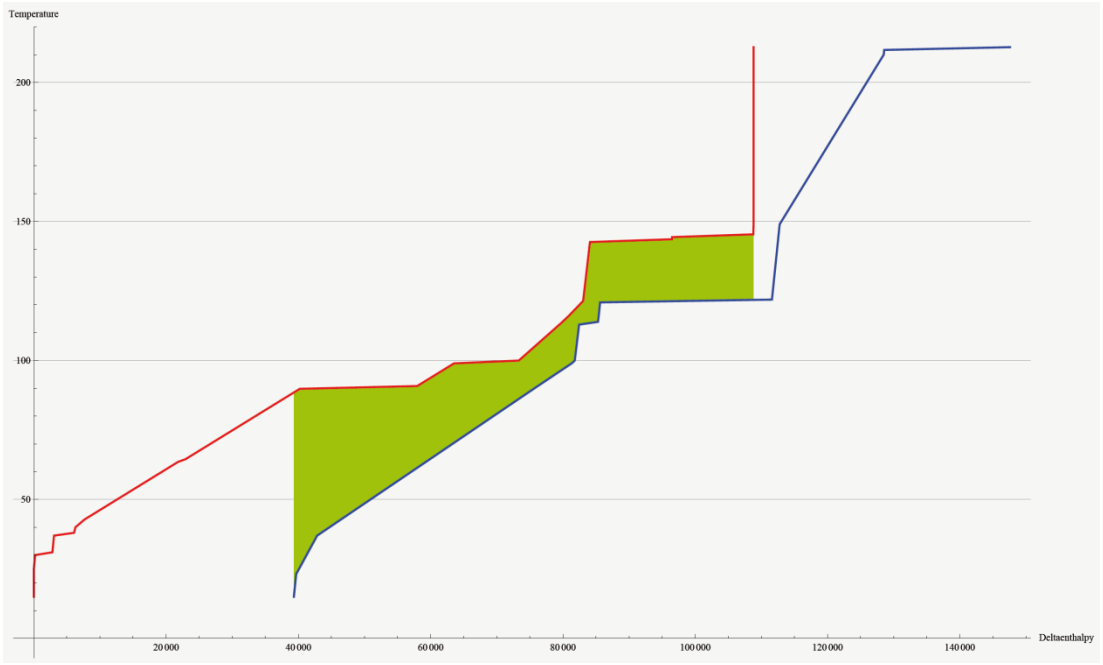


**Figure D-21:** **CCC and HCC of the overall bioethanol process including a 2-column distillation and a biogas production with a minimum temperature difference of 7°C**

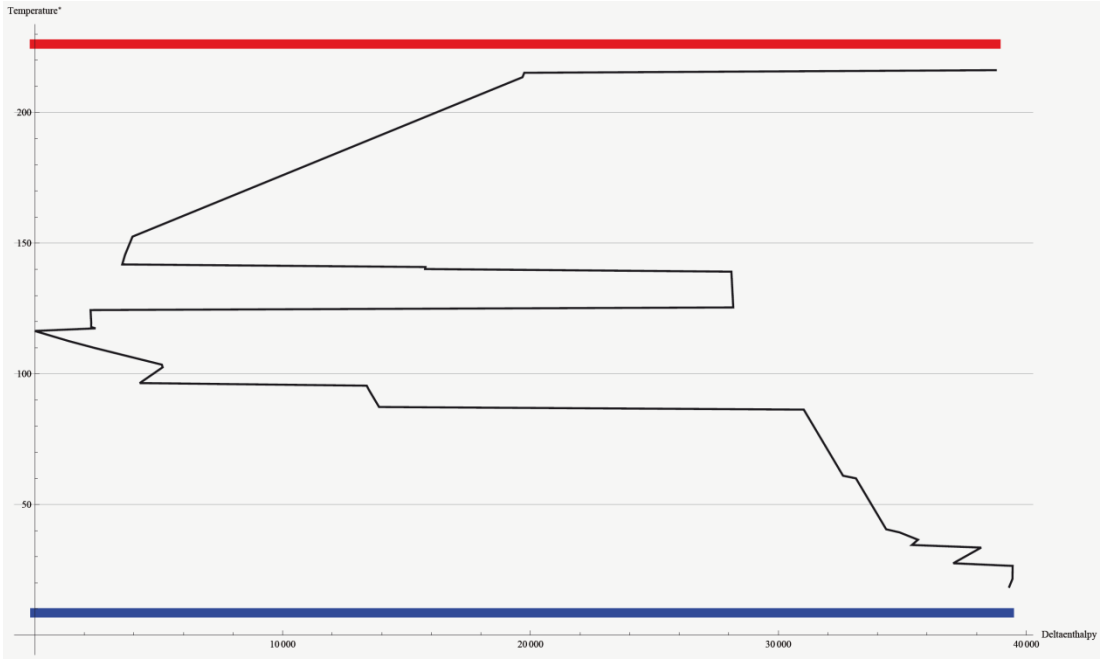


**Figure D-22:** **GCC of the overall bioethanol process including a 2-column distillation and a biogas production with a minimum temperature difference of 7°C**

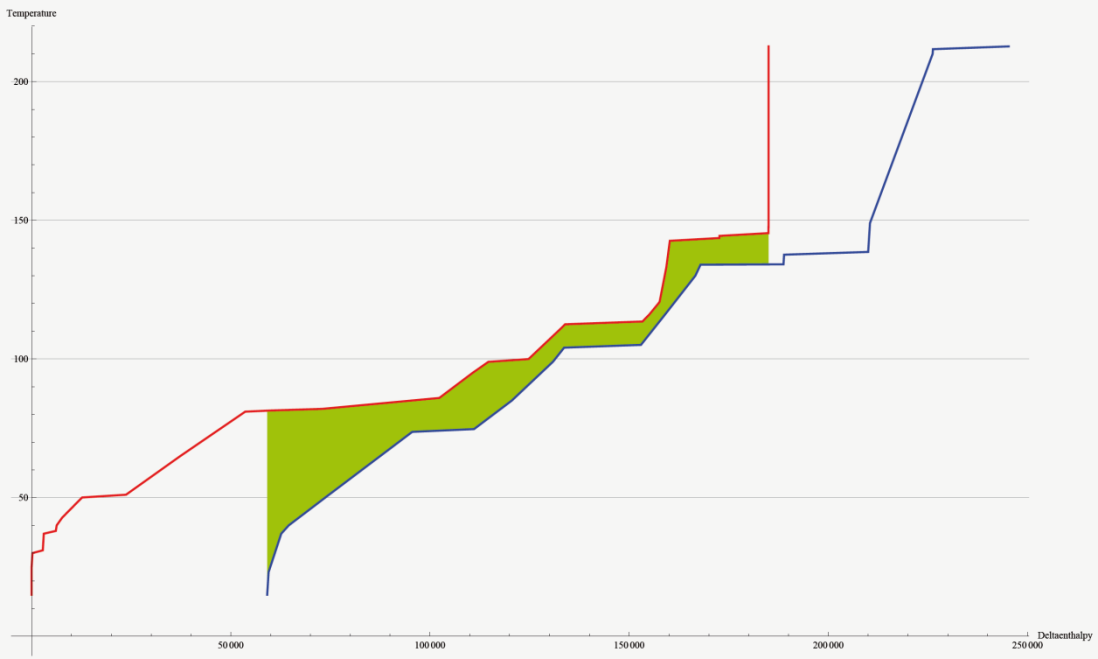


**Figure D-23:** **CCC and HCC of the overall ethanol process including a 3-column distillation and a multi-stage evaporation with a minimum temperature difference of 7°C**

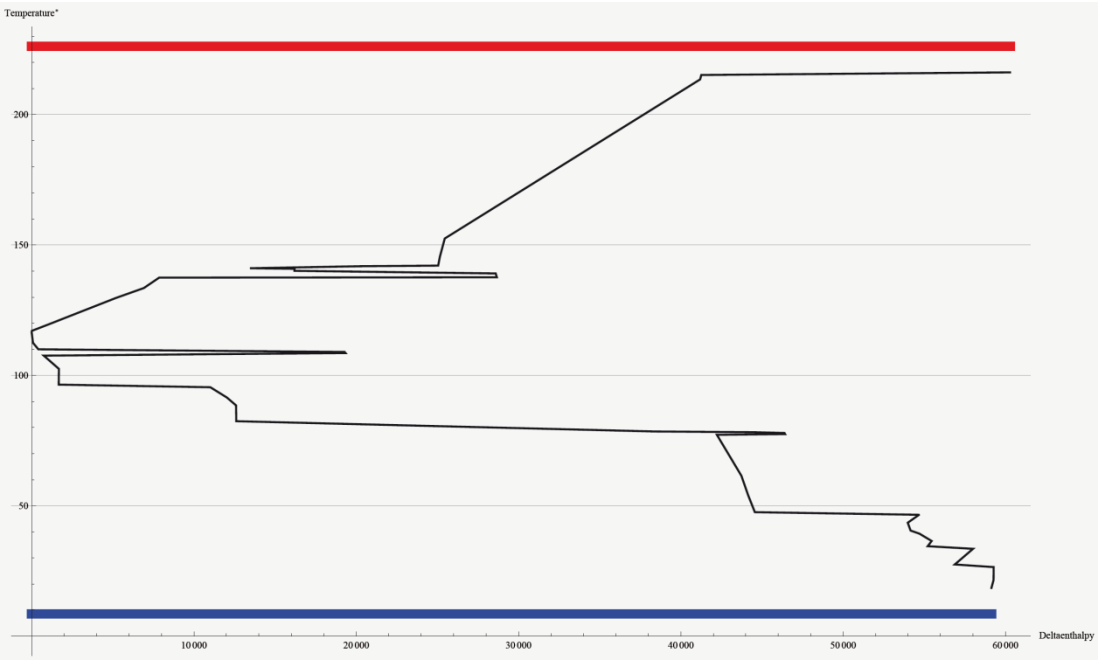


**Figure D-24:** **GCC of the overall ethanol process including a 3-column distillation and a multi-stage evaporation with a minimum temperature difference of 7°C**

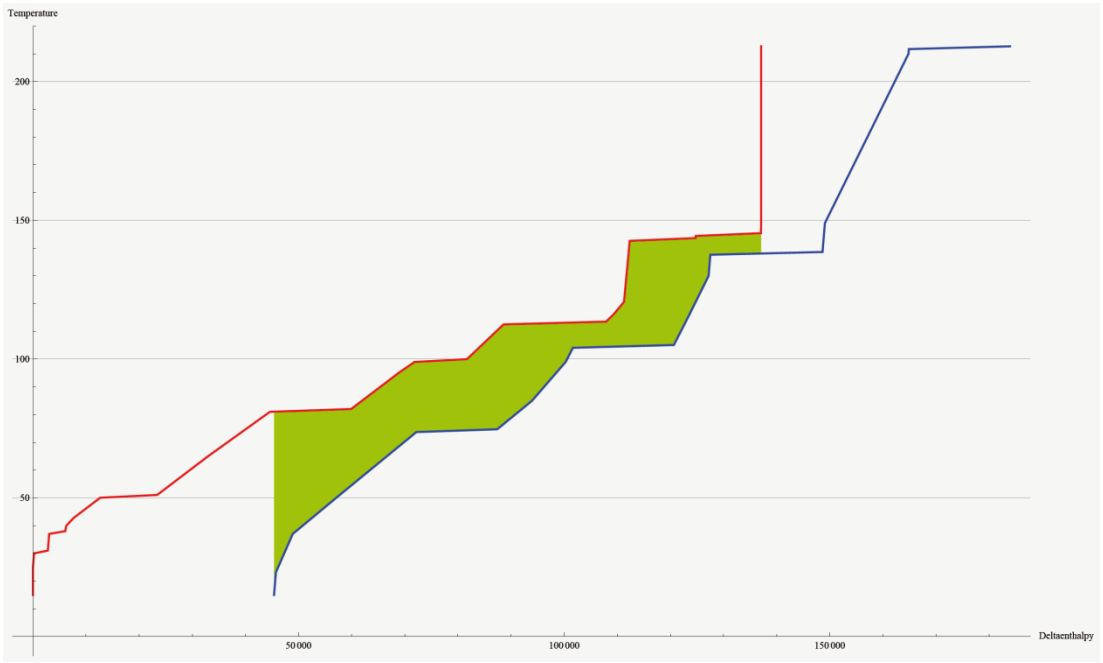


**Figure D-25:** **CCC and HCC of the overall ethanol process including a 3-column distillation and a biogas production with a minimum temperature difference of 7°C**

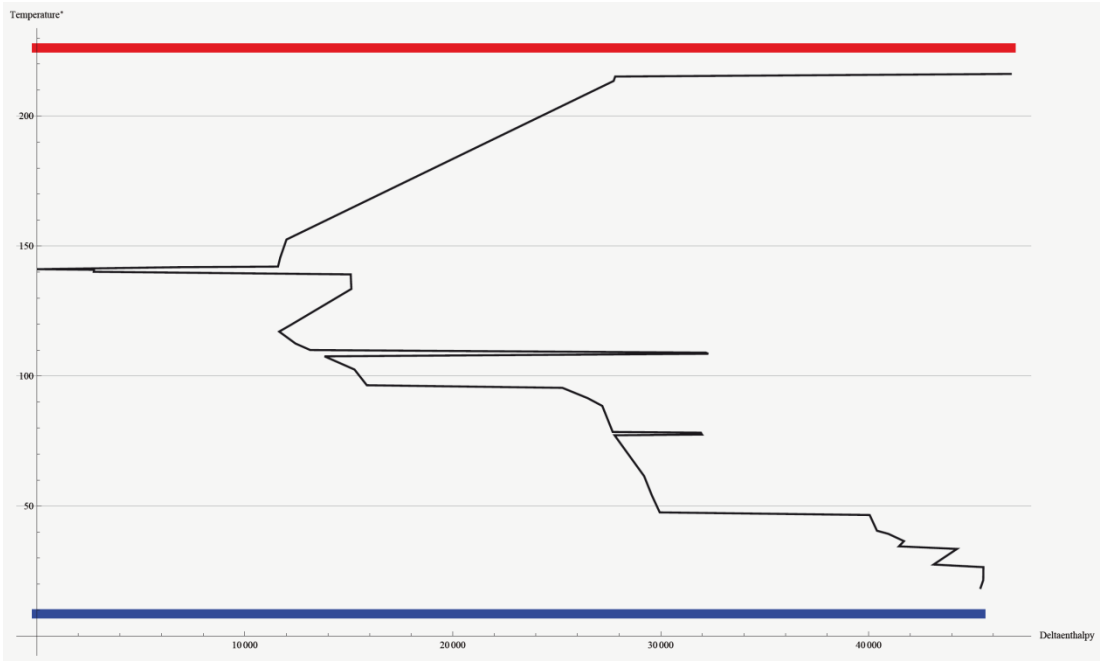


**Figure D-26:** **GCC of the overall ethanol process including a 3-column distillation and a biogas production with a minimum temperature difference of 7°C**

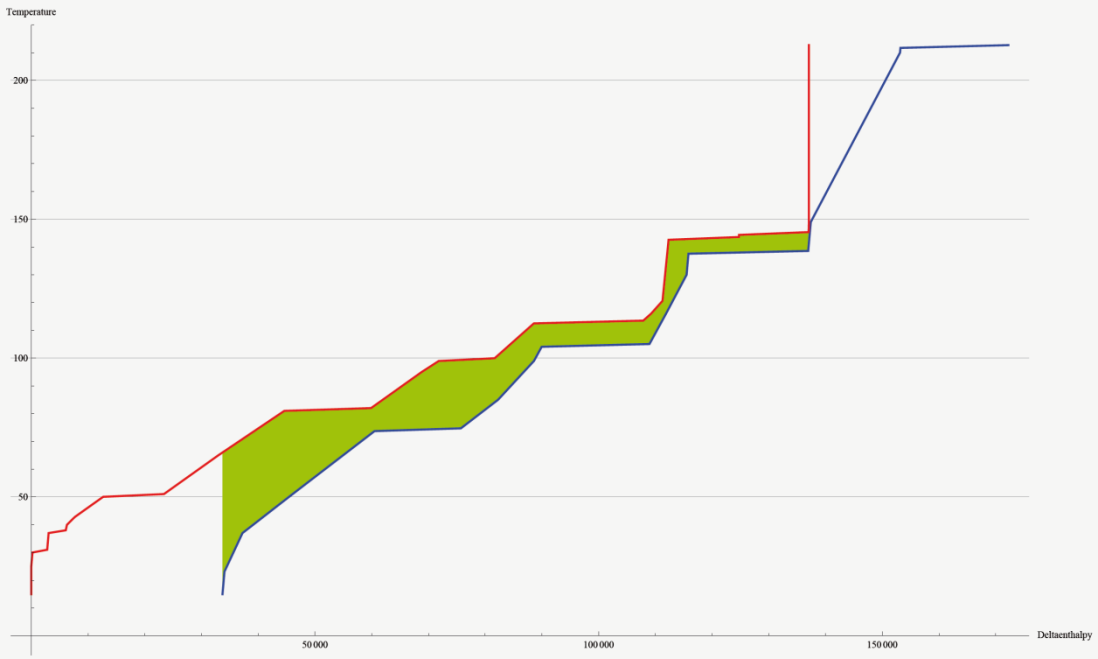


**Figure D-27:** **CCC and HCC of the overall ethanol process including a 3-column distillation and a biogas production with a minimum temperature difference of 5°C**

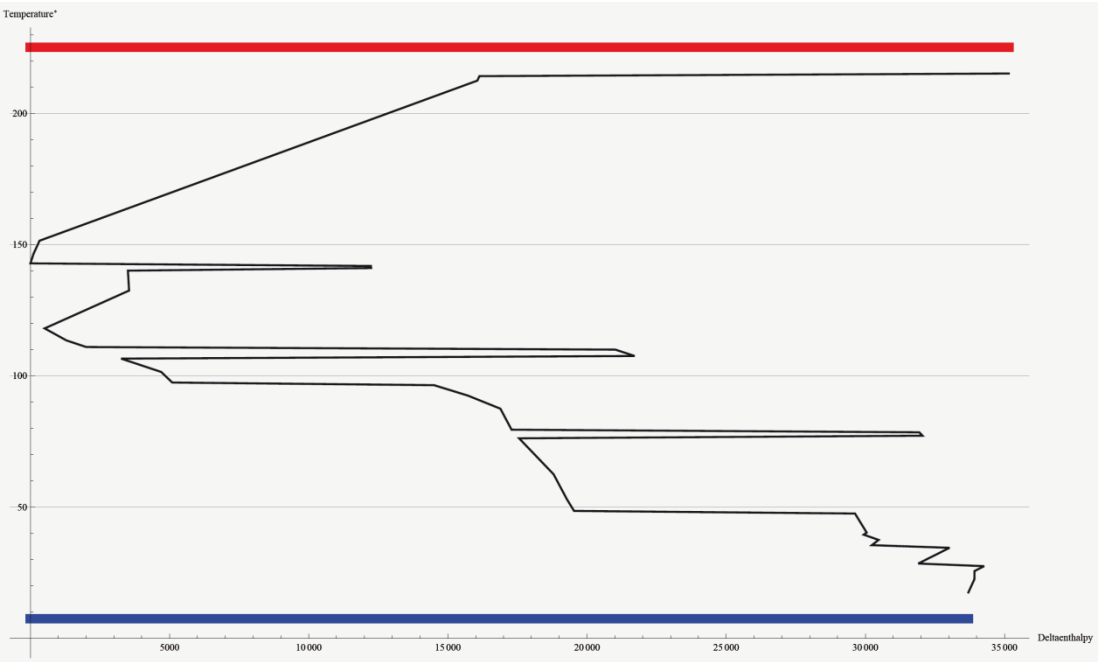


**Figure D-28:** **GCC of the overall ethanol process including a 3-column distillation and a biogas production with a minimum temperature difference of 5°C**